NUMERICAL STUDY ON EARTHQUAKE INDUCED DYNAMIC RESPONSE OF SKEWED AND CURVED INTEGRAL BRIDGES

A Thesis Submitted by

DEBANJAN PAL

(University Roll no - 002110402030)

(Examination Roll no – M4CIV23013)

In partial fulfillment of the requirements for the award of degree of

MASTER OF ENGINEERING IN CIVIL ENGINEERING

Specialization:

STRUCTURAL ENGINEERING

Under the guidance of

Dr. Dipankar Chakravorty

DEPARTMENT OF CIVIL ENGINEERING

JADAVPUR UNIVERSITY

KOLKATA – 700032, WEST BENGAL, INDIA

2023

DEPARTMENT OF CIVIL ENGINEERING
FACULTY OF ENGINEERING AND TECHNOLOGY
JADAVPUR UNIVERSITY
KOLKATA – 700 032

CERTIFICATE OF RECOMMENDATION

This is to certify that the thesis entitled, "**Numerical Study on Earthquake Induced Dynamic Response of Skewed and Curved Integral Bridges**" submitted by **Debanjan Pal** (Examination Roll No. M4CIV23013, Class Roll No. 002110402030, Registration No. 160042 of 2021-2022) of Jadavpur University is absolutely based upon her own work under the supervision of **Dr. Dipankar Chakravorty.** I hereby recommend that the thesis be accepted in partial fulfilment of the requirements for awarding the degree of '**Master of Engineering in Civil Engineering (Structural Engineering)**'.

Supervisor
(Dr. Dipankar Chakravorty)
Professor
Department of Civil Engineering
Jadavpur University,
Kolkata - 700032

Head of the Department
(Dr. Partha Bhattacharya)
Head of the Department
Department of Civil Engineering
Jadavpur University,
Kolkata - 700032

Dean, FET
Prof. Ardhendu Ghoshal
Jadavpur University,
Kolkata - 700032

DEPARTMENT OF CIVIL ENGINEERING
FACULTY OF ENGINEERING AND TECHNOLOGY
JADAVPUR UNIVERSITY
KOLKATA -700032

CERTIFICATE OF APPROVAL

This thesis paper is hereby approved as a credible study of an engineering subject carried out and presented in a manner satisfactorily to warrant its acceptance as a pre-requisite for the degree for which it has been submitted. It is understood that, by this approval the undersigned do not necessarily endorse or approve any statement made, opinion expressed or conclusion drawn therein but approved the thesis paper only for the purpose for which it is submitted.

Committee of Thesis Paper Examiners

____

Signature of Examiner

____

Signature of Examiner

DECLARATION

I, Debanjan Pal, Master of Engineering in Civil Engineering (Structure Engineering), Faculty of Engineering and Technology, Jadavpur University, hereby declare that the work being presented in the thesis work titled, "**Numerical Study on Earthquake Induced Dynamic Response of Skewed and Curved Integral Bridges**", is an authentic record of work that has been carried out in the Department of Civil Engineering, Jadavpur University, Kolkata under the guidance of **Dr. Dipankar Chakravorty**. Professor, Head of Department, Department of Civil Engineering, Jadavpur University, Kolkata. This work has not previously been submitted for a degree or diploma in any University. To the best of my knowledge and belief, the thesis contains no material previously published or written by another person except where due reference is made in the thesis itself.

Place: Kolkata

Date:

Debanjan Pal

Examination Roll No.: M4CIV23013

Roll No.: 002110402030

Registration No.: 160042 of 2021-2022

Acknowledgement

I would like to take this opportunity to convey my sincere gratitude and appreciation for my supervisor **Dr. DIPANKAR CHAKRAVORTY** Professor of the Department of Civil Engineering, Jadavpur University, Kolkata. I am indebted to him for his methodical guidance, motivation and constant support given to me throughout the thesis work. He has identified my potentials and kept faith in me. It is because of his confidence that I was able to successfully accomplish the targets. I am extremely thankful to him as without him my thesis could not have reached this state.

I also thankfully acknowledge my gratefulness to all Professors and staffs of Civil Engineering Department, Jadavpur University, Kolkata, for extending all facilities to carry out the present study.

I also thankfully acknowledge the assistance and encouragement received from my family members, friends and others during the preparation of this Thesis.

Date:

……………………………..

Debanjan Pal

Roll No – 002110402030

Examination Roll No.: M4CIV23013

Registration No.: 160042 of 2021-2022

CONTENTS

List of figures

List of graphs

Variation of dead load

Variation of time period

Variation of base reaction

Variation of the moment at side wall in longitudinal seismic condition

Variation of the moment at middle wall in longitudinal seismic condition

<u>Variation of the moment at side wall in transverse seismic condition</u>

Variation of the moment at middle wall in transverse seismic condition

List of tables

Abstract

Road alignment including the bridge geometry in plan depends on a number of factors related to vehicle speed, alignment of existing roads, availability of land, funds and more. These practical compulsions often necessitate provision of skewed and curved bridges. Seismic performance of bridges is an important issue of infrastructure development for maintaining uninterrupted flow of traffic for considerable life span of the bridges. Bridge construction is specialized, cost and skilled labour intensive and so ensuring a long-life span of a bridge has great economic implications. Integral bridges are relatively light weight and these indeterminate and stable structures have been recommended by IRC: SP: 114 – 2018 in high earthquake risk zones.

Although several analytical and experimental results are available in the literature regarding straight integral bridges but similar study on skewed and curved integral bridges are nor found. Hence this study considers the effect of various parameters like central angle, radius of curved bridges, skew angle of skewed bridges on important design parameters like time period, bending moment, torsional moment, support reaction etc. The Midas Civil software is used to generate results of numerical analysis which are interpreted from practical engineering point of view. Future scope of research is also indicated.

Chapter – 1: Introduction

1.1 General

A bridge is a structure carrying a road, path, railway, etc. across a river, water body, valley, road, or other obstacle without blocking the way underneath. It is constructed for the purpose of providing smooth passage over the obstacle, which is usually something that is otherwise difficult or impossible to cross. There are many different designs of bridges, each serving a particular purpose and applicable to different situations. Designs of bridges may be in various shapes, sizes and with different materials depending on factors such as the function of the bridge, the nature of the terrain where the bridge is constructed and anchored, and the material used to make it, and the funds available to build it.

Bridges are designated in different terms such as:-

- When it carries road traffic or railway traffic or a pipe line over a channel or a valley: it is designated as *bridge*.
- When it carries the traffic or pipe over a communication system like roads or railways, it is designated as *fly-over/over-bridge*.
- Bridge (several small spans) constructed over a busy locality, a valley, dry or wetland, or forming a flyover to carry the vehicular traffic, it is designated as *viaduct*.

1.2 History of bridge engineering

The history of bridge engineering is closely associated with the progress of human civilization spread over several centuries. The earliest bridge on record is traced to the lake dwellers of Switzerland who pioneered the timber trestle construction for crossings of rivers around 4000 B.C. The oldest bridge still standing is a pedestrian stone slab bridge which is at least 2800 years old built across the Meles river in Smyrna, Turkey. Many of the important ancient bridges were built by armies. As per Homerand Herodotus, the floating bridges were made of inflated skins (used as floats) around 800 B.C. A bridge of this kind was built in the year 556 B.C. by King Cyrus.

Around 320 B.C, Alexander the Great built floating bridges for the passage of his army during his great conquest of the East. India was the birth place of wooden cantilever bridges in the Himalayas with planks of wood anchored at the two banks using heavy stones and the wooden planks corbelled out progressively towards the mid-stream until the gap could be spanned by a single plank.

The period between 200 B.C. and 260 A.D. witnessed the widespread use of stone arches by Romans using massive piers. After the fall of Rome, the bridge activity in Europe was mainly promoted by the religious orders. The Pont d'Avignon with 20 arch spans of about 34 m built by St. Benezet over the river Rhone in 1188 and the old London bridge across the river Thames with 19 pointed arch spans of varied length built by Peter Colechurch in 1209 belong to this period. The medieval period bridges were loaded with decorative and defensive towers, chapels, statues, shops and dwellings. The Rialto Bridge in Venice, Italy built in 1591 having a single arch span of 27 m is a typical example of the many bridges built during the Renaissance period.

In middle age, number of bridges were constructed in Europe e.g. over Thames in London (1209), over Arno in Florence (1177 and 1569) and over Grand Canal in Venice (1591).

The first treatise on bridge engineering was published in 1714 by the French Engineer, Robert Guiter ushering the age of reason.

Advancement of bridge engineering has been taken place in 19th century due to production of alloy steel and cement, manufacture of heavy load lifting equipment and construction machinery, advancement in construction methodology and engineering design.

Reinforced concrete bridges gained popularity in the 20th century due to their versatility in construction, economy and ease of maintenance. These bridges can be casted at site in any shape and form to meet the architectural requirement. Again, locally available material e.g. coarse aggregate and fine aggregate can be utilized eliminating high carriage cost. Reinforced concrete bridges have been further improved in prestressed concrete bridge. Now a days, extra dosed bridge, cable stayed bridge are being used as long span bridges, where the deck is being made of reinforced concrete/prestressed concrete

1.3 Importance of bridge

There are several reasons why bridges are important. They offer a way to cross rivers, mountains, and other barriers, allowing people and vehicles to move from one side to the other. This enables improved accessibility and connectivity between various places. Additionally, bridges are essential to transportation because they provide buses, trains, and other vehicles a way to move quickly and safely. Bridges can also serve to facilitate the flow of goods and services and lessen traffic congestion. Additionally, bridges are crucial for tourism and recreational purposes. They may be a lovely and captivating attraction for both tourists and residents. They are also very important economically for the towns or areas where they are found. So, there are several economic, social and political importance of bridges.

1.4 Classification of bridges

There are various types of bridges classified based on span, materials, types of bridge structures, functions, utility and position etc. A bridge is structure which allows passage over an obstruction. The obstructions may be river, valley, rail route or road way etc. Bridges are classified into so many types based on different criteria. They are explained below.

- Types of bridges based on utility.
  - Temporary bridge.
  - Permanent bridge.

- Types of bridges based on high flood level (HFL)
  - Low level bridge.
  - High level bridge.

- Classification of bridges (according to form (or) type of superstructures)
  - Slab bridge.
  - Beam bridge (RCC, Steel or PSC).
  - Truss bridge.
  - Arch bridge.
  - Cable stayed (or) suspended bridge.
  - Extra dosed bridge.

- Classification of bridges (According to material of construction of superstructure)
  - Timber bridge.
  - Stone/Stone masonry bridge.
  - Brick Masonry bridge.
  - R.C.C bridge.
  - Steel bridge.
  - P.C.C bridge.
  - Composite bridge.
  - Aluminum bridge.

- Classification of bridges (According to inter-span relationship)
  - Simply supported bridge.

- Integral bridge.
- Cantilever bridge.
- Continuous bridge.

➢ According to length of bridge
- Culvert bridge (less than 6 m).
- Minor bridge (less than 6 m-60m).
- Major bridge (more than 60 m).
- Long span bridge (more than 120 m).

➢ According to function
- Aqueduct bridge (canal over a river).
- Viaduct (road or railway over a valley or approach of bridge/ROB).
- Pedestrian bridge.
- Highway bridge.
- Railway bridge.
- Road-cum-rail.
- Flyover.
- Utility/pipe line bridge.
- Cattle of animal underpass/overpass.

1.5 Bridge geometry

Bridge geometry is typically established to follow a determined roadway alignment. Roadway geometric designers take a number of variables into consideration when establishing these alignments. They work within the limits of a particular site to optimize the functionality of a roadway while considering user safety. The resulting impact on bridge geometry can be small when roadway needs are straightforward, as for simple grade separations, or quite complex, as in the case of congested urban interchanges.

Present day traffic requirements demand straight alignment of the road in view of the fast traffic and this in turn necessitates the use of skew crossings or curved bridges. In addition to overcoming these geometrical constrain, construction of skewed-curved Integral bridges is becoming increasingly popular for economic and aesthetic reasons.

1.6 Curvature in bridge

As a result of complicated geometrics, limited rights of way, and traffic mitigation, horizontally curved bridges are becoming the norm of highway interchanges and urban expressways.

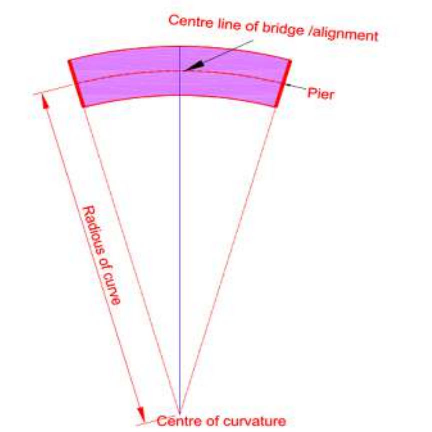

Fig 1. Curved bridge

When the axis of the bridge girder system is having a curvature in plan (Figure 1), the bridge is called curved bridge. Curvature of a particular span is measured by central angle. Curvature of a girder may be achieved either by a single curve or joining small straight beam elements. Due to geometric complexities, the gravity load will induce torsional shear stresses, warping normal stresses, and flexural stresses to the structural components of horizontally curved bridges. To determine these stresses, special analysis accounting for torsion is required. Most refined methods are forms of finite-element analysis. Grillage analysis as well as three-dimensional (3-D) models have been used successfully to analyze curved bridges. The grillage method assumes that the member can be represented in a series of beam elements. 3-D view of a curved bridge is shown in Figure 2.

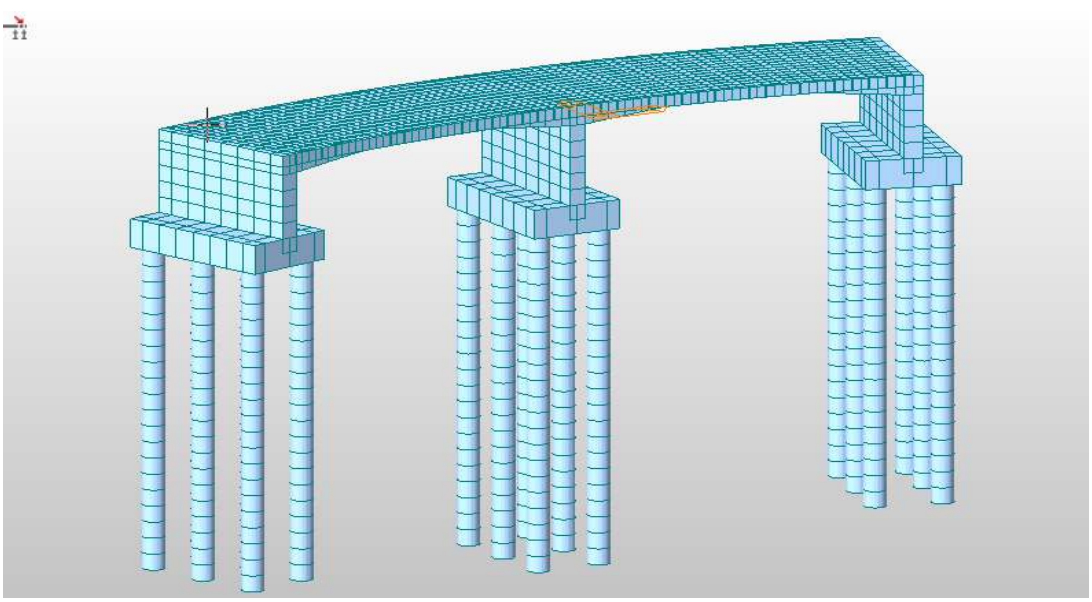

Fig 2. 3D view of a curved bridge.

1.7 Skewed bridge

A bridge, built obliquely between abutments/piers is called as skewed bridge. The angle between the normal to the center line of the bridge and the center line of the abutment(s) or the angle between directions of traffic with the normal to the abutment(s) is known as skew angle. A clockwise rotation of the bridge abutment normal with respect to the traffic direction is denoted as positive skew (θ_1 and θ_2) while a counter-clockwise rotation represents negative skew (θ_3 and θ_4) as shown in Figure 3.

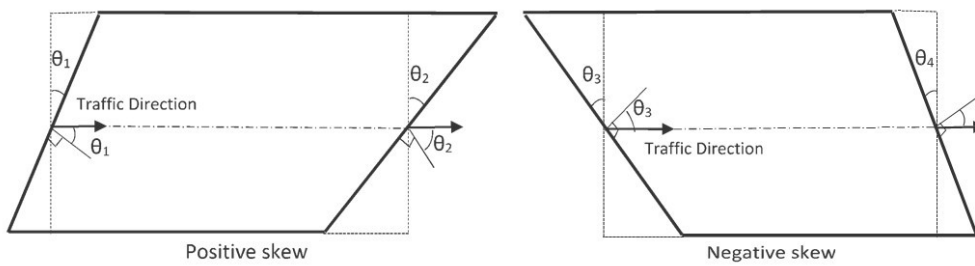

Fig 3. 3D Types of skew deck**.**

The load path (force transfer mechanism), in straight bridges, is found along the direction of span, while in skew bridges load tends to take the shortest path along the obtuse corners. Due to change in load transfer mechanism, higher reactions are developed at obtuse corner while lower reactions are observed at acute corners. Moreover, due to skewness in the bridges, additional torsional and transverse moments are developed; though, the longitudinal moments are reduced. It is well documented in the literature that the bridges with small skew angles (< 15–20°) may be analyzed and designed similar to the straight bridges with little/no modifications. But, the structural behavior of the bridges with large skewness substantially differs from the straight bridges.

1.8 Integral bridge

An Integral bridge (IB) is a structure where there are no bearings over the abutments and no expansion joints in the superstructure. IB's are characterized by monolithic connection between the superstructure and the substructure (piers and abutments), unlike the traditional bridge construction, where the superstructure is supported on bearings and transfers all the forces to substructure and foundation through bearings. Provision of expansion joints and bearings in traditional bridges allows movement and rotation of the bridge deck, without transferring any force to abutment / pier and foundation due to thermal / creep / shrinkage induced movements. In case of IB's, the deck carries the movement of deck to the abutment as well as to the backfill soil behind the abutment. The approach slab between the bridge end and the pavements accommodates the necessary movements, which leads to a strong soil-structure interaction.

1.9 Integral bridge practices in various parts of the world

Experience on construction of integral bridges in the United States of America dates back to late 1930's and early 1940's. Ohio, South Dakota, and Oregon were the first states to routinely use continuous construction with integral abutments. California followed suit in 1950's. Tennessee and other states in USA began moving toward integral bridges from 1960's. New Zealand's experience with joint-less bridges began in 1930's. Standardized design drawings for concrete bridges of this type have been developed by the New Zealand Ministry of Works and Development (NZMWD) as far back as 1950's. In the 1970's, Britain started to research on IB's. Currently in UK, the bridges with span length less than 60 m and skew not exceeding 30º are generally required to be continuous over intermediate piers and integral at abutments2. The thermally induced cyclic movement at each abutment is restricted to ± 20 mm in case of IB's as per the British Advisory Note. In Japan, the first integral bridge was built in 1996. Generally the integral bridge length in Japan is restricted to 30 m. In Australia, the integral bridge construction is practiced by Queensland Main Roads Department (QMRD) since 1975. China began to build Integral bridges since 1990's.

European experience of integral bridge is significantly less and dates back to 1960 onwards. However the experience gained by Europe has been positive and as a result, the trend is towards making integral bridges a larger percentage of all newly constructed bridges in Europe. In Switzerland, many integral bridges were constructed on the national motorway network during the period 1960-85. The long term experiences of these structures have been overwhelmingly positive, both in terms of construction and maintenance. More than 40% of the existing bridges on FEDRO (Federal Roads Office of Switzerland) network are integral or semi integral structures. The scientists at EPFL (Ecole Polytechnique Federale de Lausanne) are currently conducting research program on abutment and approach slab construction techniques, with the challenge to build long span bridges with integral concepts (i,e. bridges of length > 200m). A sample elevation of integral bridge is shown in Figure 4.

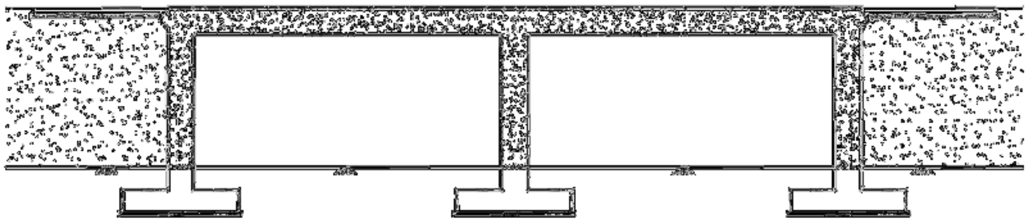

Fig 4. Elevation of integral bridge

1.10 Integral bridge characteristics

There are some significant differences between integral and conventional bridges. The most important is that integral bridges are rigid in their structure and conventional bridges are not. These differences are illustrated in Figure 5.

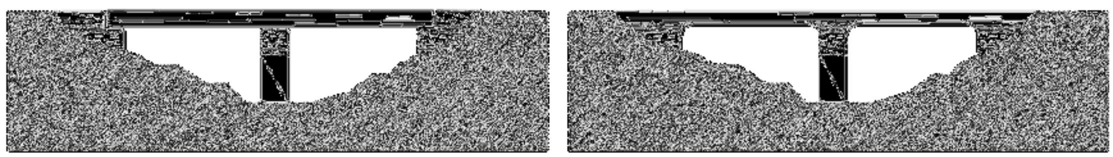

Fig 5: Elevation fundamental differences between conventional bridge (left) and integral bridge construction (right)

It can be seen than the conventional bridges have expansion joints and bearings in their structure, while integral bridges are built monolithically without bearings or expansion joints.

The idealization of the bridge in simple form is shown in Figure 6. Such bridges are the solution for small and medium-length bridges where bearings and expansion joints can either be eliminated altogether or reduced to a minimum. Their decks are continuous and connected monolithically to the abutment with a moment-resistant connection. This leads the structure to act as one unit. So far, this type of bridge has had a good record of initial cost savings, with economical use of material and maintenance. The absence of expansion joints at the abutment and bridge deck leads to reduced construction and maintenance costs. Engineers are therefore increasingly interested in using integral bridges, although there are still many problems to be overcome, such as soil-structure interaction and cracking. In Figure 6, soil is modelled as a series of springs acting horizontally and vertically to support the structure.

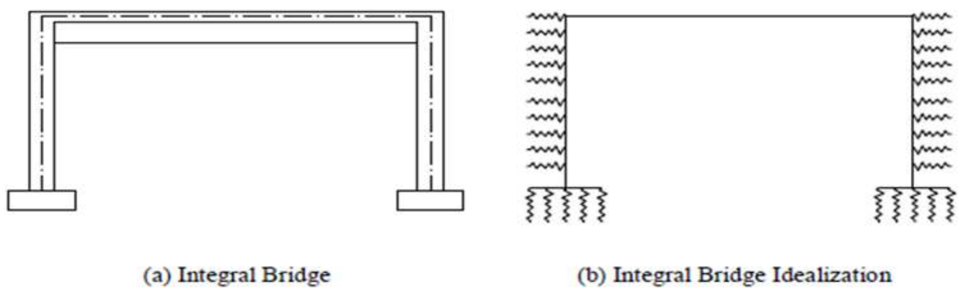

Fig 6: Idealization of integral bridge

1.11 Advantages and disadvantages of using integral bridges

Advantages

- Added redundancy with improved seismic performance
- Improved structural reliability and redundancy
- Improved ride-quality and noise reduction
- Improved durability due to absence of expansion joints, which is the source of moisture ingress
- Potential for reduced initial cost
- Reduced maintenance requirement
- Reduced traffic disruption
- Lower whole-of-life cost and
- Improvement of bridge appearance
- Simplified widening and replacement detail
- Useful concept for strengthening of existing bridges

Disadvantages

- Added redundancy with improved seismic performance
- Limited span range due to restraints to movements caused by thermal, creep and shrinkage.
- Differential settlement between foundations resting on varying strata or varying scour conditions in case of river bridges.
- Climatic conditions with large variation in maximum and minimum ambient temperatures.
- Need for complex structural analysis involving soil-structure interaction. Improved ride-quality and noise reduction

1.12 Behavior of integral bridges under earthquake loads and soil structure interaction

The basic difference between integral and conventional bridges is the inclusion of the superstructure, the substructure and the surrounding soil in a single structural model. in the case of the integral bridge, the superstructure has a necessary and direct impact on the substructure, so it needs to be modelled as a unit. For the substructure itself, it is important to incorporate the influence of the backfill behind the abutments into the structural model. The influence of the backfill is addressed by soil springs, which are applied in the abutment. These soil springs are applied horizontally, in other words transverse to the back of the abutment. This soil interaction with the abutments and superstructure as a unity is called soil-structure interaction. As an integral bridge is a rigid structure, then this soil-structure interaction is important and needs to be considered in designing this type of bridge.

An integral bridge, especially when its main span is long, is subjected to longitudinal displacements due to daily and seasonal temperature fluctuations. This effect, which is usually expressed as expansion and contraction of the bridge, will be restrained by the abutment backfill and interactive substructure, as shown in Figure 7.

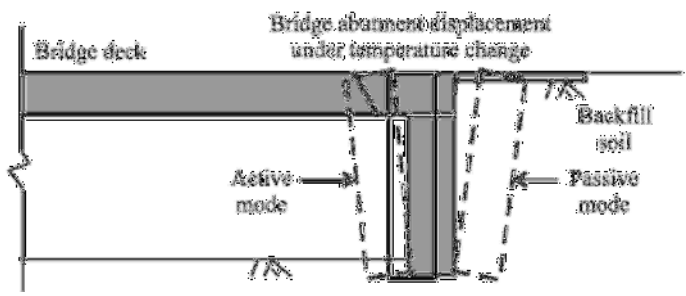

Fig 7: Abutment wall: active and passive states (Alizadeh, et al., 2010)

Figure 7 explains the process of fluctuations in the length of the bridge due to temperature changes. An increase in temperature drives the expansion and makes the back soil denser. When the structure contracts, the abutment will move away from the back soil and it may reduce the density of the soil. This condition will cause sliding over the wall and create an active earth pressure behind the abutment wall.

When external forces, such as earthquakes, act on these systems, neither the structural displacements nor the ground displacements are independent of each other. The process in which the response of the soil influences the motion of the structure and the motion of the structure influences the response of the soil is an example of soil-structure interaction. The structure imposes stresses and forces to the ground, and this will give additional force and deformation to the bridge as a consequence. This process continues until the structure and the soil reach their equilibriums or fail (in the case of excessive loading and deformations of the system). However, in general, structural analysis simplifies soil behavior, while geotechnical analysis simplifies structural behavior.

Lateral earth pressure is mainly influenced by the soil's properties and responses. Modelling the soil is an important aspect in analysis of integral bridges. This is because the performances of the integral abutment bridges are known to be affected by the interaction between the backfill soil and the abutment, as shown in Figure 8; this involves the relative displacement and soil stress-strain behavior due to the lateral earth pressure. Therefore, a reasonable soil constitutive model needs to be used to represent the soil properties in an analysis. Soil constitutive models are drastic idealizations of soil characteristics and a requirement for practical applications.

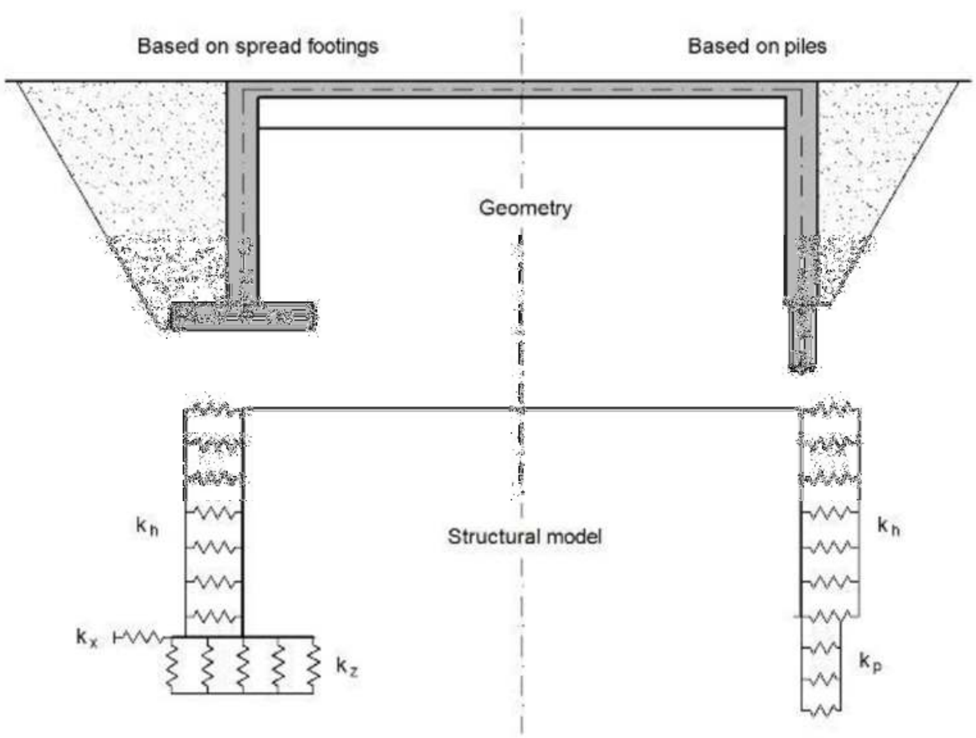

Fig 8: Soil spring idealization of the integral bridge.

Moreover, considering the soil-structure interaction effect increases the effective damping ratio of the system. The smooth idealization of the design spectrum suggests smaller seismic response with the increased natural periods and effective damping ratio, due to soil-structure interaction. With this assumption, it was traditionally considered that soil-structure interaction can conveniently be neglected for conservative design. In addition, neglecting soil-structure interaction significantly reduces complexity in the analysis of structures, which has tempted designers to neglect the effect of soil-structure interaction in the analysis.

Since integral abutment analysis is a typical soil-structure interaction problem, a very realistic and reliable modelling approach has to be adopted. The approach employed to model the soil-structure interaction should be able to provide reliable and accurate analysis results.

The search for a physically close and mathematically simple model to represent the soil media in the soil–structure interaction problem has produced two classic approaches, namely the Winklerian and the Continuum approaches. The earliest mathematical idealization of the foundation medium is due to Winkler, who assumed a linear load versus settlement relation (Chandra et al., 1985). The model is thus referred to as the Winkler method; it can be seen in Figure 9. Winkler represented the case of a finite soil layer resting on basement rock by a family of linear springs resting on a rigid base, as shown in the figure above; a Winkler model requires only one parameter, the elastic spring constant. A number of researchers have modified the original model in an effort to make it more realistic. To do this, an additional parameter is needed, and these modified models are usually referred to as two-parameter elastic models.

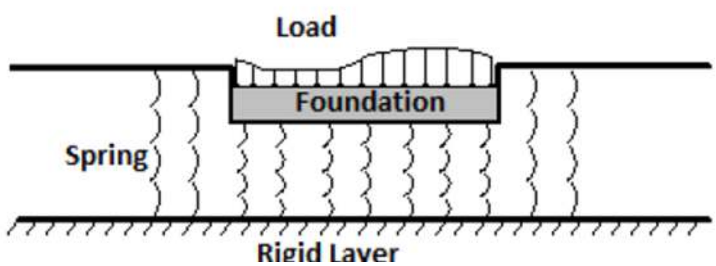

Fig 9: Winkler spring approach.

1.13 Provisions in IRC codes in seismic analysis

The geography of India is extremely diverse, with landscape ranging from snow-capped mountain ranges to deserts, plains, hills and plateaus. India comprises most of the Indian subcontinent situated on the Indian Plate, the northerly portion of the Indo-Australian Plate. It is the seventh-largest country in the world, with a total area of 3,287,263 square kilometers (1,269,219 sq mi). India measures 3,214 km (1,997 mi) from north to south and 2,933 km (1,822 mi) from east to west. It has a land frontier of 15,200 km (9,445 mi) and a coastline of 7,516.6 km (4,671 mi). So, all the parts in India are not equally vulnerable to seismic.

So, on the basis of the levels of intensities sustained during past earthquakes, understanding gained from the geology, the seismo-tectonics and the seismic activity in the country, India has been divided into four Zones (Zone-II, III, IV and V) (Figure 10) by Bureau of Indian Standards (BIS). As the divisions of zones are prepared chronologically ascending forms, hence, zone – V will be the most critical zone in regards of earthquake intensity and calamity.

IRC also released several publications for adaptation earthquake forces in bridges.

1. In the year 1958, seismic provisions were introduced for the first time, for bridge design in IRC: 6, wherein the country was divided into 4 regions based on the damage likely to occur.
2. In the year 1981 IRC-6 came up with a different map with five seismic zones. Also, for computation of seismic force, horizontal seismic coefficient, importance factor and a coefficient to account for different soil and foundation system were introduced in
3. In 2003 IRC: 6 came up with a new seismic map of India showing four seismic zones along with zone factor. For computation of seismic force, a force-based approach was adopted using spectral acceleration (included for three different types of soil), importance factor, dead load and part live load and a single response reduction factor for all bridge components. Also, mandatory provisions were included to prevent dislodgment of superstructure and ductile detailing of piers to minimize the damage, especially in seismic zones IV and V. Also, to mitigate earthquake forces, special seismic devices such as base isolation bearings, STUs, etc. were recommended.
4. Subsequently, the Interim Seismic provisions, mentioned above, were replaced with new seismic force clause in 2008, which essentially adopted a force-based design approach and addressing the issues like- consideration of simultaneous action of seismic forces acting in three different directions, near field effects, dynamic earth pressure and hydrodynamic forces during earthquake.
5. Till the year 2011, the bridges were being designed based on working stress approach. Meanwhile there had been rapid developments in state-of-the-art in the area of seismic resistant design of bridges, like capacity design approach, which have been incorporated in many international standards.
6. In the year 2018 separate IRC code has been published IRC: SP: 114-2018 for seismic forced calculation of bridges.

Major scope and the application of IRC: SP: 114- 2018 are: -

- The guidelines are applicable for bridges with design life up to 100 years and shall be designed for design basis earthquake (DBE) only. Bridges having design life more than 100 years are not covered under this guideline.

- The methodology of estimation of seismic forces given in these guidelines can be adopted for seismic evaluation of existing bridges and retrofitting of existing structures.
- Bridges having complex geometry and situated at locations requiring special investigations and detailed studies have also been covered under these guidelines.
- Guidelines for ductile detailing, seismic isolation devices, hydro dynamic effect, method of assessment of liquefaction assessment of soil is also included in these guidelines.
- The earthquake resistant design due to ground motion effects has been included in these guidelines. The ground surface rupture, tsunami, landslides and near-field effects of earthquake hazards are not included in these guidelines.
- Relaxation given for culverts and minor bridges upto span 10m in all seismic zone and simply supported span with total length not exceeding 60m need not to be designed for seismic effects and dynamic earth pressures on abutments during earthquakes shall not be considered in Zones II and III.

General principles for design according to this code are –

- The bridge should be designed for DBE/MCE according to the design philosophy specified in the guidelines, using limit state design procedure employing force-based method of seismic design and response reduction factors. The force-based design should meet the design philosophy and the principles of capacity design should be followed to protect the structure from collapse.
- Seismic forces and displacements in site specific data shall not be less than response spectra in this code.
- The scour to be considered during seismic design shall be based on average of yearly maximum design floods. The maximum of 0.9 times the maximum design scour depth and average of consecutive 7 years' data should be used in design.
- The earthquake accelerations should be applied to full mass in case of submerged structures and not on buoyant mass.
- The seismic force on live load should be considered on reduced live load in transverse direction only. No seismic of live load in longitudinal direction will be applied.
- The earthquake accelerations on embedded portion of bridge foundation should be considered in design.

- *For bridges in curve*, transverse movement of superstructure translates into longitudinal movement at a joint, which could lead to unseating of deck. So, proper bearing arrangement to be installed.
- *For skewed bridge,* the centre of mass usually does not coincide with centre of stiffness, which causes rotation of superstructure and large displacements at supports. Also, bridges with large skew angle could rotate and unseat the superstructure under seismic action.

The Design Philosophy of this code is

- Under Design Basis Earthquake (DBE), a moderate earthquake, which may occur more frequently in the life of a structure; the bridge should be able to withstand earthquake with minor structural damage.
- Under Maximum Considered Earthquake (MCE), a large earthquake, which may occur once in the life of a structure; the bridge may be subjected to significant structural damage but not collapse. The damage should be readily accessible for inspection and repair.
- The bridges with design life of up to 100 years may be designed for DBE only. The bridges with design life of more than 100 years may be designed both for DBE and MCE.

Preferred structural system and configurations are listed below –

As per type of Superstructure:

- ***Integral bridges are preferred in high seismic zone. Because it helps to avoid unseating of superstructure from support. It also improves seismic response due to its high redundancy.***
- Continuous bridges.
- Superstructure with low seismic mass is always most acceptable for bridges in high seismic zones.
- Bridges with mild curvature and small skew.

As per type of Substructure:

- Multiple columns bent instead of wall type piers as it has large difference in stiffness in two orthogonal directions.
- Adjacent piers are with near height (variation of stiffness <25%) otherwise shorter column will be affected with shear brittle failure due to stiffness irregularities.
- Piers with such shapes where plastic hinge forms above the top of the foundation as

inspection can be done during earthquake.

- PCC and masonry piers are not recommendable in seismic zone of IV and V.
- Bridges are without pier shaft is also not desired.
- Flair in Piers at top and bottom is also to be avoided.
- RCC / PSC piers are design as under reinforced and adequately detailed to avoid premature failure due to shear and bond. Plastic hinge region to be provided with close spaced transverse stirrups to confine the compressed concrete within the core region and to prevent the buckling of longitudinal reinforcement.

Special investigation and detailed seismic studies shall be required for following type of bridges

- For bridges with individual span length more than 150 m and/or pier height is more than 30 m in zone IV and V, extradosed, cable stayed and suspension bridges and Arch bridges having more than 50 m span Site-specific response spectrum of the bridge including geometrical nonlinearity, P-delta effect and soil structure interaction is needed. Dynamic analysis may be done to ascertain the energy dissipation characteristics of ductile members.
- For continuous bridge of length between expansion joint larger than 600 m spatial variation of ground motion shall be considered.
- Bridge site close to a fault (< 10 km) detail geological / seismological study is required to calculate the fault movement.
- In zone IV and V, if the soil condition is poor, consisting of marine clay or loose sand with little or no fines (e.g., where the soil up to 30 m depth has average SPT N value equal to or less than 20) site specific spectrum shall be obtained.
- For loose sand or poorly graded sands with little or no fines, liquefiable soil, liquefaction analysis is required.
- For horizontally curved Bridge having ≤ 100 m radius and bridge with high skew- ≥ 30-degree 3D modeling with substructure and foundation to be done. Torsional motions of the bridge about a vertical axis under seismic action shall be considered. Possibility of unseating of bridge deck about acute corner to be checked and ruled out. In single span bridges Bearings shall be designed to resist torsional effects.

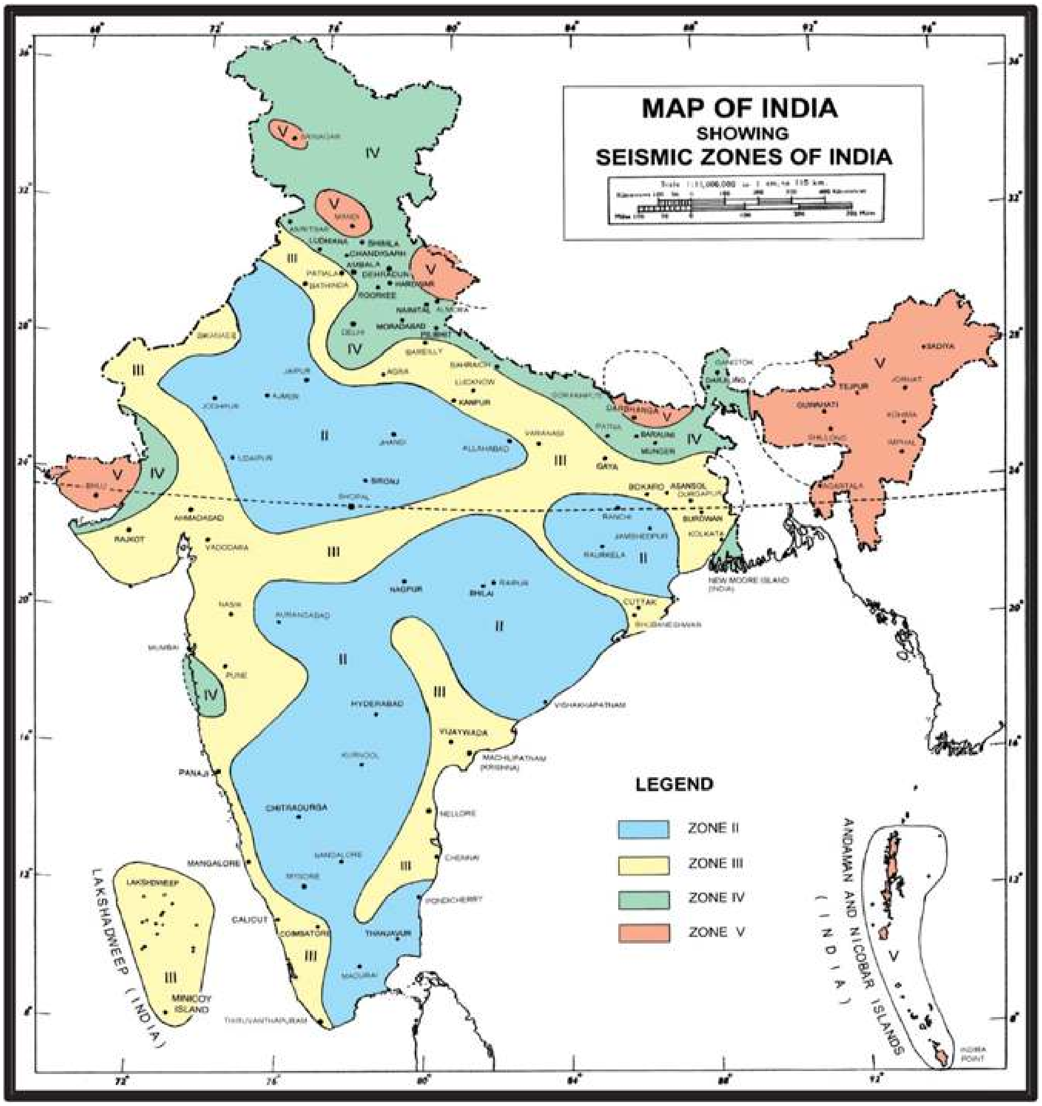

Fig 10. Seismic zone map of India(Ref:- IRC:SP:114-2018).

Chapter – 2: Literature review

To have a detailed study on skewed and curved integral abutment bridges, three different subjects should be considered: curved bridges, skewed bridges and integral bridges. This is attributed to the fact that the problems associated with a curved jointed bridge or a straight integral bridge may be inherited by a curved integral bridge. Therefore, the literature review is carried out in four steps. First, the available IRC code (IRC: SP:115-2018) has been reviewed. Then, the previous research works on straight integral bridges are reviewed. These studies mainly include the investigations on response of integral bridge and examination of the available field monitoring data related to integral bridges. After that, research works on curved bridges are reviewed. These studies mainly include the investigations on response due to curvature and examination of the available field monitoring data related to integral bridges. Then, research papers on skewed bridges are studied. This part presents a summary of research on the behavior of skewed bridges, their design requirements and the approaches to evaluate their strength. And then, studies on integral abutment bridges are briefly summarised.

2.1 IRC: SP: 115-2018 (Guidelines for design of integral bridges)

In this code, the general guidelines for design and construction of integral bridge are provided. In order to use the simplified design methods as per this guideline, the structure should satisfy the following requirements:

- The characteristic thermal movement at the end of the deck does not exceed ±20 mm under normal case from the position at the time of restraints during construction.
- Shall have a skew angle less than or equal to 30 degrees.
- Shall be a straight bridge or a curved bridge with radius of curvature exceeding 100 m.
- Shall not have connected splayed wing wall.

Integral bridges perform better under seismic induced forces due to the fixity and restraints at the abutments. The multiple degree of redundancy in the structure helps to minimize the risk of failure of the structure. Therefore, in high seismic zone, integral bridges are preferred.

Type of superstructure usually used:

- Cast in-situ RC solid slab/voided slab deck
- Precast prestressed/RCC girder with in-situ composite deck.
- Steel girder with in-situ concrete composite deck

Type of substructure usually used:

- Cast bank seat abutments
- Framed abutments with fixed base (i.e. with open foundation or foundation with multi-row piles).
- Framed Abutments with hinged base (i.e. foundation with single row piles)
- Embedded wall abutments
- Flexible support abutments.

Geometry of the structure

A complex geometry creates problems in the design of integral bridges. Irregular structures, sharply skewed structures and structures with sharp curvatures (that is, where there are abrupt or unusual changes in the mass, stiffness or geometry along the span) should be avoided.

For an integral structure, it is preferable that the spans are symmetrically placed and the adjacent pier stiffness does not differ substantially (say by more than 25 percent). Though curvature and skew can be accommodated, it would be desirable to avoid large skew (say, more than 30º) and high degree of curvature (Say R<100 m).

Integral Bridges, for all their simplicity of construction, are complicated structural systems. To thoroughly analysed a given structure, the designer must not only design for primary loads (dead, live, wind, etc.) but must also accurately account for secondary loads (creep, shrinkage, settlement, temperature effects, etc.). To additionally complicate the analysis, the response of a structure to a given set of external forces is very dependent on the geometry, materials, configuration, soil-structure interaction, and construction details of the individual system.

Loads and load combinations

The forces due to applied loads must also be accommodated, and these are the dead loads, the vehicular live loads plus impact, the horizontal force due to wind, vehicle braking and centrifugal force and seismic force as applicable. Besides that, other loads to be considered are

- The effects of temperature difference, shrinkage, and creep should also be considered in accordance with relevant clauses of IRC:6 and IRC:112.
- Bridges which are curved, or not symmetric, experience thermal movements relative to a zero-movement point. The position of the zero-movement point can be determined from a stiffness analysis employing horizontal stiffness at supports and abutments.
- Earth pressure.

2.2 Literature review on straight integral bridges

Several researchers have been researched on skewed integral bridges. To carry out this study some literatures have been studied and summarized below-

Faraji et al. (2001) have studied non-linear analysis of integral bridges by finite element method. They described the implementation of a full 3D finite-element model of an integral bridge system incorporating the nonlinear soil response. They represented the results from a small parametric study on a sample bridge where the soil compaction levels in the cohesion less soils behind the wall and adjacent to the piles were varied. These results show that the level of compaction in the granular backfill strongly dominates the overall soil reaction, and that this reaction greatly impacts the overall structural response of the bridge system.

The effect of modelling assumptions and simplifications on the seismic analyses results of integral bridges (IBs) is investigated by Dicleli and Erhan(2010). They have prepared five structural models of integral bridges in decreasing levels of complexity starting from a nonlinear structural model including the true behaviour of the foundation and backfill soil. They gradually simplified the model to a level where the effect of backfill and foundation soil is totally excluded. With these models nonlinear time history analyses are performed using a set of ground motions with various intensities representing small, medium and large intensity earthquakes. The analyses results are then used to assess the effect of modelling complexity level on the seismic behaviour of integral bridges. In this paper the nonlinear soil-bridge interaction is found to have considerable effects on the seismic behaviour of integral bridges under medium and large intensity earthquakes.

Bardakis and Fardis(2011) are performed nonlinear dynamic and elastic analysis for seismic deformation demands in concrete bridges having deck integral with the piers. Eight bridge configurations with prestressed box girder deck with bonded tendons, having three or five spans and piers of various cross-sections and about equal or very different heights are studied. Two versions of each bridge are considered: one of conventional, force-based design and another having much less over-strength in the piers and developing less inelastic action in the deck. Seven spectrum-compatible motions with peak ground acceleration (PGA) of 0.25, 0.35 and 0.45 g on rock are applied in the longitudinal or transverse direction with 5% damping. They have found modal response spectrum analysis gives on average good and safe-sided predictions of inelastic deformation demands at the deck and the piers of regular bridges, especially under longitudinal earthquake. They found that the result underestimates inelastic deformation demands in bridges having piers of very different height, even when design measures are taken to harmonize stiffness across the piers. The stronger the ground motion, the larger are on average the elastic predictions of deformations relative to those from nonlinear dynamic analysis.

Zordan et al. (2011) have performed the nonlinear parametric and pushover analysis on a 400m long integral bridge built in the Province of Verona-Italy. They implemented a 2D simplified finite element model and performed non linear analysis of the bridge with different soil properties behind the back-walls and around the piles. They also performed temperature pushover analysis to assess the failure pattern of the bridge caused by a temperature change. They also studied the effect of abutment stiffness. In the study they have found following points:-

- The bending moment at the structure's ends is high where concentration of stiffness at the abutments is high.
- The axial forces in the girders and piles are greatly influenced by positive and negative temperature variations.
- Different soil conditions greatly affect the bending moment near abutments and axial force along the girder.
- The internal force distribution, at abutments and in the end parts of the structure, is greatly influenced by significant temperature variations.
- Slender and flexible piers respond more uniformly and predictably to temperature variations.
- For this flexible abutments or pin connections between girder and abutments should be considered as the preferred solution.
- Negative temperature variations need to be considered with the utmost attention

Shreedhar and Hosur (2011) have studied the soil-pile interaction for integral abutment bridges. In the study they have prepared a 3D finite element model using commercially available structural analysis software STAAD Pro 2006 as linear elements while the soil reaction adjacent to the piles and behind the abutment walls are modeled as nonlinear support springs. In the study they have found following points:-

- The combined effect of temperature variation and different type of soil may act as more significant case for integral abutment bridges.
- Analysis shown linear response due to selected temperature change ranges.
- The properties of soil adjacent to the abutment and pile are major factors governing the response of integral abutment bridges to thermal loads.
- For a particular temperature change, looser soil behind abutments results in larger displacement and subsequently larger maximum bending moment. As the soil gets denser,

displacement decreases thereby reducing the value of the maximum bending moment.

- Pile top displacement is reduced as there is increase in relative compaction of the soil behind the abutment.

Fartaria (2012) has studied the soil-structure interaction in integral abutment bridges. In the study, she has proposed a stabilization solution through the use of soil-cement columns, executed with the jet-grouting technique, and a resilient EPS layer. For this she has performed a numerical analysis by a 2D finite element model in PLAXIS 2D which was allowed both the identification of the critical phenomena, as well as the quantification of the lateral earth pressure reduction achieved by the use of an elastic inclusion. She found that the use of a compressible inclusion (resilient EPS) leads to a high reduce in lateral earth pressures. The resilient EPS have been the material of choice to use as a compressible inclusion. Its low stiffness and elastic behavior make it a suitable material to perform as a joint. Although the current and proposed stabilization solutions will increase the construction cost of integral abutment bridges, they should be cost effective and make up that cost by reducing future maintenance and repair costs.

Mohtashami and Shooshtari (2012) have performed the seismic assessment of integral reinforced concrete bridges using adaptive multi-modal pushover analysis soil-pile interaction. This paper they have used a new adaptive pushover procedure to account for the effect of higher modes in order to estimate the seismic response of bridges more accurate. They have performed the parametric study for regular and irregular configuration of integral bridges which includes 9 bridge configurations having 4 spans with the varying length of spans and height of piers. In each step of the nonlinear analysis, the updated displacement capacity of the structure, obtained by the proposed method and compared with the updated displacement demand. They conducted the procedure step by step until the performance point of the structure was found. Numerical results indicate that in most cases studied in this research, the proposed method is capable of predicting displacements as well as internal forces with desirable accuracy. The response of the proposed procedure is in good agreement with the response of inelastic time-history analysis and is believed to be quite satisfactory in comparison with the current pushover procedures.

Bloodworth et al. (2012) describes a method in which the results of laboratory cyclic stress-path testing within a numerical model have been used to determine the thermal cycling effects. For this samples of sand and stiff clay were tested in the tri-axial apparatus under stress paths that are typical behind an integral abutment. Both the soils showed distinct behavior, in which stiff clay attains relative little built up of lateral stress with cycles, whereas in case of sand stresses were found to be increasing continuously, exceeding at-rest pressure and finally reaching to full passive pressures. Also, a numerical model was developed in order to determine the implications of these findings on soil-abutment interaction and to estimate the lateral stresses acting on the abutment as a whole. It was found that the numerical model gave good agreement with published centrifuge and field data, indicating that the stress profile specified in some current standards is conservative.

Masrilayanti (2013) studied the effect of earthquakes on integral bridges built on several different soil types, through computer simulation of an integral abutment bridge. The study was made based on Eurocode 8 recommendations, which provides data for different types of soil to be used for earthquake analysis. A symmetrical medium length integral bridge obtained from an existing structure is used for the analysis. Artificial EC8 spectrum compatible time histories (with a 0.35 g peak ground acceleration) ware applied to the structure for a range of soil stiffnesses. She studied both static and dynamic relative displacement. Synthetic time histories for 5 different types of soil were created using Mathcad. The synthetic acceleration time history was validated using Seismospect (by Seismosoft). The time histories were then used to carry our full integration time history analyses in ANSYS (engineering simulation software) to simulate the dynamic response of the bridge. She found that those relative displacements play an important role in overall structural response of the integral bridge, compared to the pure dynamic response. The results also confirm that lower stiffness soils suffer a more detrimental effect of the earthquake compared to a soil of higher stiffness.

Erhan et al. (2014) compared the seismic performance of integral and conventional bridges considering the differences at their abutments. Three conventional jointed bridges were designed from the existing integral bridges having one, two and three spans and then the structural models of the integral and conventional bridges were created taking into account the nonlinear structural and dynamic soil–bridge interaction effects. The nonlinear time of the bridge models are conducted using a set of ground motions. In the analyses, the ground motions are scaled to peak ground accelerations ranging between 0.2 and 0.8 g to assess the seismic performance of integral bridges in relation to that of conventional bridges at various ground motion intensities and associated performance levels. The analyses results revealed that integral bridges have superior seismic performance compared to conventional bridges in terms of smaller inelastic rotations at piers and piles, deck displacements, pile axial forces, abutment rotations, pier column drifts and bearing displacements for the bridges under consideration.

Far et al. (2015) have studied the combined effect of the thermal and seismic loads for integral bridges. They have prepared a 2D finite element combined pile-soil-structure interactive model considering nonlinear behavior for near field soil behind the abutments. The soil around the piles modeled by nonlinear springs based on p-y curves. The uniform temperature changes occurring at the time of some significant earthquakes around the world are gathered and applied simultaneously with the corresponding earthquake time history ground motions. They compared the results of these analyses to prescribed AASHTO LRFD load combinations and observed that pile forces and abutment stresses are affected by this new load combination. This effect is more severe for contraction mode which is caused by negative uniform temperature changes.

Wood (2015) has reviewed the earthquake performance of bridges with integral abutments and the available design methods of determining the stiffness, passive pressure resistance and damping for different types of integral abutments. He has found that bridges with integral abutments have performed well in strong ground shaking in both NZ and California because the passive resistance and damping at the abutments limits the longitudinal response leading to less damage than for bridges with seat type abutments. He also found that the friction slabs used with integral abutments to limit gapping increased damping.

Peric et al. (2015) assembled an entire finite element model of a three span integral bridge subjected to combined gravity and thermal loads. The substructure of bridge included the two sets of concrete piers, two abutments, and fourteen HP steel piles (seven at each abutment), having its strong axis of bending oriented parallel to the longitudinal direction of the bridge. Various load cases representing different amount of temperature increase in presence of different type of the backfill soil were simulated. The results of the analysis indicated that the effects of the amount of compaction on backfill and magnitude of thermal loading have opposite behavior on substructure elements as compared to that of superstructure.

Panikkavettil and Raveendran (2017) has studied the seismic performance of different span integral bridges by carrying out static analysis, modal analysis and response spectrum analysis in ANSYS2015 and the effectiveness of bridge with respect to increase in span is also studied. They used a simplified finite-element model of the East Logansport Bridge at West and performed static analysis modal analysis and response spectrum analysis. The have prepared a design chart which helps to extend the design of the bridge to any span length and the validity of the chart is also tested by ANSYS.

Kozak et al. (2018) studied the seismic performance of integral abutment highway bridges in Illinois. They modeled two Integral bridges subjected to design-level earthquakes; one using pre stressed concrete girders, and the other using steel plate girders as the main superstructure elements. Two analysis types were conducted for each 3-span Integral Abutment Bridge in both directions i.e. transverse and longitudinal directions:

i. Static pushover analysis
ii. Dynamic analysis

The design-level shaking was provided by 20 ground motions, for a 1000-year return period hazard-level, developed for the southern Illinois city of Cairo. They found that, yielding of piles at the abutments is a main limit state, which occurs in both the steel and concrete span Integral Abutment Bridges for all dynamic analysis. Damage to the pier columns and retainers are more extreme in the concrete span Integral Abutment Bridge as compared to steel span Integral Abutment Bridge. The final location of consistent damage is in the retainers of the both bridge when subjected to transverse excitation. For this they recommended two solutions
a) To increase abutment pile size.
b) Smaller retainer anchor bolt for Steel Integral abutment bridges.
c) Increase the size of pier column.

Mahjoubi and Maleki (2018) presented a comprehensive non-linear finite element (FE) model of integral abutment bridges to facilitate the analysis of such bridges using commercial software, especially under seismic loading. The presented model is capable of capturing non-linearity in both the structure and soil, in addition to considering far-field soil response. The model is simple enough to be used for practical purposes. On the other hand, many aspects of seismic behaviour of integral abutment bridges are unclear, due to complicated soil–structure interaction. Using the presented model, a parametric study is performed to identify the effects of bridge length, abutment type and soil type on seismic behaviour of integral abutment bridges. Non-linear direct integration finite element analyses are performed on the integral abutment bridge models. The results of the parametric analyses demonstrate the importance of non-linear modelling of soil and pile in capturing a realistic seismic response of integral abutment bridges.

Choi et al. (2019) studied the nonlinear behavior and seismic capacity of the fully integral bridge to assess the appropriate stiffness of the end-restraining abutment to sufficiently resist design earthquake loadings through a rigorous parametric study. They used OpenSees software to perform the finite element method of nonlinear static pushover analysis to obtain the force-deflection curves of the models. They found that the fully integral bridge prototype in the study meets the seismic performance criteria specified by Caltrans. The nonlinear static pushover analysis results reveal that, due to the end-restraining effect of the abutment, the lateral displacement of the fully integral bridge is reduced, and the intermediate piers sustain less lateral force and displacement. Then, the sectional member forces are well controlled in the intermediate piers by a proper application of the end restraining abutments.

Ibrahim et al. (2019) studied the theoretical dynamic characteristics of integral bridge abutment with bored piles by the FE modal analysis using ABAQUS software. A single-span integral bridge located in Pahang, Malaysia has been selected as the case study. The modal characteristics of the same design of bridge with simply supported bridge yield different values of modal frequency, which are higher. From the FE modelling result, they found that the integral bridge with the bored piles type of foundation possess lower natural frequencies compared to the simply supported bridge of similar type of foundation.

Malekjafarian et al. (2020) introduced a novel pier scour indicator, which uses the ratio between mode shape amplitudes identified at two points on an integral bridge structure to monitor the progression of scour erosion. The mode shape ratio (MSR) is investigated as an additional parameter to complement the use of changes in natural frequency as a scour indicator. The approach is demonstrated using numerical modelling and the MSR is extracted from acceleration signals arising in the structure due to modelled ambient and vehicle-induced vibrations. The MSR shows higher sensitivity to scour erosion than the more commonly researched natural frequency. Furthermore, the variation in MSR under temperature fluctuations is inversely related to that of frequency, in that it increases with increasing temperature whereas frequency decreases with increasing temperature. This inverse relationship potentially enables the separation of the scour effect from the temperature influence on the dynamics of the system.

Naji et al. (2020) studied the parameters of integral abutment bridges considering soil structure interaction to recognize the most effective parameters of analysis IABs. They found that no significant effect of stresses to the abutment occurred due to vertical load. The behaviour of abutment may be greatly affected by thermal load and soil pressure. Again the bridge length significantly influences girder axial force, pile lateral force, pile moment and pile head displacement. The influence of bridge length on girder bending moment is relatively weak. Again they found that the backfill material behind the IABs has a significant effect on the performance of IABs. Using a compressible material behind the abutments would enhance the in-service performance of IABs. Finally, behaviour of abutment may be greatly affected by thermal load and soil pressure. Thermal expansion coefficient significantly influences girder axial force, girder bending moment, and pile head/abutment displacement.

Joshi and Patel (2020) reviewed the analysis and design of integral bridges for different type of span using finite element method. They found that the structural system offered by bridges made integral between superstructure and abutments can provide structural efficiencies as well as enables the elimination of bearings and expansion joints. In some circumstances the durability of the bridge is improved and maintenance costs reduced. These bridges are single span or multispan bridges. The abutments, being cast integral with the superstructure so as to avoid the expansion joints and movement bearings that otherwise require regular maintenance. The piers for integral abutment bridges may be constructed either integrally with or independently .The benefits of Integral Bridges are principally the elimination of expansion joints and bearings, leading to simpler structures that are easier and less expensive to maintain.

Shilpa et al. (2021) studied the seismic analysis of this integral bridge and their behaviour for major earthquakes and to determine its suitability and safety in seismic regions especially for Bangalore region. They have modeled a 150-m long viaduct portion of the flyover consists of five continuous spans of reinforced concrete (RC) voided deck slab having individual spans of 22.5m + 30m + 40m + 30m + 22.5 m with 2.5m overhang on either side with the help of SAP 2000. The total deck width is 9.9m having 9-m wide clear carriageway and 450-mm wide crash barriers (at base level) on either side. They analyzed the model as per loads given in IRC:6-2000 and Seismic analysis performed for Seismic Zone-II. The found that the DL+temp is a critical combination compared to others and that shrinkage induces compressive stresses and creep induces tensile stresses. Again, they found that the stiffness in vertical direction is smaller compared to horizontal direction and deflection in deck and pier joint is more in horizontal direction than vertical direction.

2.3 Literature review on skewed integral bridges

Several researchers have been researched on skewed integral bridges. To carry out this study some literatures have been studied and summarized below-

Greimann et al. (1983) surveyed the highway departments of all 50 states to obtain information on the design and performance of skewed bridges with integral abutments and tried to establish tentative recommendations on maximum safe lengths and skew angles for concrete and steel skewed bridges with integral abutments. They found that the survey responses indicated that 26 states use integral-type abutments on skewed bridges. Most states design integral abutments on skewed bridges based on empirical experience and no theoretical analysis was introduced in design. For integral abutments on skewed bridges, 15 states orient their piles with the web of the piles perpendicular to the centerline of the abutment so that bending will be primarily about the strong axis. Thus, thermally induced biaxial bending stresses will be introduced into the piles. But the survey responses show that most states ignored the thermally induced bending stress due to transverse thermal movement. The major reasons given for using pile orientation are as follows:

- The restraint provided by the integral abutment reduced the magnitude of the thermal move-ment. Orienting the pile with the strong axis parallel to the centerline of the bearings gives more rigidity tor earthquake loads.
- Thermal expansion is actually very small, and the backfill material around the abutment and the piling seems to yield sufficiently so that no distress is apparent. The piling was oriented to resist the force of earth pressure from the abutment backfill rather than the force of thermal expansion.
- Temperature forces would act along the center- line of the roadway, not parallel to the pile web, and active soil pressure would act against the strong axis of the pile. Temperature effects are somewhat compensated for by predrilling for driven piles and filling the voids with pea gravel or sand.

Kaviani et al. (2011) have conducted parametric response-sensitivity analyses to identify the key parameters that control the seismic behavior of skewed bridges. They described simplified modeling technique, which takes bridge-abutment interaction into account, along with the analysis results. Three short bridges located in California were used as subjects. These bridges have different arrangements of number of spans and number of columns per bent. They used three bridges located in California as seeds for our parametric study. These bridges mainly differ in their global torsional resistance. Multiple analytical bridge models were generated from each of three seed bridges by varying the original bridges' geometrical properties, which included abutment skew angle, span arrangement, and column height. In addition, they studied effects of ground motion characteristic on the seismic response of skewed bridges by introducing three types of ground motions into our response-sensitivity analyses. These were soil-site, rock-site, and pulse-like ground motions. They observed that less gap size between the deck and the backwall results in more effective impact forces that mobilize the backfill soil and leads to higher deck rotation; especially when the bridge is subjected to pulse-like ground motions. Column drift ratio is significantly sensitive to the column height, abutment skew angle, and number of columns in each bent. Abutment unseating increases by increasing skew angle, particularly for bridges with tall columns.

Akib et al. (2011) investigated the effects of different parameters on the structural behavior of a skewed integral bridge. Flow velocities affected the scour depths at the piles, and subsequently, affected the structural behavior of the bridge's substructure. Different loading locations had varying influences on the scour depth, as well as the structural behavior of the integral bridge. Laboratory tests on a scaled down hydraulic model were undertaken to simulate the structural behavior of the scoured integral bridge. The scale of the model was chosen to simulate the actual bridge dimensions, material properties, and loading. Three different velocities were accounted for, based on the actual flow velocities of the river under the bridge, and were scaled according to the model size. Two different truck locations were adopted. The main data acquired from the experiment were the displacements and strains at specific locations on the deck slab and piles. Specifically, the results of this investigation can be utilized to identify and provide accurate design parameters for the design of a skewed integral bridge. Furthermore, results can subsequently be applied in the design of a better scour protection system. They found that the flow velocities affected scouring over time and scour depth had a direct effect on the structural behavior, such as strains and displacements of the bridge substructure. Strain increased as the scour depth increased for almost all of the strain gauges (STs) and scour depth intervals. Flow velocity had a direct effect on the structural behavior of the integral bridge, due to increase of flow force. Strains and displacement on the slab and piles varied, due to location and the flow velocities. Finally, vehicle location had a different influence on the structural behavior.

Wright et al. (2015) conducted the field monitoring of two bridges located in northern Illinois, include a 30-degree skew four-span continuous integral abutment bridges and a 42.5-degree skew single-span integral abutment bridges, both of which have steel superstructures and incorporate pile top relief for HP14 piles. Construction of the bridges began in the spring of 2013, and instrumentation data has been collected since May 2014. Field instrumentation includes pile, girder, and concrete embedment strain gages, as well as displacement transducers and tiltmeters. They collected the field data for one year with the bridges experiencing a summer- to-winter-to-summer temperature cycle and compared made with 3-D finite element models of each instrumented integral abutment bridges. After the first year of data collection, a general understanding of overall bridge behavior emerged. Specifically, at the UPRR Bridge, low pile strain readings at the gage locations indicated that the pile capacity was adequate and piles are not expected to yield under typical service conditions. The tiltmeter readings shown small differential rotations between the bridge girders and abutments, which was a sign that the connections are mostly behaving rigidly as commonly assumed. Furthermore, the superstructure movement as measured by the crackmeter displacement at the pier-girder interface was less than what was expected from free expansion, which was a trend that agrees with what has been observed in the companion parametric study. Other response parameters such as girder, deck, and approach slab strains investigated and compared with finite element models as well. Overall, the data collected follows expected trends.

Popoola and Waslu (2015) studied the long-term performance of skewed integral bridges. They modelled four types of integral bridges using the Midas Civil software and analysed the results in terms of displacement, deflection, moments and torsion. Creep and shrinkage, traffic and temperature loadings ware taken into account. Skew angles were increased and sizes of abutments varied. They found that the skewed bridge had the majority of displacement on the short term of 40 days and a considerable percentage of displacement takes place on the long term up to 25%. The abutment angle affects the displacement of the skewed bridges where the abutment with the acute angle had horizontal displacement of 27.2 mm while the abutment with the obtuse angle had less horizontal displacement of 13.2 mm on the long term when the abutment size was 0.5 m. So the deflection of skewed bridges ware more deflection than the square bridges. Increasing the skew angle, the deflection increases. On the long term, it was discovered that about 5% of the deflection takes place. Comparing the result of the skew to the square bridge, the 8.6° bridge had 73% displacement more than the prestress bridge and 44.5% more than the non-prestress bridge. The 13° skew bridge has higher deflection comparing with the non-prestress and prestress respectively. There were hogging moments because of the traffic loading that was considered during the modelling of the bridges. Normally, without a skew angle, the deck will act like it was simply supported with positive moments (sagging). The greatest sagging moment occurred in the non-prestress 13° skew bridge deck with a magnitude of 6499.77 kN-m on the long term while the hogging moment has -1157.1 kN-m on the obtuse angle side of abutment. When the skew angle was increased, hogging moments increased as well.

Mallick and Raychowdhury (2015) performed the seismic analysis of highway skewed bridges with nonlinear soil–pile interaction. They investigated the effect of skew angle on seismic response of a bridge-foundation system including nonlinear soil–pile interaction subjected to bi-directional ground motions. They observed that the rotational demand of the bridge deck is greatly affected by the skewness, indicating an increased vulnerability of skewed bridges due to rotational movement of the deck leading to deck unseating. They also observed that the shear and moment demand of the piers increase significantly with increasing skew angle, as much as 54% and 37%, respectively. The maximum bending moment of the pile shaft is also found to increase upto 55%, indicating higher design requirements for the foundation components of the skew bridges compared to a similar normal bridge.

Muhammad et al. (2015) researched to assess the effect of concrete creep on long-term performance of skewed Integral Abutment Bridge. They conducted time-history transient analysis using Finite Element method for 75-year period in LUSAS on bridge total length

(60m,90m,150m), skew angles (0º,10º,20º,30º,40º), backfill soil stiffness (dense sand, loose sand). They studied the behaviour of the bridge measured by girder and abutment displacement, moment and shears. Three-dimensional nonlinear thick beam element with CEP-FIP 1990 creep material properties was used to model bridge girders and for other structural members were modelled using three-dimensional thick beam element. They found that bridge span and skew angle have predominant influence on behaviour of skewed integral abutment Bridges than backfill soil stiffness. They should therefore be given great attention when designing skewed IABs. Loose sandy backfill soil results in higher values of deformations in comparison to dense sandy soils. Most of the deformations are regular from zero to 20° skew, variations in deformation mostly occur after 20° skew.

Haymanmyintmaung and kyawlinnhtat (2017) studied the integral bridge with various span length of 40m, 50m, 60m and 70m non-skew and skews angles of 15°, 30°, 45° and 60°. They designed, and modelled the bridges in SAP2000 software and investigated skew angle, span length and stress reduction methods. The geometric dimensions of the Integral Bridge and the loading used were in compliance with AASHTO standard specifications. Static analysis and dynamic nonlinear time history analysis were performed to assess the seismic performance of integral bridge. They checked shears and bending stresses, axial force and deflection by allowable stress method. Extreme stresses that exceed allowable limit were reduced by using six different stress reduction methods. They found that in skew angle bridge, cross frame member stress increase greatly as skewed bridge tend to rotate during a seismic event, which can cause excessive transverse movement and also found that MSE+HLAC method was the best stress reduction method for all non-skew and skew angle bridge. According to analysis result, integral bridge maximum skew angle can be extend up to 60° and span length up to 60 m can be extended using stress reduction method under extreme seismic loading.

Haymanmyintmaung and Kyawlinnhtat (2017) studied the performance of skewed integral bridge under dynamic loading. They designed by modeling the integral and simply supported bridge with total length of 200 m non-skew and skews in SAP2000 software and analyzed the results in terms of moments, shears and stresses under static and dynamic loading and checked with allowable stress method. Extreme stresses that exceed allowable limit in the superstructure and substructure of integral bridges were reduced by using six different stress reduction methods. They compared the analysis results with that of simply support bridge result to analyze skew effect and integral effect. The propose of this study was to analyze behaviour of integral, skew angle, and to reduce extreme stress of integral bridge under dynamic loading. The parameters investigated in this analytical study were bridge support type, skew angle and stress reduction methods. The geometric dimensions of the integral bridge and the loading used were in compliance with AASHTO standard specifications. Static analysis and dynamic analysis of moving load analysis and nonlinear time history analysis were performed to assess the seismic performance of integral bridge. The FEA results indicate that under static live load, integral bridge girder shear force was minimum in skew 60°, but maximum moment that was opposite to simply supported bridge girder. Under dynamic moving load analysis, integral abutment bored pile moment and shear force were maximum in skew 60°, but maximum in skew 15° for integral pier bored pile. Under dynamic seismic time history analysis, maximum bending and shear stress occurred at integral abutment foundation and integral pier foundation in non-skew (0°) and minimum skew angle 15° bridge, among six stress reduction method, MSE wall and HLAC method can reduce stress within allowable limit for non-skewed and skewed bridge over 90% and 23% respectively. According to analysis result, MSE wall is the best stress reduction method in skewed and non-skewed integral bridge.

Parachos and Amde (2020) investigated the relation between depth of predrilled holes and reduction in pile bending stresses. They developed three-dimensional nonlinear finite element model for this parametric study. The model includes the bridge superstructure and substructure as well as the soil behind and below the integral abutments. The model consists of shell elements for the deck slab, girders, and piles; solid elements for the abutments; and nonlinear spring elements for the soil. The study was conducted using the ABAQUS general-purpose nonlinear finite element analysis program. The results of this study point out to a number of observations related to the behavior of skewed integral abutment bridges. This includes the following: (1) increased bridge length and skew angle induces higher bending stresses in the piles supporting the integral abutments, (2) increased number of spans and use of predrilled holes around the piles of integral abutments results in reduced pile bending stresses, and (3) use of predrilled holes increases the vertical pile load carrying capacity. Again, the analysis suggest that the use of predrilled holes filled with loose sand around the piles of skewed integral abutment bridges is an effective method to reduce bending stresses in the piles and increase their vertical load carrying capacity. The depth of predrilled holes is 2.75 m measured from the bottom of the integral abutment.

Zhao et al. (2021) studied the seismic response of skewed integral abutment bridges under near-fault ground motions, including soil–structure interaction. They analyzed the nonlinear dynamic response of a skewed integral abutment bridge (SIAB) under near-fault pulse and far-fault non-pulse type ground motions considering the soil–structure interaction, along with parametric studies on bridge skew angle and compactness of abutment backfill. They selected three sets of near-fault pulse ground motion records for the analyses on the bridge site conditions, and three corresponding far-field non-pulse artificial records fitted by their acceleration response spectra. They found that the near-fault pulse type ground motions generally more destructive than the non-pulse motions on the nonlinear dynamic response of SIABs, but the presence of abutment backfill will mitigate the pulse effects to some extent. Coupling of the longitudinal and transverse displacements as well as rotation of the bridge deck would increase with the skew angle, and so do the internal forces of steel H piles. The influence of the skew angle would be most obvious when the abutment backfill is densely compacted.

2.4 Literature review on curved integral bridges

Several researchers have been researched on skewed integral bridges. To carry out this study some literatures have been studied and summarized below-

Kalayci et al. (2009) studied the effect of curvature and Backfill material on response of curved integral bridges using results 3D finite element models (FEMs) having the structural characteristics of bridge in Vermont. The bridge models are differed by varying the degree of curvature (0º to 50º) of the superstructure and backfill material properties (loose sand and dense sand), thus forming total 10 models. The influence of curvature and backfill material on integral abutment bridges thermal response was determined through the comparison of longitudinal and vertical deformations of the bridge deck, abutment displacements and rotations, weak and strong axis pile moments, and backfill pressures behind abutments under the effect of thermal loading. It was found that temperature increase cause decrease in vertical displacement. The maximum vertical displacement in all cases increases with curvature. Backfill material had minimal effect on vertical deflection of bridge deck. Changes in abutment displacements and rotations with increased bridge curvature were dominated by self - weight; curvature of the bridge did not affect abutment displacements and rotations induced by thermal loading as strongly.

Kalayci et al. (2012) conducted the parametric study on the thermal response of curved integral abutment bridges. The modeled abutment–pile and abutment–superstructure connections in curved integral abutment bridges using finite element (FE) modeling. A detailed, three-dimensional, FE model of a curved integral abutment bridge located in Stockbridge, Vermont, USA was used as a prototype to evaluate the behavior of curved integral abutment bridges under thermal loading. A parametric study was carried out to investigate the effects of bridge curvature and abutment backfill soil type. Moreover, additional FE models were created to investigate the effect of degree of lateral restraint provided by the U-shaped wingwalls integral with abutments and the interior pier. The results, including abutment displacements, moments at abutment piles, earth pressures on abutments and wingwall, and bridge superstructure forces, are reported and compared with the responses of conventional curved bridges containing expansion joints.

Kataria and Jangid (2013) carried out the seismic response of horizontally curved concrete box girder bridge isolated by the elastomeric rubber bearings. They studied the effect of curved geometry on the performance of isolation system under excitation with four different ground motions of different frequency spectrum characteristic, and each ground motion contains three-directions. The selected bridge consists of three span continuous concrete box girder superstructure supported on piers and abutments. In the modeling of the bridge, the deck is modeled as a single spine beam, made up of small straight beam elements with 6 DOF at each node. The coupled equations of motion for isolated system are derived and solved in the incremental form using Newmark's step-by-step method. In addition, comparison is made between the response of curved isolated bridge with straight isolated bridge (having the same cross section and material property) in order to study the effect of curved geometry on the response of the isolation system. They found that the elastomeric rubber bearings system was effective for controlling the seismic response of curved bridge and effect of curved geometry makes no significant difference in peak response of elastomeric rubber bearings system.

Phares (2014) conducted field monitoring of curved girder bridges with integral abutments. The primary objective of this work was to monitor and evaluate the behavior of six in-service, horizontally curved, steel-girder bridges with integral and semi- integral abutments. In addition, the influence and behavior of fixed and expansion piers were considered. The bridges were monitored over a period of approximately 18 months for the long-term health assessment. During this period, the strains, temperatures, and displacements were recorded under a variety of loading conditions. In addition, the short-term behavior was investigated by conducting a series of live load tests. He found following observations

- They found no measurable difference between the horizontally curved bridges and straight bridges regard to bridge behavior under thermal effects. They recorded internal strains in the composite girders as a result of thermally induced restrained expansion and contraction and, of the recorded strains, axial strain showed the largest ranges; the bridges expanded and contracted with seasons and showed more expansion and contraction near expansion piers than fixed piers.
- The equivalent cantilever method of steel pile analysis fell short of accurately predicting

the relationship between weak axis bending strain in the piles and the pile head displacement; the measured internal stress in the abutment piles due to expansion and contraction of the bridge were generally below 50 percent of yield stress; and the soil pressures on the abutment backwalls were generally below approximate passive soil pressures.

- With regards to the live loading, moment distribution factors were heavily influenced by the amount of curvature and the V-Load equation provided an approximation of lateral bottom flange bending with minimal bridge skews.
- Since AASHTO requires a three-dimensional analytical model of the bridge and support conditions to calculate lateral bending stresses for the final design of all curved bridges, this model should also be used to calculate thermal stresses for final design of the curved bridge. However, with a 10 degree skew and 0.06 radians arc span length to radius ratio (i.e., meeting the geometrical requirements to ignore curvature for strong axis bending), the curved and skewed integral abutment bridges can be designed as a straight bridge if a stress tolerance of 10% is acceptable.
- An expansion pier does reduce the thermal stresses in the girders of the straight bridge but does not appear to absolutely reduce the stresses in the girders of the curved and skewed bridge even though the overall restraint is reduced.

Deng et al. (2015) carried out field monitoring program and a numerical based analysis in order to determine the behavior of curved and skewed bridge with integral abutments. The behavioral study of a newly constructed three span one lane bridge was done through field monitoring system under changing ambient conditions and was tested by a dump truck across the bridge walkway. Also, parametric study was conducted to predict the behavior of such bridges under design load conditions. It was concluded that with the changes in curvature and skew there were significant changes in the stresses. Also, it was found that thermal stress and its magnitude relative to the maximum stress can reach up to 3 ksi and 15% of the maximum stress, respectively.

Jayeshbhai and Sanghvi (2020) reviewed the behavior of curved integral bridges. They found following observations: -

- The value of thermal stress and its magnitude relative to the maximum stress can reach up to 3 ksi and 15% of the maximum stress, respectively.
- There is considerable effect on stress due to change in curvature and skew of the integral bridges.
- The effect of backfill compaction and thermal changes are inverse in case of substructure

elements as compared to that of super structural elements.

- The increase in the curvature resulted in an increase in the maximum vertical deflection of bridge.
- Yielding of piles at the abutments is a main limit state, which occurs in both the steel and concrete.
- The temperature increase resulted in decrease in the vertical displacement.

Civjan et al. (2021) carried out field monitoring of four no's curved steel girder integral abutment bridges in Vermont, Usa. Spans of these bridges range from 86 ft. to 140 ft., which are typical of many bridge replacement projects. Arc span divided by girder radius, ranges from 0.067 to 0.358 radians and girder stiffness varies across the spans. Each has distinct characteristics that are notable, from curvature of 23.87 degrees with superelevation and grade change at the Danby Bridge, 30 degree skew and curvature of 2.75 degrees at the Bradford Bridge, and two-span structure with curvature of 11.25 degrees and twelve years in service of the Stockbridge Bridge. Site visits were made to all four structures and the current condition was documented, including any observed cracking. Any distress noted was not attributable to the bridge curvature, but was common to the detailing used. The condition of all four of these bridges is very good, based on author site visits and bridge inspection reports and they are performing as expected.

2.5 Critical discussion

From the above literature review following salient points may be concluded:

Several analytical as well as experimental results are available on seismic effect of non-skewed and non-curved integral bridges but similar research reports on skewed and curved integral bridges are really scanty. Only a few researchers have worked on Indian Environment and IRC codal provisions. Seismic recommendations as mentioned in IRC-SP-114: 2018 may be applied on skewed and curved integral bridges to study the earthquake response of such bridges. Whether the recommendations of national and international codes in terms of suggesting working formulas for determining a pseudo- static seismic force or by proposing a single response spectrum widely over a vast area are enough to capture the actual structural response of skewed, curved or skewed-curved integral bridge under seismic excitations may be an interesting study. The effect of soil structure interactions on the gross seismic response of skewed, curved and skewed- curved bridges have not been studied though the effect of such interaction is an extremely important contributing factor. Also, the different effects of shallow or deep foundations on the seismic behavior of the abovementioned class of bridges have not received due attention.

The effect of continuous loading-unloading-reloading of the bridge structure under repetitive bidirectional ground shaking reduces the fatigue life of these structures and this aspect has not been addressed in the published papers. A study of the seismic response of bridge with time – dependent degradation of concrete property may help to determine the residual life span of the bridge and may also help in formulating the repair and retrofitting strategies under the ever-changing seismic vulnerability in different parts of Indian sub-continent. This aspect has not been focused at by the researchers which demands due attention. Seismic response of integral bridges with long piers may also be an area for researchers' attention.

2.6 Scope of the present study

From the discussion presented as critical discussion, it is found that substantial study, both analytical and experimental, are to be worked out to understand the structural behavior of curved and skewed integral bridges individually against seismic excitation. Very little research has been carried out on skewed and curved bridges in Indian conditions for different arrangements of substructure and foundation. It has also been seen that the recommendations of national and international codes are also not enough to capture the variations of structural response of skewed, curved integral bridges particularly in locations of high seismic risk.

Keeping in mind the abovementioned lacunae, the scope of the present work has been outlined as given below-

- Developing the structural model of a straight integral bridge by using Midas Civil 2022(v1.2) and comparing the response spectrum outputs of the model with those calculated through IRC: SP: 114-2018 recommendations.
- Having realised the importance of computing seismic response parameters by actual time history analysis to the data available for the earthquake at India-Burma border on 06.08.1988 recorded at station Dipu by IITR, will be applied on curved and skewed integral bridges. The only work on seismic analysis of integral bridges was reported by Shilpa et al.(2021) considering low risk zone II.

Variations of practical parameters like skew angle, radius of curvature, superstructure and foundation arrangements will be considered to arrive at conclusions of engineering significance which will be important inputs for seismic design of integral bridges.

Chapter – 3: Modeling and analysis

There are several methodologies used in research such as simulation, case study and experiment. In this research, the methodology used is to conduct a case study and carry out a series of simulation analyses using 3D finite element model. A procedure is generated to obtain geometric and graphical variations of seismic parameters with respect to different load transfer arrangement variations which are then used to study the seismic behavior of a bridge.

In this study, the behaviour of integral bridges subject to bi-axial earthquake ground motion are analyzed separately. Theoretical evaluation of anticipated seismic performance mostly requires a structural simulation which is based on the concept of structural likeness. Simulation of bridge, soil and earthquakes in this research is carried out using a computer software programs, namely Midas Civil. For the simulation of earthquake and soil conditions, reference to IRC: SP:114-2018 is made. The main purpose of this research is to obtain knowledge and insight into the structural response to earthquakes of an integral bridge. Both longitudinal and transverse ground shaking will be modeled.

3.1 Flowchart of methodology

In this research finite element methods used to learn the seismic behaviour of an integral bridge with simplicity and idealization. Beginning with the collection of earthquake data, these are then applied to the structure boundaries, also incorporating different time histories are used in combination in the same model. Hence the responses of the structure are analyzed. The flowchart in Figure 11 describes these steps. Data collection was conducted by observing integral bridges which are suitable for this research. Northeast region is a high-risk earthquake region in India. So, data of northeast India is used. The details of the bridge are presented in the following sub-chapter; some modifications have been made to comply with the limited scope of the research.

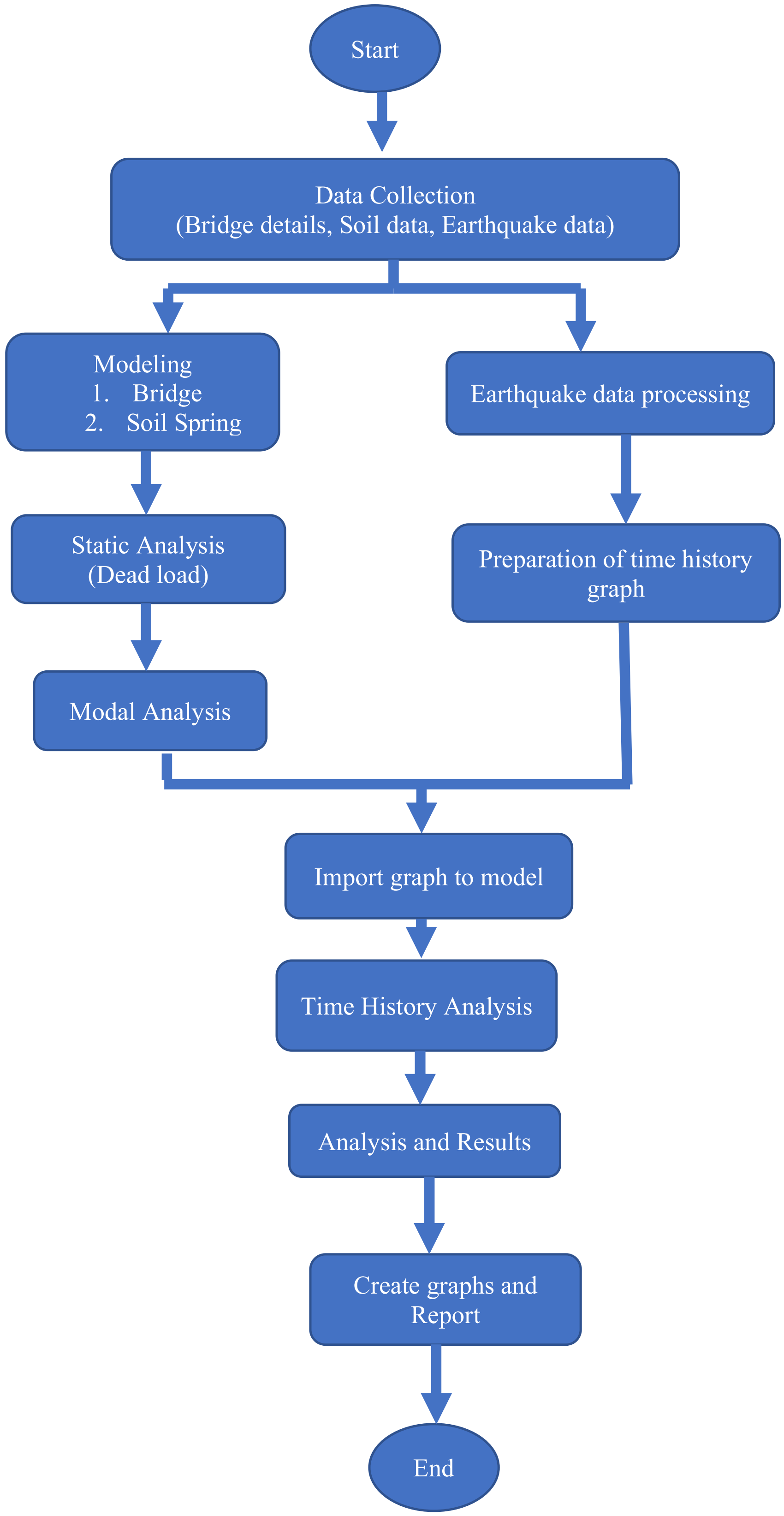

Fig 11. Flow chart of the study.

3.2 Finite element modeling

In this research finite element methods used to learn the seismic behaviour of integral bridge. finite element method is also popular tool for the solution of complicated structural engineering problems which is capable of accommodating many complexities in the solution. In this method, the actual continuum is replaced by an equivalent idealized structure composed of discrete elements, referred to as finite elements, connected together at a number of nodes. Hence, the finite element method may be seen to be very general in application and it is sometimes the only valid form of analysis for difficult deck problems. For the evaluation and assessment of existing bridges, and also for new design, FE modelling allows for a more rigorous analysis approach to be adopted that can often lead to significantly more accurate and economical results being obtained over some codified methods. In the past, structural design codes such as those from the British Standards Institution allowed for a departure from a 'codified' approach. Others, such as the newly introduced Eurocodes have been more prescriptive often mentioning that FE analysis should be carried out.

The finite element method has a number of advantages; they include the ability to -

- Model irregularly shaped bodies and composed of several different materials.
- Handle general load condition of unlimited numbers and kinds of boundary conditions.
- Handle nonlinear behavior existing with large deformation and non- linear materials.

3.3 Modelling the structure

For the case study, a two-span RCC integral slab bridge is used as the basis for a parametric study to determine the influence of variables encountered in integral bridges. 2x20 m span integral slab is adopted. The dimension details of the structure are shown in Figure 12, 13 and 14.

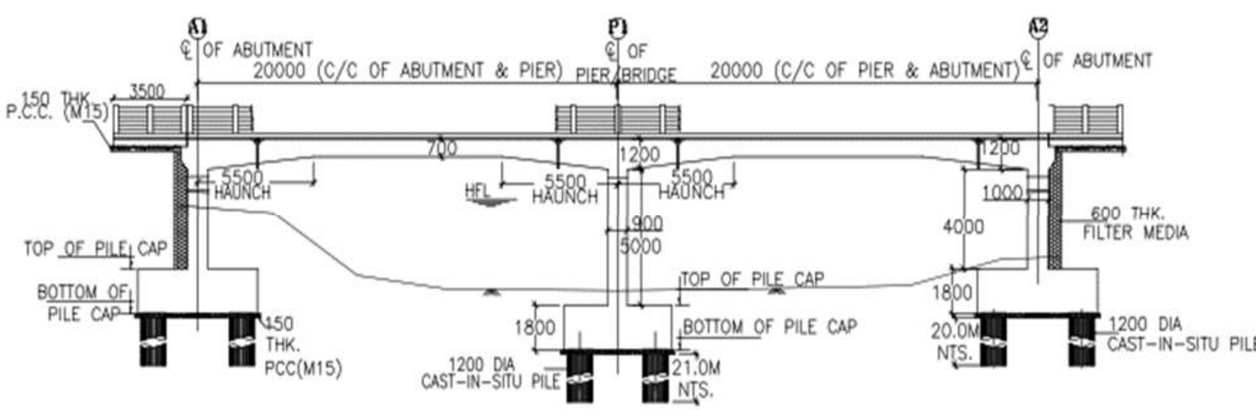

Fig 12. Elevation of the bridge.

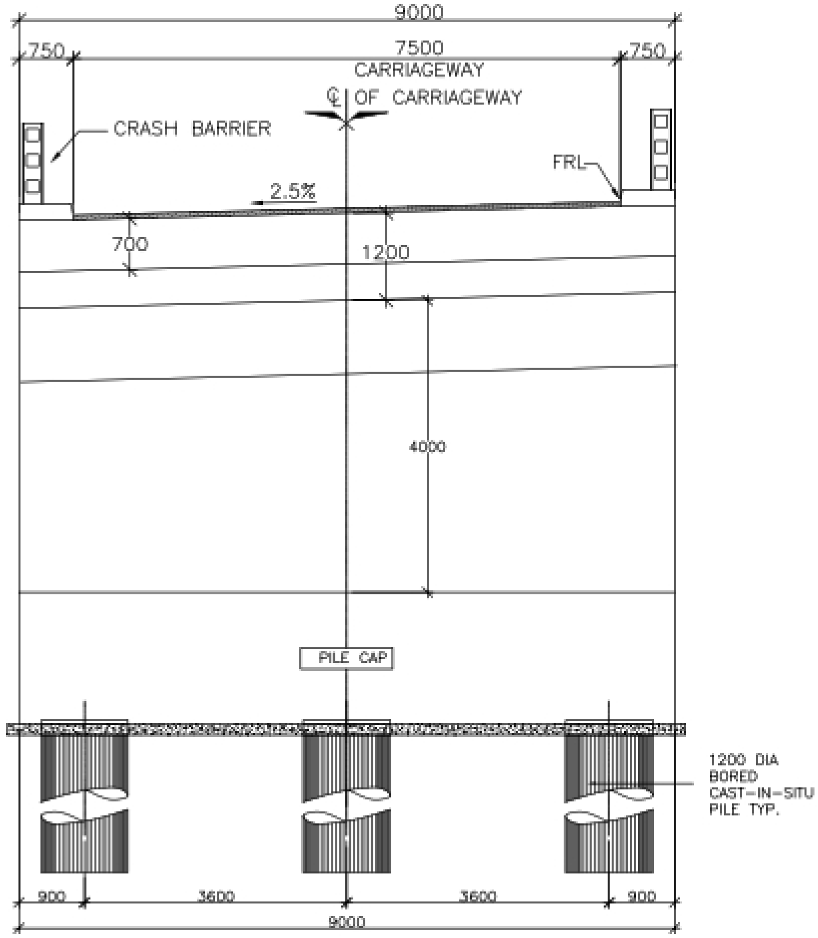

Fig 13. Cross section of the bridge.

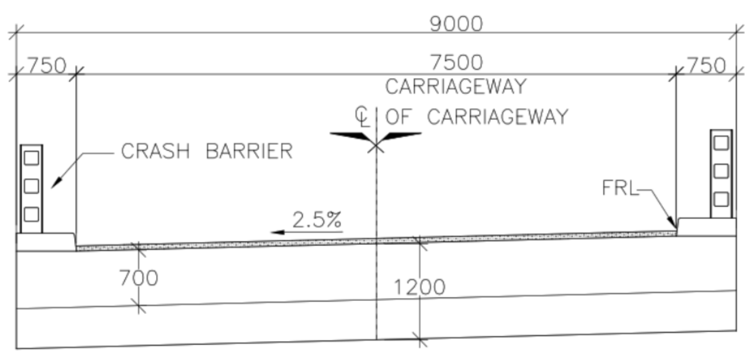

Fig 14. Cross section of the superstructure.

The bridge consists of two 20-metre spans which are supported by reinforced concrete piers and abutments. The piers and abutments are constructed on a pile cap which has a thickness of 1.8 meters. The size of the pier is 5 meter high and 0.9 m thickness. The size of the abutments are 4 meter high and 1 m in thickness. There are six nos concrete piles with 1.2 m diameter in pier and 8 nos pile of 1200 mm dia in abutment. Length of piles in abutment is 20m and pier is 21m. The concrete material density is 2500 kg/m^3. The slab superstructure is of thickness 0.7 m at middle and 1.2 m at support. The carriageway of the bridge is 7.5m and total width 9 m. A detailed 3D study of the bridge was chosen for a number of reasons. First, this would provide a simple approach capturing the 'in-plane' longitudinal response. Regarding behaviour relating to the bridge width, it was judged that bridge width and capacity would tend to provide adequate strength in most cross-deck loading scenarios. Torsion may be of concern, however; at locations where the bridge deck is supported by piers, the torsional stiffness would be larger and also be likely to possess adequate torsional capacity in most scenarios. Only in the deck spans could potential torsional displacements be larger, and the deck section used was judged to possess sufficient deformation and forced capacity to withstand this.

3.4 Element type and properties in Midas Civil

M35 material as per IRC: 112-2020 is used for the analysis purpose. Modulus of elasticity (E) as per the code is 32 GPa. Compressive strength (f_{ck}) 35 N/mm^2. The abutments and the piers are modeled with shell element and the superstructure is done by beam element and grillage model. The piles are also done with beam element.

Details of plate element

Three or four nodes placed in the same plane define a plate element. The element is capable of accounting for in-plane tension/compression, in-plane/out-of-plane shear and out-of-plane bending behaviors. The out-of-plane stiffness used in Midas Civil includes two types, DKT/DKQ (Discrete Kirchhoff element) and DKMT/DKMQ (Discrete Kirchhoff-Mindlin element). DKT and DKQ are developed on the basis of a thin plate theory, Kirchhoff Plate theory. Whereas, DKMT and DKMQ are developed on the basis of a thick plate theory, Mindlin-Reissner Plate theory, which exhibits superb performance for thick plates as well as thin plates by assuming appropriate shear strain fields to resolve the shear-locking problem.

The in-plane stiffness is formulated according to the Linear Strain Triangle theory for the triangular element, and isoparametric plane stress formulation with incompatible modes is used for the quadrilateral element. The thicknesses can be entered separately for the calculation of in-plane stiffness and out-of-plane stiffness. In general, the thickness specified for the in-plane stiffness is used for calculating self-weight and mass. When it is not specified, the thickness for the out-of-plane stiffness will be used. The ECS for plate elements is used when the program calculates the element stiffness matrices. Graphic displays for stress components are also depicted in the ECS in the post-processing mode. The element's translational d.o.f. exists in the ECS x, y, and z-directions, and rotational d.o.f. exists in the ECS x and y-axes. The ECS uses x, y and z-axes in the Cartesian coordinate system, following the right-hand rule. The directions of the ECS axes are defined as presented in Figure 15.

In the case of a quadrilateral (4-node) element, the thumb direction signifies the ECS z-axis. The rotational direction (N1>N2>N3>N4) following the right-hand rule determines the thumb direction. The ECS z-axis originates from the center of the element surface and is perpendicular to the element surface. The line connecting the mi point of N1 and N4 to the midpoint of N2 and N3 defines the direction of ECS x-axis. The perpendicular direction to the x-axis in the element plane now becomes the ECS y-axis by the right-hand rule. For a triangular (3-node) element, the line parallel to the direction from N1 to N2, originating from the center of the element becomes the ECS x-axis. The y and z-axes are identically defined as those for the quadrilateral element.

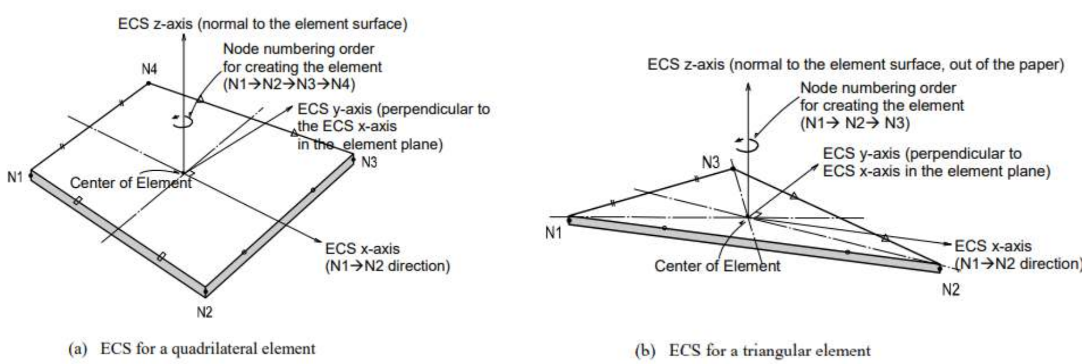

Fig 15. Direction of co-ordinate system.

The sign convention for plate element forces and stresses is defined relative to either the ECS or GCS. The following descriptions are based on the ECS.

- Output for element forces at connecting nodes.
- Output for element forces per unit length at connecting nodes and element centers.
- Output for element stresses at top and bottom surfaces at connecting nodes and element centers.

At a connecting node, multiplying each nodal displacement component by the corresponding stiffness component of the element produces the element forces. In order to calculate element forces per unit length at a connecting node or an element center, the stresses are separately calculated for in-plane and out-of-plane behaviors and integrated in the direction of the thickness. The element forces per unit length can be effectively applied to the design of concrete members. For stresses at the connecting nodes and element centers, the stresses calculated at the integration points (Gauss Points) are extrapolated. Output for element forces Figure 16 shows the sign convention for element forces. The arrows represent the positive (+) directions. Output for element forces per unit length Figure 17 shows the sign convention for element forces per unit length at connecting nodes and element centers. The arrows represent the positive (+) directions. Output for element stresses Figure 18 (a) shows the top and bottom surface locations where element stresses are produced at connecting nodes and element centers. Figure 18 (b) shows the sign convention for element stresses. Figure 19 shows a details of typical shell element used in Midas Civil.

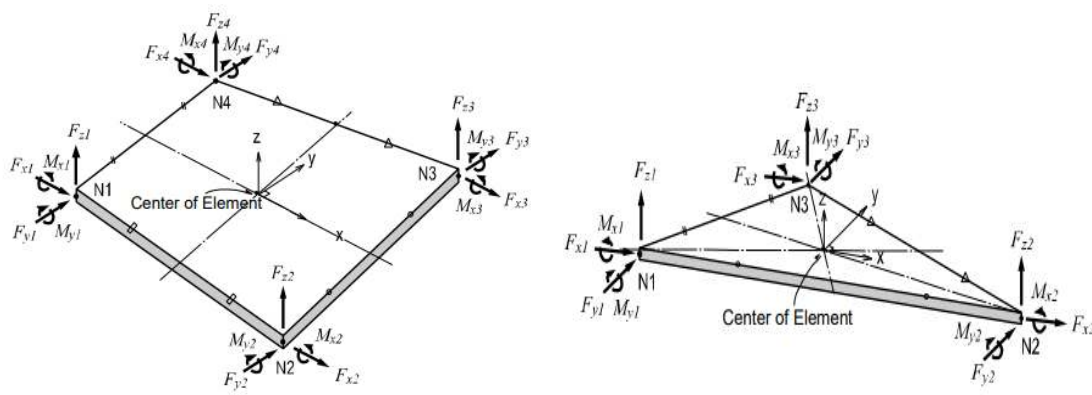

(a) Nodal forces for a quadrilateral element

(b) Nodal forces for a triangular element

Fig 16. Sign convention for nodal forces at each node of plate elements.

* Element forces are produced in the ECS and the arrows represent the positive (+) directions.

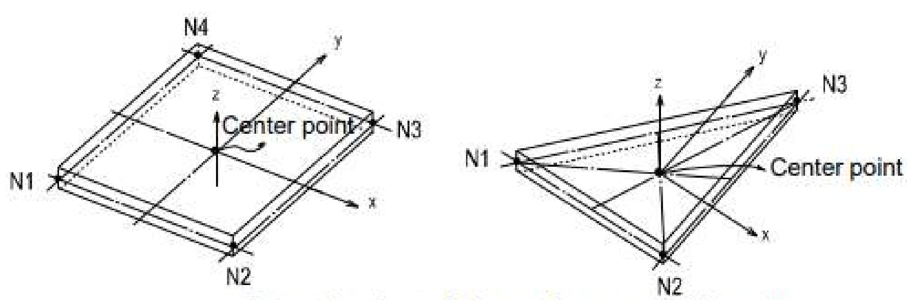

•: Out put locations of element forces per unit length

(a) Output locations of element forces

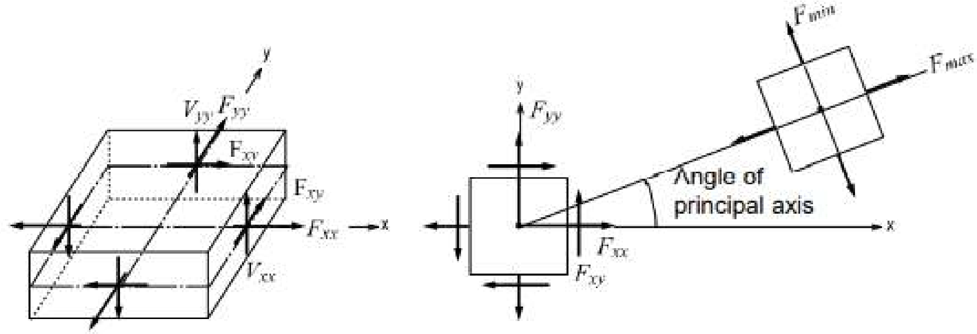

(b) Forces per unit length due to in-plane actions at the output locations

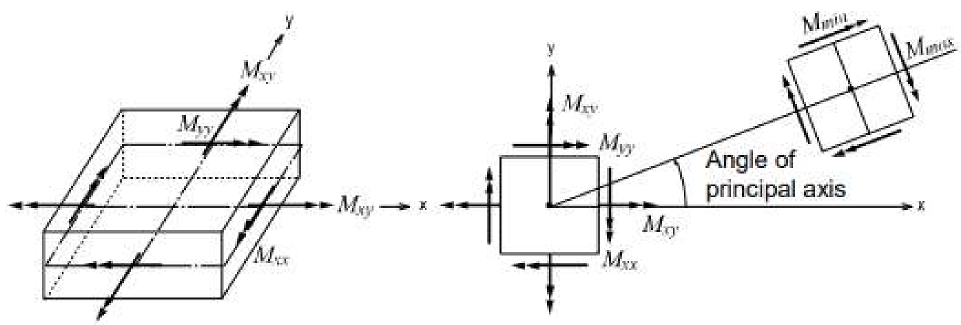

(c) Moments per unit length due to out-of-plane bending actions at the output locations

Fig 17. Output locations of plate element forces per unit length and the sign convention.

* Element forces are produced in the ECS and the arrows represent the positive (+) directions.

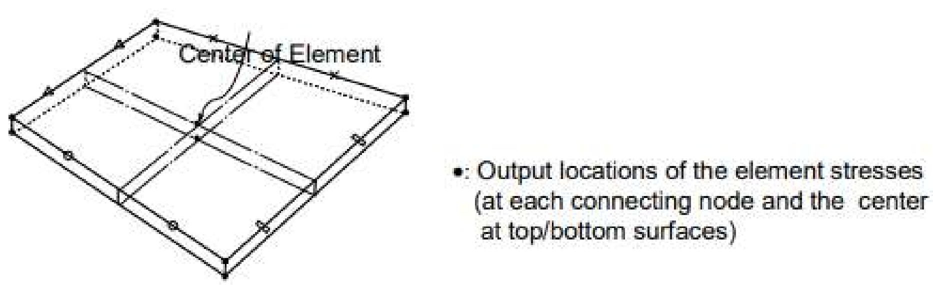

(a) Output locations of element stresses

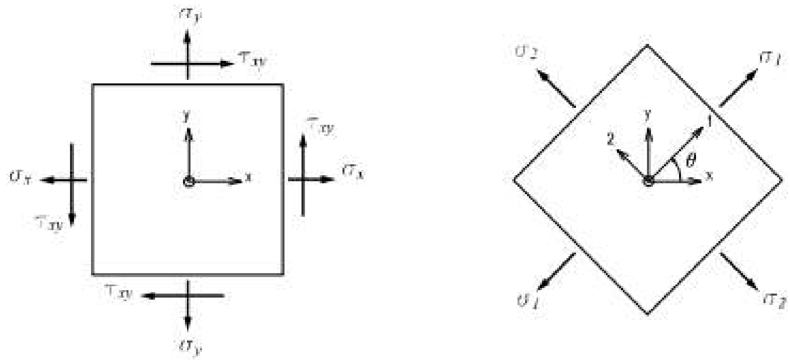

σ_x : Axial stress in the ECS x - direction

σ_x : Axial stress in the ECS y - direction

τ_{xy} : Shear stress in the ECS x - y plane

σ_1 : Maximum principal stress $= \dfrac{\sigma_x + \sigma_y}{2} + \sqrt{\left(\dfrac{\sigma_x - \sigma_y}{2}\right)^2 + \tau_{xy}^2}$

σ_2 : Minimum principal stress $= \dfrac{\sigma_x + \sigma_y}{2} - \sqrt{\left(\dfrac{\sigma_x - \sigma_y}{2}\right)^2 + \tau_{xy}^2}$

τ_{xy} : Maximum shear stress $= \sqrt{\left(\dfrac{\sigma_x - \sigma_y}{2}\right)^2 + \tau_{xy}^2}$

θ : Angle between the x - axis and the principal axis, 1

σ_{eff} : von - Mises Stress $= \sqrt{(\sigma_1^{\,2} - \sigma_1\sigma_2 + \sigma_2^{\,2})}$

(b) Sign convention for plate element stresses

Fig 18. Output locations of plate element stresses and the sign convention.

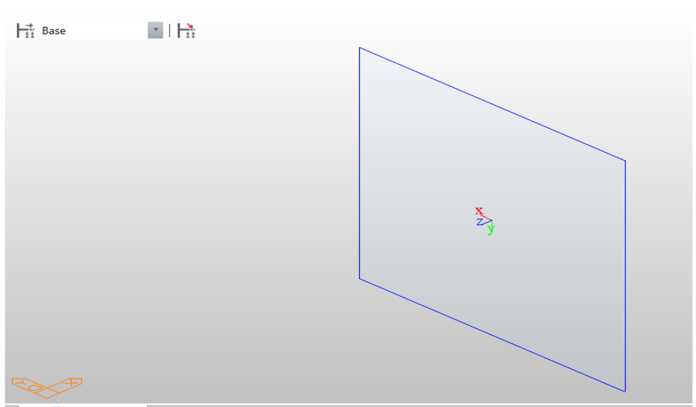

Fig 19. Details of a typical shell element used.

Details of beam element

Decks and piles are modeled as beam element. Its formulation is founded on the Timoshenko beam theory taking into account the stiffness effects of tension/compression, shear, bending and torsional deformations. In the section dialog box, only one section is defined for a prismatic beam element whereas, two sections corresponding to each end are required for a non-prismatic beam element. Midas Civil assumes linear variations for cross-sectional areas, effective shear areas and torsional stiffness along the length of a non-prismatic element. For moments of inertia about the major and minor axes, you may select a linear, parabolic or cubic variation. Each node retains three translational and three rotational d.o.f. irrespective of the ECS or GCS. The ECS for the element is identical to that for a truss element.

The sign convention for beam element forces is shown in Figure 20. The arrows represent the positive (+) directions. Element stresses follow the same sign convention. However, stresses due to bending moments are denoted by '+' for tension and '-' for compression.

Figure 21 and 22 shows the 3D view of straight integral model in Midas Civil while Figure 23 and 24 represents the 3D view of skew model and Figure 25 and 26 represents the curved model.

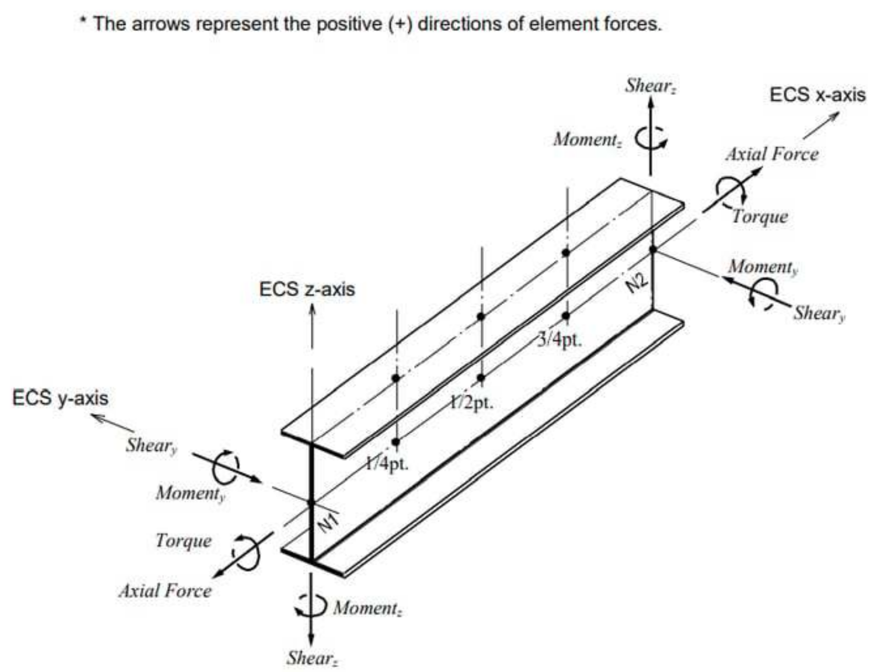

Fig 20. Details of a typical shell element used.

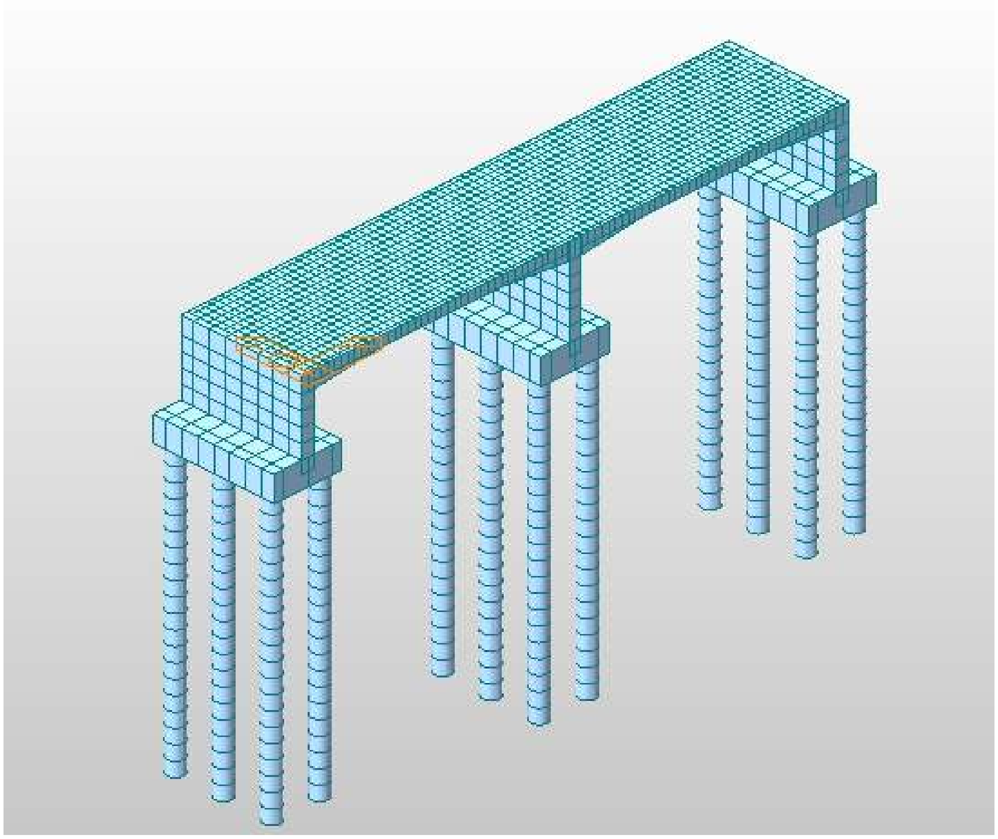

Fig 21. 3D view of straight integral bridge.

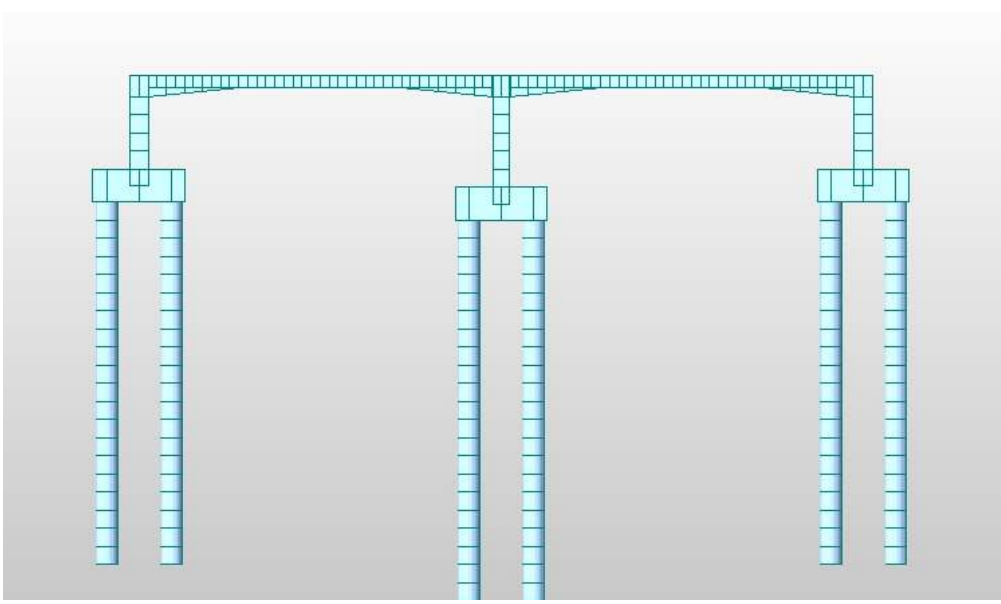

Fig 22. Elevation of straight integral bridge.

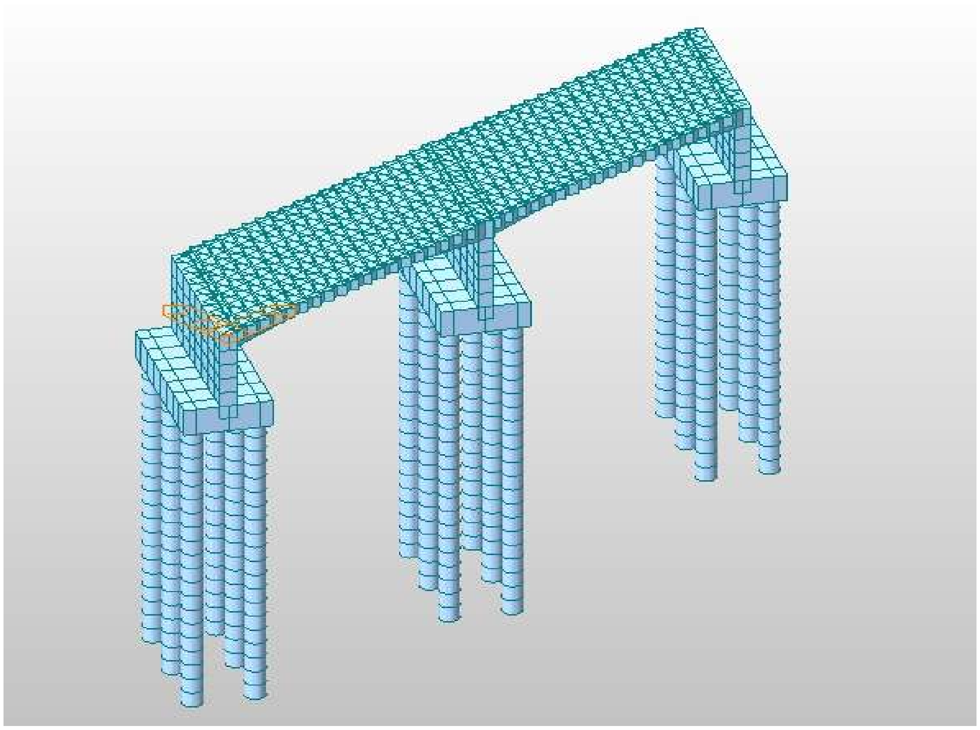

Fig 23. 3D view of skewed integral bridge.

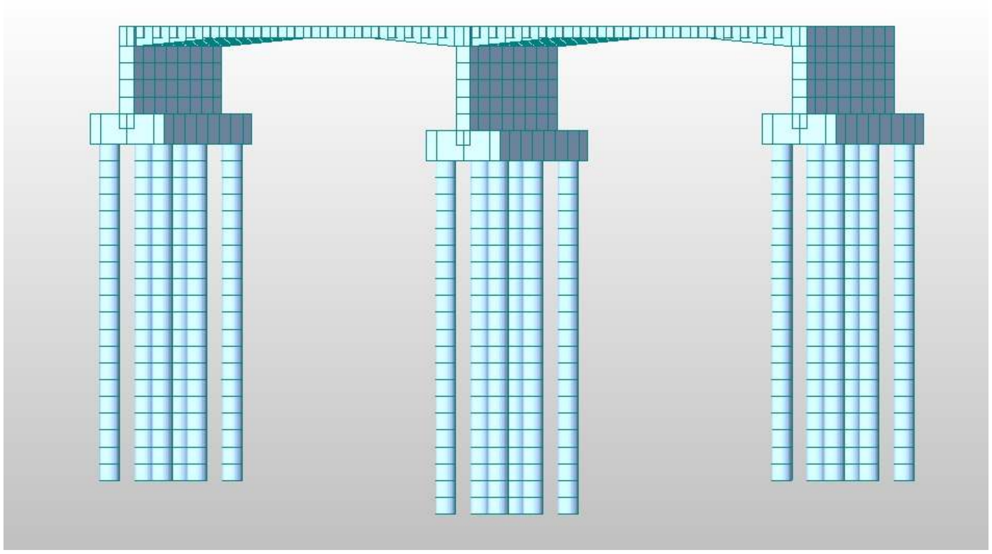

Fig 24. Elevation of skewed integral bridge.

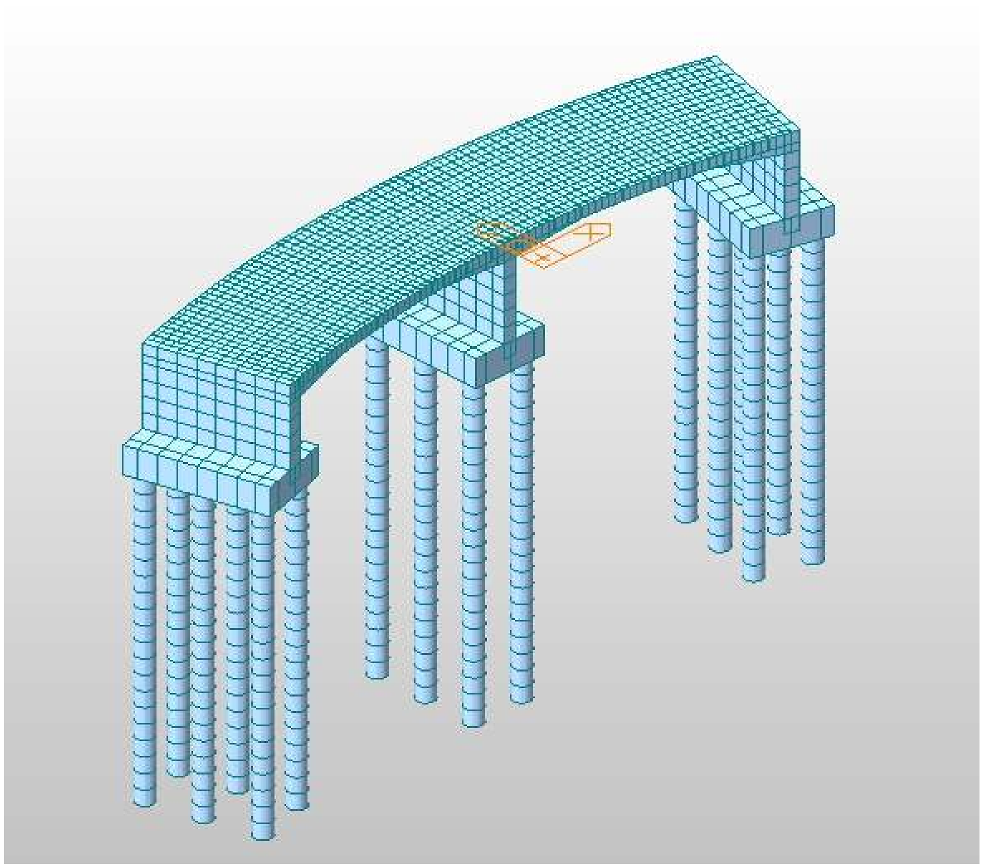

Fig 25. 3D view of curved integral bridge.

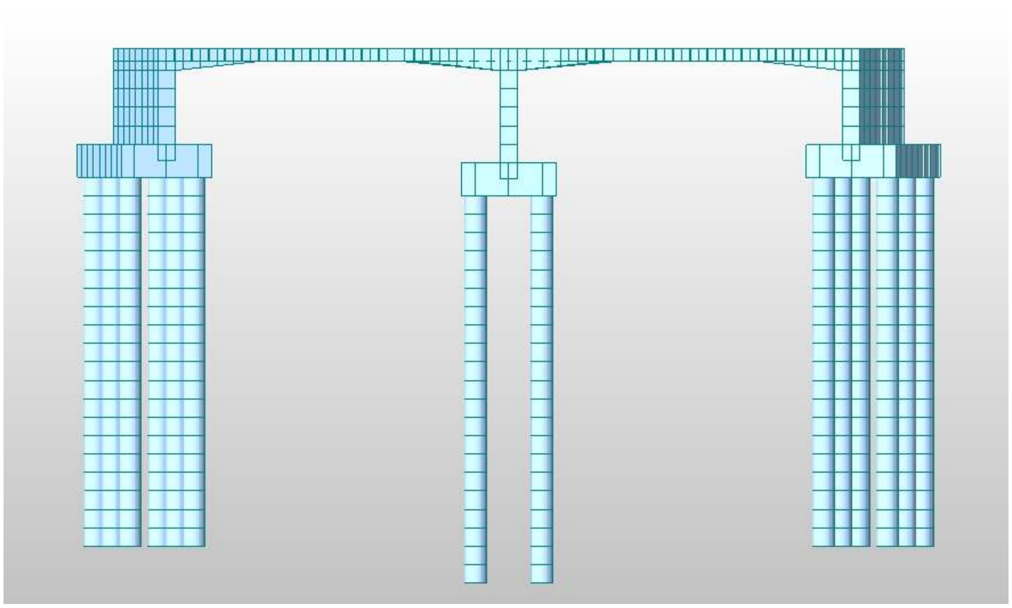

Fig 26. Elevation of curved integral bridge.

3.5 Soil properties and springs

In this thesis two types of foundations (Pile and open) are compared. So, two types of soil is used. For open foundation hard soil below the foundation is considered. Here, The bearing capacity of soil used is 60T/sqm for 25mm settlement.

So the spring stiffness is = 60*10/.0025 = 24000 Kn/m^3.

Now the properties of backfill soil is used ϕ = 30°, void ratio =0.6, specific gravity = 2.65, cycle factor =2, thermal expansion =30° C.

For Abutment pile the soil properties used is

Layer		Layer thickness (m)	Bulk Density, gms/cc	Dry Density, gms/cc	Specific gravity	Cohesion kN/sqm	Friction angle °	K0	Subgrade Modulus (kn/m^3) (K)
From (m)	To (m)								
0	11	11	1.83	1.42	2.7	63	0	1	4800
11	20	9	1.8	1.47	2.71	0.000	32	0.47	3220

For Pier pile the soil properties used is

Layer		Layer thickness (m)	Bulk Density, gms/cc	Dry Density, gms/cc	Specific gravity	Cohesion kN/sqm	Friction angle °	K0	Subgrade Modulus (kn/m^3) (K)
From (m)	To (m)								
0	10	10	1.83	1.42	2.7	63	0	1	4800
10	20	11	1.8	1.47	2.71	0.000	32	0.47	3220

The main concern for integral bridges is the effect of varying temperatures as it causes the bridge deck to deform either contraction or expansion. These repeated contractions and expansion of the deck have a significant effect on the backfill adjacent to the abutment which causes a cycle of soil compaction and soil slide, which in effect causes the modulus of subgrade reaction and pressure distribution of the backfill to vary with depth. As this cycle continues infinitely, the modulus of subgrade reaction on the backfill becomes constant. With this, a formulation is proposed by Barry Lehane to calculate this behavior through soil springs to represent the interaction between the soil and the abutment/piles. In Midas Civil, Integral Bridge function is readily available to auto-calculate these soil springs based on Barry Lehane Calculation. This function will help you in assigning corresponding Compression-only Lateral Springs and Linear Elastic Springs in abutment and piles by providing the parameters required by the function.

When the abutment Spring option is selected as the Soil Spring Type, the function will look like this (Figure-28). Using this option, backfill soil will be represented by Compression-only springs (Figure 30). For the Elements of abutment, Planar elements used. This is used if the abutment is modeled using plate elements. Direction is either Normal(+) or Normal(-), which pertains to the positive or negative side of the plate with reference to its Local Z. Compression-only Spring support will be defined on the side of the selected direction (Figure-27).

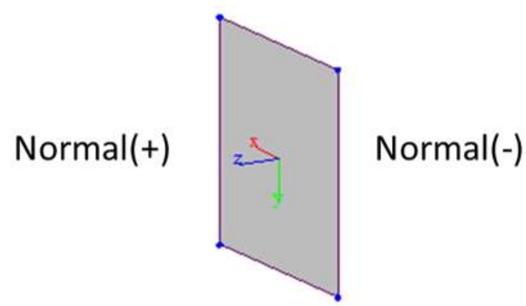

Fig 27. Planner element direction

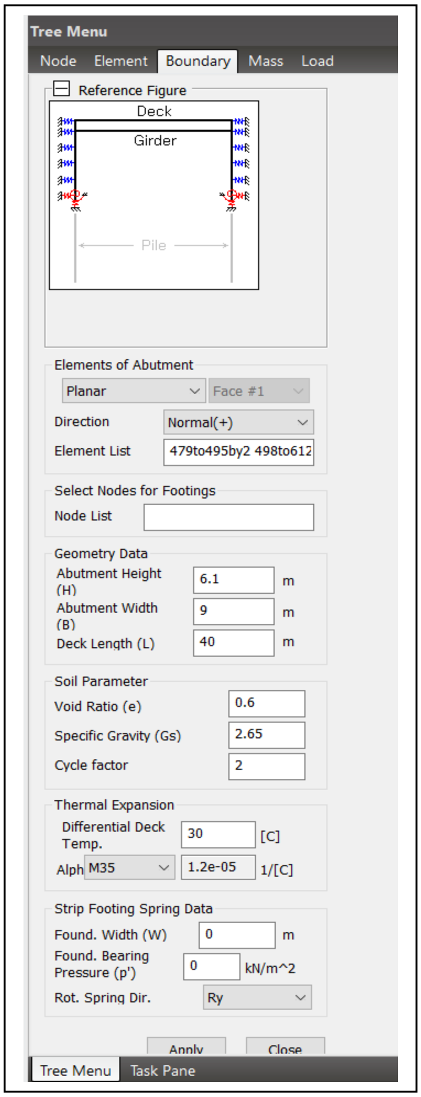

Fig 28. Details of abutment spring.

Computation of stiffness of compression-only springs for abutment backfill.

According to Broms (1971), the lateral stress-displacement relationship for abutment backfill of integral bridge is determined as shown in the Figure-29.

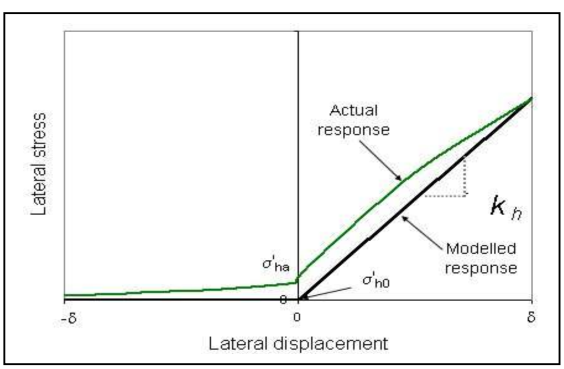

Fig 29. Lateral displacement of abutment spring.

The stiffness per unit area is calculated as follows:

$$K_S^{ave} = \frac{3.5G_{eq}}{H \times \left(\frac{B}{H}\right)^{0.5}}$$

Where, $G_{eq} = p_{atm} 600 f_{cyc} F(e) \left(\frac{p'}{p_{atm}}\right)^{0.5} \left(2.5H \times \frac{0.0001}{\Delta}\right)^{0.5}$ for $75 \times 10^{-6} < \frac{\Delta}{H} < 0.025$

$p' = 1.5\gamma_{fill}(H/2) - u \quad (u = 0)$

$= 1.5\text{g} \times \rho_d \times (H/2)$

$\rho_d = G_s \rho_w / (1 + e)$

Where, P_{atm}: Atmospheric pressure (100,000 N/m²) γ_{fill}: Unit weight of the fill g: Gravity acceleration (9.806 m/s²)

p': Mean effecitve stress of backfill ρ_w: Density of water (1000 kg/m³) B: Abutment width

f_{cyc}: Cycle factor u: Average pore pressure H: Abutment Height

G_s: Specific gravity of soil e: Void ratio L: Deck length

$F(e) = \frac{(2.17-e)^2}{1+e}$ Δ: Lateral displacement ($\Delta = \frac{\alpha \times \Delta T \times L}{2}$)

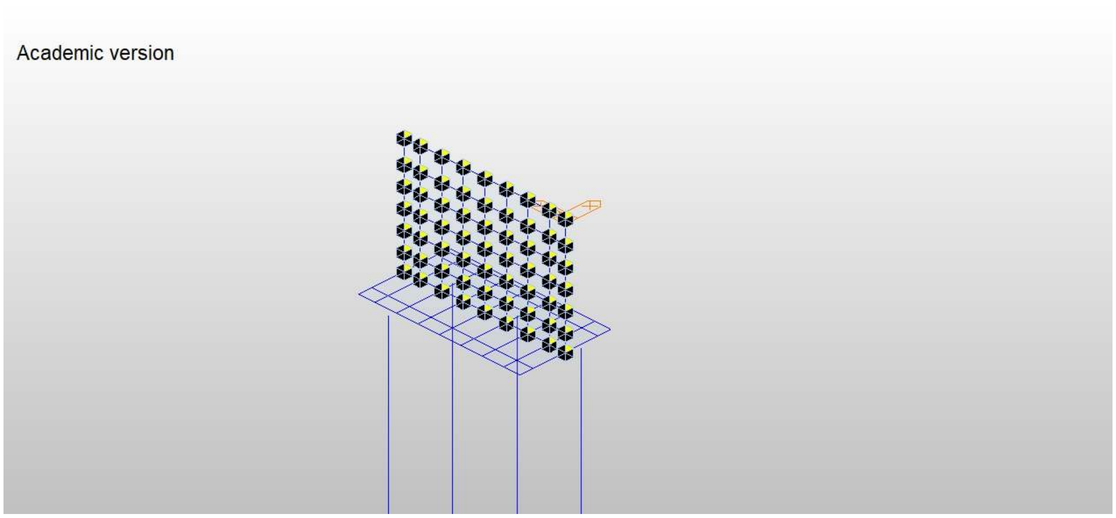

Fig 30. Abutment spring in Midas Civil

Lateral springs for the soils adjacent to piles are modeled as symmetric nonlinear elastic springs () and vertical springs for the soils adjacent to piles are modeled as linear elastic springs (). The stiffness of soil springs is automatically calculated and entered into point spring supports. Model of an abutment with soil spring in Midas Civil is shown in Figure 30.

Figure 32 and 33 shows the input used for pile spring and Figure 34 shows the model with pile spring.

The relationship between the lateral soil resistance and the lateral displacement Y at a specific depth X is represented as shown in the left (Figure.31). The values of Pk, Pm, Pu, Yk, Ym and Yu are defined at a specific depth (i.e., where pile springs are). The method of calculating Pu varies with Soil Types. The values of Pk, Pm, Yk, Ym and Yu are calculated using Pu as explained below. The calculation method is divided into two major cases - Sand and Clay. Different J values are used for soft clay and stiff clay, respectively.

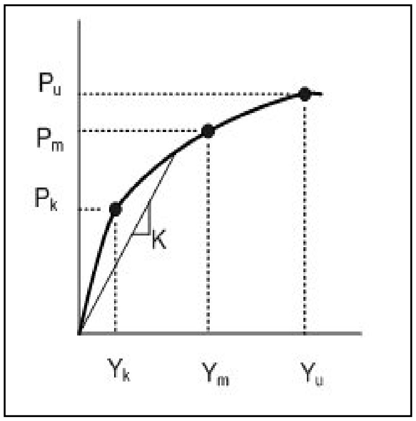

Fig 31 Pile spring.

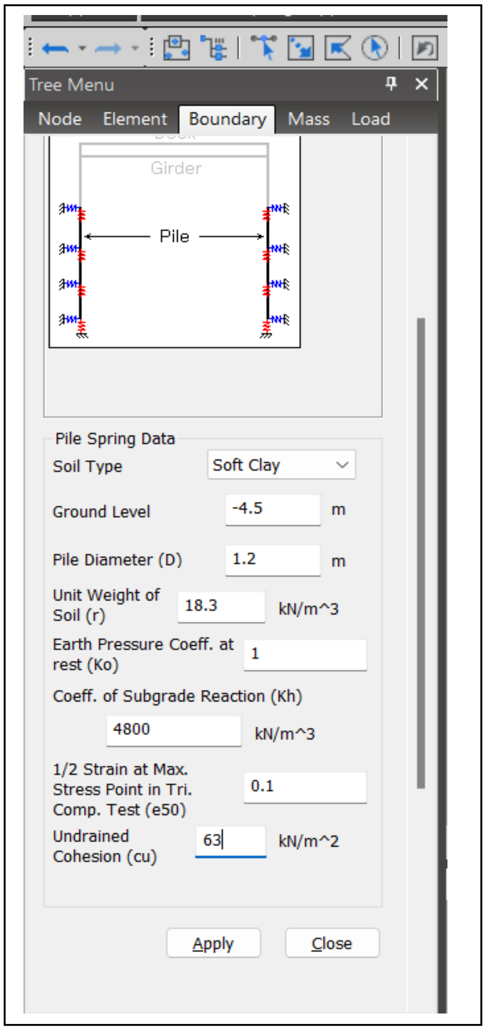

Fig 32. Pile spring in clay.

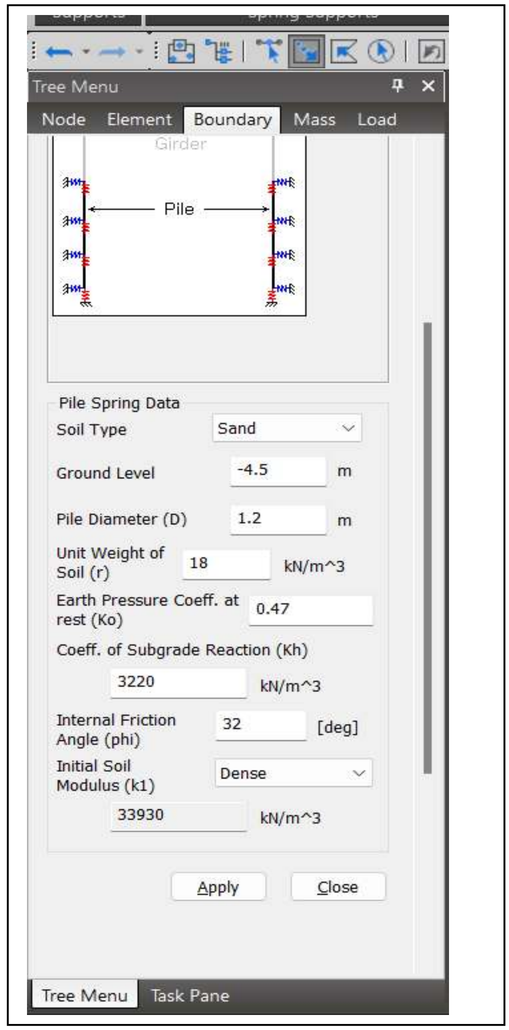

Fig 33. Pile spring in sand.

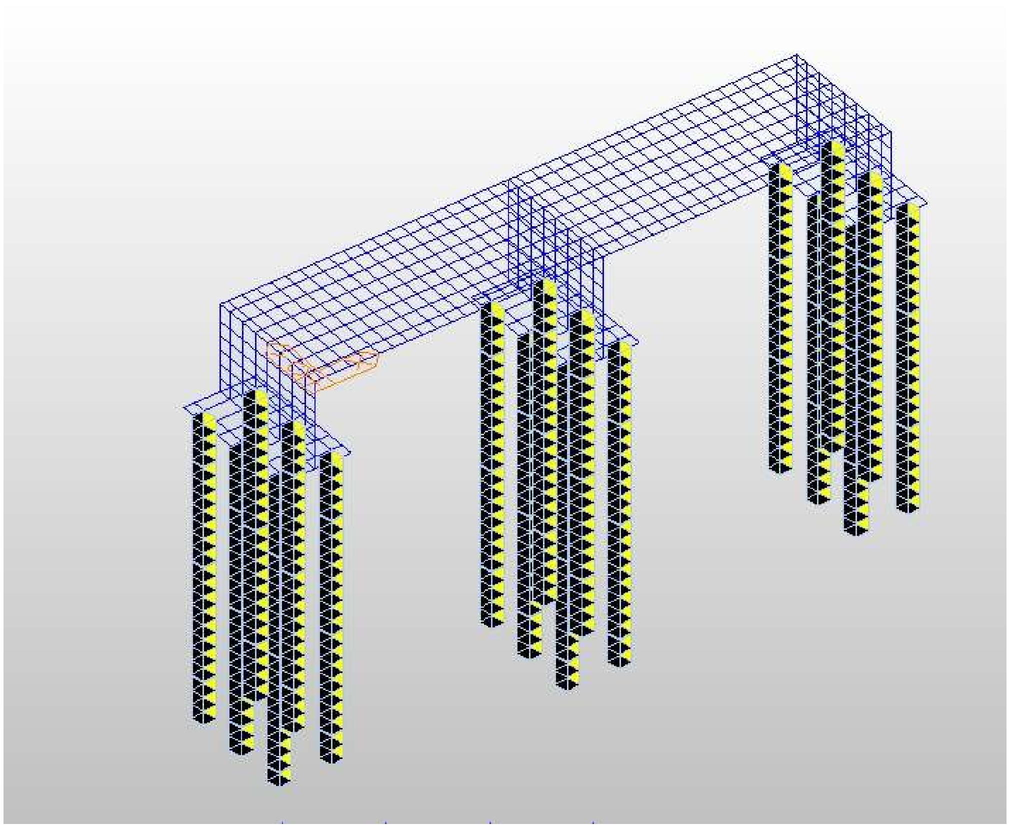

Fig 34. Pile spring in Midas Civil.

3.6 Dynamic analysis

Dynamic analysis is needed for the estimation of structural response in the process of designing earthquake-resistant structures as well as to check the vulnerability of the existing structures to seismic waves. The seismic analysis of the bridges shall be carried out using the following methods as per applicability depending upon the complexity of the structure and the input ground motion.

- Elastic seismic acceleration method (seismic coefficient method)
- Elastic response spectrum method
- Time history method

As per IRC:SP: 114 – 2018, integral bridges should be analysis in elastic response spectrum method or time history method. In this study all models have been analysed in time history method. In order to use the dynamic analysis, it is necessary to understand the design response, eigenvalue analysis and mode superposition method to calculate dynamic characteristics such as natural periods and mode shapes of structure.

3.7 Eigenvalue analysis

Structures have natural vibration characteristics depending on their shape, material, and boundary conditions. Natural vibration characteristics refers to a free vibration state that does not receive any external forces. The analysis method to find these characteristics is called mode analysis, eigenvalue analysis, or free vibration analysis. Through the eigenvalue analysis, it is possible to know the natural frequency of the structure and the corresponding eigen-mode. The natural frequency represents the degree of how quickly it repeats per unit time, and the eigen-mode refers to a shape that can be freely deformed under a given constraint.

The natural vibration characteristics of the structure can be obtained from the undamped free vibration, which is a state that is not affected by external forces. Since it is an undamped free vibration, a dynamic equilibrium equation in which the damping matrix and external force are zero can be created. Furthermore, the natural frequency and eigen-mode can be calculated by assuming the displacement vector u(t) as the product of the displacement shape function and the time function. The MDOF system can be calculated in the same way as the SDOF system, except that the stiffness and mass are in matrix form.

In general, the mode superposition method uses eigenvectors to solve equations of motion. In this case, since all of the matrix terms become diagonal matrices, each degree of freedom is transformed into an uncoupled ordinary differential equation.

For eigenvalue analysis Ritz Vector method is used as shown in Figure-35

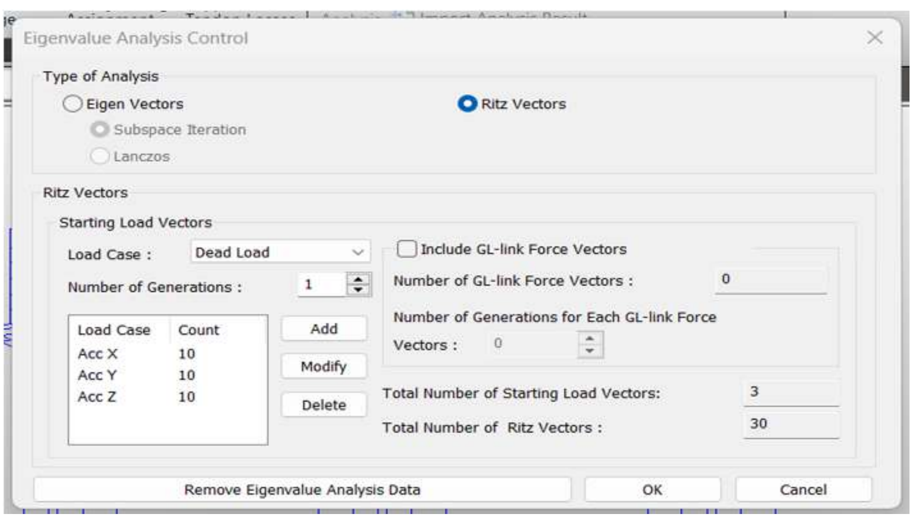

Fig 35. Eigenvalue analysis control.

3.8 Time history analysis

The time history analysis method is used to calculate the actual behavior (displacement, member forces, etc) of the structure at any given time using the dynamic characteristics of the structure and the external forces applied, and is used when the distinction between modes is not clear or nonlinear analysis is required. For this study earthquake data of earthquake happened at India-Burma border on 06.08.1988 recorded at 6.07IST is used. The data was recorded by IITR at station Dipu. The hypo central distance of the station is 210.1 Km. Peak acceleration at longitudinal direction is 2.77 m/s/s and in transverse direction is 3.31 m/s/s. For time history analysis steps in Midas Civil are shown in Figures 36, 37, 40 and 41. Figure 38 and 39 shows the time vs acceleration input for time history analysis.

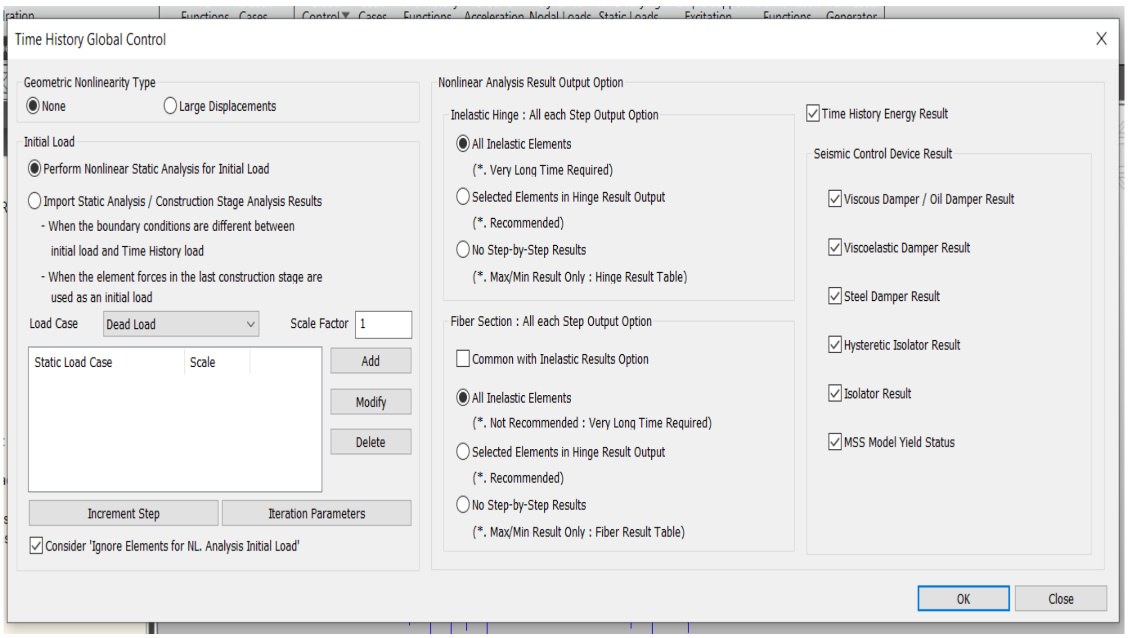

Fig 36. Time history analysis control.

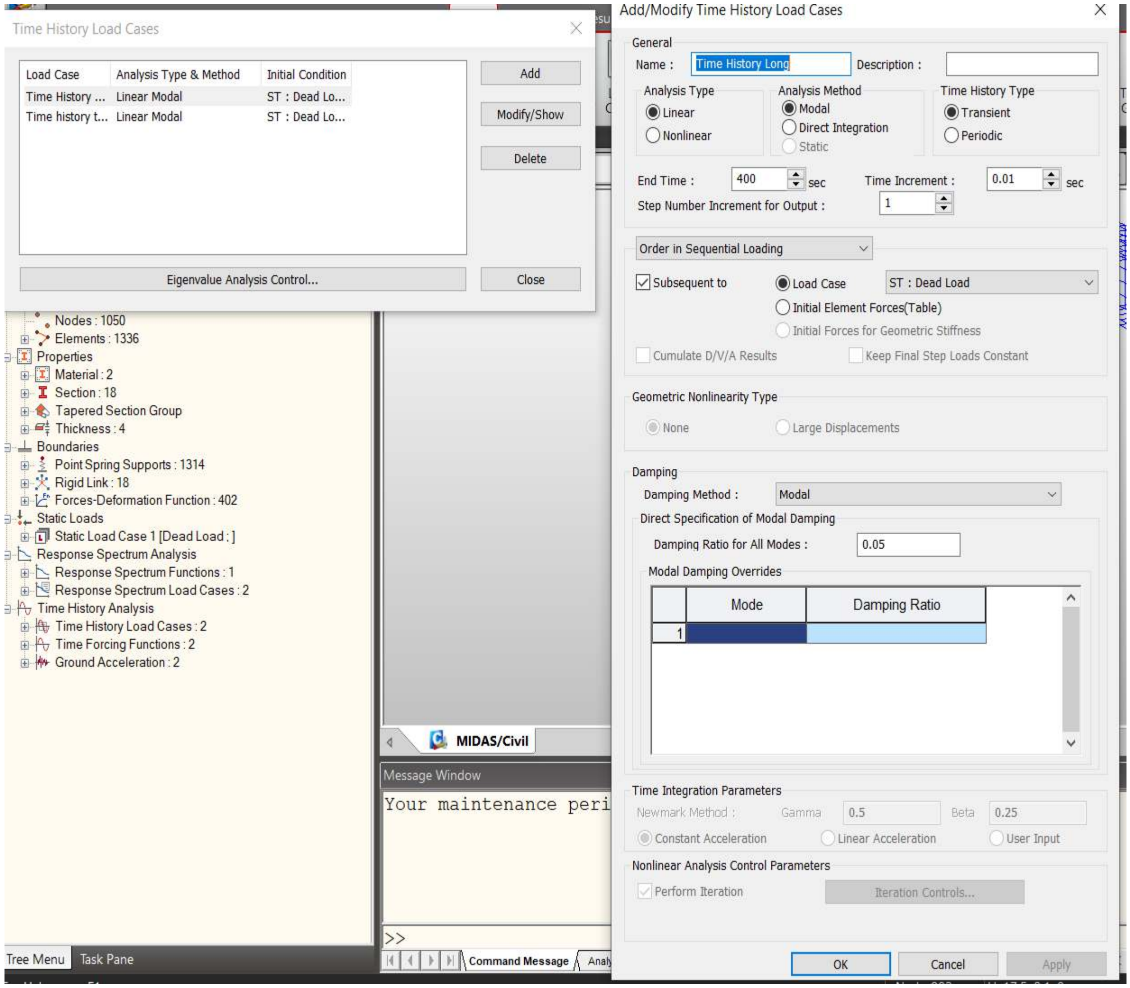

Fig 37. Time history load case control.

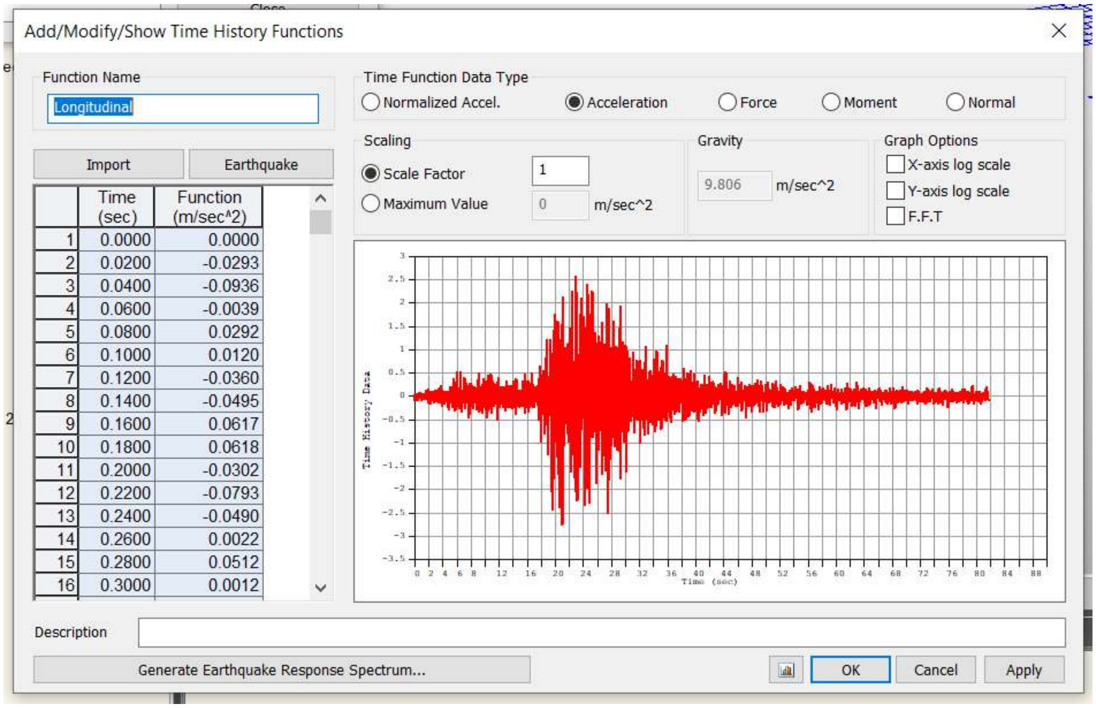

Fig 38. Time history graph longitudinal direction.

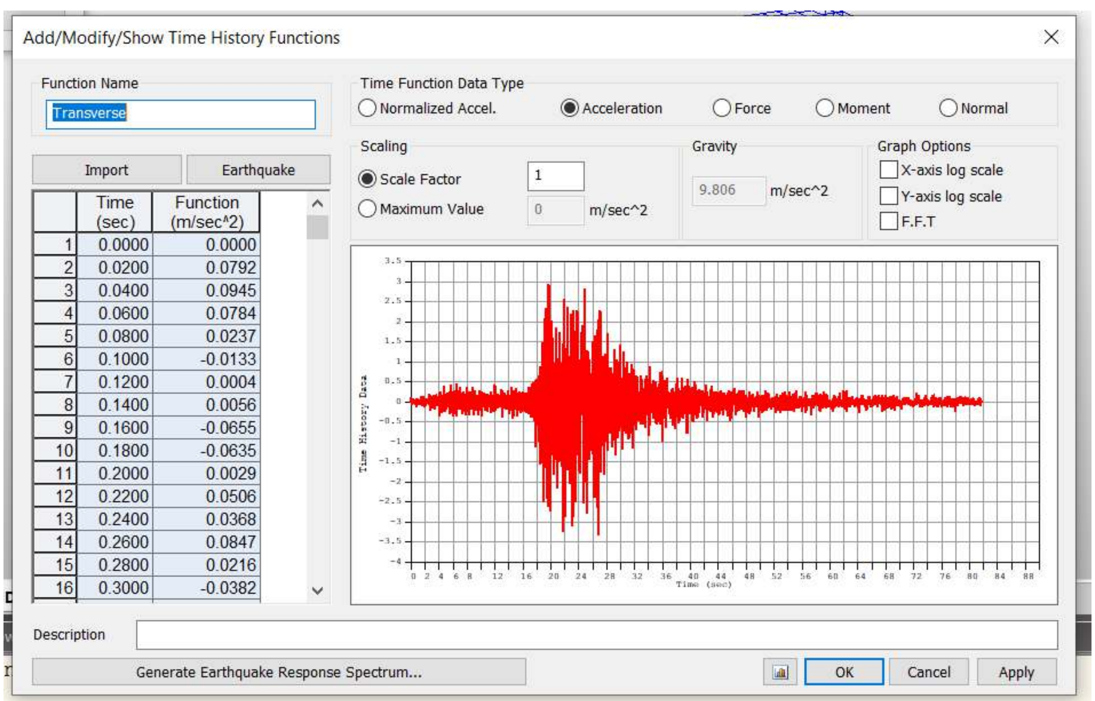

Fig 39. Time history graph transverse direction.

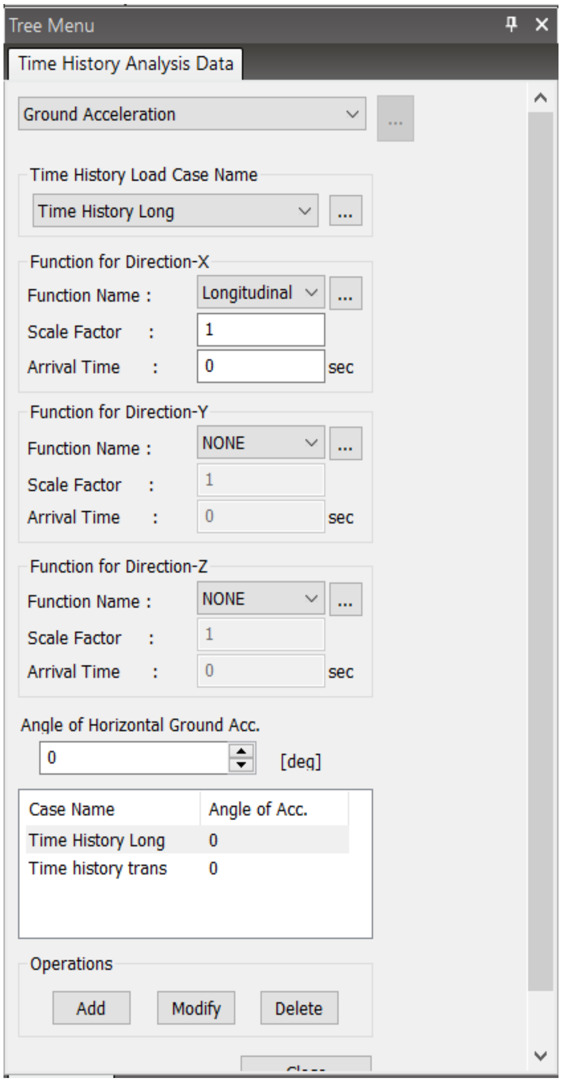

Fig 40. Time history long direction.

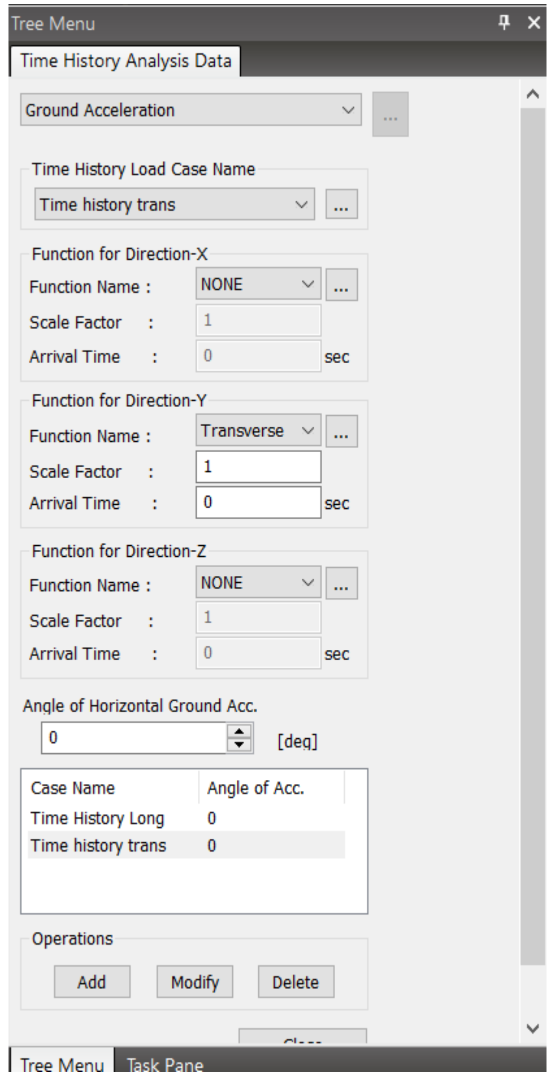

Fig 41. Time history transverse direction.

Chapter – 4: Results and discussion

Using the bridge models mentioned in the previous chapter the seismic responses of RCC integral bridge are studied and discussed for the following cases.

- Variation of first mode-time period with variation of skew angle and radius of curvature.
- Variation of base shear values with variation of skew angle and radius of curvature.
- Variation of moment (about longitudinal, transverse axis and torsional) of top and bottom of abutment and pier with variation of skew angle and radius of curvature.

4.1 Benchmark validation

To validate the present approach, a model is developed in Midas Civil as per the specifications mentioned in IRC: SP – 114: 2018 and the total base shear is calculated manually. Then the total base shear is compared with software output (Refer Table 1). Figure 42 shows the 3D model in Midas Civil software and the Figure 43 shows the output of Midas Civil software.

Manual calculation

Zone factor (Z) =	0.36	
Importance factor (I) =	1	
response reduction factor (R) =	1	
Dead load without foundation=	11832.75	KN
Total dead load =	6196.5	KN
Total dead load =	18029.25	KN

Mode No	Frequency		Period	Sa/g	Ah	Modal perticipation factor (%)	Seismic except foundation (KN)	Seismic on foundation (KN)
	(rad/sec)	(cycle/sec)	(sec)					
1	18.22082	2.899934	0.344835	2.5	0.45	0	0	0
2	19.10077	3.039981	0.328949	2.5	0.45	65.38	3481.313	911.536
3	24.75279	3.939528	0.253838	2.5	0.45	0	0.000	0.000
4	30.63122	4.87511	0.205124	2.5	0.45	3.85	205.002	53.677
5	44.15307	7.02718	0.142305	2.5	0.45	0	0.000	0.000
6	48.34855	7.69491	0.129956	2.5	0.45	0	0.000	0.000
7	50.12495	7.977633	0.12535	2.5	0.45	0.06	3.195	0.837
8	52.76323	8.397528	0.119083	2.5	0.45	15.11	804.568	210.666
9	59.4747	9.465693	0.105645	2.5	0.45	0.36	19.169	5.019
10	65.45879	10.41809	0.095987	2.440	0.439	0	0.000	0.000
11	85.98093	13.68429	0.073077	2.096	0.377	0	0.000	0.000
12	99.48866	15.83411	0.063155	1.947	0.351	0	0.000	0.000

Mode No	Frequency		Period	Sa/g	Ah	Modal participation factor (%)	Seismic except foundation (KN)	Seismic on foundation (KN)
	(rad/sec)	(cycle/sec)	(sec)					
13	102.3331	16.28681	0.061399	1.921	0.346	5.14	210.303	55.065
14	147.4817	23.47244	0.042603	1.639	0.295	0	0.000	0.000
15	178.6953	28.44025	0.035161	1.527	0.275	10.1	328.577	86.033
16	190.2258	30.27538	0.03303	1.495	0.269	0	0.000	0.000
17	218.1756	34.72373	0.028799	1.432	0.258	0	0.000	0.000
18	223.6477	35.59464	0.028094	1.421	0.256	0	0.000	0.000
19	425.9732	67.79574	0.01475	1.221	0.22	0	0.000	0.000
20	473.0918	75.29491	0.013281	1.199	0.216	0	0.000	0.000
Total						**100**	**5052.127**	**1322.833**
Total Base reaction (KN) =							**6374.960**	

Table 1: Base shear calculation for benchmark validation.

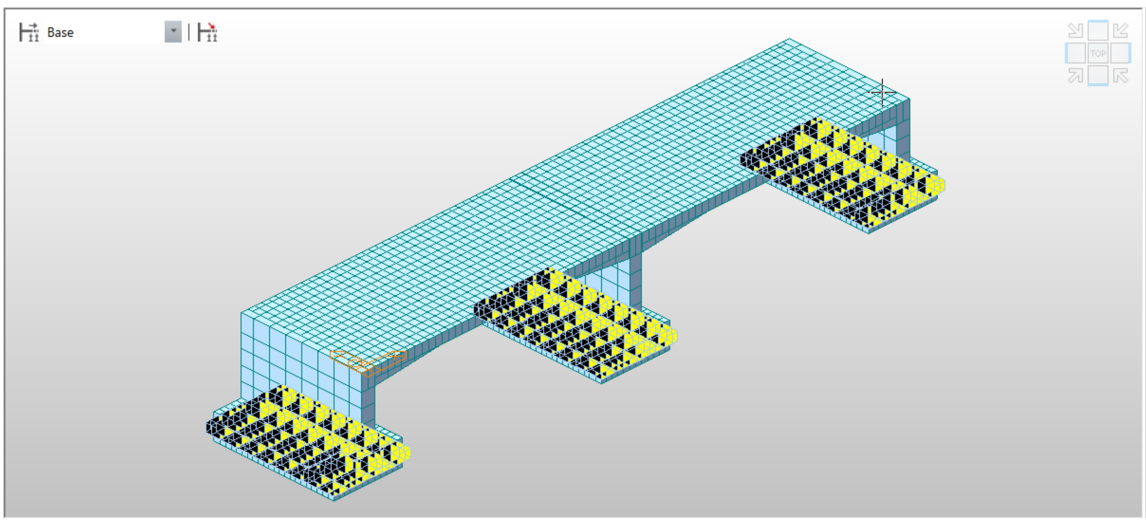

Fig 42. Total model.

SUMMATION OF REACTION FORCES PRINTOUT				
Load	FX (kN)	FY (kN)	FZ (kN)	
Dead Load	-0.000000	-0.000000	18029.250000	
RSX(RS)	6346.081315	0.000026	0.028395	
RSY(RS)	0.000024	5957.418050	0.000143	

Fig 43. Reaction output from Midas Civil.

From the above comparison it can be seen that from manual calculation the base shear is 6375 KN and from Midas Civil the total base reaction is 6346 KN in longitudinal direction. So, it can be said that the software provides the desired result as stated by the code.

4.2 Numerical study of author's own problems.

The numerical experimentations on a number of bridge models are carried out to study the seismic response of different significant design parameters. Two 20 m span of RCC integral slab bridge has been considered. Different skew angles (7.5, 15, 22.5, 30, 37.5, 45, 52.5, 60, 67.5 and 75 degree) and different radii of curvature (250m, 150m, 100m and 75m) are used. These bridges are analyzed by time history method (THM) using time history earthquake data of Dipu, Assam (Zone – V)

Considering the parametric variations, numbers of structural models has been developed and response of those bridges are studied. A table for list of the bridges are presented below (table-3):

ST = type of super -structure (ST-1 is integral slab superstructure)

AT = type of sub-structure/ abutment (AT-1 for wall type abutment)

PT = type of sub-structure/ pier (PT-1 for wall type pier)

FT = type of foundation (FT-1 for open foundation, FT-2 for pile foundation)

SAM = seismic analysis method (SAM-3 for time history analysis)

Sl no	Model ID no	Span length (L) (m)	Radius (R) (m)	Skew angle (α) (in °)	ST	AT	PT	FT	SAM	Remarks	Remarks
1	M-L20R0S0ST1AT1PT1FT2SAM3	20	0	0	1	1	1	2	3	L=20m and R=infinity skew angle varied	a. ST - 1 for integral superstructure b. PT - 1 for rectangular shape c. FT-2 for pile foundation d. SAM - 3 for Seismic analysis by time history analysis
2	M-L20R0S7.5ST1AT1PT1FT2SAM3	20	0	7.5	1	1	1	2	3		
3	M-L20R0S15ST1AT1PT1FT2SAM3	20	0	15	1	1	1	2	3		
4	M-L20R0S22.5ST1AT1PT1FT2SAM3	20	0	22.5	1	1	1	2	3		
5	M-L20R0S30ST1AT1PT1FT2SAM3	20	0	30	1	1	1	2	3		
6	M-L20R0S37.5ST1AT1PT1FT2SAM3	20	0	37.5	1	1	1	2	3		
7	M-L20R0S45ST1AT1PT1FT2SAM3	20	0	45	1	1	1	2	3		
8	M-L20R0S52.5ST1AT1PT1FT2SAM3	20	0	52.5	1	1	1	2	3		
9	M-L20R0S60ST1AT1PT1FT2SAM3	20	0	60	1	1	1	2	3		
10	M-L20R0S67.5ST1AT1PT1FT2SAM3	20	0	67.5	1	1	1	2	3		
11	M-L20R0S75ST1AT1PT1FT2SAM3	20	0	75	1	1	1	2	3		
12	M-L20R75S0ST1AT1PT1FT2SAM3	20	75	0	1	1	1	2	3	L=20m and S = 0°	
13	M-L20R100S0ST1AT1PT1FT2SAM3	20	100	0	1	1	1	2	3		

Sl no	Model ID no	Span length (L) (m)	Radius (R) (m)	Skew angle (α) (in °)	ST	AT	PT	FT	SAM	Remarks	Remarks
14	M-L20R150S0ST1AT1PT1FT2SAM3	20	150	0	1	1	1	2	3	radius of curvature varied	
15	M-L20R250S0ST1AT1PT1FT2SAM3	20	250	0	1	1	1	2	3		
16	M-L20R0S0ST1AT1PT1FT1SAM3	20	0	0	1	1	1	1	3	L=20m and R=infinity skew angle varied	a. ST - 1 for integral superstructure b. PT - 1 for rectangular shape c. FT - 1 for open / shallow e. SAM - 3 for seismic analysis by time history analysis
17	M-L20R0S7.5ST1AT1PT1FT1SAM3	20	0	7.5	1	1	1	1	3		
18	M-L20R0S15ST1AT1PT1FT1SAM3	20	0	15	1	1	1	1	3		
19	M-L20R0S22.5ST1AT1PT1FT1SAM3	20	0	22.5	1	1	1	1	3		
20	M-L20R0S30ST1AT1PT1FT1SAM3	20	0	30	1	1	1	1	3		
21	M-L20R0S37.5ST1AT1PT1FT1SAM3	20	0	37.5	1	1	1	1	3		
22	M-L20R0S45ST1AT1PT1FT1SAM3	20	0	45	1	1	1	1	3		
23	M-L20R0S52.5ST1AT1PT1FT1SAM3	20	0	52.5	1	1	1	1	3		
24	M-L20R0S60ST1AT1PT1FT1SAM3	20	0	60	1	1	1	1	3		
25	M-L20R0S67.5ST1AT1PT1FT1SAM3	20	0	67.5	1	1	1	1	3		
26	M-L20R0S75ST1AT1PT1FT1SAM3	20	0	75	1	1	1	1	3		
27	M-L20R75S0ST1AT1PT1FT1SAM3	20	75	0	1	1	1	1	3	L=20m and S = 0° radius of curvature varied	
28	M-L20R100S0ST1AT1PT1FT1SAM3	20	100	0	1	1	1	1	3		
29	M-L20R150S0ST1AT1PT1FT1SAM3	20	150	0	1	1	1	1	3		
30	M-L20R0S0ST1AT1PT1FT2SAM3	20	0	0	1	1	1	1	3		
31	M-L20R0S7.5ST1AT1PT1FT2SAM3	20	0	7.5	1	1	1	2	3	L=20m and R=infinity skew angle varied	a. ST - 1 for integral superstructure b. PT - 1 for rectangular shape c. FT-2 for pile foundation d. SAM - 3 for seismic analysis by time history analysis
32	M-L20R0S15ST1AT1PT1FT2SAM3	20	0	15	1	1	1	2	3		
33	M-L20R0S22.5ST1AT1PT1FT2SAM3	20	0	22.5	1	1	1	2	3		
34	M-L20R0S30ST1AT1PT1FT2SAM3	20	0	30	1	1	1	2	3		
35	M-L20R0S37.5ST1AT1PT1FT2SAM3	20	0	37.5	1	1	1	2	3		
36	M-L20R0S45ST1AT1PT1FT2SAM3	20	0	45	1	1	1	2	3		
37	M-L20R0S52.5ST1AT1PT1FT2SAM3	20	0	52.5	1	1	1	2	3		
38	M-L20R0S60ST1AT1PT1FT2SAM3	20	0	60	1	1	1	2	3		
39	M-L20R0S67.5ST1AT1PT1FT2SAM3	20	0	67.5	1	1	1	2	3		
40	M-L20R0S75ST1AT1PT1FT2SAM3	20	0	75	1	1	1	2	3		
41	M-L20R75S0ST1AT1PT1FT2SAM3	20	75	0	1	1	1	2	3		
42	M-L20R100S0ST1AT1PT1FT2SAM3	20	100	0	1	1	1	2	3	L=20m and S = 0° radius of curvature varied	
43	M-L20R150S0ST1AT1PT1FT2SAM3	20	150	0	1	1	1	2	3		
44	M-L20R250S0ST1AT1PT1FT2SAM3	20	250	0	1	1	1	2	3		
45	M-L20R0S0ST1AT1PT1FT1SAM3	20	0	0	1	1	1	2	3		

Sl no	Model ID no	Span length (L) (m)	Radius (R) (m)	Skew angle (α) (in °)	ST	AT	PT	FT	SAM	Remarks	Remarks
46	M-L20R0S7.5ST1AT1PT1FT1SAM3	20	0	7.5	1	1	1	1	3	L=20m and R=infinity skew angle varied	a. ST - 1 for integral superstructure b. PT - 1 for rectangular shape. FT - 1 for open / shallow. SAM - 3 for seismic analysis by time history analysis
47	M-L20R0S15ST1AT1PT1FT1SAM3	20	0	15	1	1	1	1	3		
48	M-L20R0S22.5ST1AT1PT1FT1SAM3	20	0	22.5	1	1	1	1	3		
49	M-L20R0S30ST1AT1PT1FT1SAM3	20	0	30	1	1	1	1	3		
50	M-L20R0S37.5ST1AT1PT1FT1SAM3	20	0	37.5	1	1	1	1	3		
51	M-L20R0S45ST1AT1PT1FT1SAM3	20	0	45	1	1	1	1	3		
52	M-L20R0S52.5ST1AT1PT1FT1SAM3	20	0	52.5	1	1	1	1	3		
53	M-L20R0S60ST1AT1PT1FT1SAM3	20	0	60	1	1	1	1	3		
54	M-L20R0S67.5ST1AT1PT1FT1SAM3	20	0	67.5	1	1	1	1	3		
55	M-L20R0S75ST1AT1PT1FT1SAM3	20	0	75	1	1	1	1	3		
56	M-L20R75S0ST1AT1PT1FT1SAM3	20	75	0	1	1	1	1	3		
57	M-L20R100S0ST1AT1PT1FT1SAM3	20	100	0	1	1	1	1	3	L=20m and S = 0° radius of curveture varied	
58	M-L20R150S0ST1AT1PT1FT1SAM3	20	150	0	1	1	1	1	3		
59	M-L20R250S0ST1AT1PT1FT1SAM3	20	250	0	1	1	1	1	3		
60	M-L20R0S0ST1AT1PT1FT2SAM3	20	0	0	1	1	1	1	3		

Table 2: List of analysis models

4.2.1 Variation of dead load

The dead load of the structure varies with the skew angle. As the length of substructure and pile cap/open foundation increases with the increase of skew angle the dead load increases. For both the models with abutment spring or not the dead load is same. The dead load remains same for curve models. The variation of dead load with variation of skew angle and angle of plan curvature of the Integral bridge are plotted as Graph to Graph to understand the nature of such variations due the earthquake force. The degree of curvature is measured as 1750/R, where R is the radius of curvature in m.

So, for 250 m radius degree of curvature is 1750/250 = 7 Degree. So, all graphs of curve bridge are plotted against the degree of curvature (1750/R).

4.2.1.1 Variation of dead load with skew

Graph 1. Variation of dead load with respect to skew angle for bridge with pile foundation.

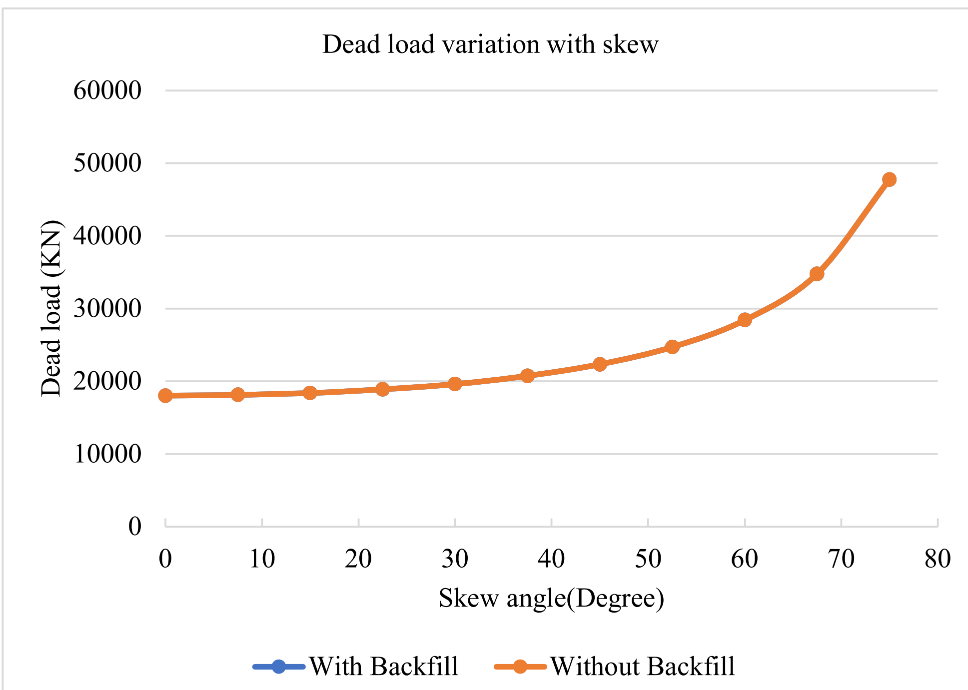

Graph 2. Variation of dead load with respect to skew angle for bridge with open foundation.

4.2.1.2 Variation of dead load with curvature

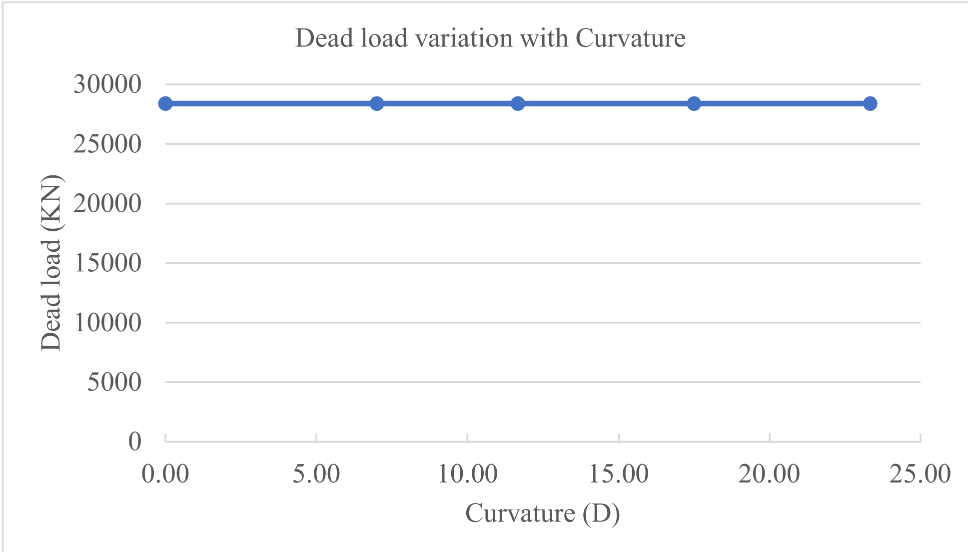

Graph 3. Variation of dead load with respect to curvature for bridge with pile foundation.

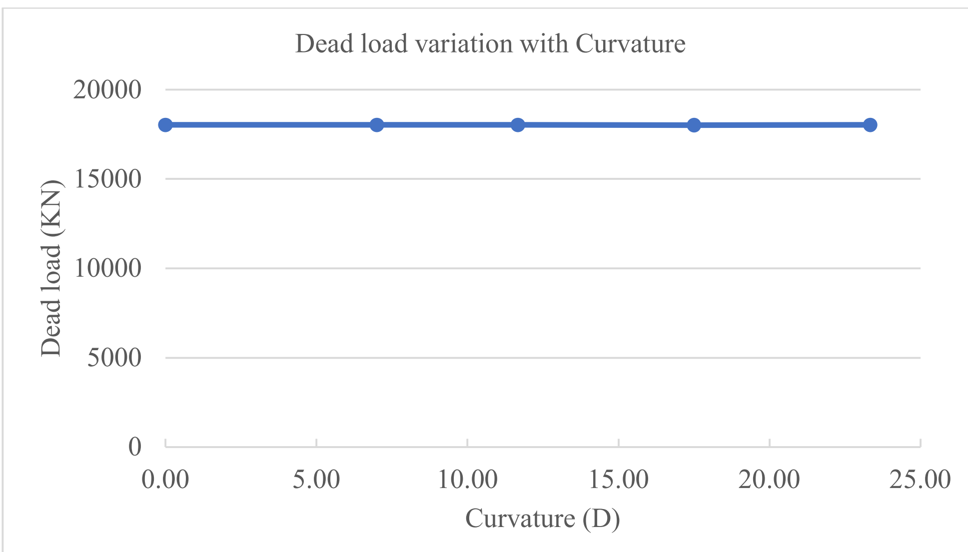

Graph 4. Variation of dead load with respect to curvature for bridge with open foundation.

Hence from the above graphs it can be said that the dead load increases with the increase of skew angle and it remains almost same for different curvature.

4.2.2 Variation of time period

Variation of time period values corresponding to 1st mode of longitudinal and transverse modes of vibration with change of skew angle and angle of plan curvature of the Integral Bridge are plotted as graphically to understand the nature of such variations due the earthquake force. The degree of curvature is measured as 1750/R, where R is the radius of curvature in m.

So, for 250 m radius degree of curvature is 1750/250 = 7 degree. So, all graphs of curved bridge are plotted against the degree of curvature (1750/R).

4.2.2.1 Variation with skew angle

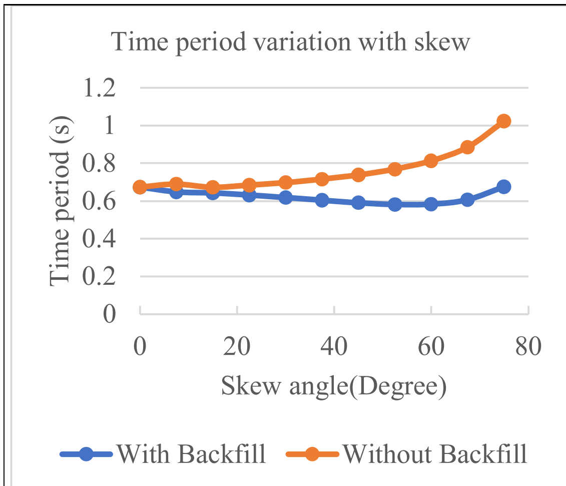

Graph 5. Comparison on variation of time period w.r.t. skew for bridge with pile foundation and with and without earth behind abutment.

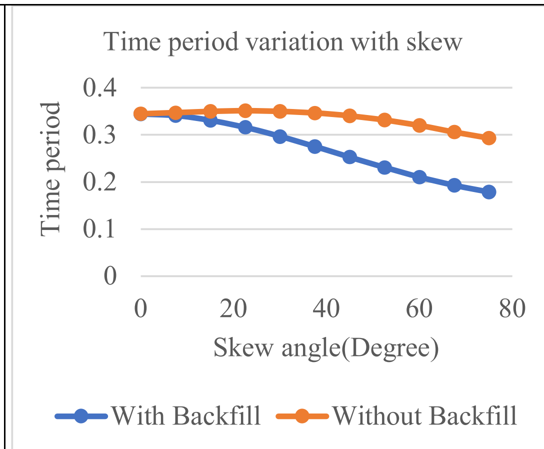

Graph 6. Comparison on variation of time period w.r.t. skew for bridge with open foundation and with and without earth behind abutment.

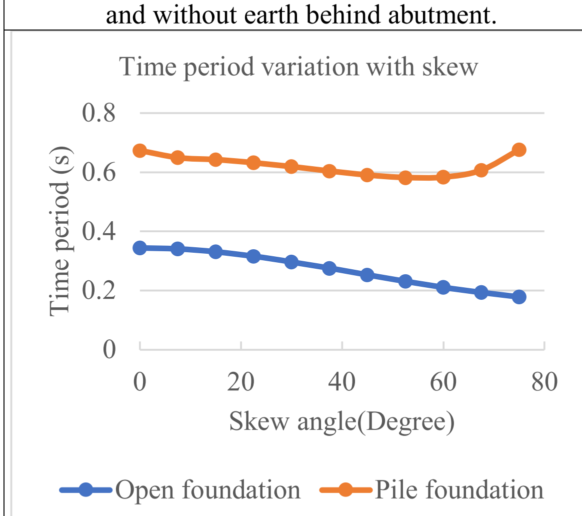

Graph 7. Comparison on variation of time period w.r.t. skew for bridge with open foundation and pile foundation with earth behind abutment.

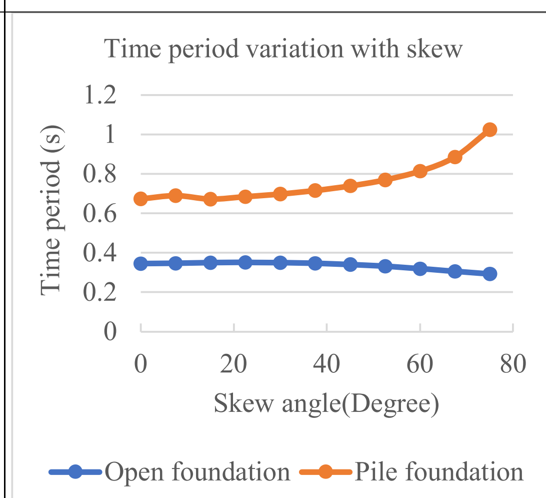

Graph 8. Comparison on variation of time period w.r.t. skew for bridge with open foundation and pile foundation without earth behind abutment.

4.2.2.2 Variation with curvature

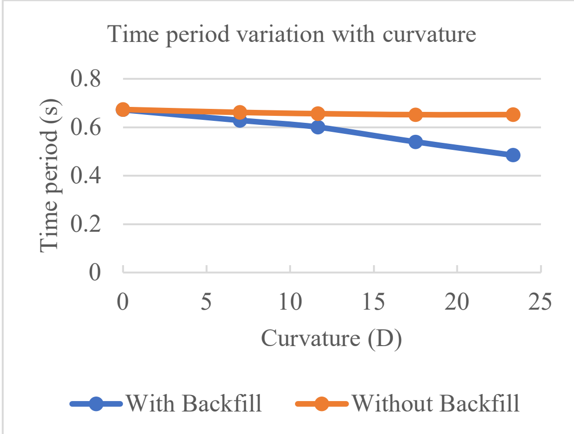

Graph 9. Comparison on variation of time period w.r.t. curvature for bridge with pile foundation and with and without earth behind abutment.

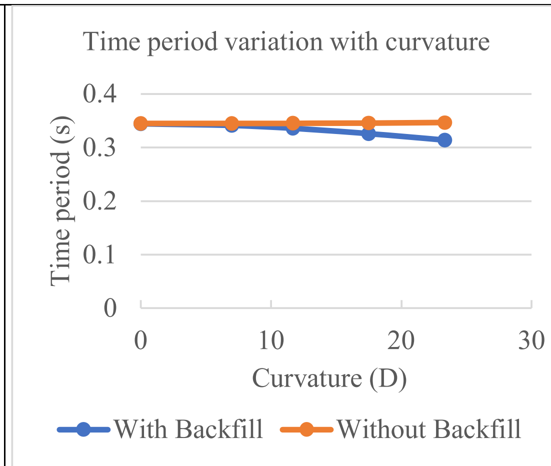

Graph 10. Comparison on variation of time period w.r.t. curvature for bridge with open foundation and with and without earth behind abutment.

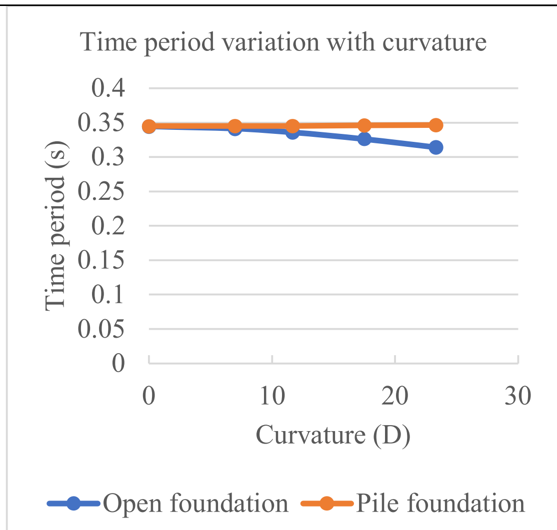

Graph 11. Comparison on variation of time period w.r.t. curvature for bridge with open foundation and pile foundation with earth behind abutment.

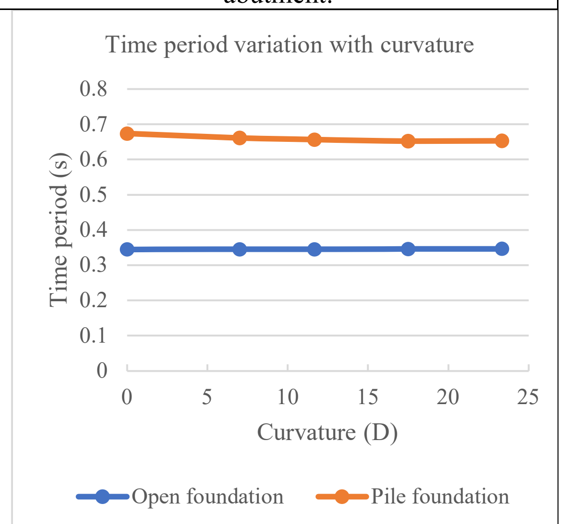

Graph 12. Comparison on variation of time period w.r.t. curvature for bridge with open foundation and pile foundation without earth behind abutment.

Hence from the above graphs following observations can be made:-

- Time period with respect to first mode for pile foundation without backfill increases with increase of skew angle and for with backfill time period initially decreases then increases.
- Time period with respect to first mode for open foundation with backfill decreases rapidly with increase of skew angle and for without backfill time period decreases slowly.

- ➢ Time period for integral bridge with pile foundation decrease with increase of curvature i.e. decrease of radius of curve. For bridge with backfill time period decreases more than without backfill.
- ➢ Time period for bridge with pile foundation is higher than the same bridge with open foundation.

4.2.3 Variation of base reaction

Base shear is the total lateral force on the base of the structure due to seismic activity. Base Shear is a very important parameter for the seismic design of bridges. The variation of the base shear for all the variants of model are studied and accumulated results are presented below. Base shear is plotted in two different ways one is total base shear against skew or curvature, in another graph ratio of base shear to total DL is plotted against skew/curve. 2nd graph will provide actual variation because the deal load is also varying with skew. So, both the graphs are plotted.

4.2.3.1 Variation with skew angle in longitudinal seismic case

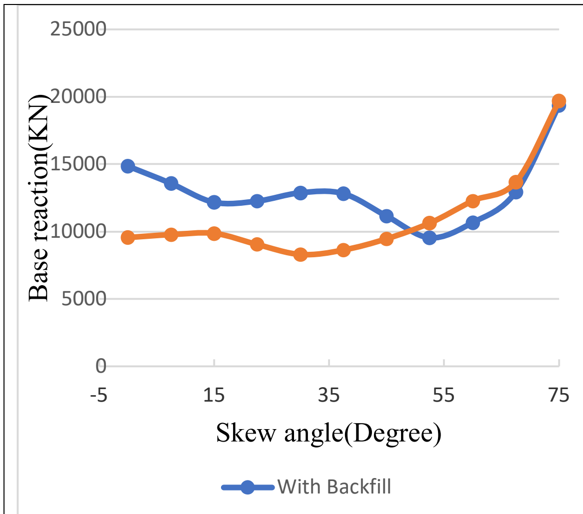

Graph 13. Comparison on longitudinal base shear w.r.t. skew with pile foundation and with or without earth behind abutment.

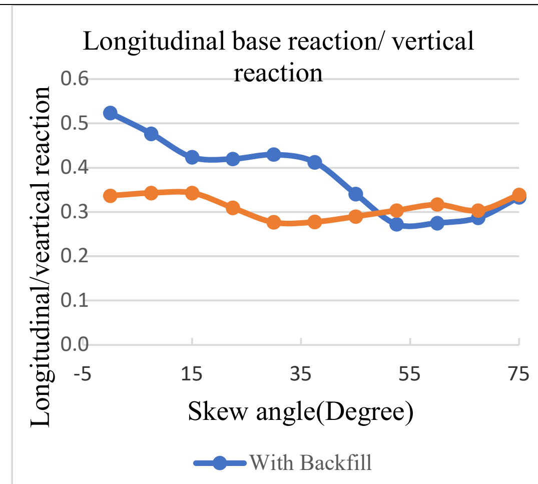

Graph 14. Comparison on longitudinal base shear/Vertical reaction w.r.t. skew with pile foundation and with or without earth behind abutment.

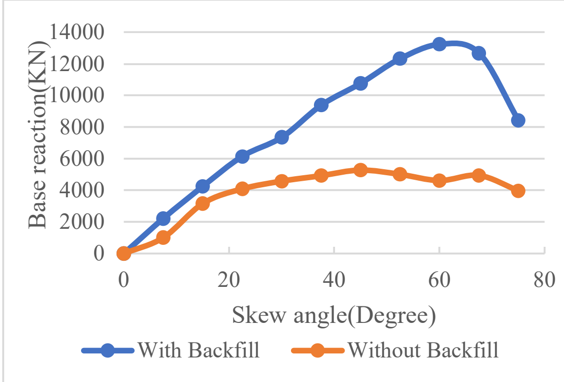

Graph 15. Comparison on transverse base shear w.r.t. skew with pile foundation and with or without earth behind abutment.

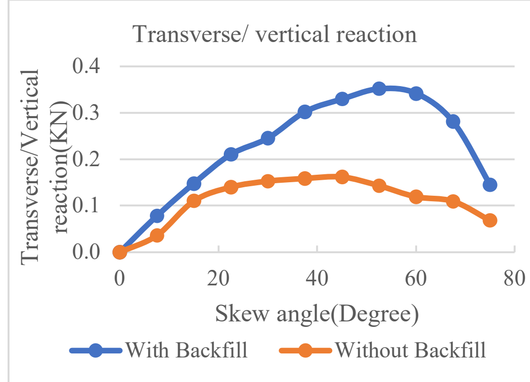

Graph 16. Comparison on transverse base shear/vertical reaction w.r.t. skew with pile foundation and with or without earth behind abutment.

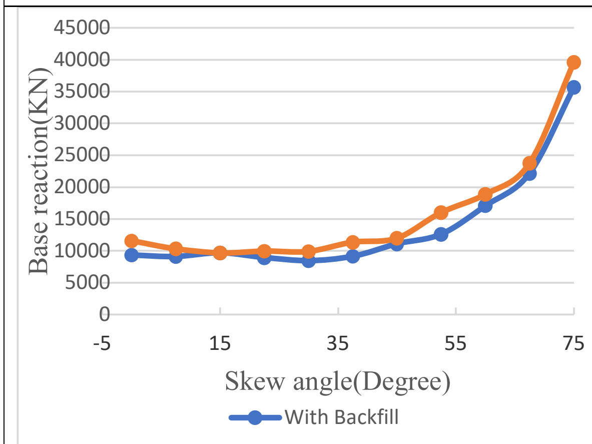

Graph 17. Comparison on longitudinal base shear w.r.t. skew with open foundation and with or without earth behind abutment.

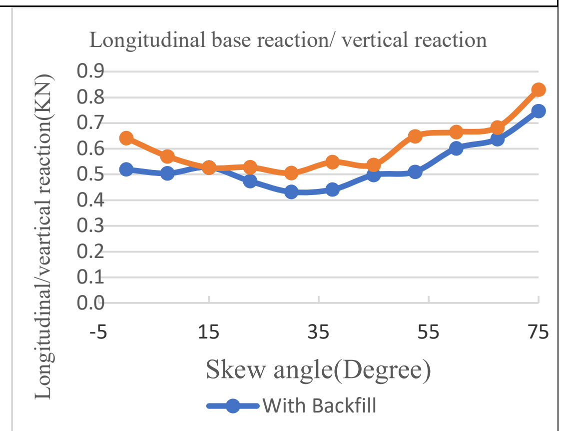

Graph 18. Comparison on longitudinal/vertical base shear w.r.t. skew with open foundation and with or without earth behind abutment.

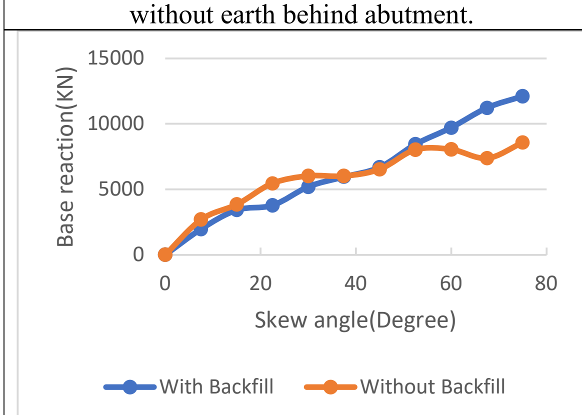

Graph 19. Comparison on transverse base shear w.r.t. skew with open foundation and with or without earth behind abutment.

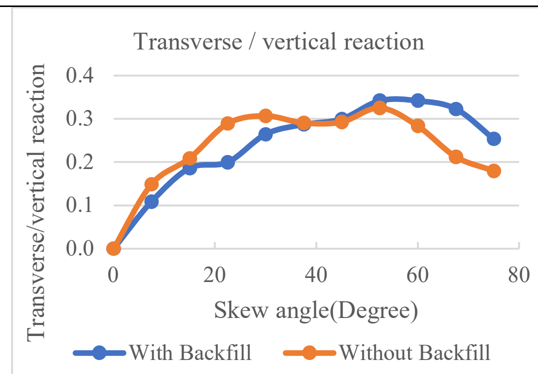

Graph 20. Comparison on transverse/vertical base shear w.r.t. skew with open foundation and with or without earth behind abutment.

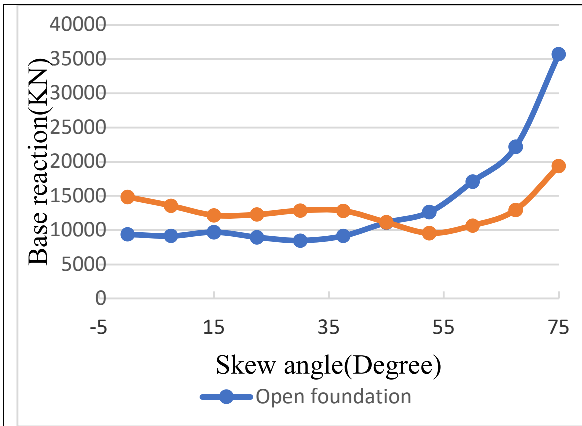

Graph 21. Comparison on longitudinal base shear w.r.t. skew with open or pile foundation and with earth behind abutment.

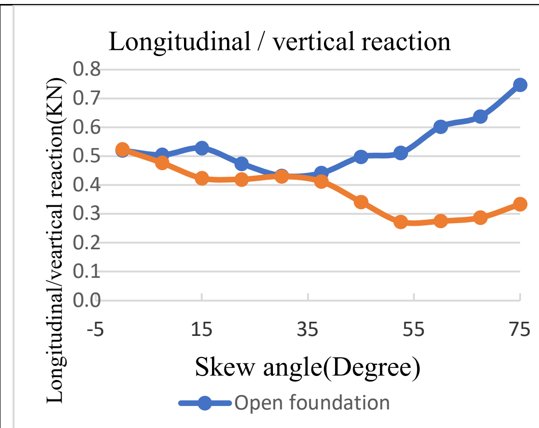

Graph 22. Comparison on longitudinal/vertical base shear w.r.t. skew with open or pile foundation and with earth behind abutment.

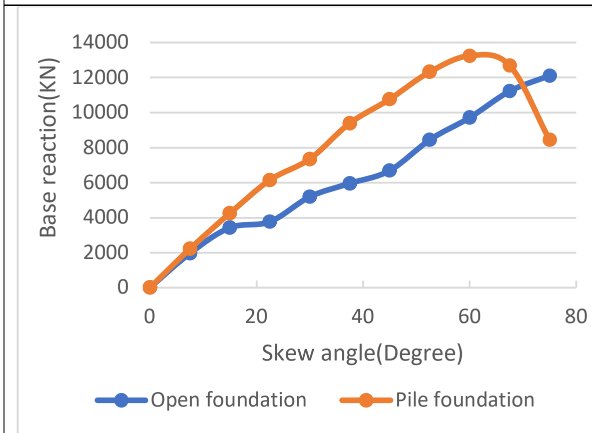

Graph 23. Comparison on transverse base shear w.r.t. skew with open or pile foundation and with earth behind abutment.

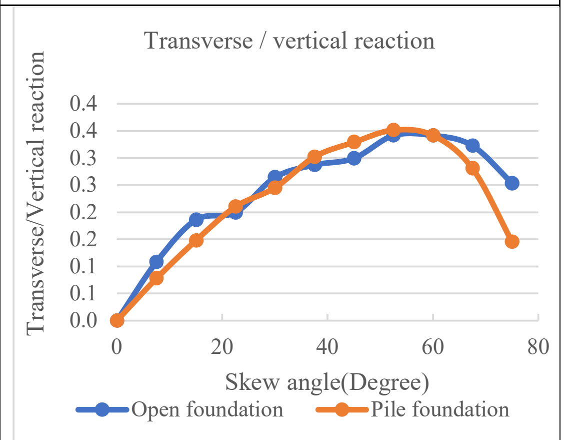

Graph 24. Comparison on transverse/vertical base shear w.r.t. skew with open or pile foundation and with earth behind abutment.

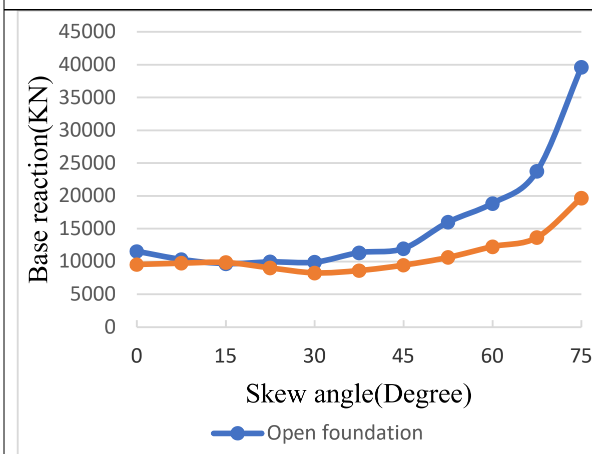

Graph 25. Comparison on longitudinal base shear w.r.t. skew with open or pile foundation and without earth behind abutment.

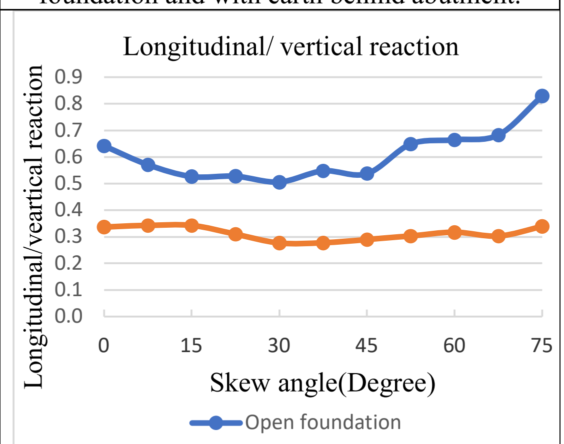

Graph 26. Comparison on longitudinal/vertical base shear w.r.t. skew with open or pile foundation and without earth behind abutment.

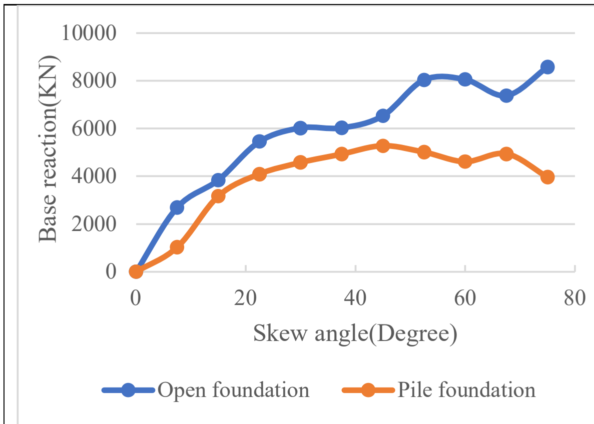

Graph 27. Comparison on transverse base shear w.r.t. skew with open or pile foundation and without earth behind abutment.

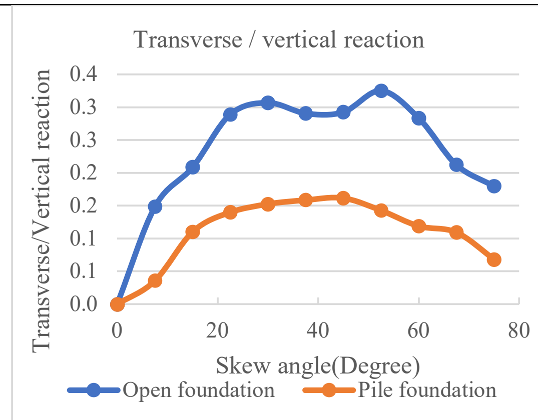

Graph 28. Comparison on transverse/vertical base shear w.r.t. skew with open or pile foundation and without earth behind abutment.

4.2.3.2 Variation with skew angle in transverse seismic case

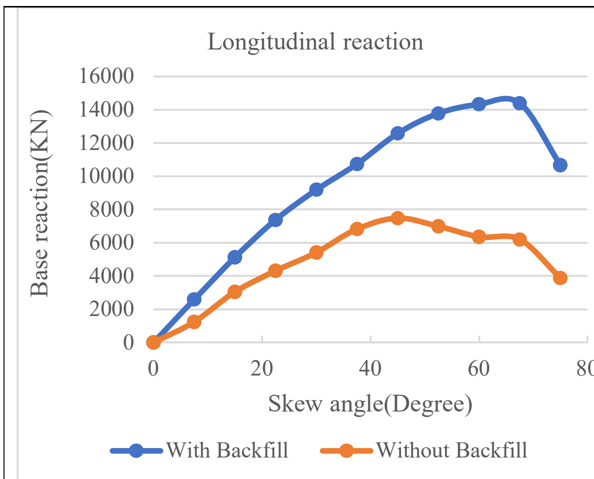

Graph 29. Variation on longitudinal base shear w.r.t. skew with pile foundation and with or without earth behind abutment.

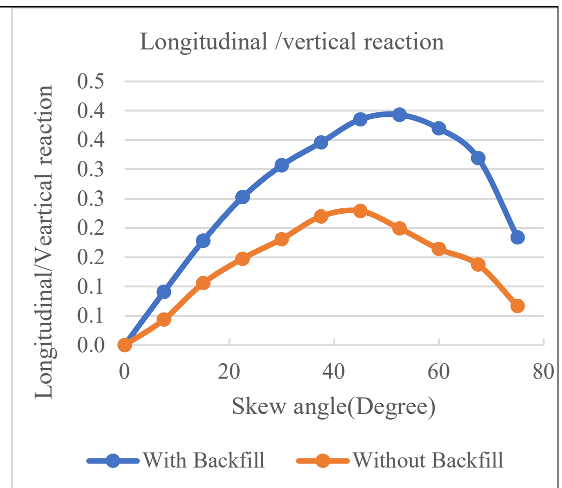

Graph 30. Variation on longitudinal base shear/vertical w.r.t. skew with pile foundation and with or without earth behind abutment.

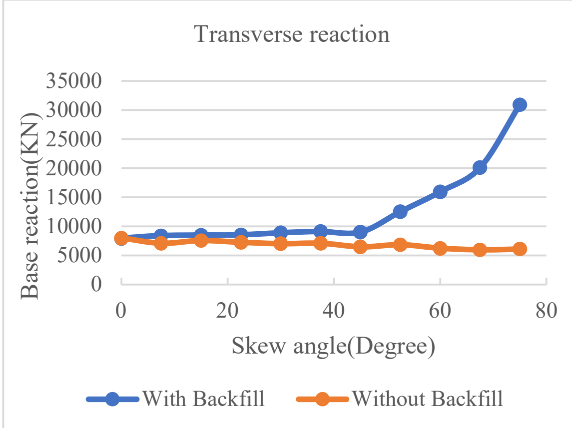

Graph 31. Variation on transverse base shear w.r.t. skew with pile foundation and with or without earth behind abutment.

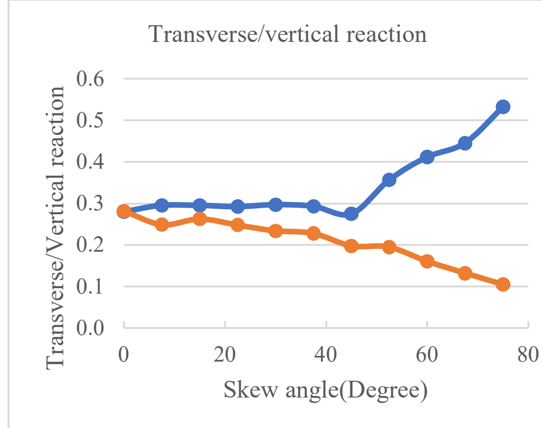

Graph 32. Variation on transverse base shear/vertical w.r.t. skew with pile foundation and with or without earth behind abutment.

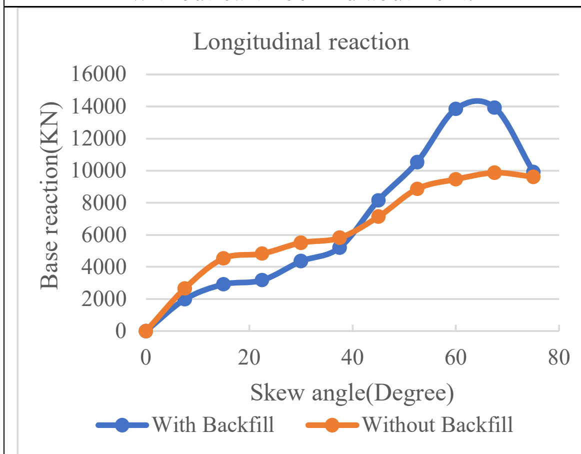

Graph 33. Variation on longitudinal base shear w.r.t. skew with open foundation and with or without earth behind abutment.

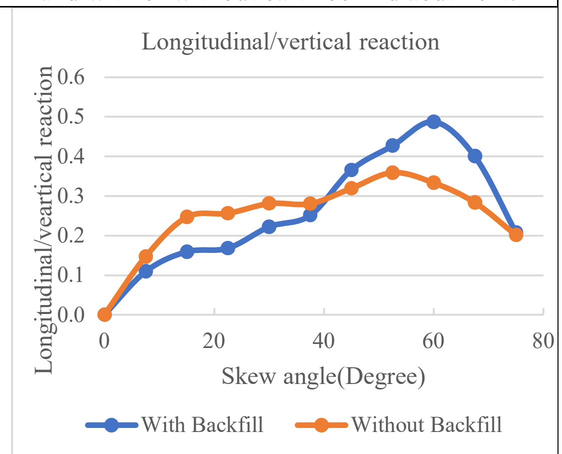

Graph 34. Variation on longitudinal base shear/vertical w.r.t. skew with open foundation and with or without earth behind abutment.

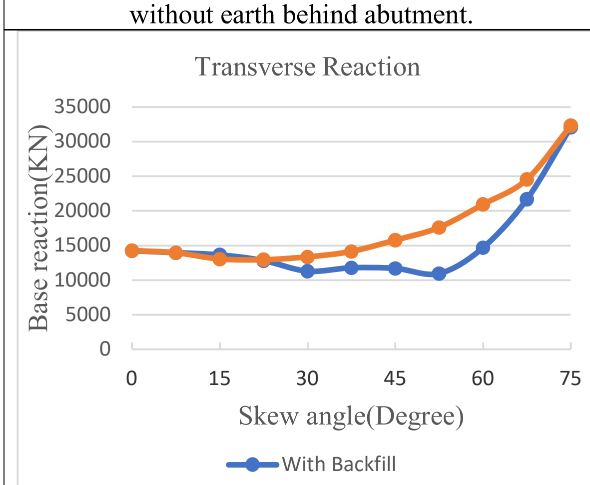

Graph 35. Variation on transverse base shear w.r.t. skew with open foundation and with or without earth behind abutment.

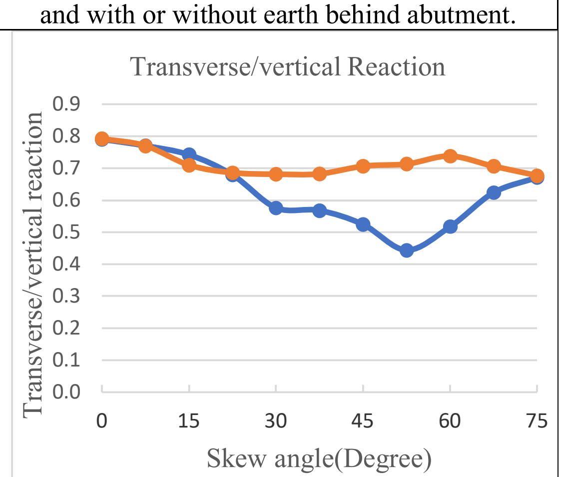

Graph 36. Variation on transverse base shear/vertical w.r.t. skew with open foundation and with or without earth behind abutment.

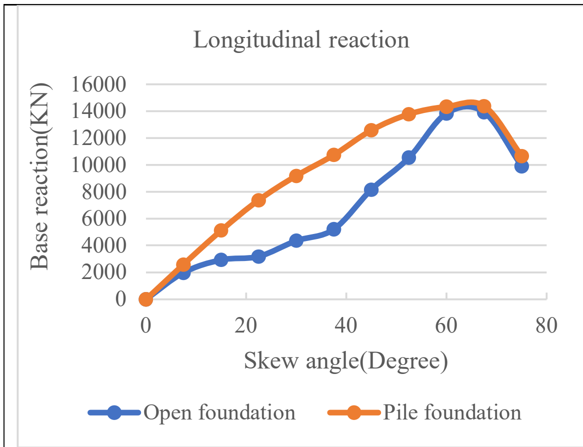

Graph 37. Variation on longitudinal base shear w.r.t. skew with open and pile foundation and with earth behind abutment.

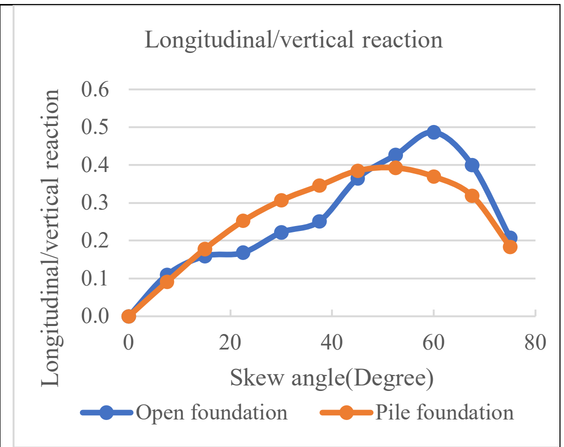

Graph 38. Variation on longitudinal base shear/vertical w.r.t. skew with open and pile foundation and with earth behind abutment.

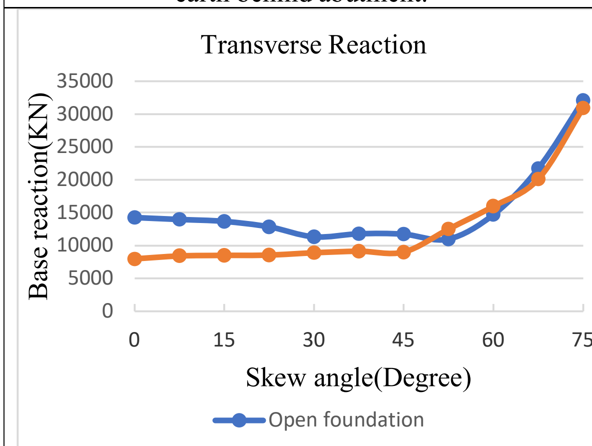

Graph 39. Variation on transverse base shear w.r.t. skew with open and pile foundation and with earth behind abutment.

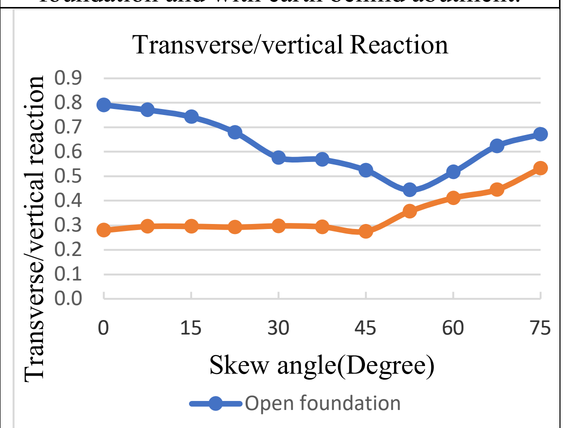

Graph 40. Variation on transverse base shear/vertical w.r.t. skew with open and pile foundation and with earth behind abutment.

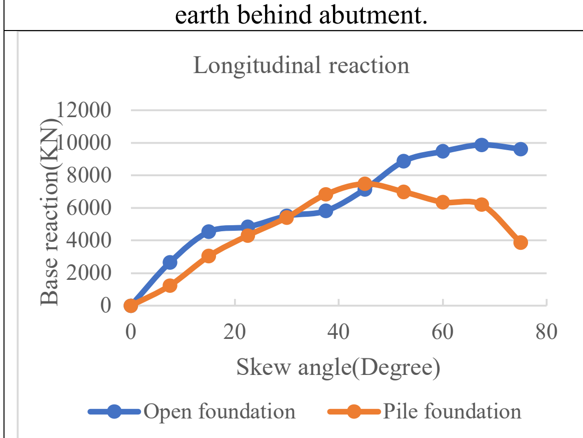

Graph 41. Variation on longitudinal base shear w.r.t. skew with open and pile foundation and without earth behind abutment.

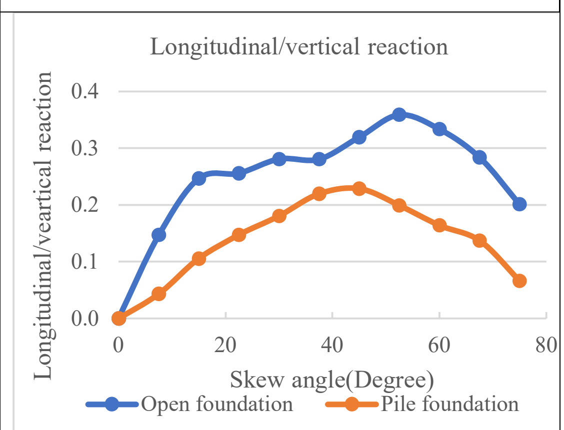

Graph 42. Variation on longitudinal base shear/vertical w.r.t. skew with open and pile foundation and without earth behind abutment.

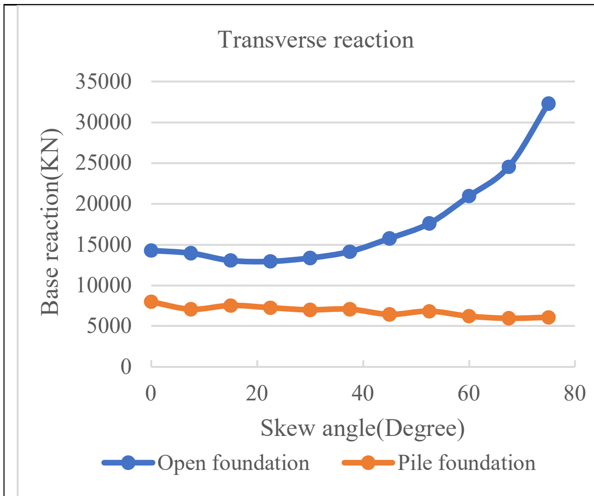

Graph 43. Variation on transverse base shear w.r.t. skew with open and pile foundation and without earth behind abutment.

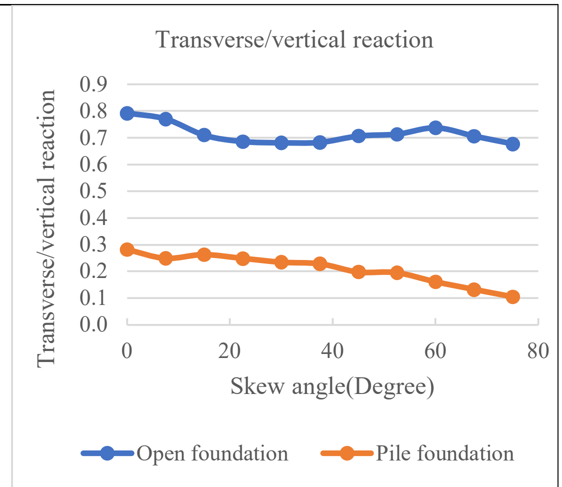

Graph 44. Variation on transverse base shear/vertical w.r.t. skew with open and pile foundation and without earth behind abutment.

4.2.3.3 Variation with curvature in longitudinal seismic case

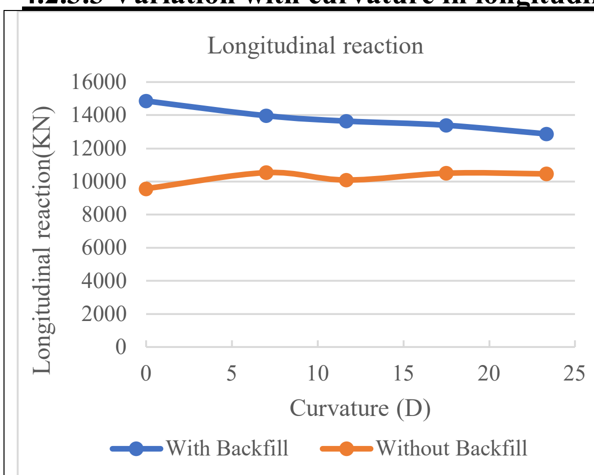

Graph 45. Variation on longitudinal base shear w.r.t. curvature with pile foundation and with or without earth behind abutment.

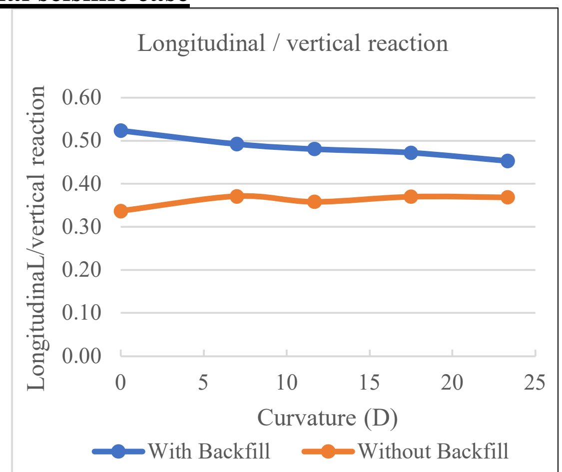

Graph 46. Variation on longitudinal base shear/vertical w.r.t. curvature with pile foundation and with or without earth behind abutment.

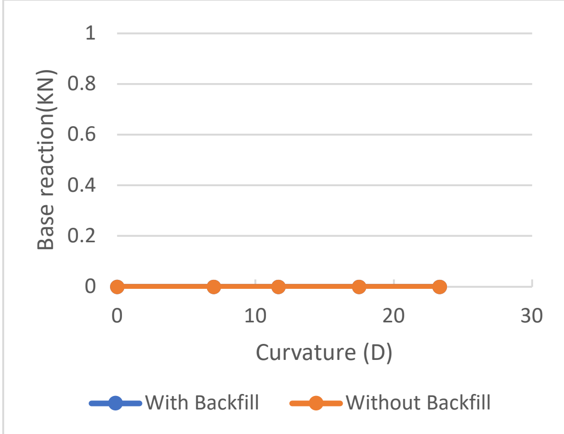

Graph 47. Variation on transverse base shear w.r.t. curvature with pile foundation and with or without earth behind abutment.

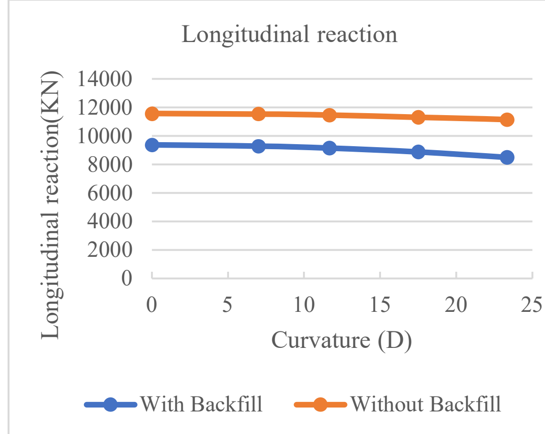

Graph 48. Variation on longitudinal base shear w.r.t. curvature with open foundation and with or without earth behind abutment.

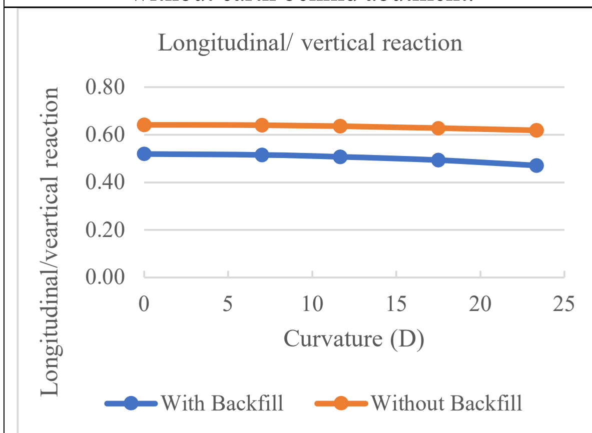

Graph 49. Variation on longitudinal base shear/vertical w.r.t. curvature with open foundation and with or without earth behind abutment.

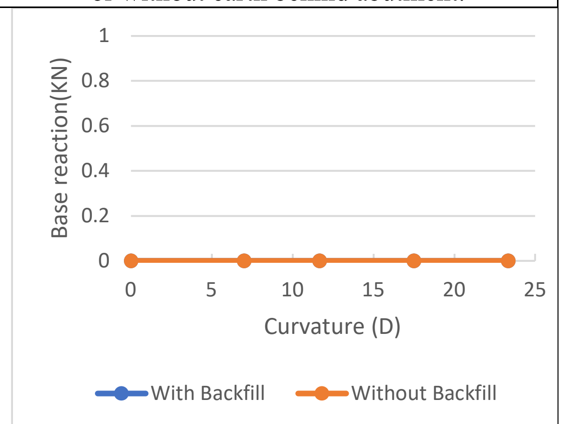

Graph 50. Variation on transverse base shear w.r.t. curvature with open foundation and with or without earth behind abutment.

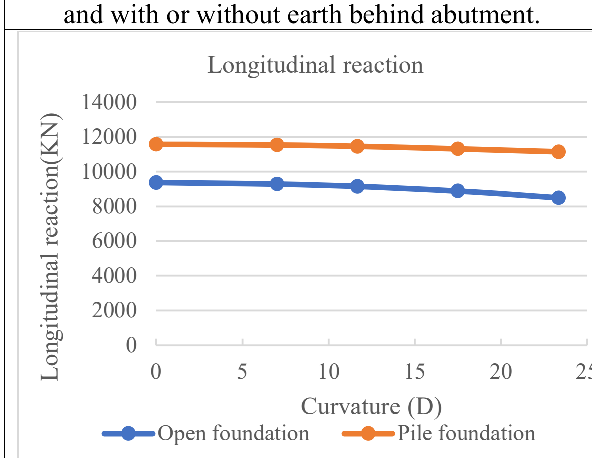

Graph 51. Variation on longitudinal base shear w.r.t. curvature with open and pile foundation and with earth behind abutment.

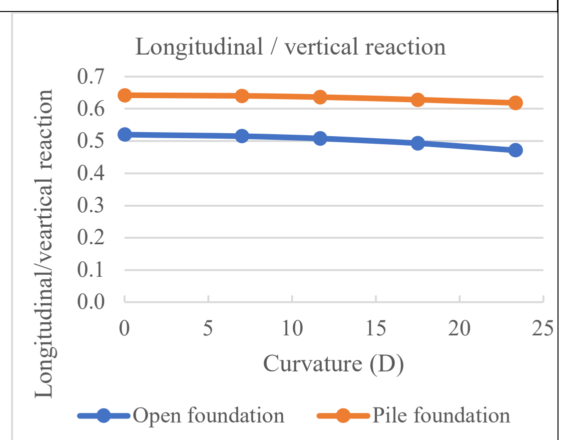

Graph 52. Variation on longitudinal base shear /vertical w.r.t. curvature with open and pile foundation and with earth behind abutment.

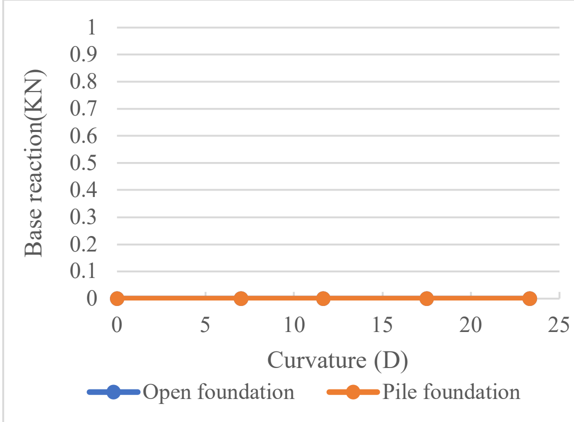

Graph 53. Variation on transverse base shear w.r.t. curvature with open and pile foundation and with earth behind abutment.

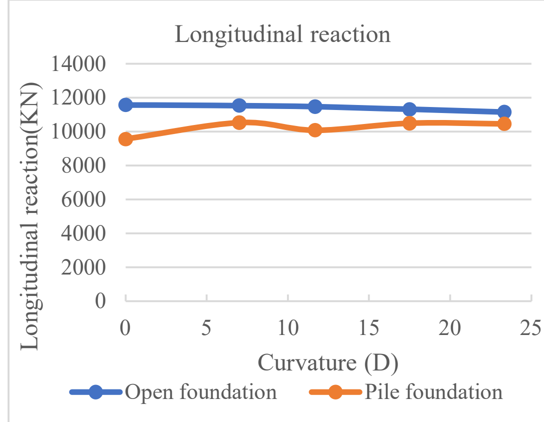

Graph 54. Variation on longitudinal base shear w.r.t. curvature with open and pile foundation and without earth behind abutment.

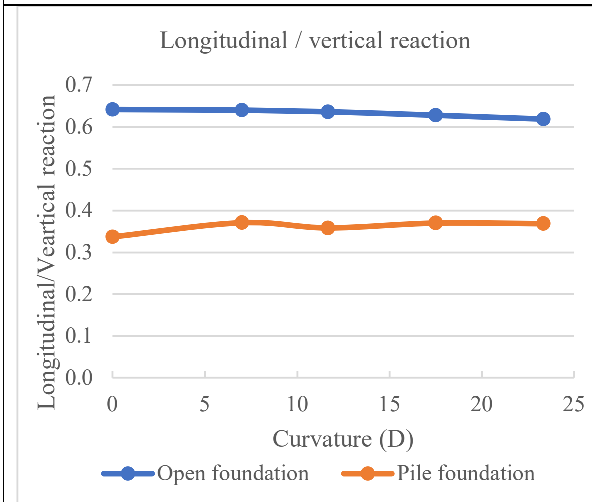

Graph 55. Variation on longitudinal base shear/vertical w.r.t. curvature with open and pile foundation and without earth behind abutment.

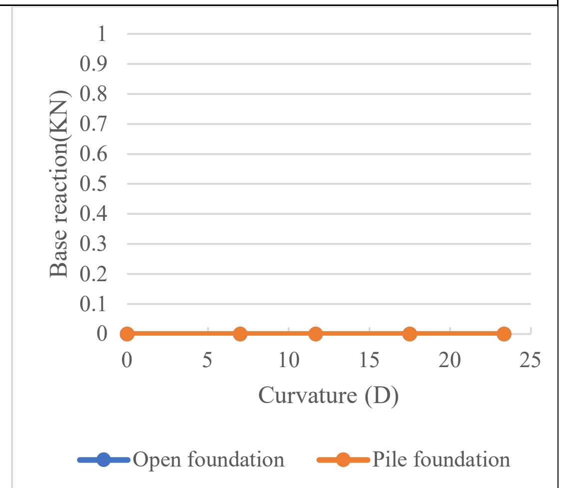

Graph 56. Variation on transverse base shear w.r.t. curvature with open and pile foundation and without earth behind abutment.

4.2.3.4 Variation with curvature in transverse seismic case

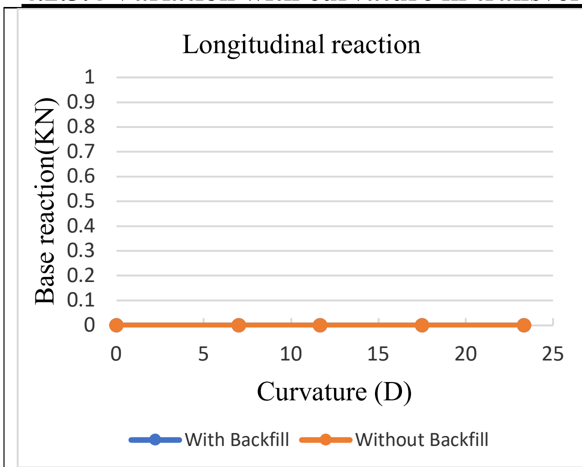

Graph 57. Variation on longitudinal base shear w.r.t. curvature with pile foundation and with or without earth behind abutment.

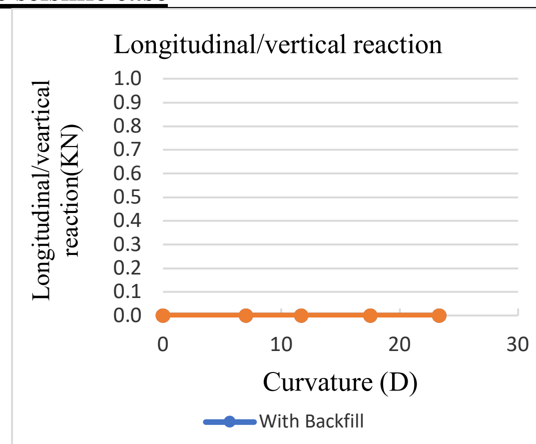

Graph 58. Variation on longitudinal base shear/vertical w.r.t. curvature with pile foundation and with or without earth behind abutment.

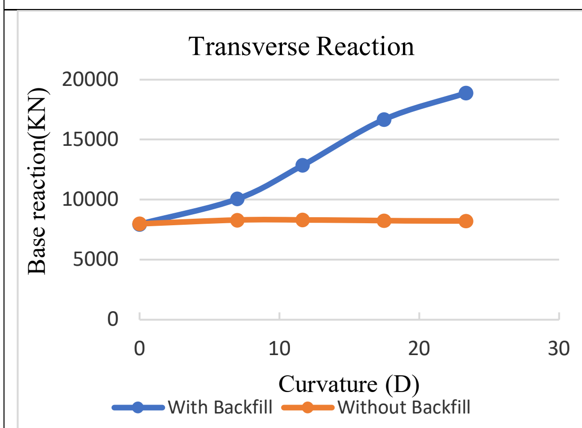

Graph 59. Variation on transverse base shear w.r.t. curvature with pile foundation and with or without earth behind abutment.

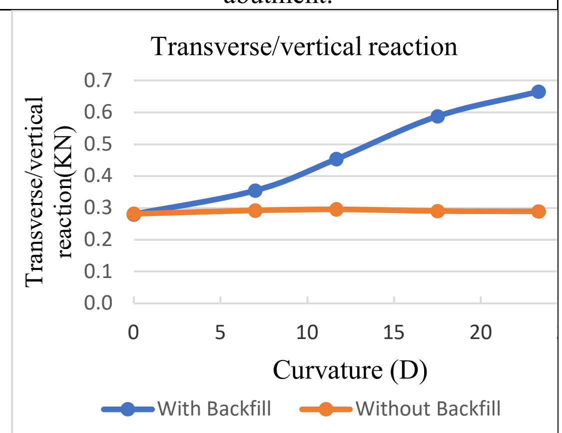

Graph 60. Variation on longitudinal base shear w.r.t. curvature with pile foundation and with or without earth behind abutment.

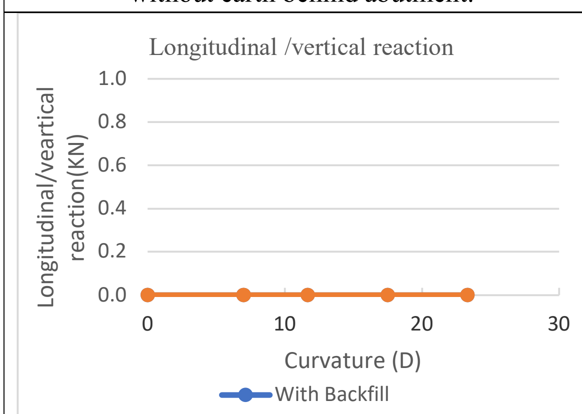

Graph 61. Variation on longitudinal base shear/vertical w.r.t. curvature with open foundation and with or without earth behind abutment.

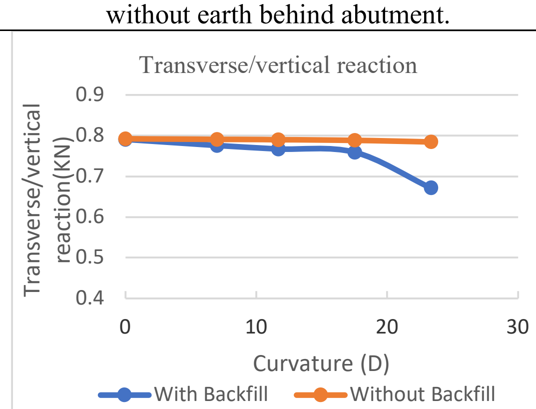

Graph 62. Variation on transverse base shear w.r.t. curvature with open foundation and with or without earth behind abutment.

Hence from the above graphs following observations can be made: -

For longitudinal seismic case

- Longitudinal base shear/vertical reaction decreases with increase of skew angle for pile foundation. The ratio initially decreases then increases with increase of skew angle for bridge with open foundation. For bridge with backfill the rate of decrease is more than bridge without backfill.
- Transverse base shear/vertical reaction initially increases then decreases with increase of skew angle. For bridge with backfill the rate of increase is more than bridge without backfill.
- Longitudinal base shear/vertical reaction is more for bridge with pile foundation. Transverse base shear/vertical reaction is more for bridge with open foundation
- Longitudinal base shear/vertical reaction is more for bridge with backfill than bridge without backfill.
- Longitudinal base shear/vertical reaction decreases slightly with increase of curvature for bridge with backfill. For bridge without backfill it is almost same.
- For bridge with open foundation longitudinal reaction is more than bridge with pile foundation.
- Transverse base shear is zero for bridge of all curvature without skew.

For transverse seismic case

- Longitudinal base shear/vertical reaction is more for bridge with backfill than bridge without backfill. The same initially increases with increase of skew angle then decreases. The same is more for bridge with open foundation than bridge with pile foundation.
- Transverse base shear/vertical reaction increases in case of bridge with backfill and decreases for bridge without backfill for bridge with pile foundation. It is more for bridge with open foundation than bridge with pile foundation.
- Longitudinal base shear is zero for bridge of all curvature without skew.
- For pile foundation with backfill transverse/vertical reaction increases with curvature. For open foundation it decreases.

4.2.4 Variation of the moment at side wall in longitudinal seismic condition

4.2.4.1 Variation of longitudinal moment at top of side wall with skew angle in longitudinal seismic

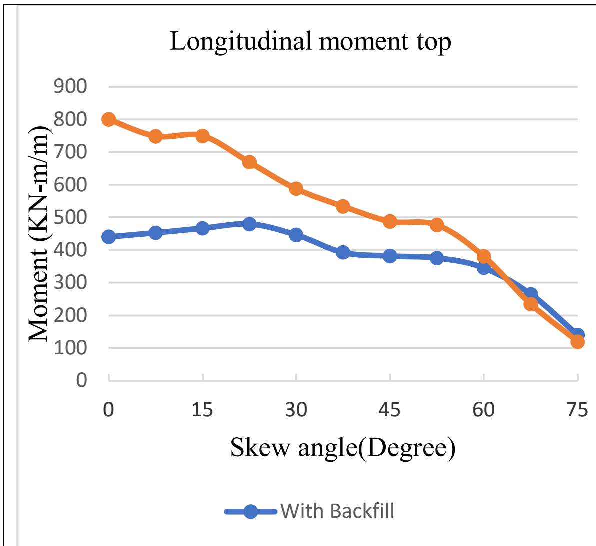

Graph 63. Variation of longitudinal moment at top of side wall w.r.t. skew with pile foundation with or with earth behind abutment.

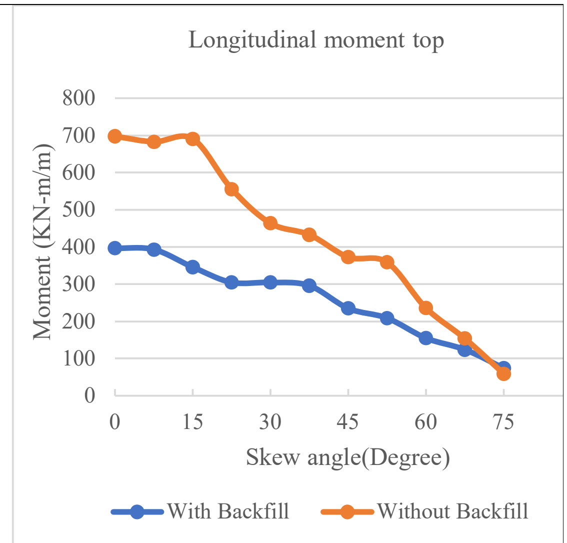

Graph 64. Variation of longitudinal moment at top of side wall w.r.t. skew with open foundation with or without earth behind abutment.

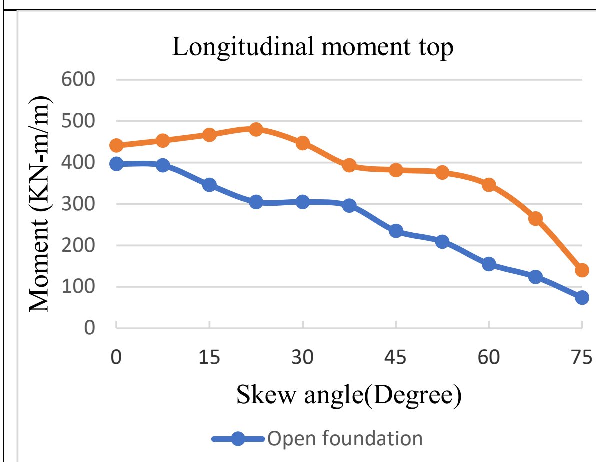

Graph 65. Variation of longitudinal moment at top of side wall w.r.t. skew between open and pile foundation with earth behind abutment.

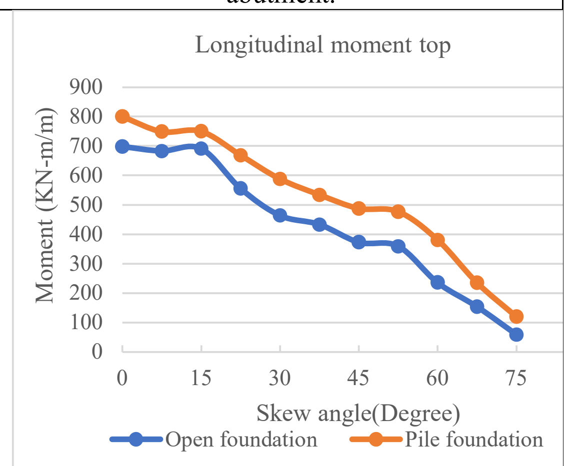

Graph 66. Variation of longitudinal moment at top of side wall w.r.t. skew between open and pile foundation without earth behind abutment.

4.2.4.2 Variation of longitudinal moment at top of side wall with curvature in longitudinal seismic

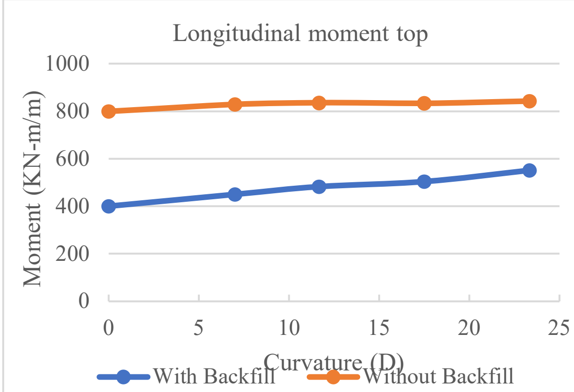

Graph 67. Variation of longitudinal moment at top of side wall w.r.t. curvature with pile foundation with or with earth behind abutment.

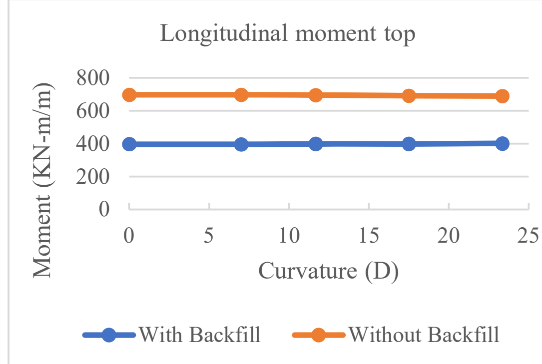

Graph 68. Variation of longitudinal moment at top of side wall w.r.t. curvature with open foundation with or without earth behind abutment.

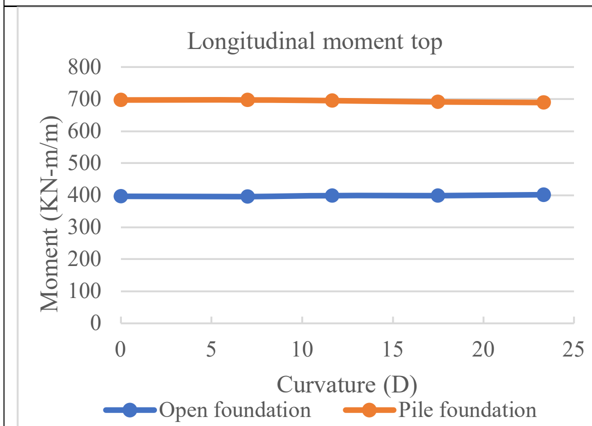

Graph 69. Variation of longitudinal moment at top of side wall w.r.t. curvature between open and pile foundation with earth behind abutment.

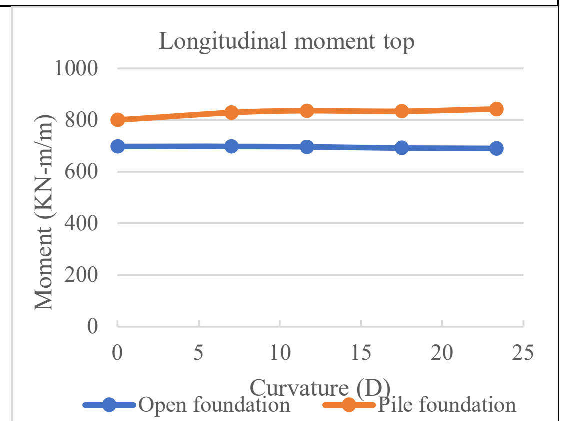

Graph 70. Variation of longitudinal moment at top of side wall w.r.t. curvature between open and pile foundation without earth behind abutment.

4.2.4.3 Variation of transverse moment at top of side wall with skew angle in longitudinal seismic

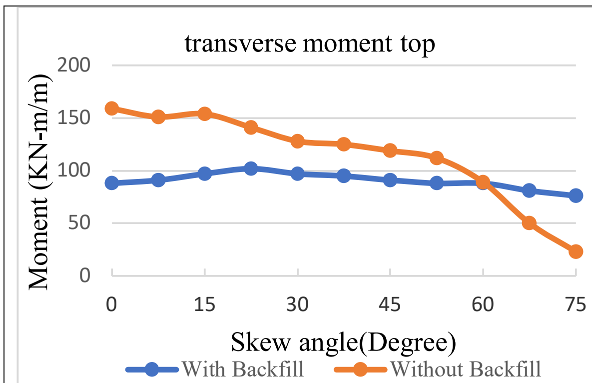

Graph 71. Variation of transverse moment at top of side wall w.r.t. skew with pile foundation with or with earth behind abutment.

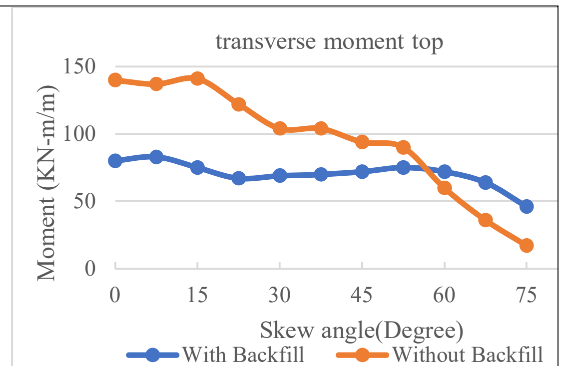

Graph 72. Variation of transverse moment at top of side wall w.r.t. skew with open foundation with or without earth behind abutment.

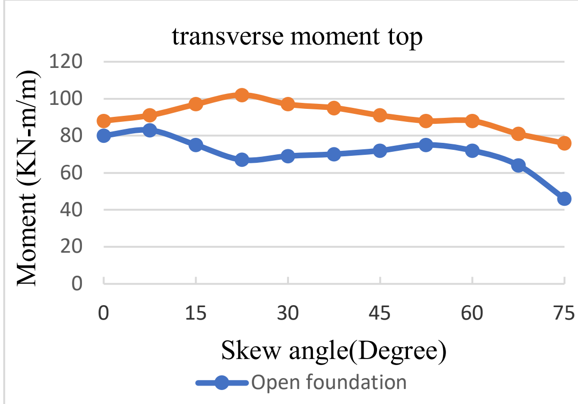

Graph 73. Variation of transverse moment at top of side wall w.r.t. skew between open and pile foundation with earth behind abutment.

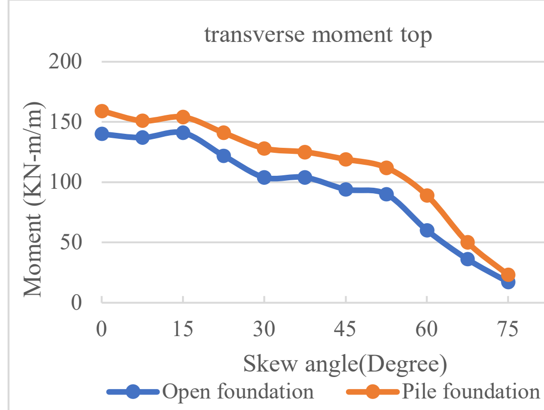

Graph 74. Variation of transverse moment at top of side wall w.r.t. skew between open and pile foundation without earth behind abutment.

4.2.4.4 Variation of transverse moment at top of side wall with curvature in longitudinal seismic

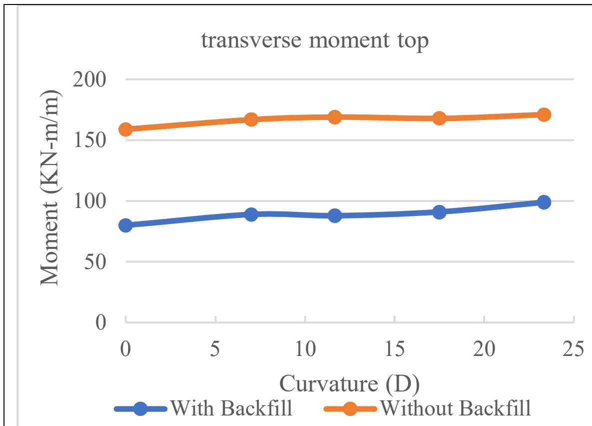

Graph 75. Variation of transverse moment at top of side wall w.r.t. curvature with pile foundation with or with earth behind abutment.

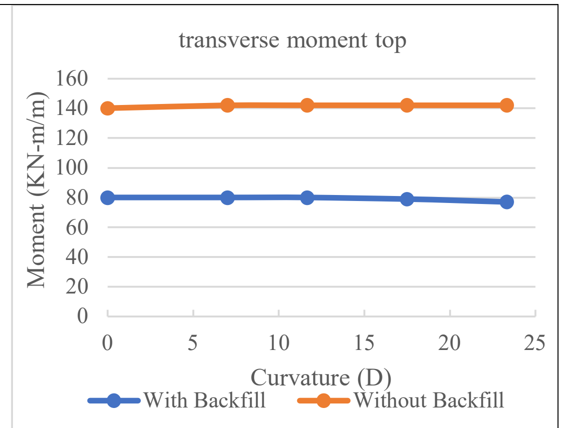

Graph 76. Variation of transverse moment at top of side wall w.r.t. curvature with open foundation with or without earth behind abutment.

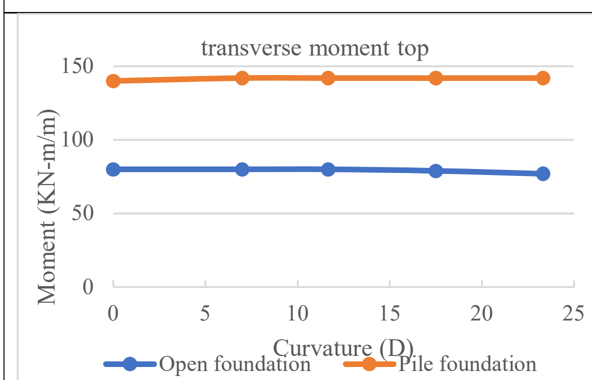

Graph 77. Variation of transverse moment at top of side wall w.r.t. curvature between open and pile foundation with earth behind abutment.

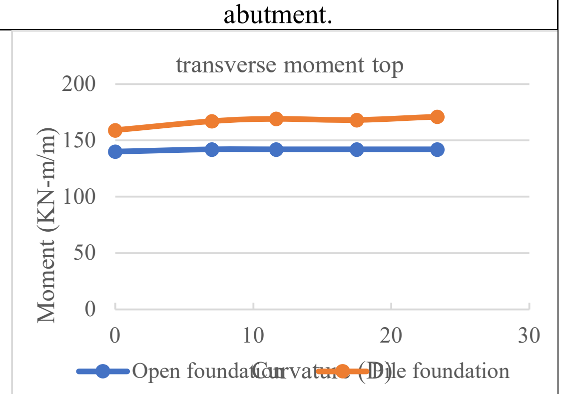

Graph 78. Variation of transverse moment at top of side wall w.r.t. curvature between open and pile foundation without earth behind abutment.

4.2.4.5 Variation of torsional moment at top of side wall with skew angle in longitudinal seismic

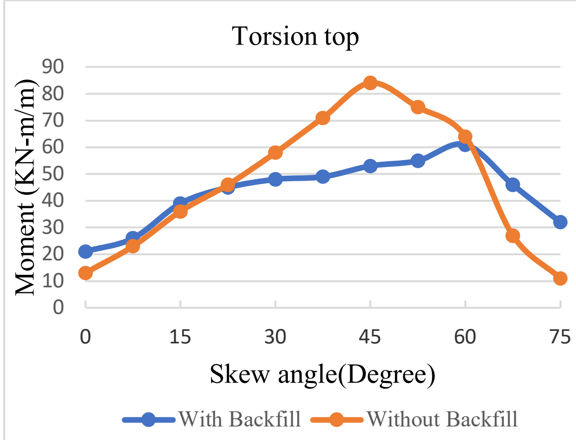

Graph 79. Variation of torsion at top of side wall w.r.t. skew with pile foundation with or with earth behind abutment.

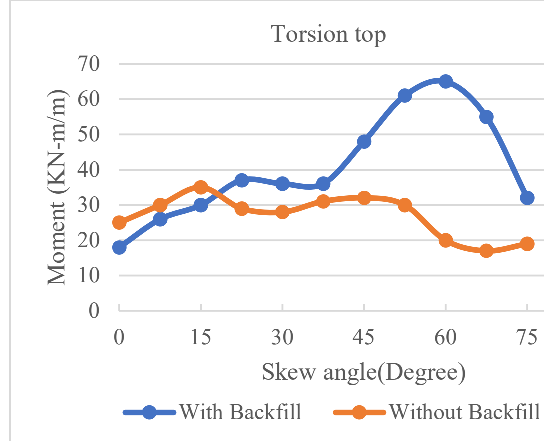

Graph 80. Variation of torsion at top of side wall w.r.t. skew with open foundation with or without earth behind abutment.

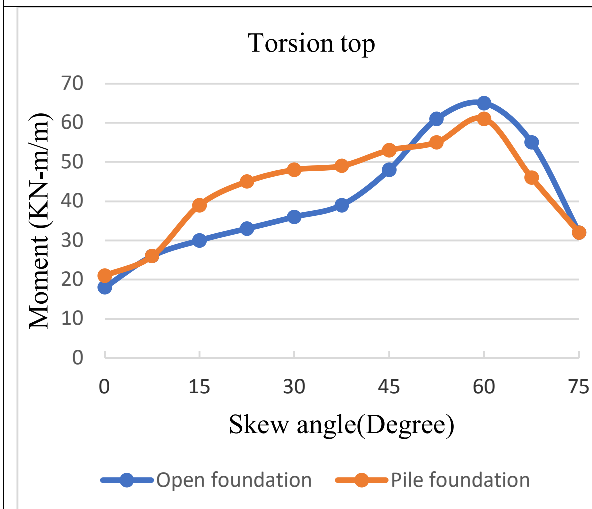

Graph 81. Variation of torsion at top of side wall w.r.t. skew between open and pile foundation with earth behind abutment.

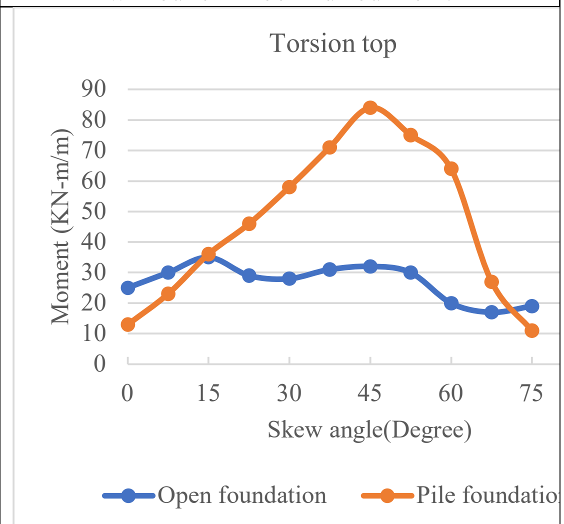

Graph 82. Variation of torsion at top of side wall w.r.t. skew between open and pile foundation without earth behind abutment.

4.2.4.6 Variation of torsional moment at top of side wall with curvature in longitudinal seismic

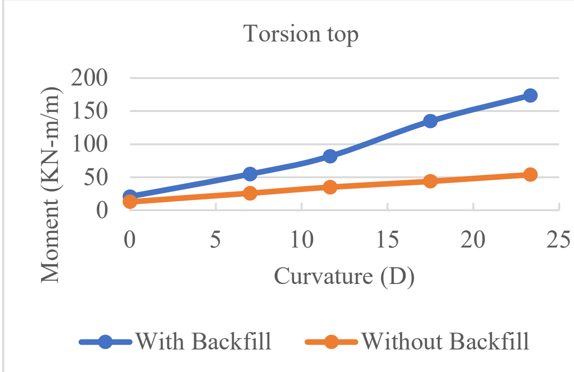

Graph 83. Variation of torsion at top of side wall w.r.t. curvature with pile foundation with or with earth behind abutment.

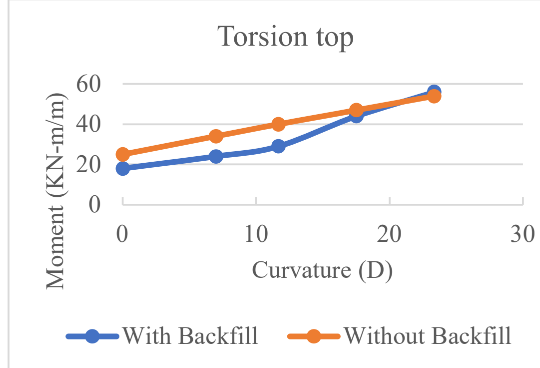

Graph 84. Variation of torsion at top of side wall w.r.t. curvature with open foundation with or without earth behind abutment.

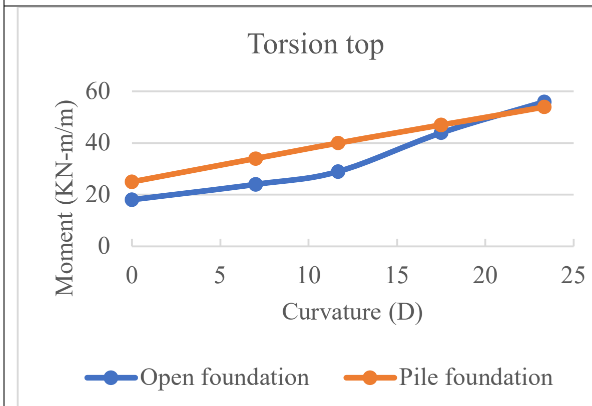

Graph 85. Variation of torsion at top of side wall w.r.t. curvature between open and pile foundation with earth behind abutment.

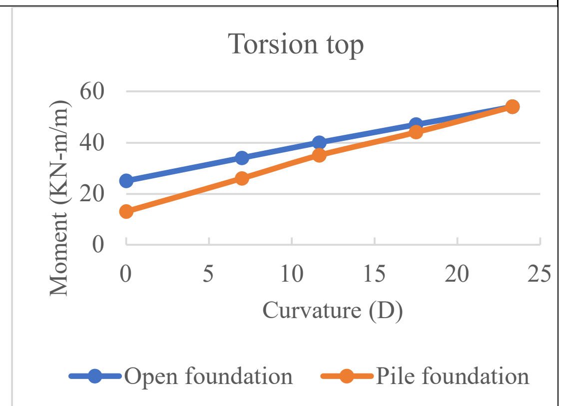

Graph 86. Variation of torsion at top of side wall w.r.t. curvature between open and pile foundation without earth behind abutment.

4.2.4.7 Variation of longitudinal moment at bottom of side wall with skew angle in longitudinal seismic

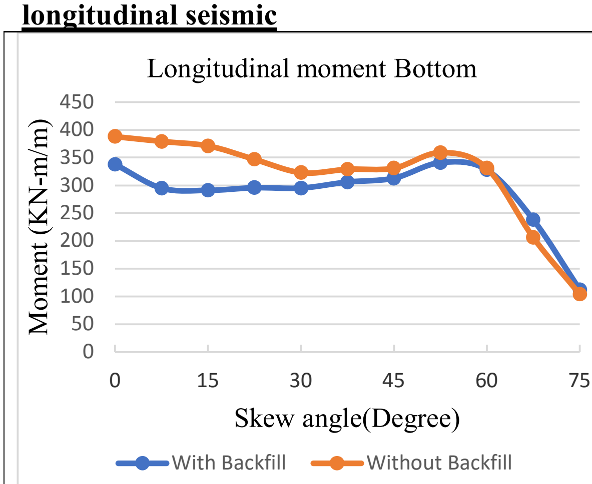

Graph 87. Variation of longitudinal moment at bottom of side wall w.r.t. skew with pile foundation with or with earth behind abutment.

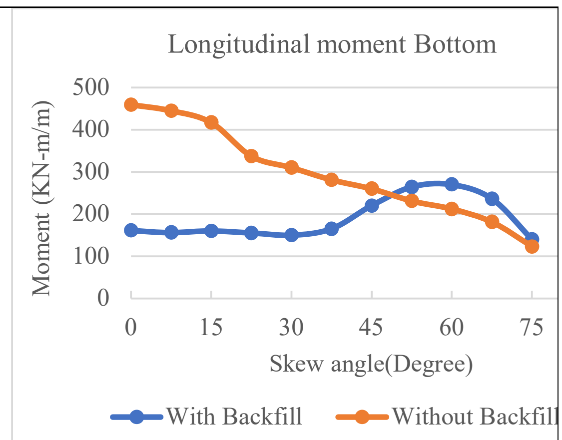

Graph 88. Variation of longitudinal moment at bottom of side wall w.r.t. skew with open foundation with or without earth behind abutment.

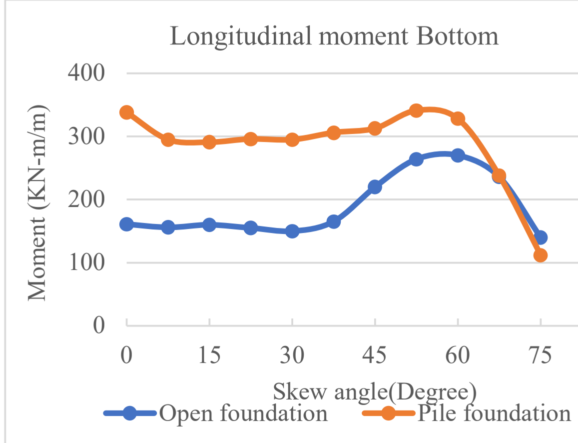

Graph 89. Variation of longitudinal moment at bottom of side wall w.r.t. skew between open and pile foundation with earth behind abutment.

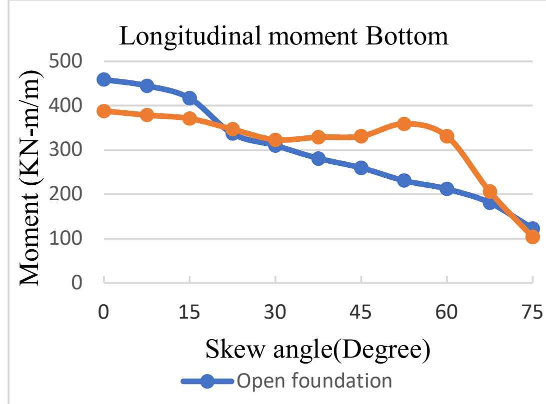

Graph 90. Variation of longitudinal moment at bottom of side wall w.r.t. skew between open and pile foundation without earth behind abutment.

4.2.4.8 Variation of longitudinal moment at bottom of side wall with curvature in longitudinal seismic

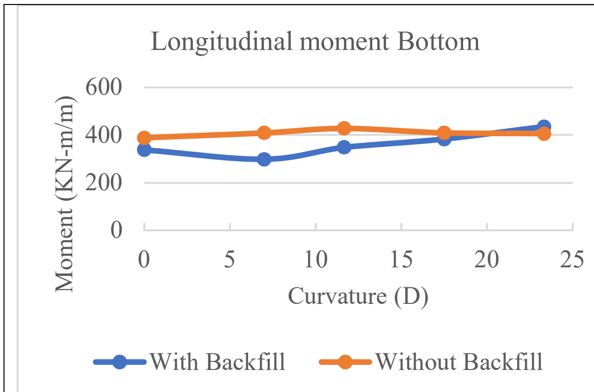

Graph 91. Variation of longitudinal moment at bottom of side wall w.r.t. curvature with pile foundation with or with earth behind abutment.

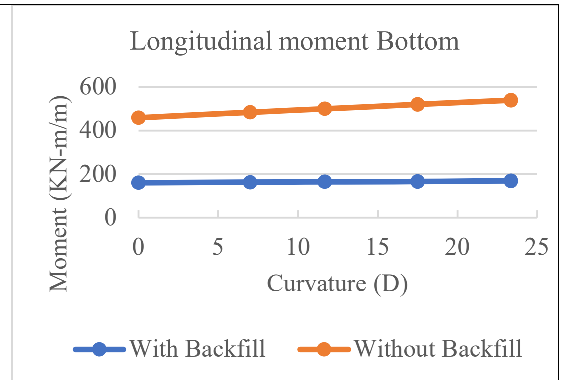

Graph 92. Variation of longitudinal moment at bottom of side wall w.r.t. curvature with open foundation with or without earth behind abutment.

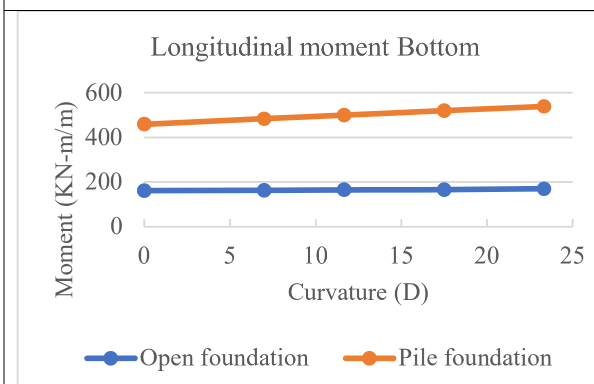

Graph 93. Variation of longitudinal moment at bottom of side wall w.r.t. curvature between open and pile foundation with earth behind abutment.

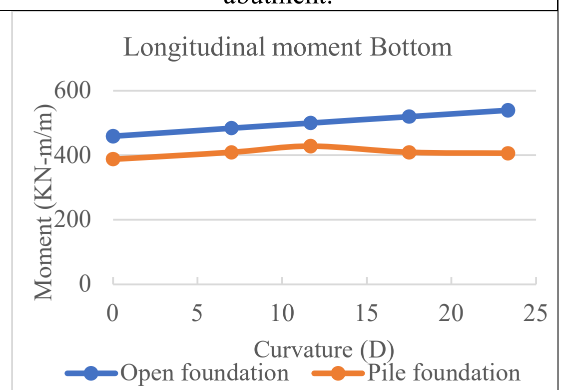

Graph 94. Variation of longitudinal moment at bottom of side wall w.r.t. curvature between open and pile foundation without earth behind abutment.

4.2.4.9 Variation of transverse moment at bottom of side wall with skew angle in longitudinal seismic

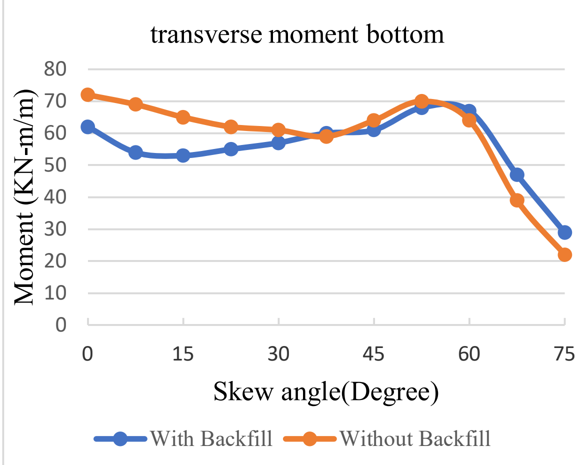

Graph 95. Variation of transverse moment at bottom of side wall w.r.t. skew with pile foundation with or with earth behind abutment.

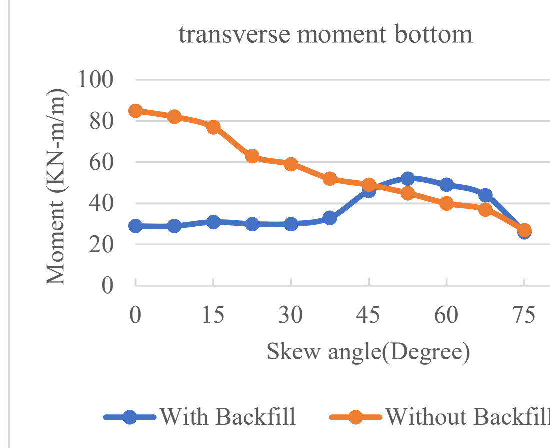

Graph 96. Variation of transverse moment at bottom of side wall w.r.t. skew with open foundation with or without earth behind abutment.

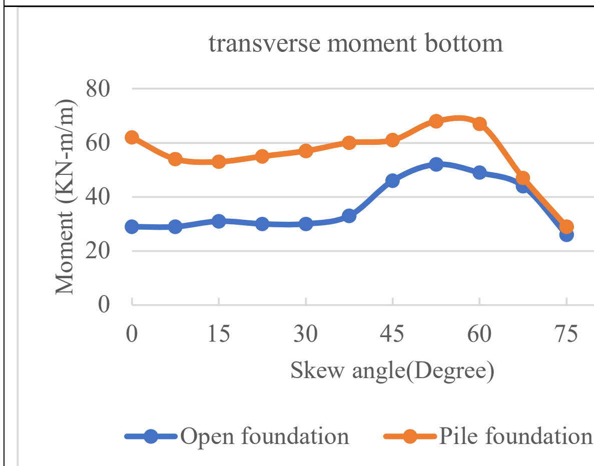

Graph 97. Variation of transverse moment at bottom of side wall w.r.t. skew between open and pile foundation with earth behind abutment.

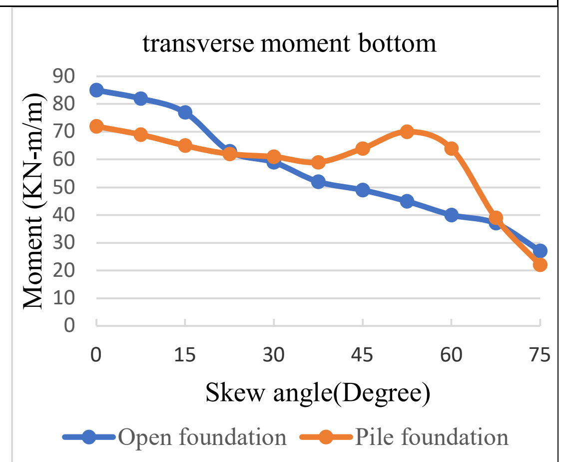

Graph 98. Variation of transverse moment at bottom of side wall w.r.t. skew between open and pile foundation without earth behind abutment.

4.2.4.10 Variation of transverse moment at bottom of side wall with curvature in longitudinal seismic

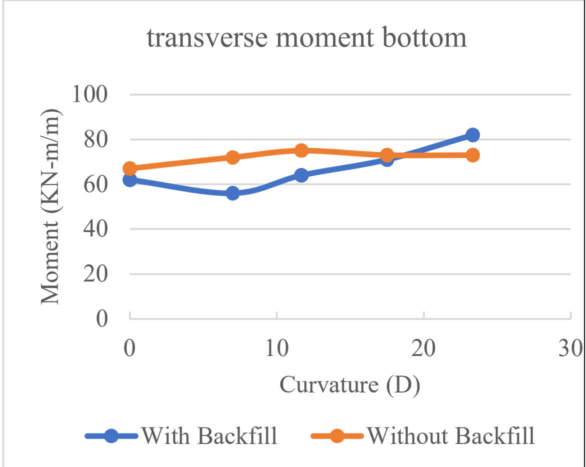

Graph 99. Variation of transverse moment at bottom of side wall w.r.t. curvature with pile foundation with or with earth behind abutment.

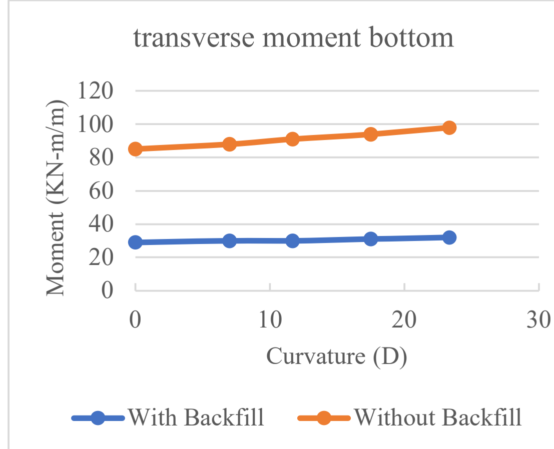

Graph 100. Variation of transverse moment at bottom of side wall w.r.t. curvature with open foundation with or without earth behind abutment.

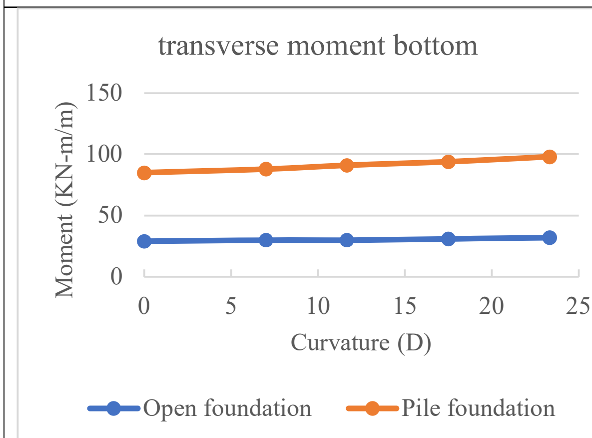

Graph 101. Variation of transverse moment at bottom of side wall w.r.t. curvature between open and pile foundation with earth behind abutment.

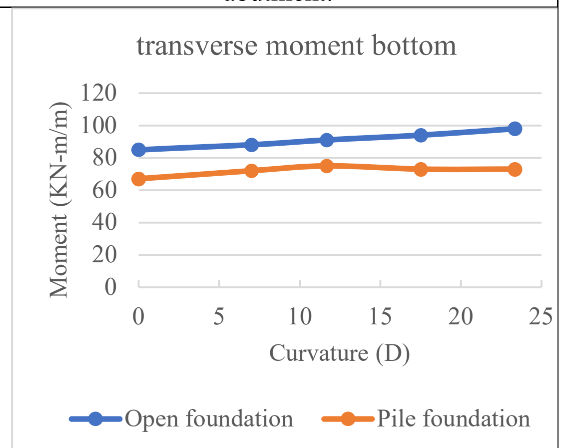

Graph 102. Variation of transverse moment at bottom of side wall w.r.t. curvature between open and pile foundation without earth behind abutment.

4.2.4.11 Variation of torsional moment at bottom of side wall with skew angle in longitudinal seismic

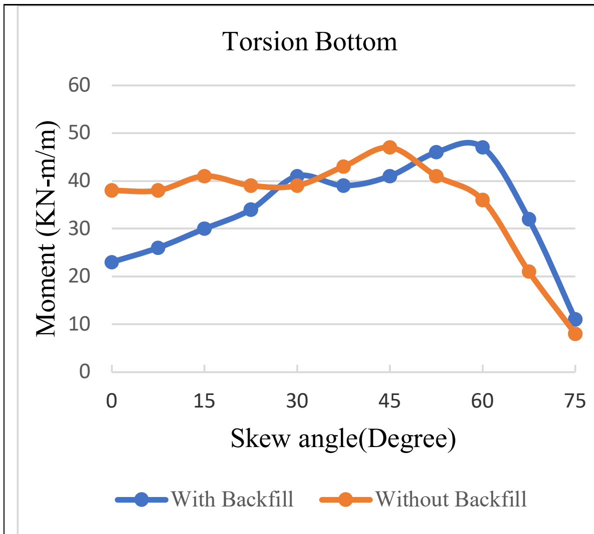

Graph 103. Variation of torsion at bottom of side wall w.r.t. skew with pile foundation with or with earth behind abutment.

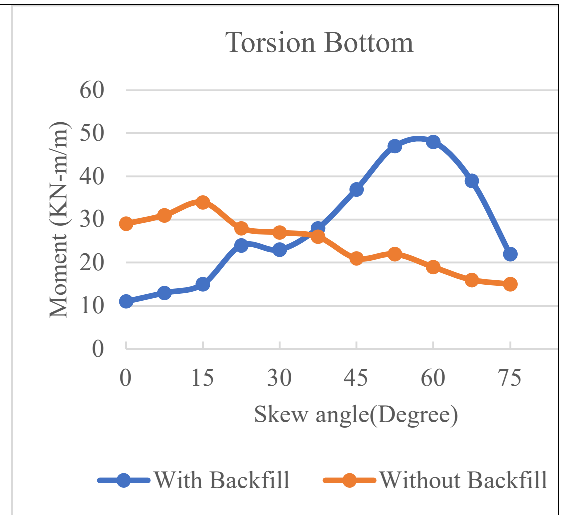

Graph 104. Variation of torsion at bottom of side wall w.r.t. skew with open foundation with or without earth behind abutment.

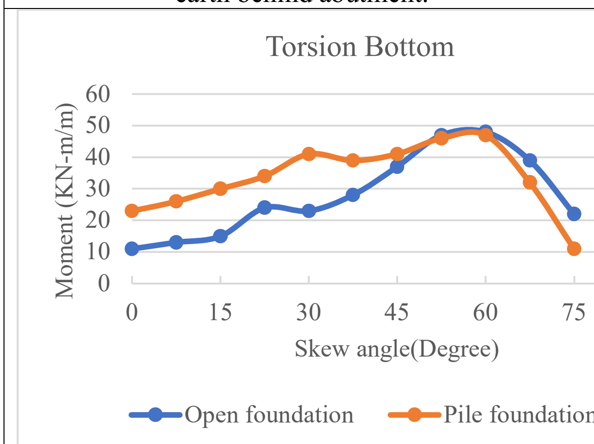

Graph 105. Variation of torsion at bottom of side wall w.r.t. skew between open and pile foundation with earth behind abutment.

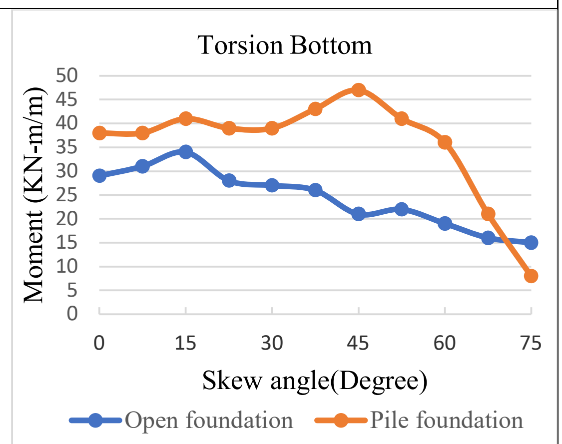

Graph 106. Variation of torsion at bottom of side wall w.r.t. skew between open and pile foundation without earth behind abutment.

4.2.4.12 Variation of torsional moment at bottom of side wall with curvature in longitudinal seismic

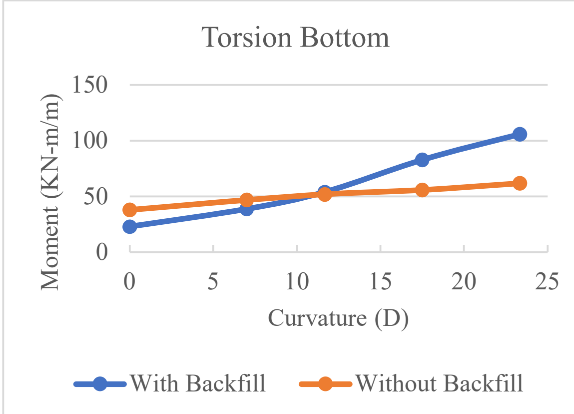

Graph 107. Variation of torsion at bottom of side wall w.r.t. curvature with pile foundation with or with earth behind abutment.

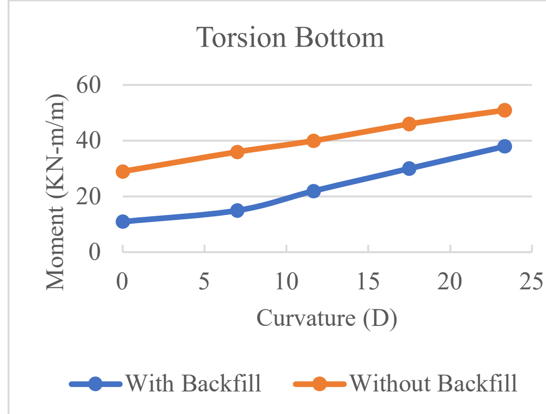

Graph 108. Variation of torsion at bottom of side wall w.r.t. curvature with open foundation with or without earth behind abutment.

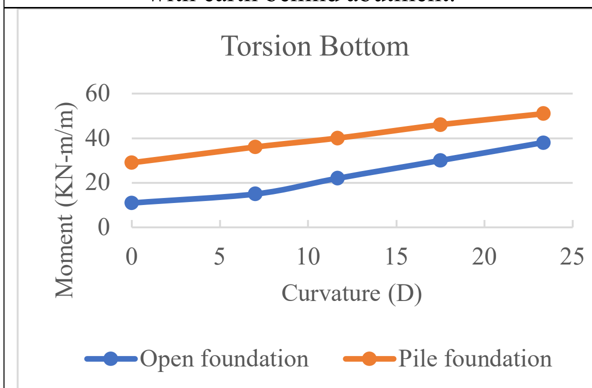

Graph 109. Variation of torsion at bottom of side wall w.r.t. curvature between open and pile foundation with earth behind abutment.

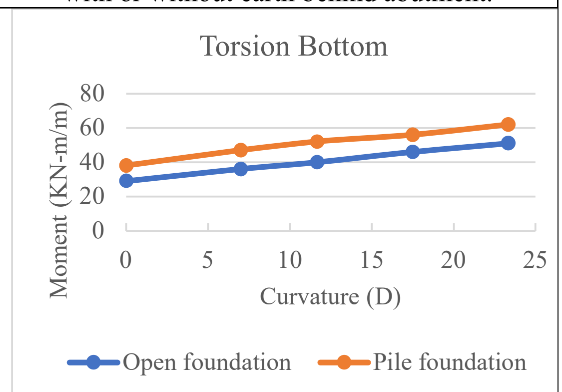

Graph 110. Variation of torsion at bottom of side wall w.r.t. curvature between open and pile foundation without earth behind abutment.

Hence from the above graphs following observations can be made: -

For longitudinal seismic case

- Longitudinal moment at top of side wall decreases with increase of skew angle for both open and pile foundation. The moment is more for bridge without backfill than bridge with backfill. Moment is more for pile foundation than open foundation.
- Longitudinal moment at top of side wall increases with increase of curvature for both open and pile foundation. The moment is more for bridge without backfill than bridge with backfill. Moment is more for pile foundation than open foundation.
- Transverse moment at top of side wall decreases with increase of skew angle for both open and pile foundation. The rate of decrease is more for bridge without backfill. Moment is more for pile foundation than open foundation.
- Transverse moment at top of side wall increases with increase of curvature for pile

foundation. For open foundation it is almost same. The moment is more for bridge without backfill than bridge with backfill.

- Torsion at top of side wall initially increases then decreases with increase of skew angle for both open and pile foundation.
- Torsion at top of side wall increases with increase of curvature for both open and pile foundation. The rate of increase is more for bridge with backfill than bridge without backfill.
- Longitudinal moment at bottom of side wall decreases with increase of skew angle for both open and pile foundation. The rate of decrease is more for bridge without backfill.
- Longitudinal moment at bottom of side wall increases with increase of curvature for both open and pile foundation.
- Transverse moment at bottom of side wall decreases with increase of skew angle for bridge without backfill. For bridge with backfill it increases initially then decreases with increase of skew angle.
- Transverse moment at bottom of side wall increases slightly with increase of curvature.
- Torsion at bottom of side wall initially increases then decreases with increase of skew angle except the bridge with open foundation without backfill. For bridge with open foundation and without backfill torsion decreases with increase of skew angle.
- Torsion at bottom of side wall increases with the increase of curvature. And for curved bridges torsion is more for bridges with pile foundation than open foundation.

4.2.5 Variation of the moment at middle wall in longitudinal seismic condition

4.2.5.1 Variation of longitudinal moment at top of middle wall with skew angle in longitudinal seismic

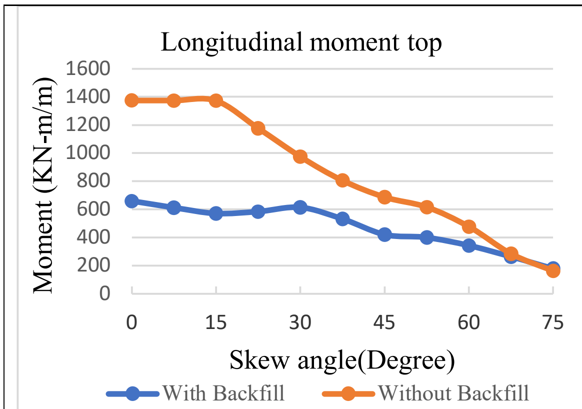

Graph 111. Variation of longitudinal moment at top of middle wall w.r.t. skew with pile foundation with or with earth behind abutment.

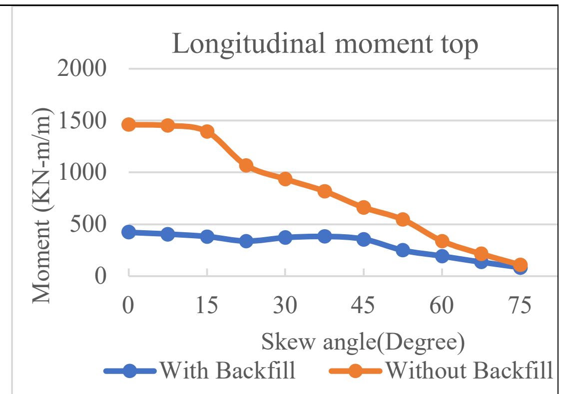

Graph 112. Variation of longitudinal moment at top of middle wall w.r.t. skew with open foundation with or without earth behind abutment.

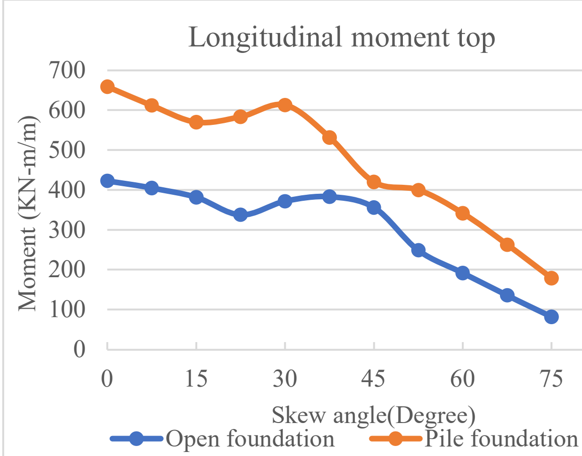

Graph 113. Variation of longitudinal moment at top of middle wall w.r.t. skew between open and pile foundation with earth behind abutment.

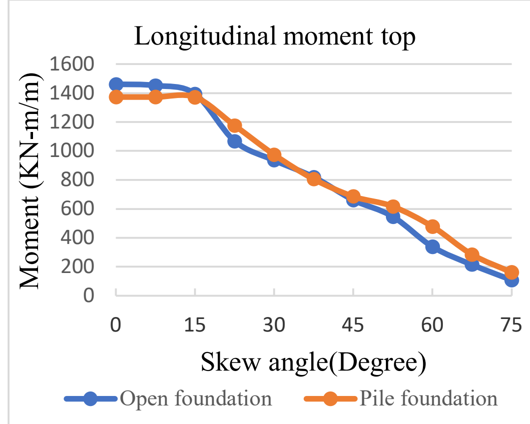

Graph 114. Variation of longitudinal moment at top of middle wall w.r.t. skew between open and pile foundation without earth behind abutment.

4.2.5.2 Variation of longitudinal moment at top of middle wall with curvature in longitudinal seismic

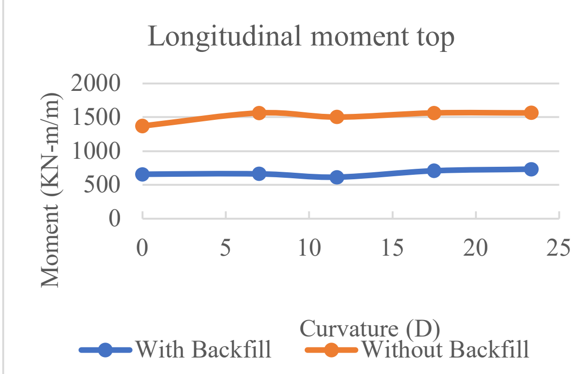

Graph 115. Variation of longitudinal moment at top of middle wall w.r.t. curvature with pile foundation with or with earth behind abutment.

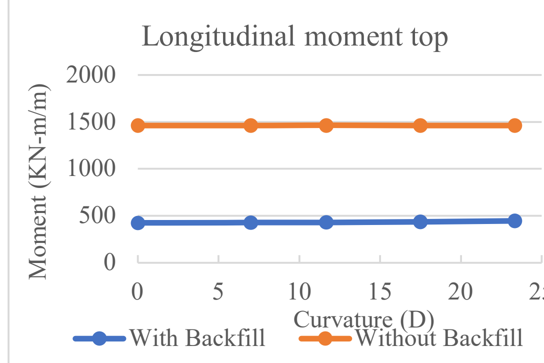

Graph 116. Variation of longitudinal moment at top of middle wall w.r.t. curvature with open foundation with or without earth behind abutment.

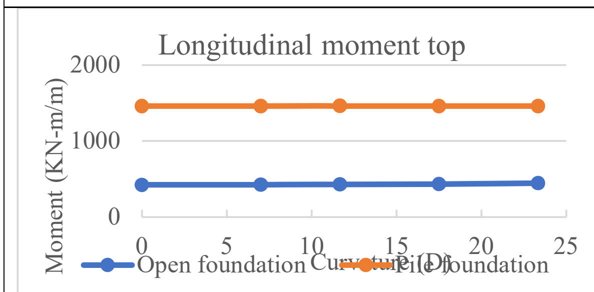

Graph 117. Variation of longitudinal moment at top of middle wall w.r.t. curvature between open and pile foundation with earth behind abutment.

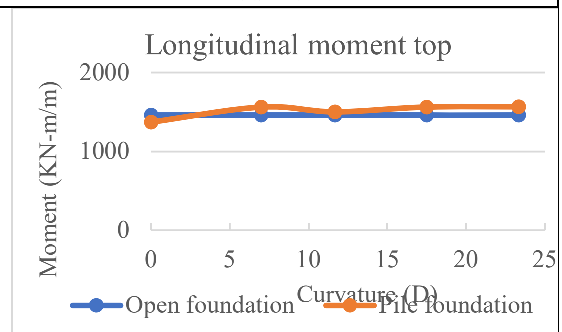

Graph 118. Variation of longitudinal moment at top of middle wall w.r.t. curvature between open and pile foundation without earth behind abutment.

4.2.5.3 Variation of transverse moment at top of middle wall with skew angle in longitudinal seismic

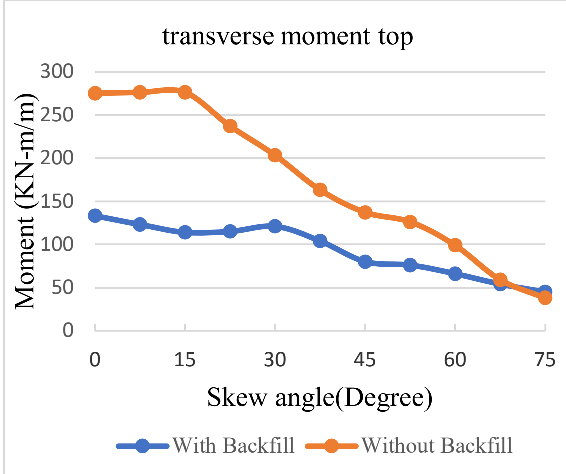

Graph 119. Variation of transverse moment at top of middle wall w.r.t. skew with pile foundation with or with earth behind abutment.

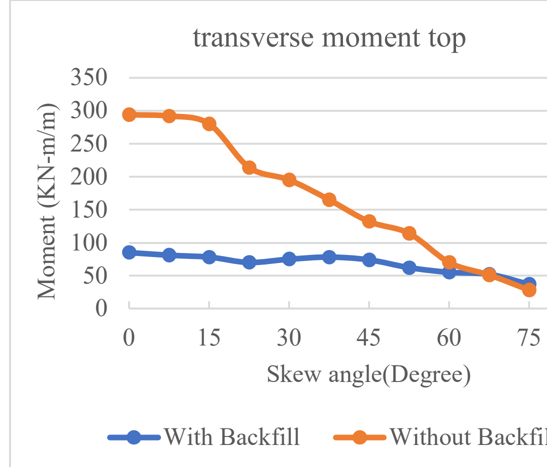

Graph 120. Variation of transverse moment at top of middle wall w.r.t. skew with open foundation with or without earth behind abutment.

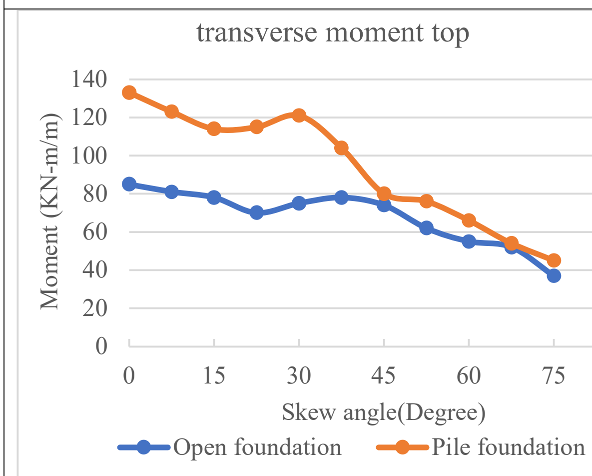

Graph 121. Variation of transverse moment at top of middle wall w.r.t. skew between open and pile foundation with earth behind abutment.

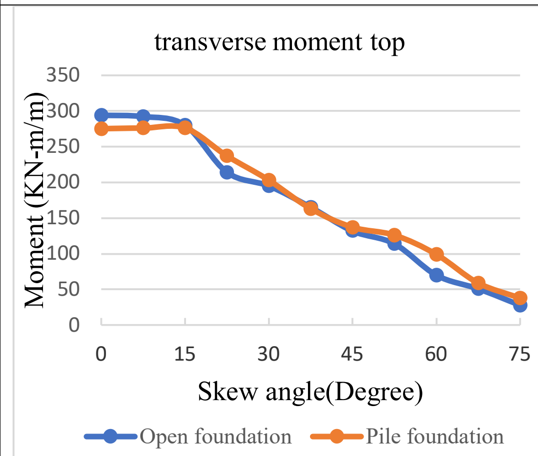

Graph 122. Variation of transverse moment at top of middle wall w.r.t. skew between open and pile foundation without earth behind abutment.

4.2.5.4 Variation of transverse moment at top of middle wall with curvature in longitudinal seismic

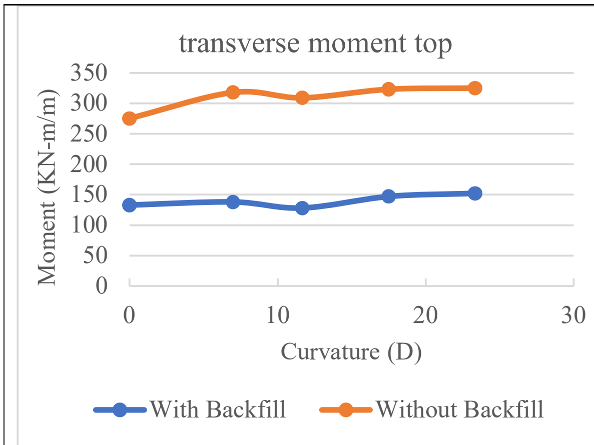

Graph 123. Variation of transverse moment at top of middle wall w.r.t. curvature with pile foundation with or with earth behind abutment.

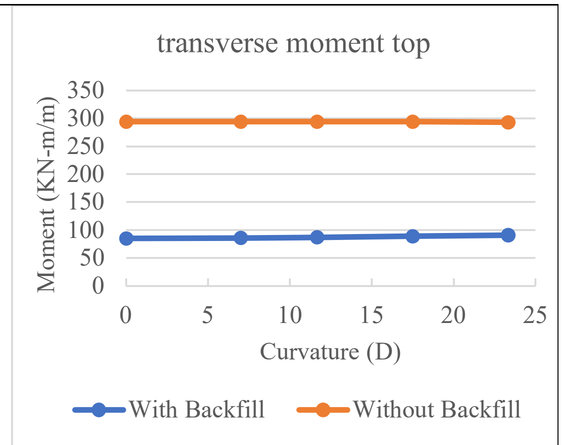

Graph 124. Variation of transverse moment at top of middle wall w.r.t. curvature with open foundation with or without earth behind abutment.

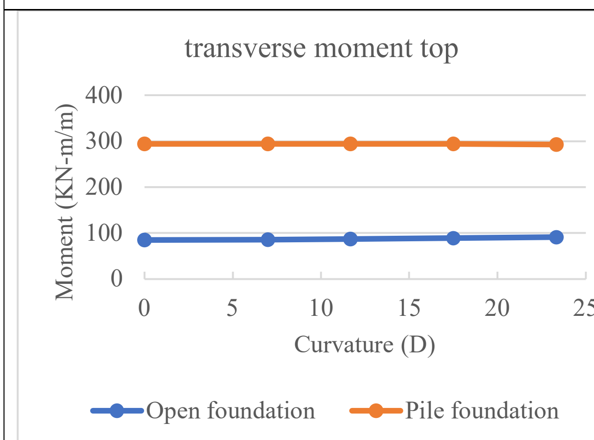

Graph 125. Variation of transverse moment at top of middle wall w.r.t. curvature between open and pile foundation with earth behind abutment.

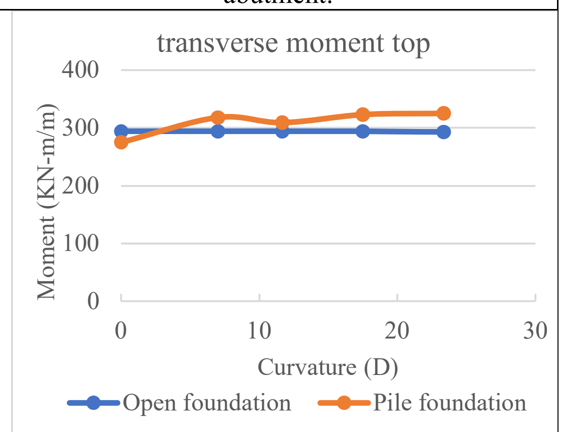

Graph 126. Variation of transverse moment at top of middle wall w.r.t. curvature between open and pile foundation without earth behind abutment.

4.2.5.5 Variation of torsional moment at top of middle wall with skew angle in longitudinal seismic

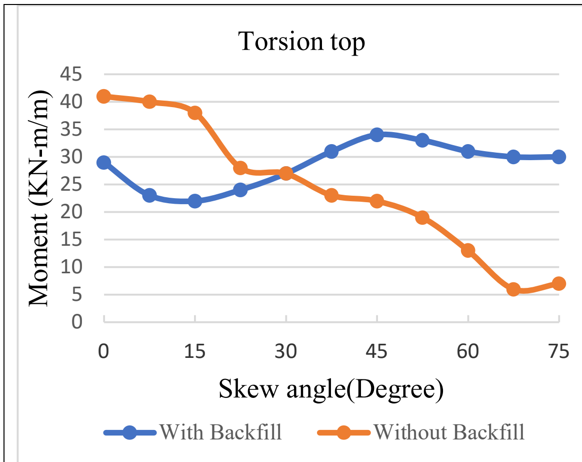

Graph 127. Variation of torsion at top of middle wall w.r.t. skew with pile foundation with or with earth behind abutment.

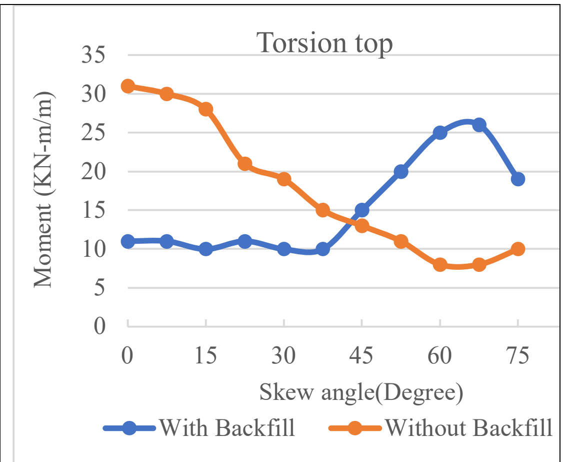

Graph 128. Variation of torsion at top of middle wall w.r.t. skew with open foundation with or without earth behind abutment.

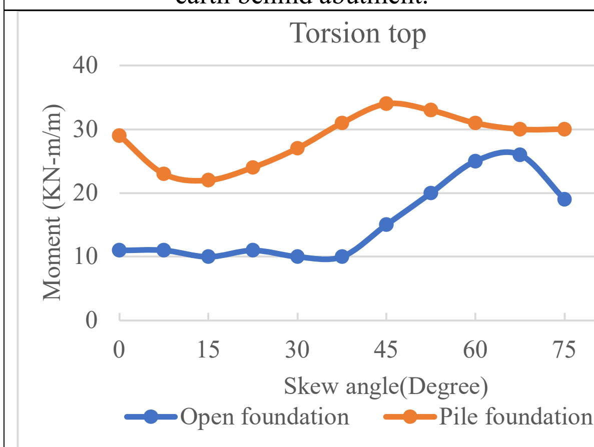

Graph 129. Variation of torsion at top of middle wall w.r.t. skew between open and pile foundation with earth behind abutment.

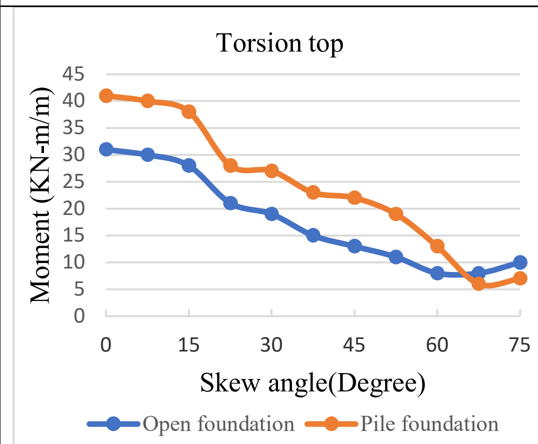

Graph 130. Variation of torsion at top of middle wall w.r.t. skew between open and pile foundation without earth behind abutment.

4.2.5.6 Variation of torsional moment at top of middle wall with curvature in longitudinal seismic

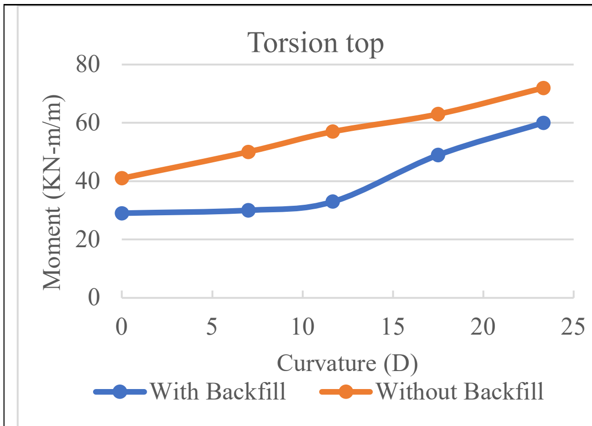

Graph 131. Variation of torsion at top of middle wall w.r.t. curvature with pile foundation with or with earth behind abutment.

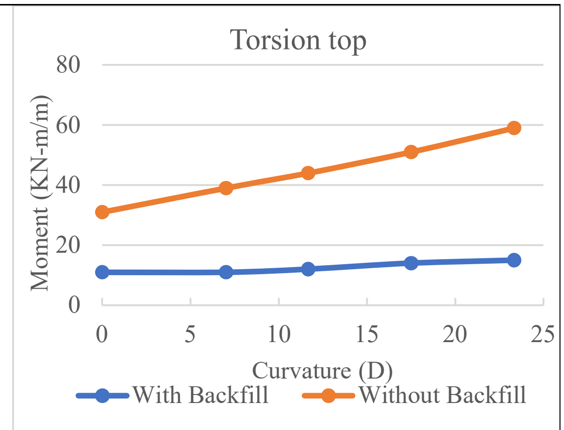

Graph 132. Variation of torsion at top of middle wall w.r.t. curvature with open foundation with or without earth behind abutment.

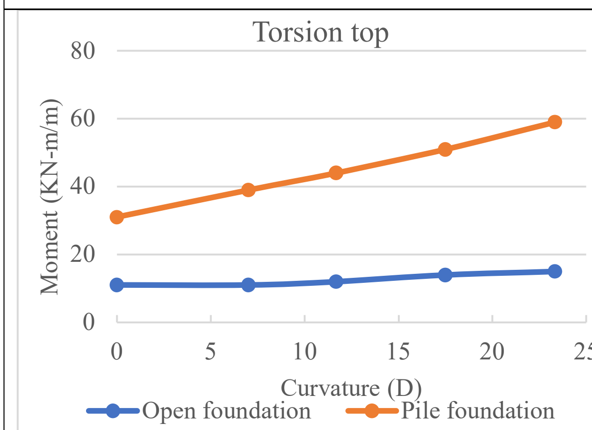

Graph 133. Variation of torsion at top of middle wall w.r.t. curvature between open and pile foundation with earth behind abutment.

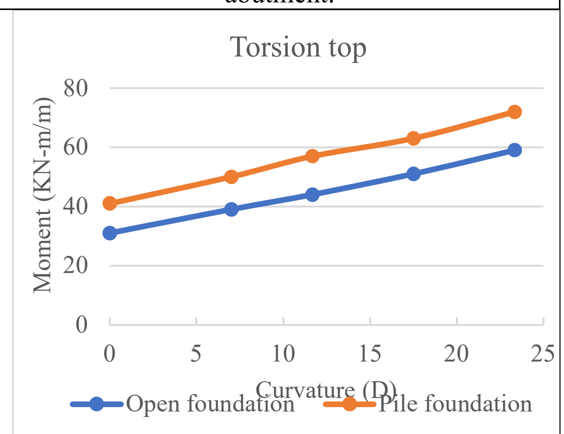

Graph 134. Variation of torsion at top of middle wall w.r.t. curvature between open and pile foundation without earth behind abutment.

4.2.5.7 Variation of longitudinal moment at bottom of middle wall with skew angle in longitudinal seismic

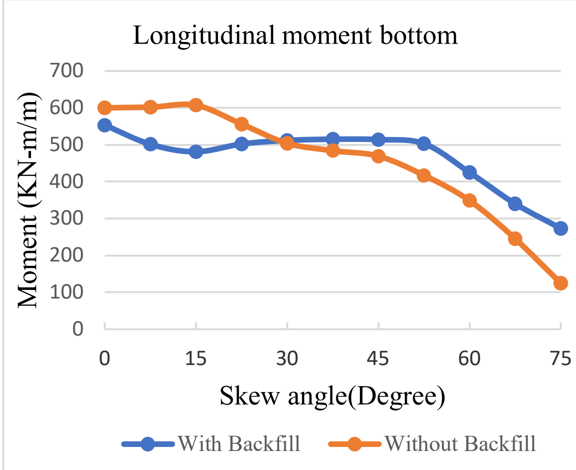

Graph 135. Variation of longitudinal moment at bottom of middle wall w.r.t. skew with pile foundation with or with earth behind abutment.

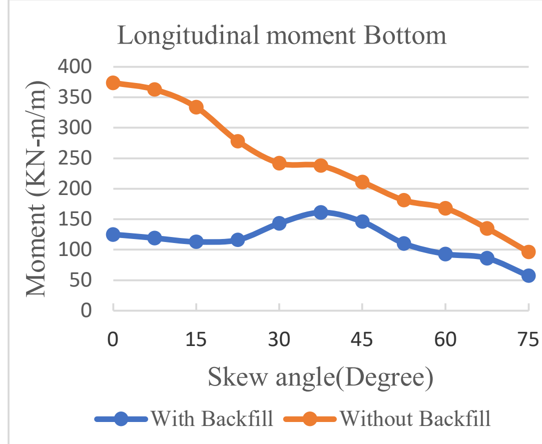

Graph 136. Variation of longitudinal moment at bottom of middle wall w.r.t. skew with open foundation with or without earth behind abutment.

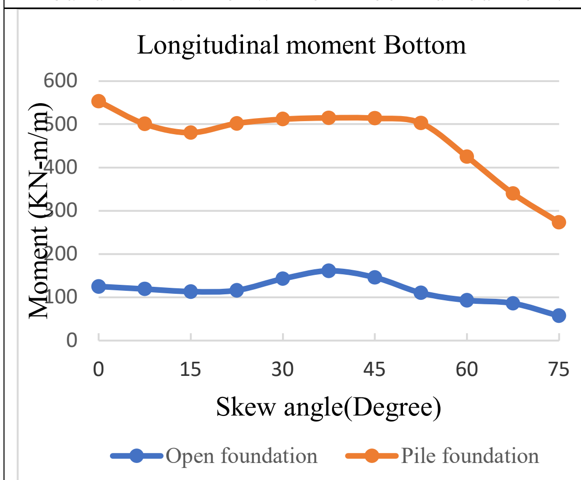

Graph 137. Variation of longitudinal moment at bottom of middle wall w.r.t. skew between open and pile foundation with earth behind abutment.

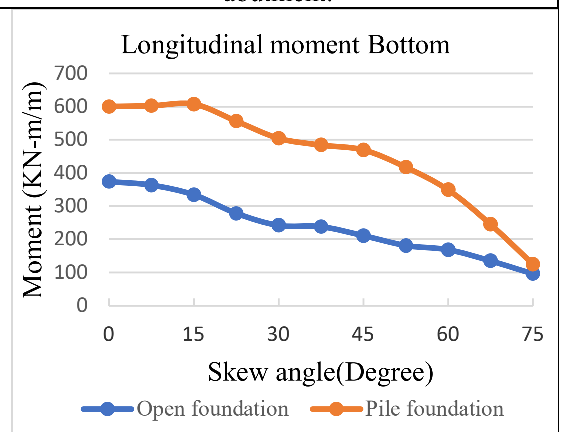

Graph 138. Variation of longitudinal moment at bottom of middle wall w.r.t. skew between open and pile foundation without earth behind abutment.

4.2.5.8 Variation of longitudinal moment at bottom of middle wall with curvature in longitudinal seismic

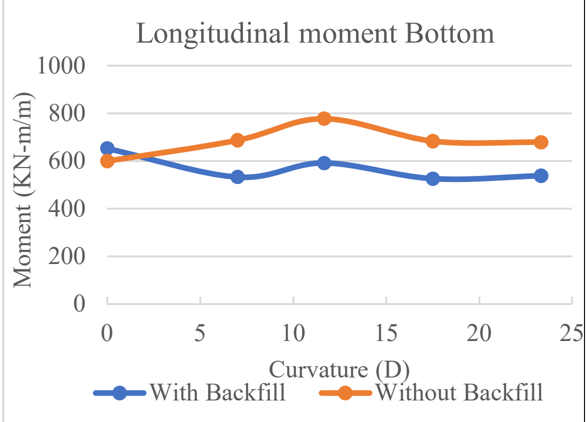

Graph 139. Variation of longitudinal moment at bottom of middle wall w.r.t. curvature with pile foundation with or with earth behind abutment.

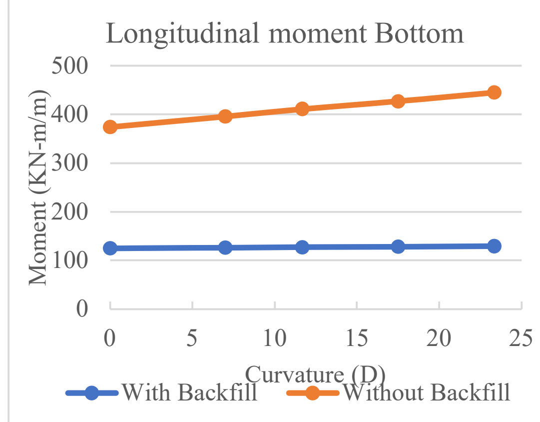

Graph 140. Variation of longitudinal moment at bottom of middle wall w.r.t. curvature with open foundation with or without earth behind abutment.

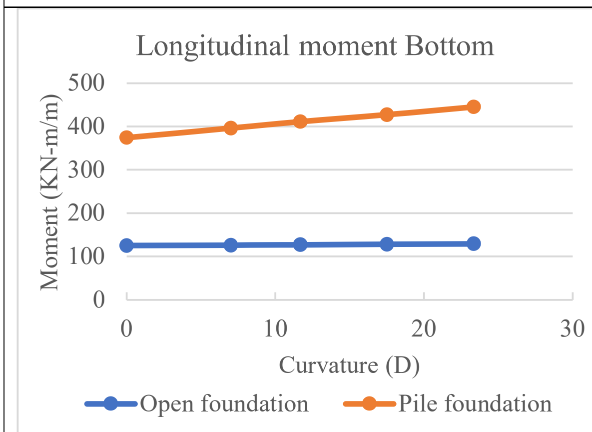

Graph 141. Variation of longitudinal moment at bottom of middle wall w.r.t. curvature between open and pile foundation with earth behind abutment.

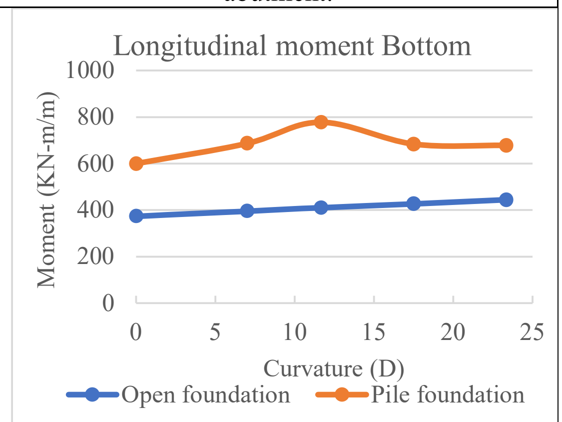

Graph 142. Variation of longitudinal moment at bottom of middle wall w.r.t. curvature between open and pile foundation without earth behind abutment.

4.2.5.9 Variation of transverse moment at bottom of middle wall with skew angle in longitudinal seismic

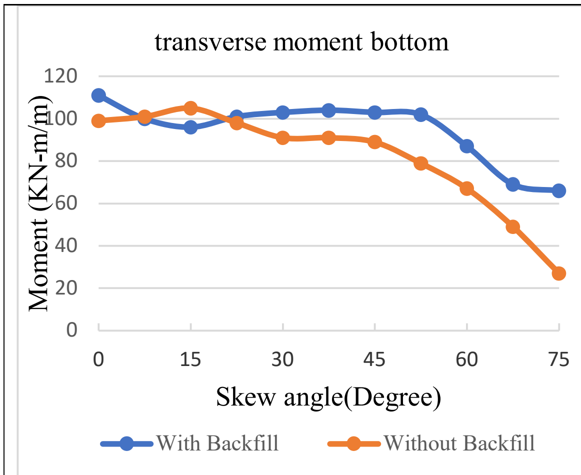

Graph 143. Variation of transverse moment at bottom of middle wall w.r.t. skew with pile foundation with or with earth behind abutment.

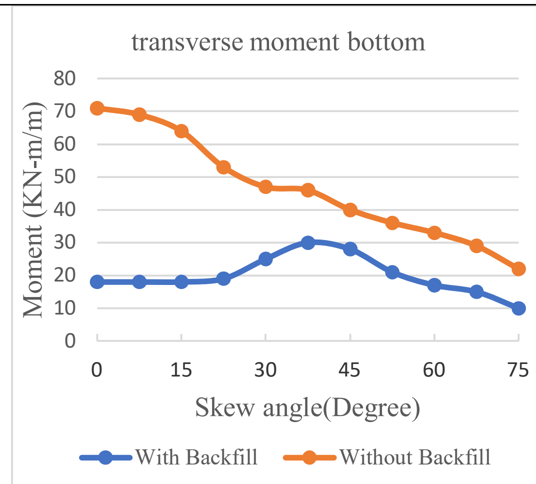

Graph 144. Variation of transverse moment at bottom of middle wall w.r.t. skew with open foundation with or without earth behind abutment.

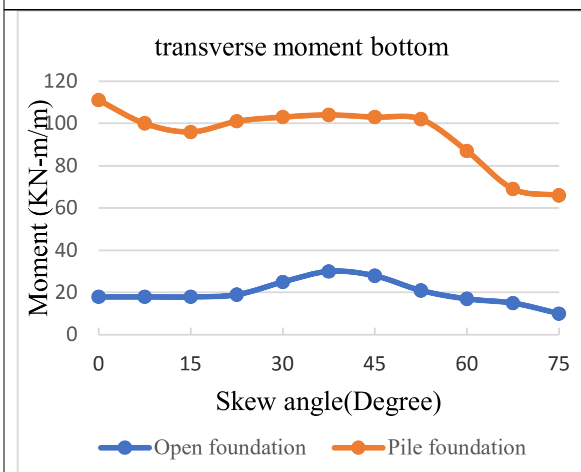

Graph 145. Variation of transverse moment at bottom of middle wall w.r.t. skew between open and pile foundation with earth behind abutment.

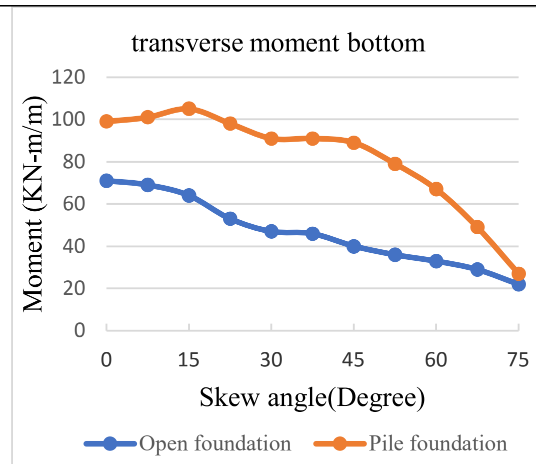

Graph 146. Variation of transverse moment at bottom of middle wall w.r.t. skew between open and pile foundation without earth behind abutment.

4.2.5.10 Variation of transverse moment at bottom of middle wall with curvature in longitudinal seismic

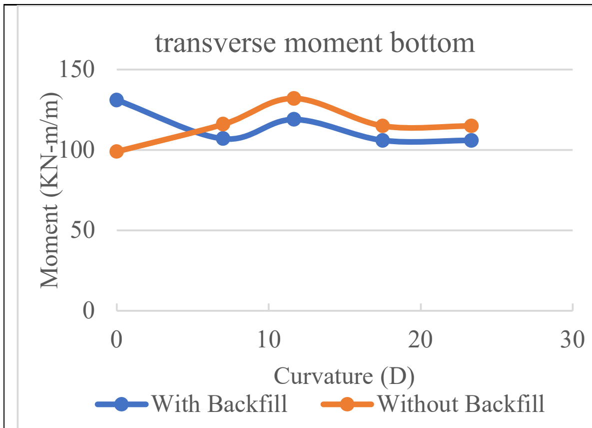

Graph 147. Variation of transverse moment at bottom of middle wall w.r.t. curvature with pile foundation with or with earth behind abutment.

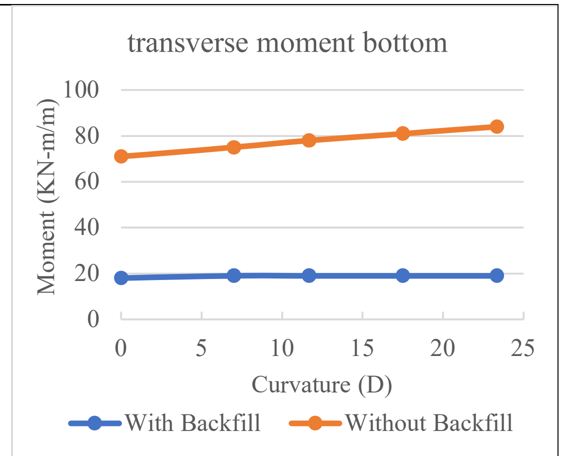

Graph 148. Variation of transverse moment at bottom of middle wall w.r.t. curvature with open foundation with or without earth behind abutment.

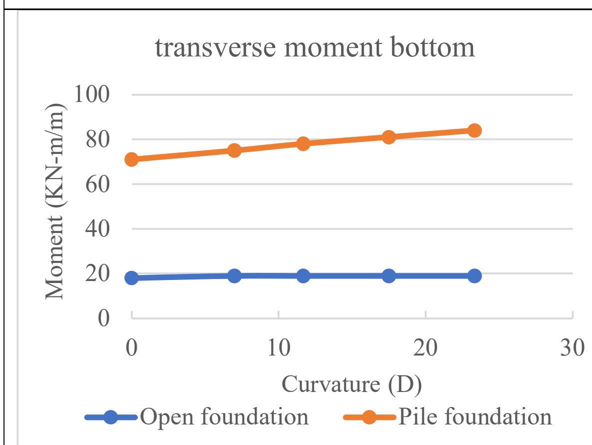

Graph 149. Variation of transverse moment at bottom of middle wall w.r.t. curvature between open and pile foundation with earth behind abutment.

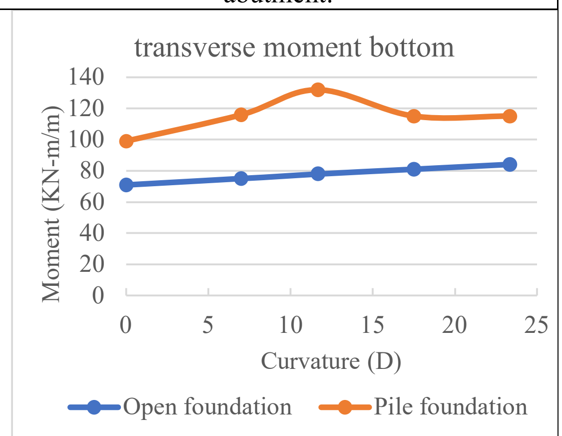

Graph 150. Variation of transverse moment at bottom of middle wall w.r.t. curvature between open and pile foundation without earth behind abutment.

<u>4.2.5.11 Variation of torsional moment at bottom of middle wall with skew angle in longitudinal seismic</u>

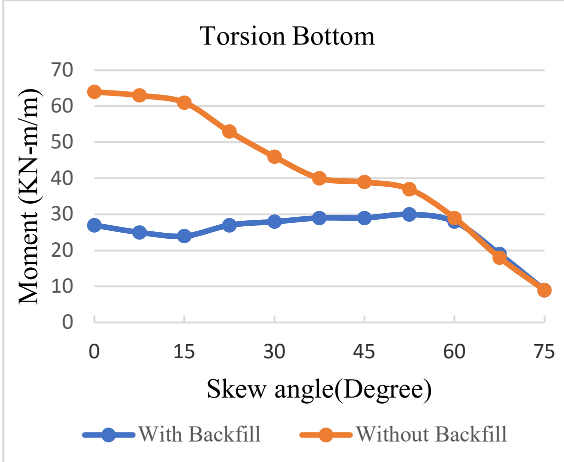

Graph 151. Variation of torsion at bottom of middle wall w.r.t. skew with pile foundation with or with earth behind abutment.

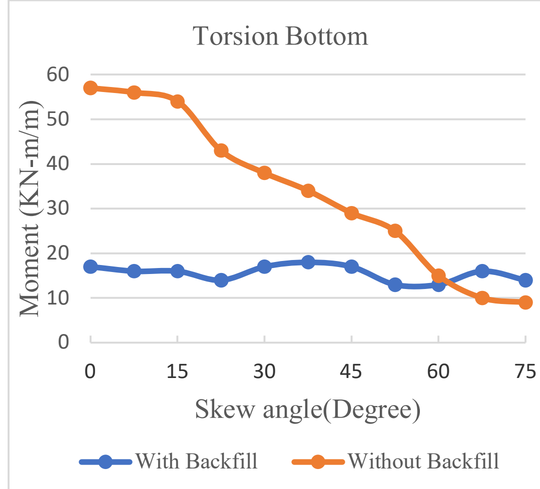

Graph 152. Variation of torsion at bottom of middle wall w.r.t. skew with open foundation with or without earth behind abutment.

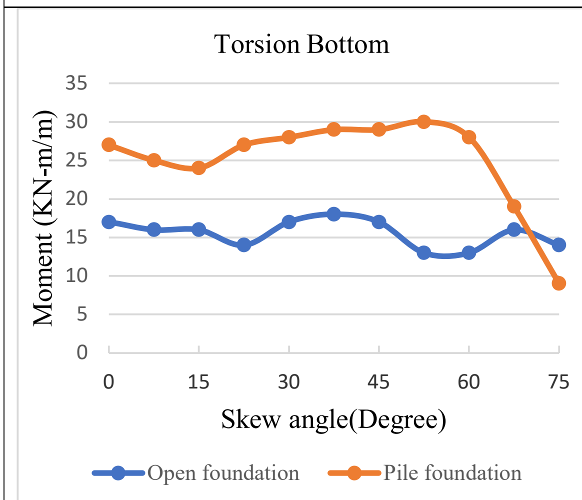

Graph 153. Variation of torsion at bottom of middle wall w.r.t. skew between open and pile foundation with earth behind abutment.

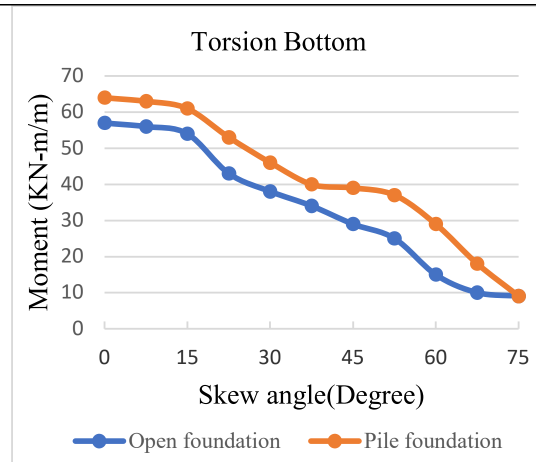

Graph 154. Variation of torsion at bottom of middle wall w.r.t. skew between open and pile foundation without earth behind abutment.

4.2.5.12 Variation of torsional moment at bottom of middle wall with curvature in longitudinal seismic

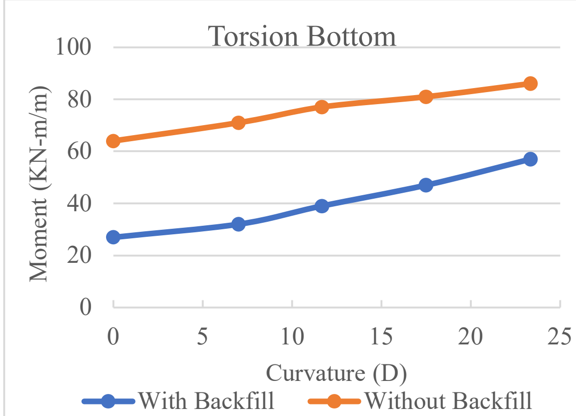

Graph 155. Variation of torsion at bottom of middle wall w.r.t. curvature with pile foundation with or with earth behind abutment.

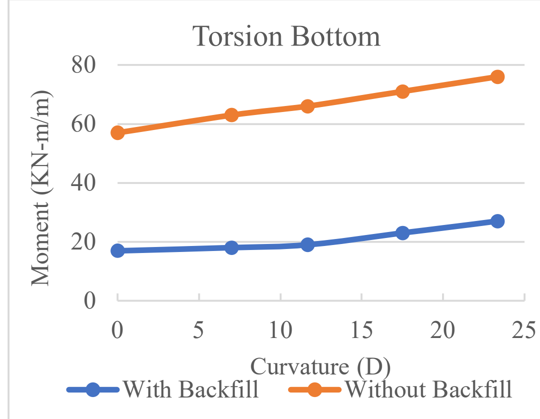

Graph 156. Variation of torsion at bottom of middle wall w.r.t. curvature with open foundation with or without earth behind abutment.

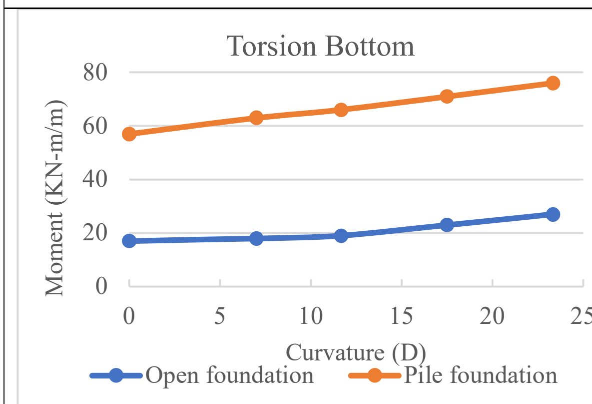

Graph 157. Variation of torsion at bottom of middle wall w.r.t. curvature between open and pile foundation with earth behind abutment.

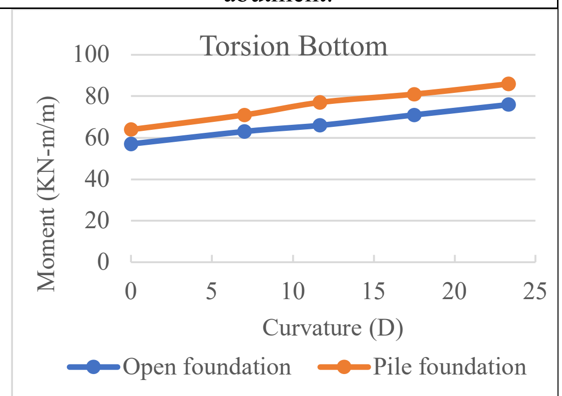

Graph 158. Variation of torsion at bottom of middle wall w.r.t. curvature between open and pile foundation without earth behind abutment.

Hence from the above graphs following observations can be made: -

For longitudinal seismic case

- Longitudinal moment at top of middle wall decreases with increase of skew angle for both open and pile foundation. The moment is more for bridge without backfill than bridge with backfill.
- Longitudinal moment at top of middle wall is almost same with changing of curvature. The moment is more for bridge without backfill than bridge with backfill.
- Transverse moment at top of middle wall decreases with increase of skew angle for both open and pile foundation. The rate of decrease is more for bridge without backfill.
- Transverse moment at top of middle wall at top of middle wall is almost same with

changing of curvature. The moment is more for bridge without backfill than bridge with backfill.

- Torsion at top of middle wall initially decreases with increase of skew angle for bridges without backfill.
- Torsion at top of middle wall increases with increase of curvature for both open and pile foundations. It is more for bridge without backfill and bridge with pile foundation than bridge with backfill and bridge with open foundation.
- Longitudinal moment at bottom of middle wall decreases with increase of skew angle for both open and pile foundations. It is more for bridge with pile foundations than bridge with open foundations.
- Longitudinal moment at bottom of middle wall increases with increase of curvature for both open and pile foundation.
- Transverse moment at bottom of middle wall decreases with increase of skew angle.
- Transverse moment at bottom of middle wall increases with increase of curvature.
- Torsion at bottom of middle wall decreases with increase of skew angle for bridge without backfill. For bridge with backfill it is almost same. The rate of decrease is more for bridge without backfill.
- Torsion at bottom of middle wall increases with increase of curvature.

4.2.6 Variation of the moment at side wall in transverse seismic condition

4.2.6.1 Variation of longitudinal moment at top of side wall with skew angle in transverse seismic

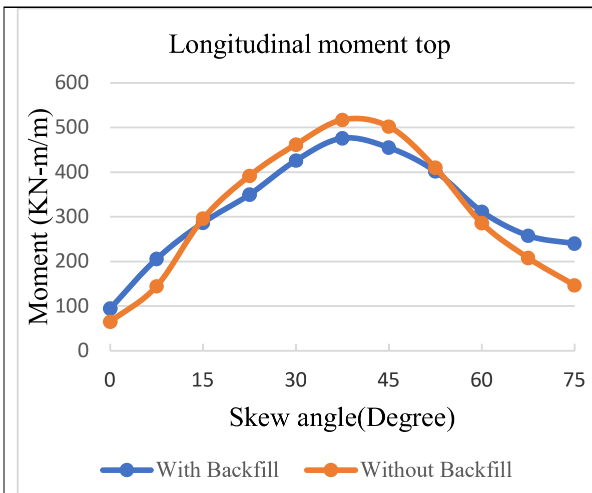

Graph 159. Variation of longitudinal moment at top of side wall w.r.t. skew with pile foundation with or with earth behind abutment.

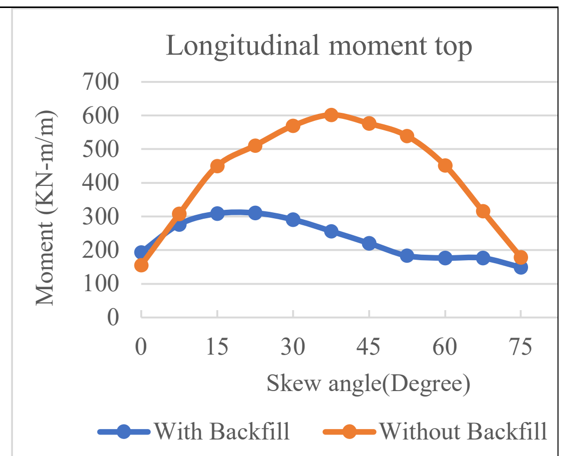

Graph 160. Variation of longitudinal moment at top of side wall w.r.t. skew with open foundation with or without earth behind abutment.

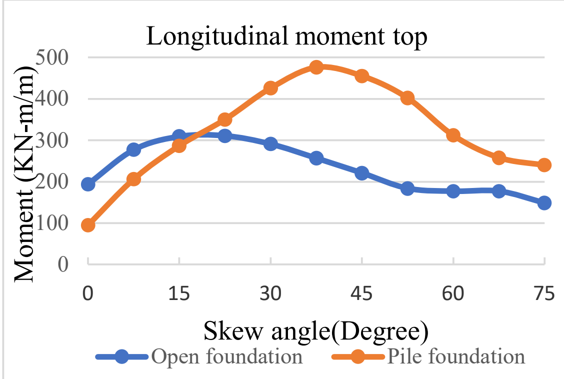

Graph 161. Variation of longitudinal moment at top of side wall w.r.t. skew between open and pile foundation with earth behind abutment.

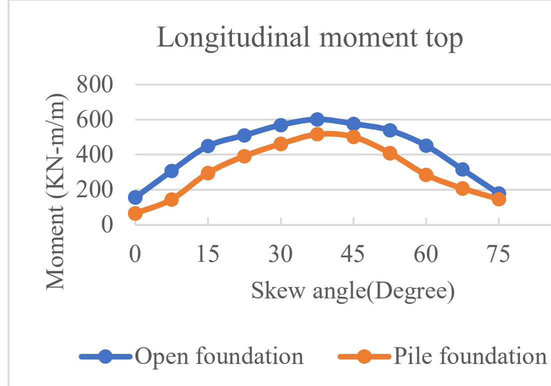

Graph 162. Variation of longitudinal moment at top of side wall w.r.t. skew between open and pile foundation without earth behind abutment.

4.2.6.2 Variation of longitudinal moment at top of side wall with curvature in transverse seismic

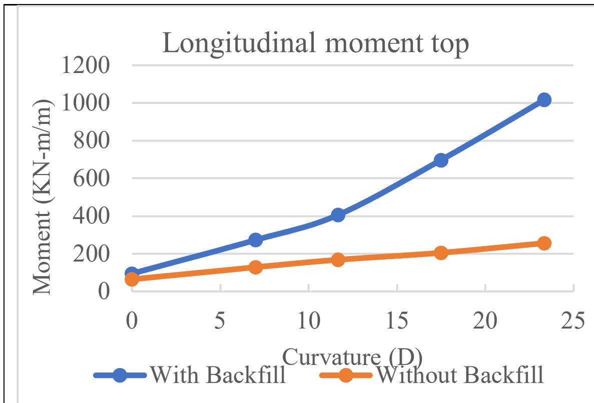

Graph 163. Variation of longitudinal moment at top of side wall w.r.t. curvature with pile foundation with or with earth behind abutment.

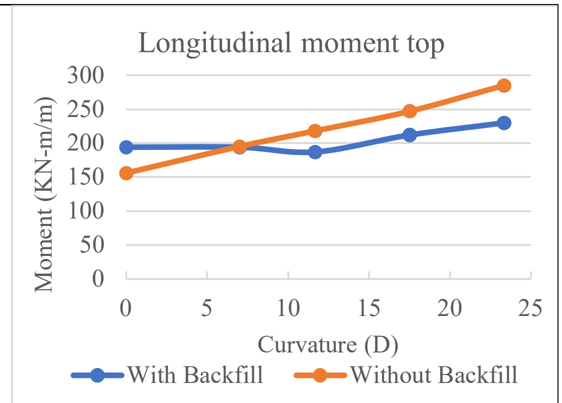

Graph 164. Variation of longitudinal moment at top of side wall w.r.t. curvature with open foundation with or without earth behind abutment.

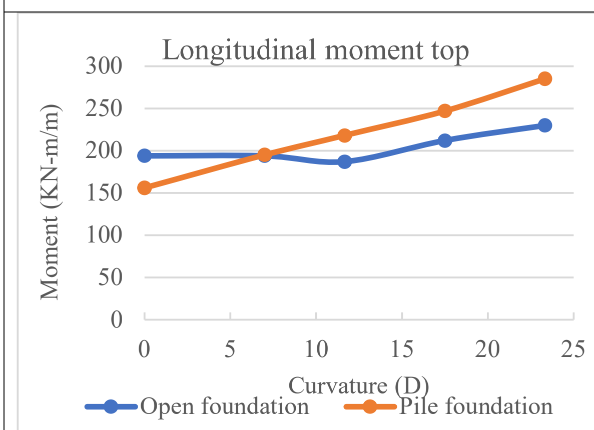

Graph 165. Variation of longitudinal moment at top of side wall w.r.t. curvature between open and pile foundation with earth behind abutment.

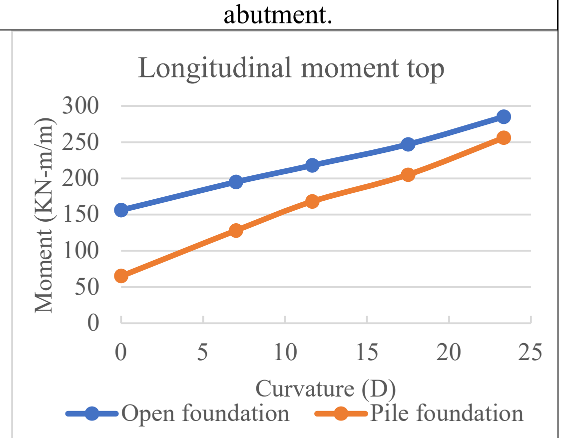

Graph 166. Variation of longitudinal moment at top of side wall w.r.t. curvature between open and pile foundation without earth behind abutment.

4.2.6.3 Variation of transverse moment at top of side wall with skew angle in transverse seismic

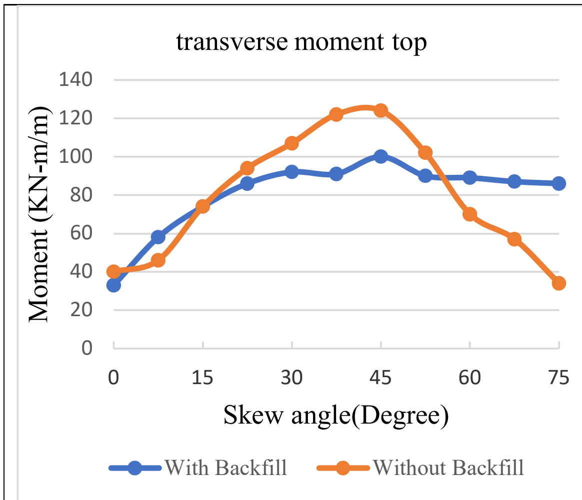

Graph 167. Variation of transverse moment at top of side wall w.r.t. skew with pile foundation with or with earth behind abutment.

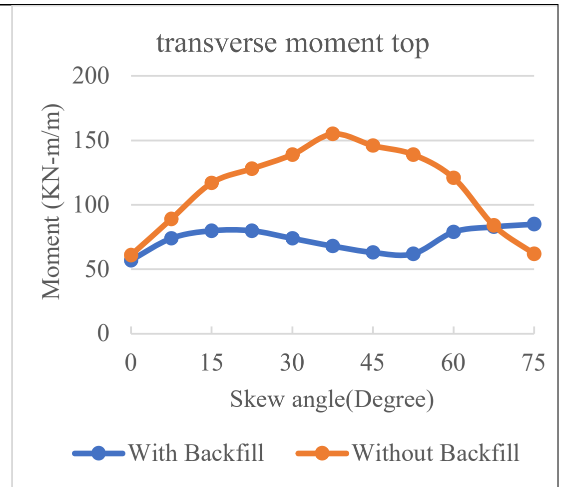

Graph 168. Variation of transverse moment at top of side wall w.r.t. skew with open foundation with or without earth behind abutment.

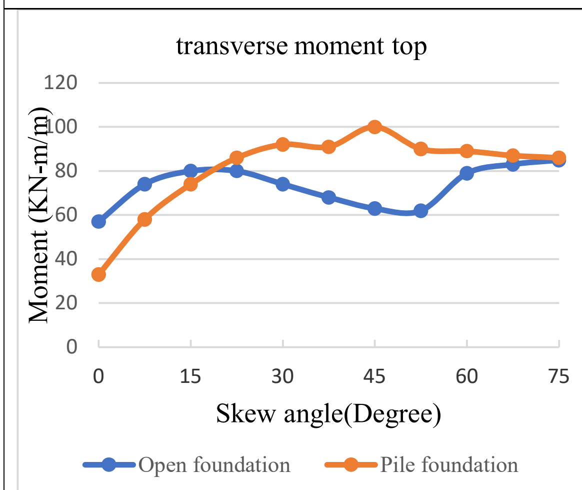

Graph 169. Variation of transverse moment at top of side wall w.r.t. skew between open and pile foundation with earth behind abutment.

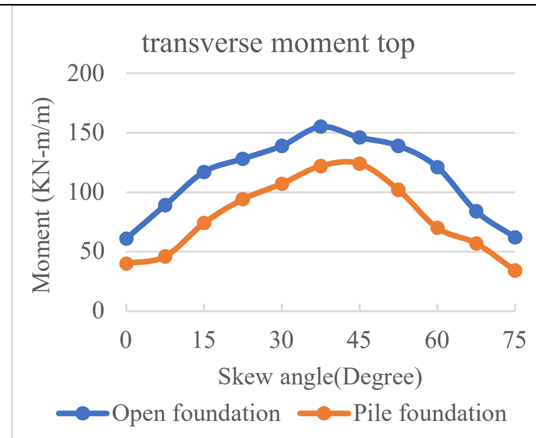

Graph 170. Variation of transverse moment at top of side wall w.r.t. skew between open and pile foundation without earth behind abutment.

4.2.6.4 Variation of transverse moment at top of side wall with curvature in transverse seismic

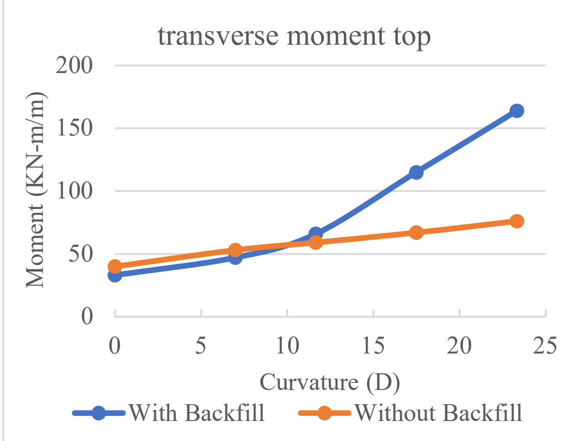

Graph 171. Variation of transverse moment at top of side wall w.r.t. curvature with pile foundation with or with earth behind abutment.

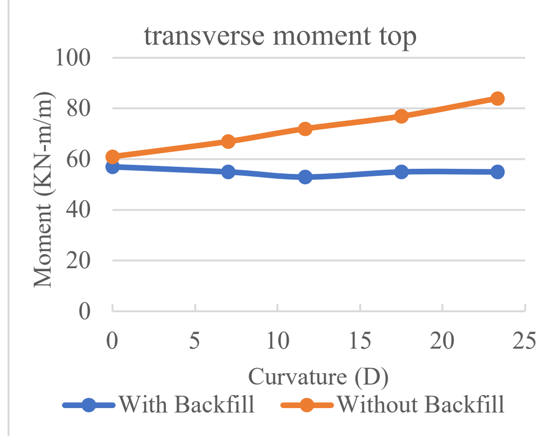

Graph 172. Variation of transverse moment at top of side wall w.r.t. curvature with open foundation with or without earth behind abutment.

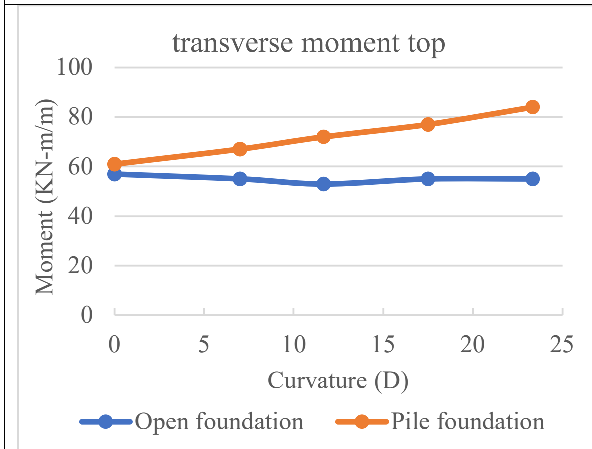

Graph 173. Variation of transverse moment at top of side wall w.r.t. curvature between open and pile foundation with earth behind abutment.

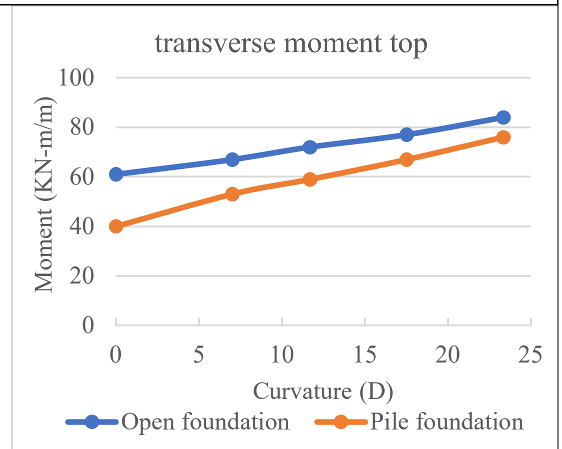

Graph 174. Variation of transverse moment at top of side wall w.r.t. curvature between open and pile foundation without earth behind abutment.

4.2.6.5 Variation of torsional moment at top of side wall with skew angle in transverse seismic

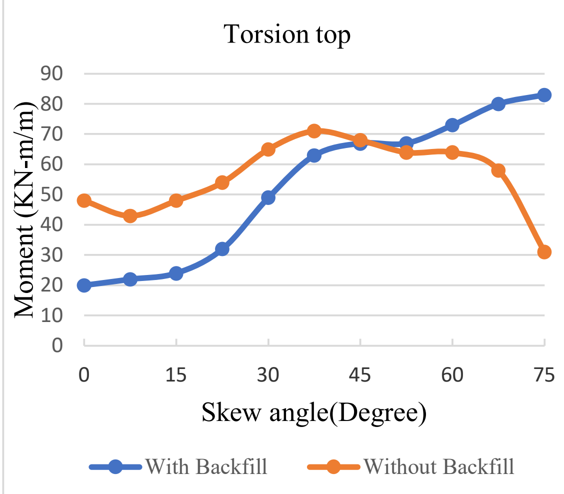

Graph 175. Variation of torsion at top of side wall w.r.t. skew with pile foundation with or with earth behind abutment.

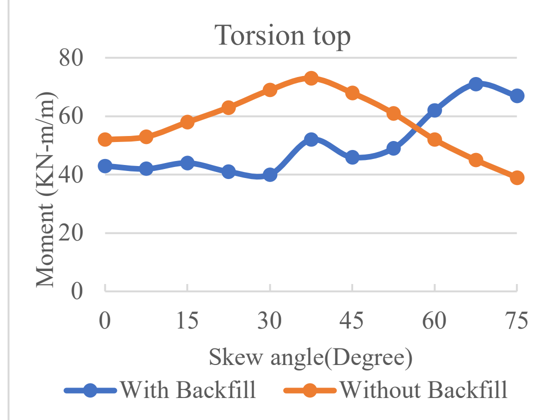

Graph 176. Variation of torsion at top of side wall w.r.t. skew with open foundation with or without earth behind abutment.

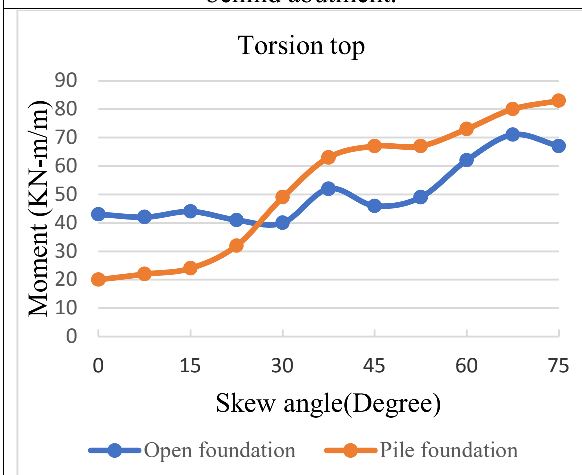

Graph 177. Variation of torsion at top of side wall w.r.t. skew between open and pile foundation with earth behind abutment.

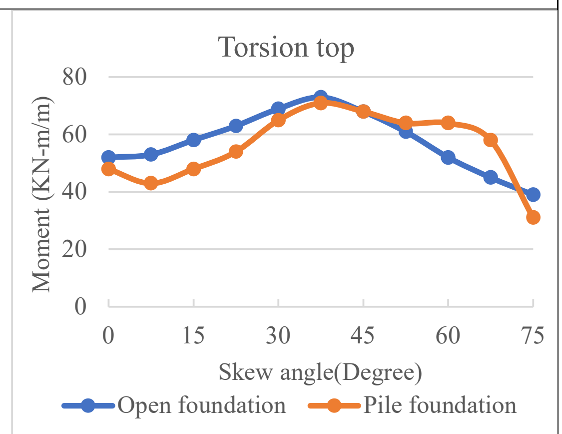

Graph 178. Variation of torsion at top of side wall w.r.t. skew between open and pile foundation without earth behind abutment.

4.2.6.6 Variation of torsional moment at top of side wall with curvature in transverse seismic

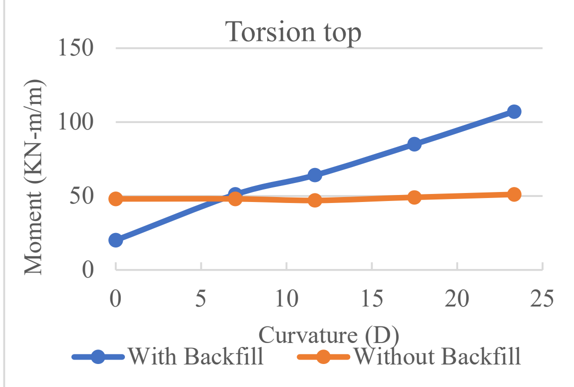

Graph 179. Variation of torsion at top of side wall w.r.t. curvature with pile foundation with or with earth behind abutment.

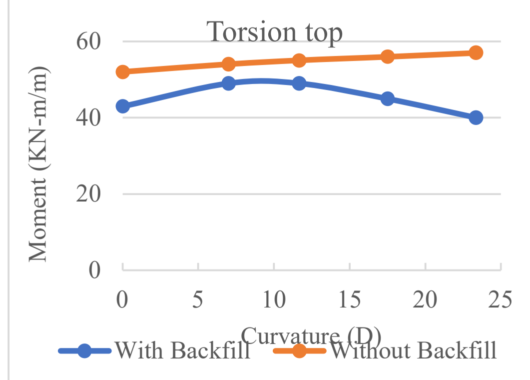

Graph 180. Variation of torsion at top of side wall w.r.t. curvature with pile foundation with open foundation with or without earth.

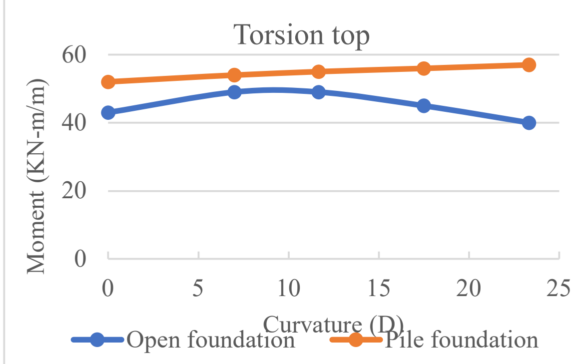

Graph 181. Variation of torsion at top of side wall w.r.t. curvature between open and pile foundation with earth behind abutment.

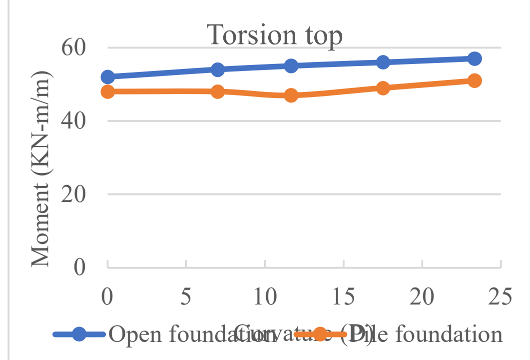

Graph 182. Variation of torsion at top of side wall w.r.t. curvature between open and pile foundation without earth behind abutment.

4.2.6.7 Variation of longitudinal moment at bottom of side wall with skew angle in transverse seismic

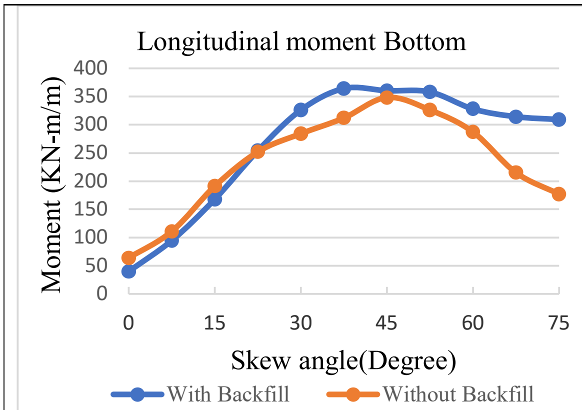

Graph 183. Variation of longitudinal moment at bottom of side wall w.r.t. skew with pile foundation with or with earth behind abutment.

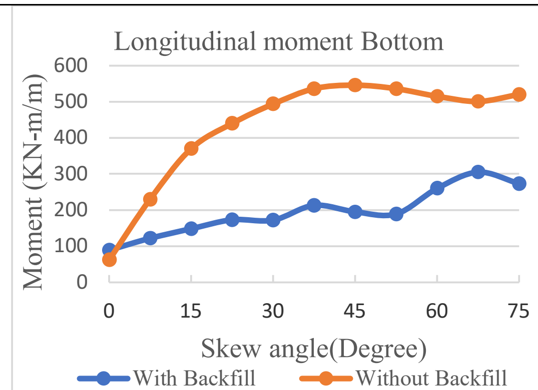

Graph 184. Variation of longitudinal moment at bottom of side wall w.r.t. skew with open foundation with or without earth behind abutment.

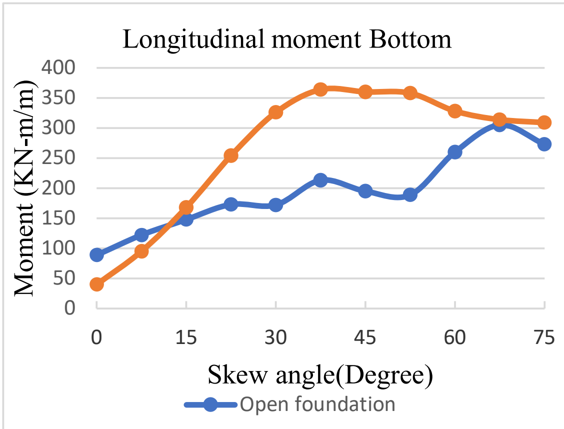

Graph 185. Variation of longitudinal moment at bottom of side wall w.r.t. skew between open and pile foundation with earth behind abutment.

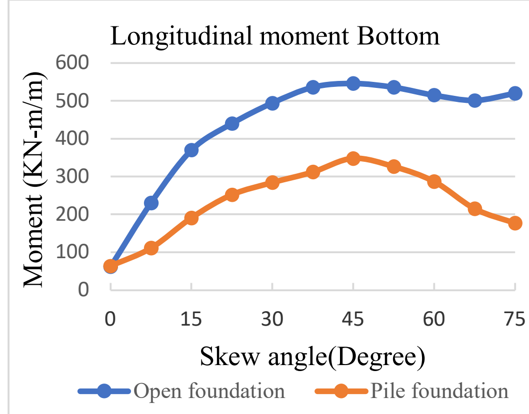

Graph 186. Variation of longitudinal moment at bottom of side wall w.r.t. skew between open and pile foundation without earth behind abutment.

4.2.6.8 Variation of longitudinal moment at bottom of side wall with curvature in transverse seismic

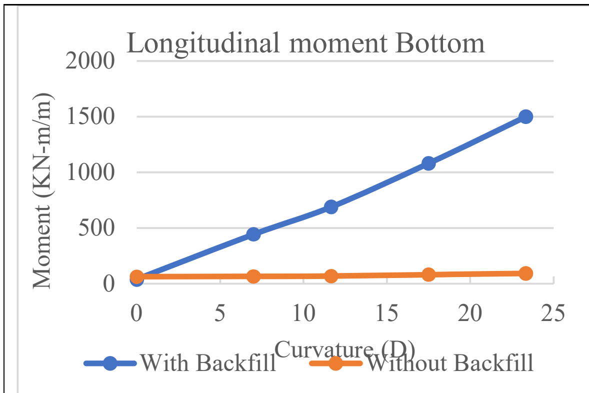

Graph 187. Variation of longitudinal moment at bottom of side wall w.r.t. curvature with pile foundation with or with earth behind abutment.

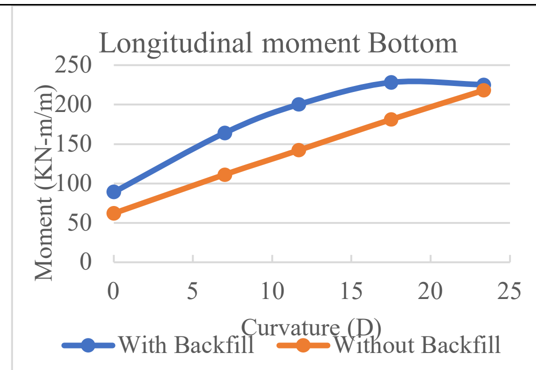

Graph 188. Variation of longitudinal moment at bottom of side wall w.r.t. curvature with open foundation with or without earth behind abutment.

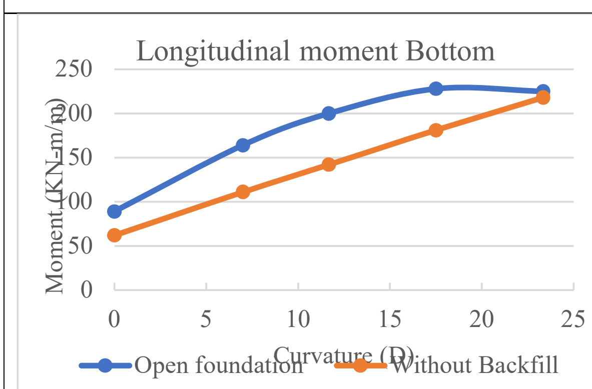

Graph 189. Variation of longitudinal moment at bottom of side wall w.r.t. curvature between open and pile foundation with earth behind abutment.

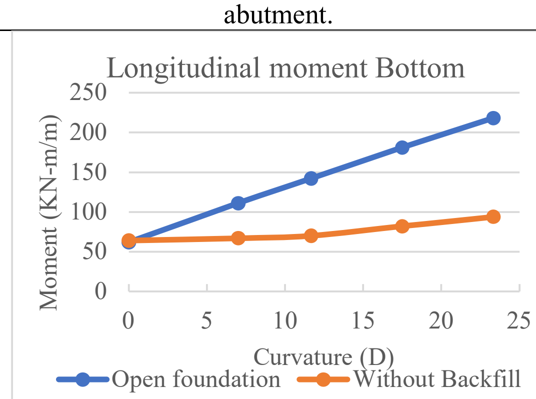

Graph 190. Variation of longitudinal moment at bottom of side wall w.r.t. curvature between open and pile foundation without earth behind abutment.

4.2.6.9 Variation of transverse moment at bottom of side wall with skew angle in transverse seismic

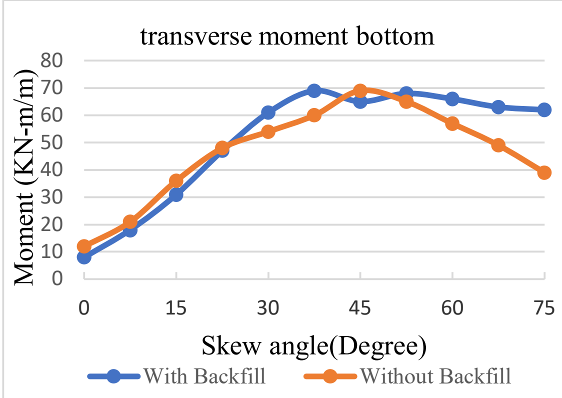

Graph 191. Variation of transverse moment at bottom of side wall w.r.t. skew with pile foundation with or with earth behind abutment.

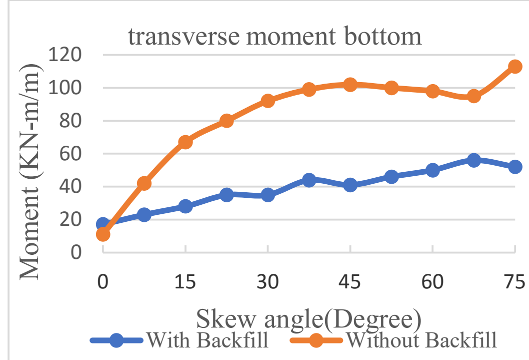

Graph 192. Variation of transverse moment at bottom of side wall w.r.t. skew with open foundation with or without earth behind abutment.

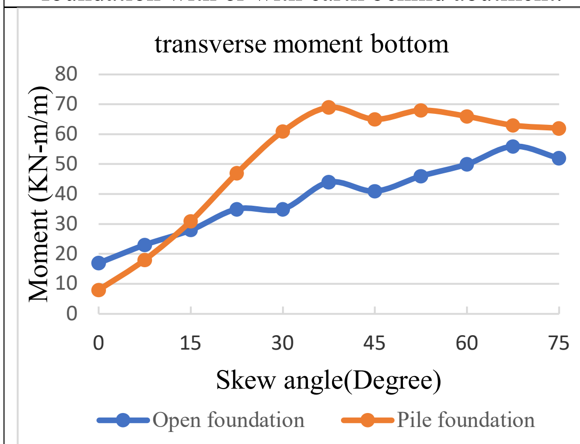

Graph 193. Variation of transverse moment at bottom of side wall w.r.t. skew between open and pile foundation with earth behind abutment.

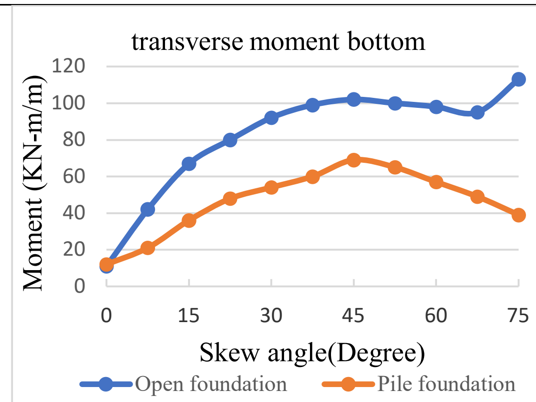

Graph 194. Variation of transverse moment at bottom of side wall w.r.t. skew between open and pile foundation without earth behind abutment.

4.2.6.10 Variation of transverse moment at bottom of side wall with curvature in transverse seismic

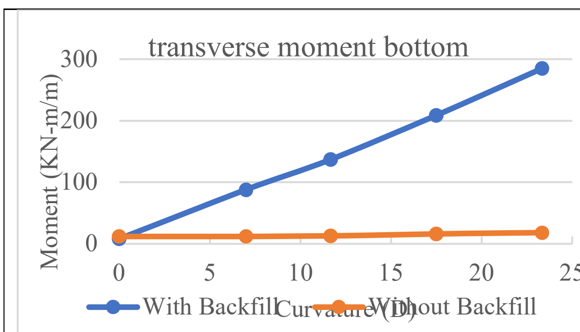

Graph 195. Variation of transverse moment at bottom of side wall w.r.t. curvature with pile foundation with or with earth behind abutment.

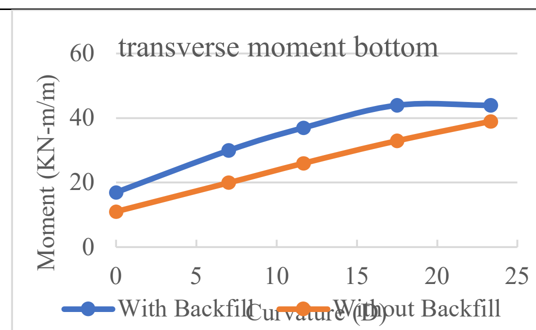

Graph 196. Variation of transverse moment at bottom of side wall w.r.t. curvature with open foundation with or without earth behind abutment.

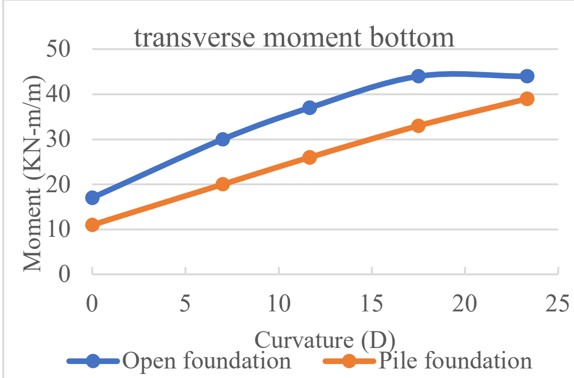

Graph 197. Variation of transverse moment at bottom of side wall w.r.t. curvature between open and pile foundation with earth behind abutment.

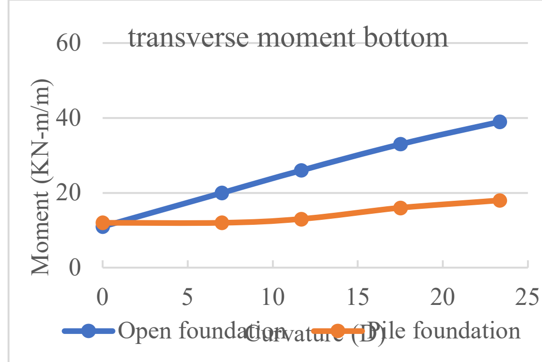

Graph 198. Variation of transverse moment at bottom of side wall w.r.t. curvature between open and pile foundation without earth behind abutment.

4.2.6.11 Variation of torsional moment at bottom of side wall with skew angle in transverse seismic

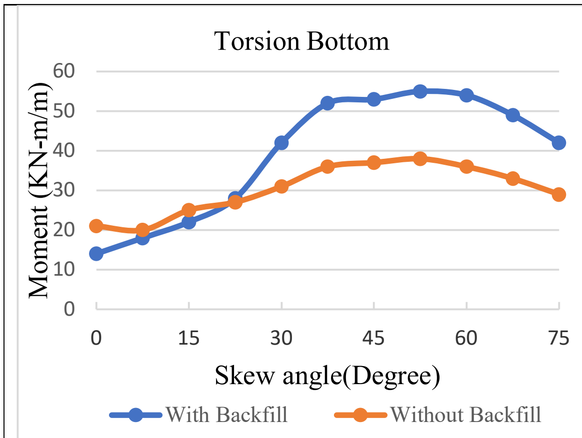

Graph 199. Variation of torsion at bottom of side wall w.r.t. skew with pile foundation with or with earth behind abutment.

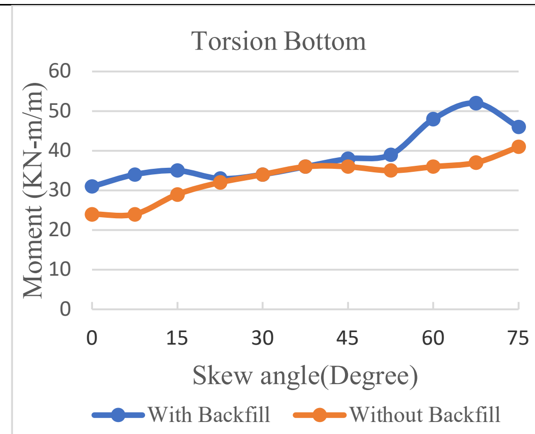

Graph 200. Variation of torsion at bottom of side wall w.r.t. skew with open foundation with or without earth behind abutment.

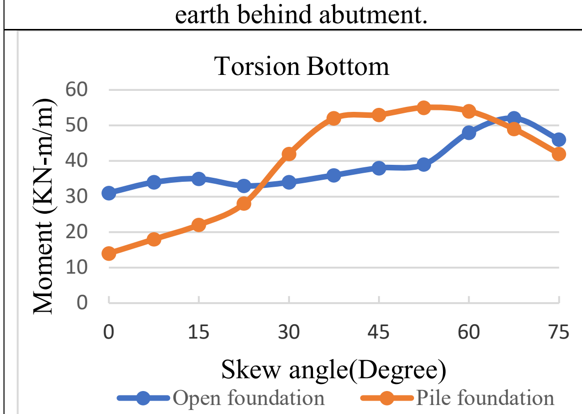

Graph 201. Variation of torsion at bottom of side wall w.r.t. skew between open and pile foundation with earth behind abutment.

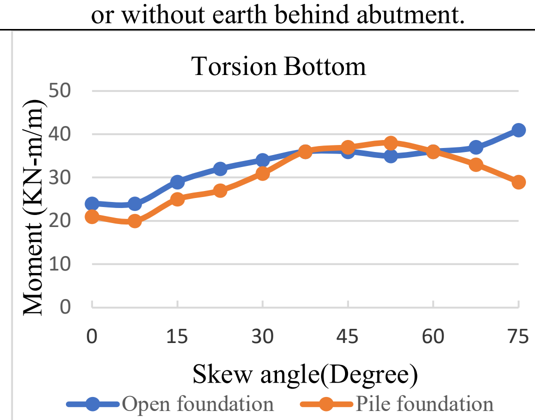

Graph 202. Variation of torsion at bottom of side wall w.r.t. skew between open and pile foundation without earth behind abutment.

4.2.6.12 Variation of torsional moment at bottom of side wall with curvature in transverse seismic

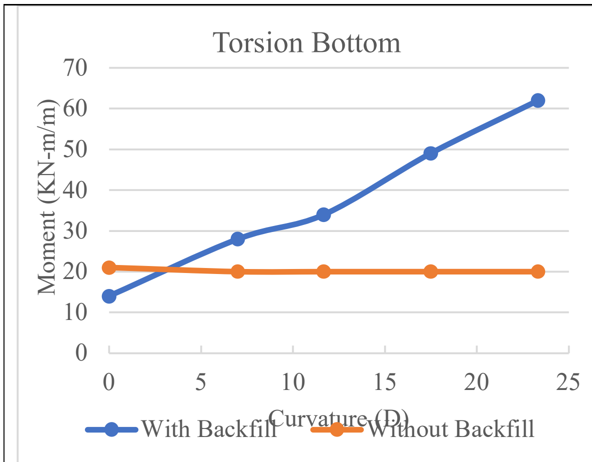

Graph 203. Variation of torsion at bottom of side wall w.r.t. curvature with pile foundation with or with earth behind abutment.

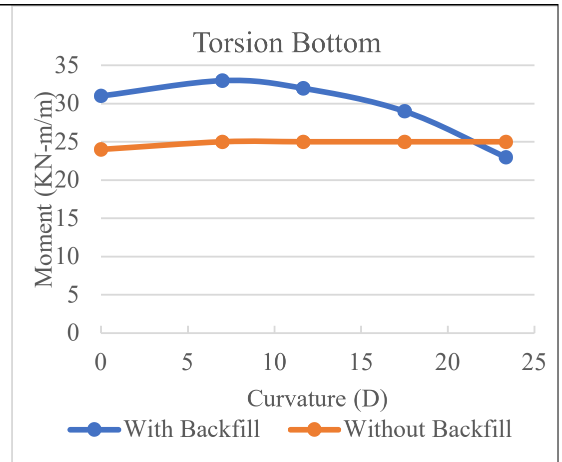

Graph 204. Variation of torsion at bottom of side wall w.r.t. curvature with open foundation with or without earth behind abutment.

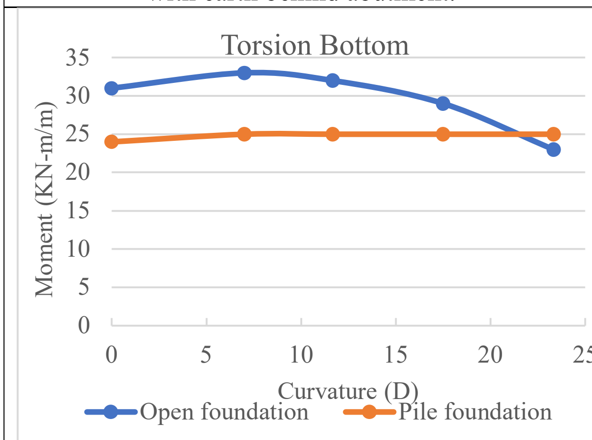

Graph 205. Variation of torsion at bottom of side wall w.r.t. curvature between open and pile foundation with earth behind abutment.

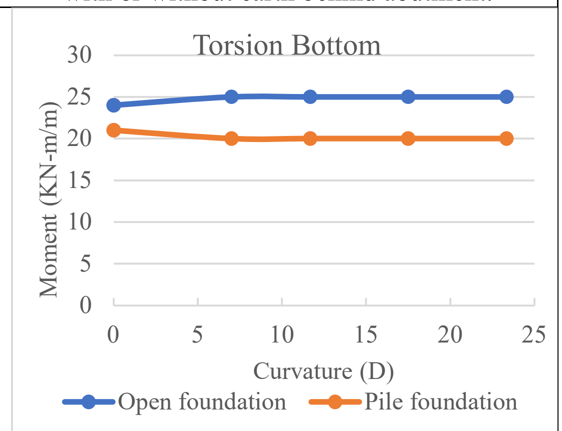

Graph 206. Variation of torsion at bottom of side wall w.r.t. curvature between open and pile foundation without earth behind abutment.

Hence from the above graphs following observations can be made: -

For transverse seismic case

- Longitudinal moment at top of side wall initially increases then decreases with increase of skew angle for both open and pile foundation. The moment is more for bridge without backfill than bridge with backfill.
- Longitudinal moment at top of side wall increases with increase of curvature for both open and pile foundation.
- Transverse moment at top of side wall initially increases then decreases with increase of skew angle for both open and pile foundation.
- Transverse moment at top of side wall increases with increase of curvature for open

and pile foundation.

- Torsion at top of side wall initially increases then decreases with increase of skew angle for bridges without backfill. For bridges with backfill it increases with increase of skew angle.
- Torsion at top of side wall increases with increase of curvature for both open and pile foundations.
- Longitudinal moment at bottom of side wall initially increases then decreases with increase of skew angle for both open and pile foundations.
- Longitudinal moment at bottom of side wall increases with increase of curvature for both open and pile foundation. It is more for bridge with backfill and pile foundation.
- Transverse moment at bottom of side wall increases with increase of skew angle.
- Transverse moment at bottom of side wall increases with increase of curvature.
- Torsion at bottom of side wall decreases with increase of skew angle and also with increase of curvature. The rate of decrease is more for bridge without backfill.

4.2.7 Variation of the moment at middle wall in transverse seismic condition

4.2.7.1 Variation of longitudinal moment at top of middle wall with skew angle in transverse seismic

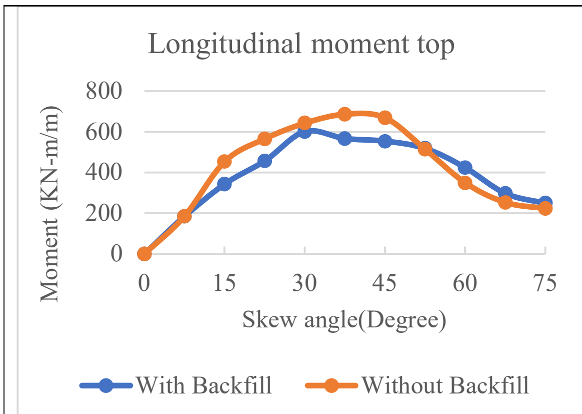

Graph 207. Variation of longitudinal moment at top of middle wall w.r.t. skew with pile foundation with or with earth behind abutment.

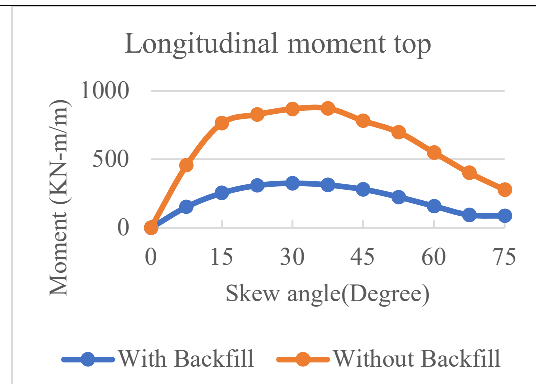

Graph 208. Variation of longitudinal moment at top of middle wall w.r.t. skew with open foundation with or without earth behind abutment.

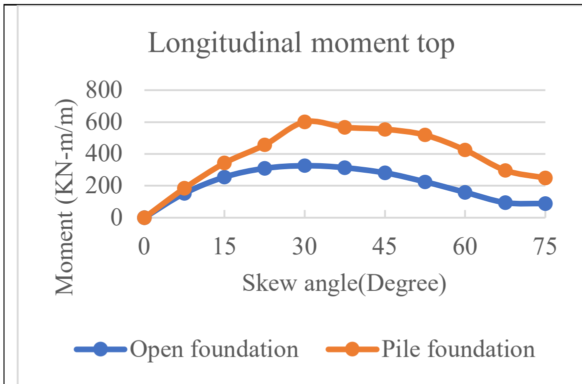

Graph 209. Variation of longitudinal moment at top of middle wall w.r.t. skew between open and pile foundation with earth behind abutment.

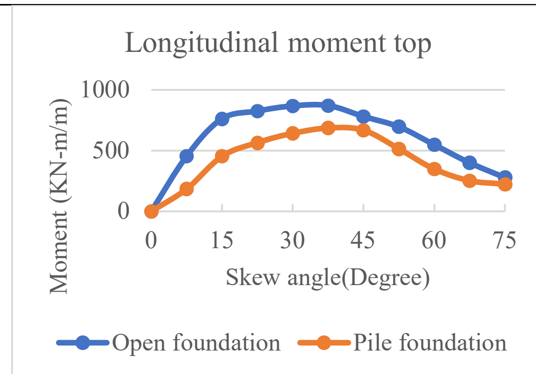

Graph 210. Variation of longitudinal moment at top of middle wall w.r.t. skew between open and pile foundation without earth behind abutment.

4.2.7.2 Variation of longitudinal moment at top of middle wall with curvature in transverse seismic

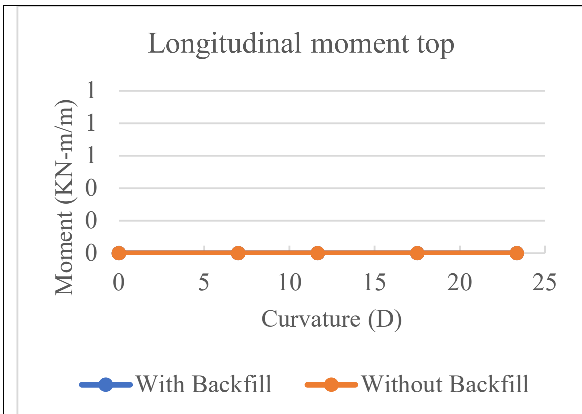

Graph 211. Variation of longitudinal moment at top of middle wall w.r.t. curvature with pile foundation with or with earth behind abutment.

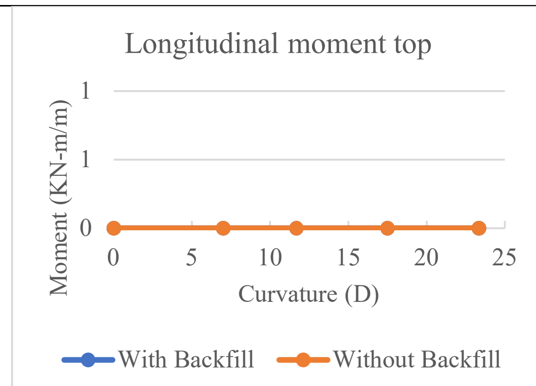

Graph 212. Variation of longitudinal moment at top of middle wall w.r.t. curvature with open foundation with or without earth behind abutment.

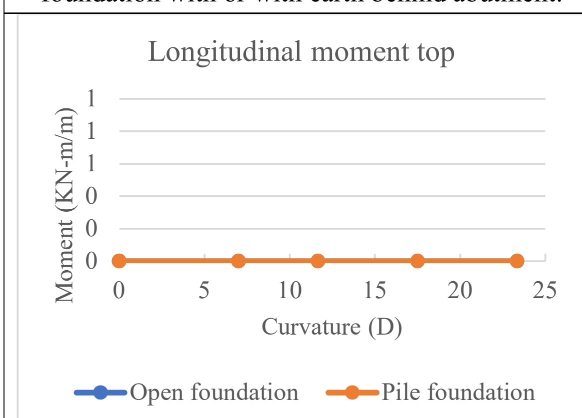

Graph 213. Variation of longitudinal moment at top of middle wall w.r.t. curvature between open and pile foundation with earth behind abutment.

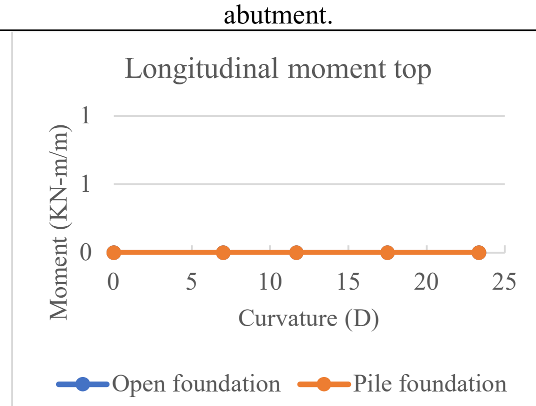

Graph 214. Variation of longitudinal moment at top of middle wall w.r.t. curvature between open and pile foundation without earth behind abutment.

4.2.7.3 Variation of transverse moment at top of middle wall with skew angle in transverse seismic

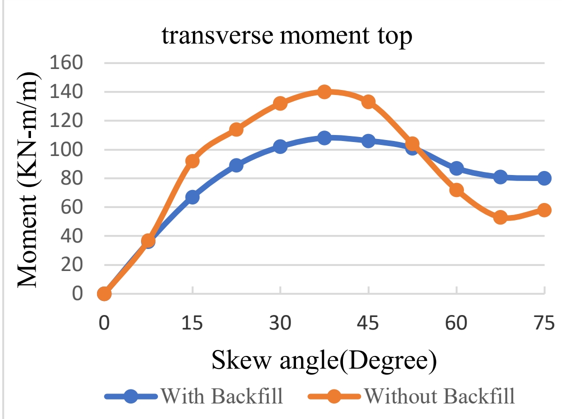

Graph 215. Variation of transverse moment at top of middle wall w.r.t. skew with pile foundation with or with earth behind abutment.

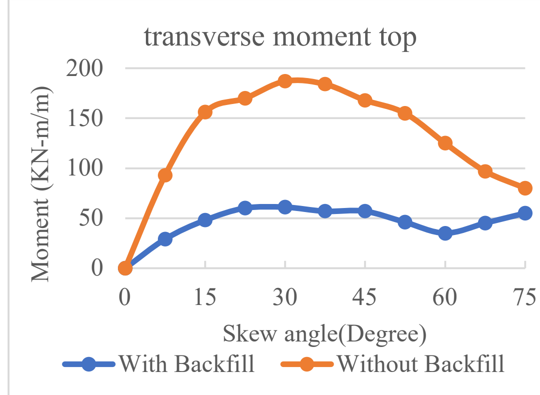

Graph 216. Variation of transverse moment at top of middle wall w.r.t. skew with open foundation with or without earth behind abutment.

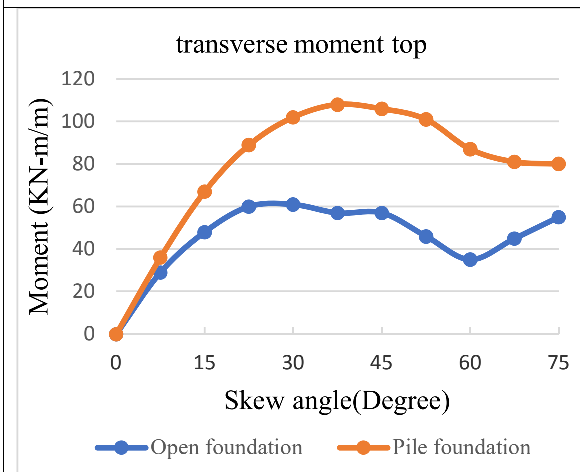

Graph 217. Variation of transverse moment at top of middle wall w.r.t. skew between open and pile foundation with earth behind abutment.

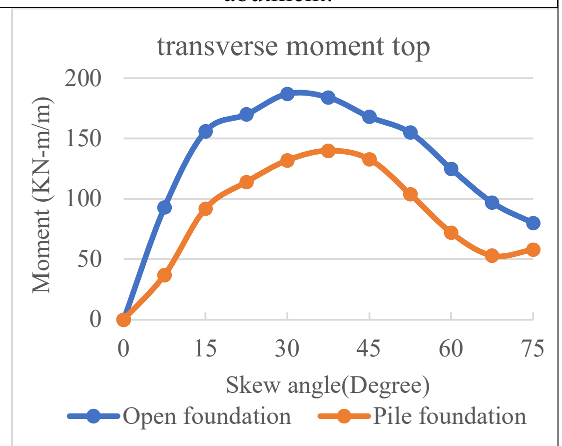

Graph 218. Variation of transverse moment at top of middle wall w.r.t. skew between open and pile foundation without earth behind abutment.

4.2.7.4 Variation of transverse moment at top of middle wall with curvature in transverse seismic

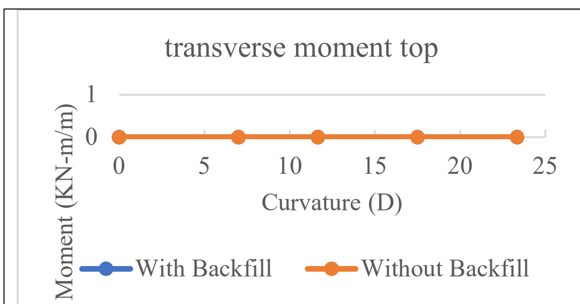

Graph 219. Variation of transverse moment at top of middle wall w.r.t. curvature with pile foundation with or with earth behind abutment.

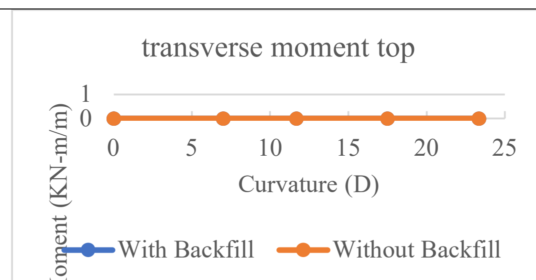

Graph 220. Variation of transverse moment at top of middle wall w.r.t. curvature with open foundation with or without earth behind abutment.

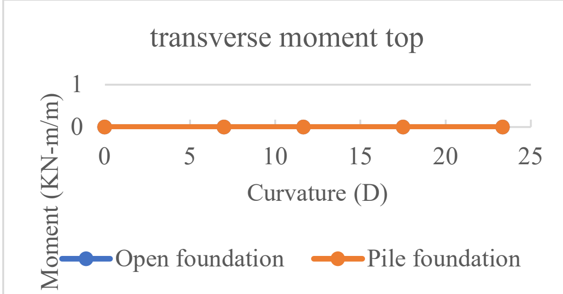

Graph 221. Variation of transverse moment at top of middle wall w.r.t. curvature between open and pile foundation with earth behind abutment.

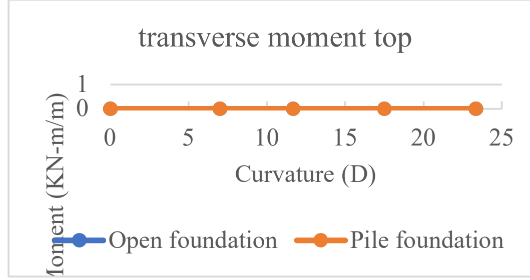

Graph 222. Variation of transverse moment at top of middle wall w.r.t. curvature between open and pile foundation without earth behind abutment.

4.2.7.5 Variation of torsional moment at top of middle wall with skew angle in transverse seismic

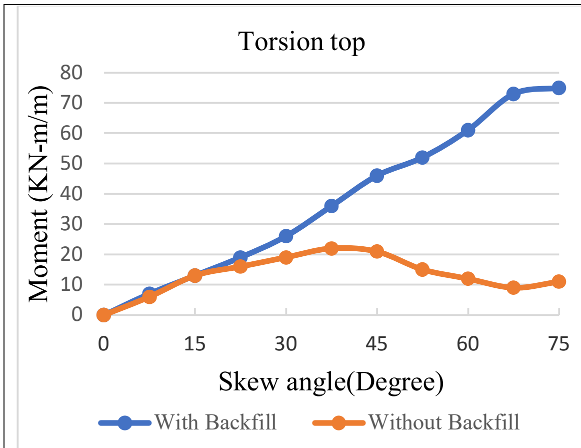

Graph 223. Variation of torsion at top of middle wall w.r.t. skew with pile foundation with or with earth behind abutment.

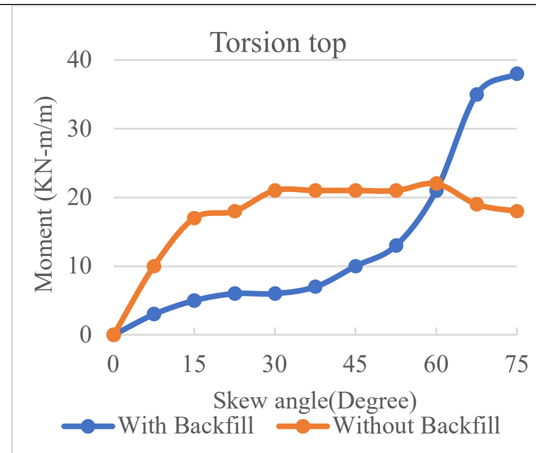

Graph 224. Variation of torsion at top of middle wall w.r.t. skew with open foundation with or without earth behind abutment.

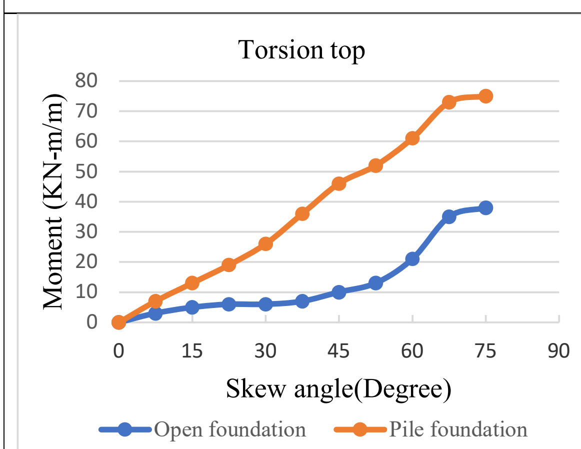

Graph 225. Variation of torsion at top of middle wall w.r.t. skew between open and pile foundation with earth behind abutment.

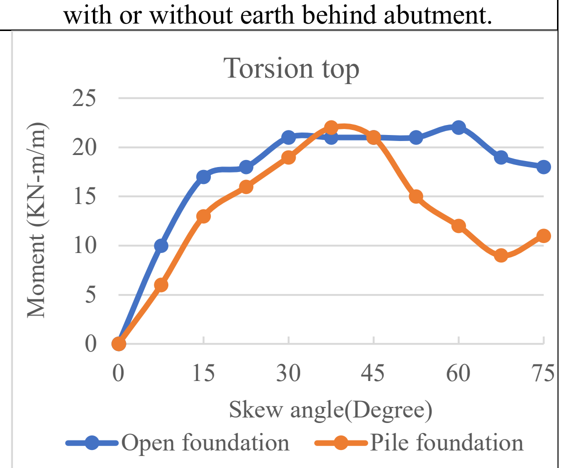

Graph 226. Variation of torsion at top of middle wall w.r.t. skew between open and pile foundation without earth behind abutment.

4.2.7.6 Variation of torsional moment at top of middle wall with curvature in transverse seismic

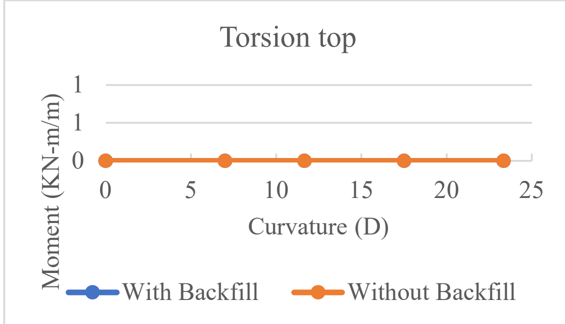

Graph 227. Variation of torsion at top of middle wall w.r.t. curvature with pile foundation with or with earth behind abutment.

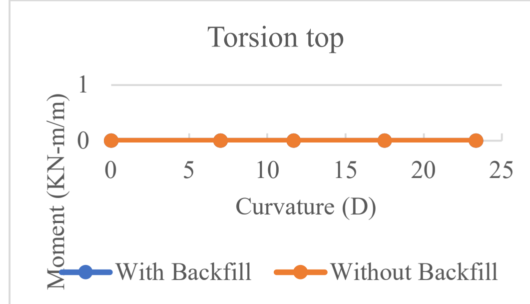

Graph 228. Variation of torsion at top of middle wall w.r.t. curvature with open foundation with or without earth behind abutment.

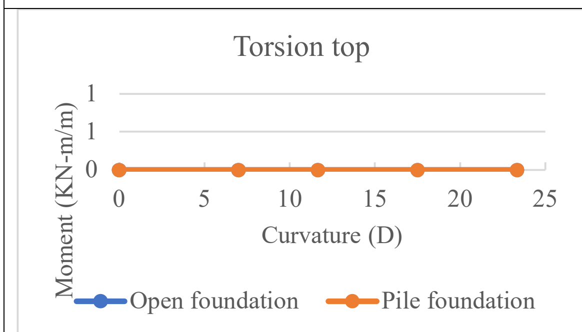

Graph 229. Variation of torsion at top of middle wall w.r.t. curvature between open and pile foundation with earth behind abutment.

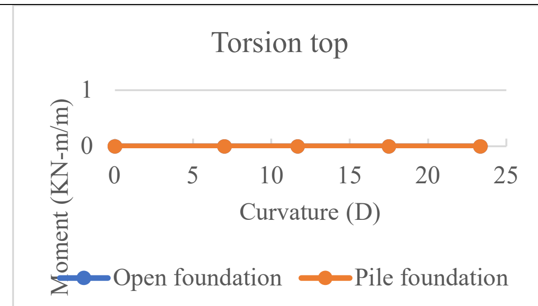

Graph 230. Variation of torsion at top of middle wall w.r.t. curvature between open and pile foundation without earth behind abutment.

4.2.7.7 Variation of longitudinal moment at bottom of middle wall with skew angle in transverse seismic

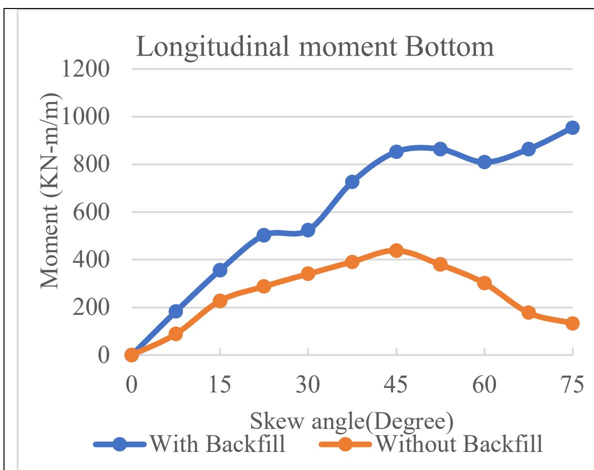

Graph 231. Variation of longitudinal moment at bottom of middle wall w.r.t. skew with pile foundation with or with earth behind abutment.

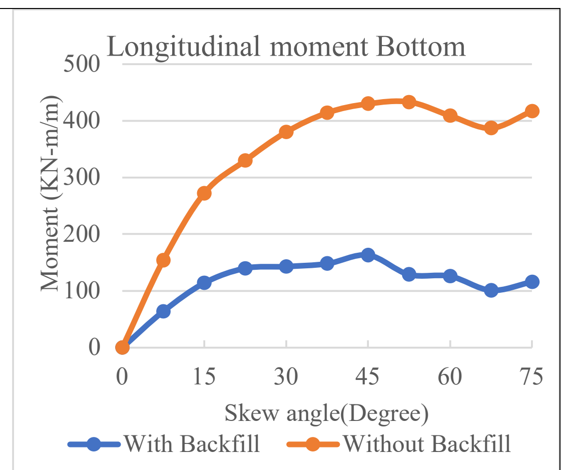

Graph 232. Variation of longitudinal moment at bottom of middle wall w.r.t. skew with open foundation with or without earth behind abutment.

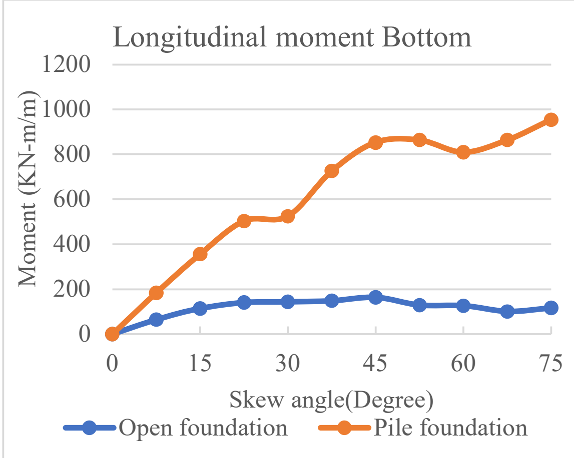

Graph 233. Variation of longitudinal moment at bottom of middle wall w.r.t. skew between open and pile foundation with earth behind abutment.

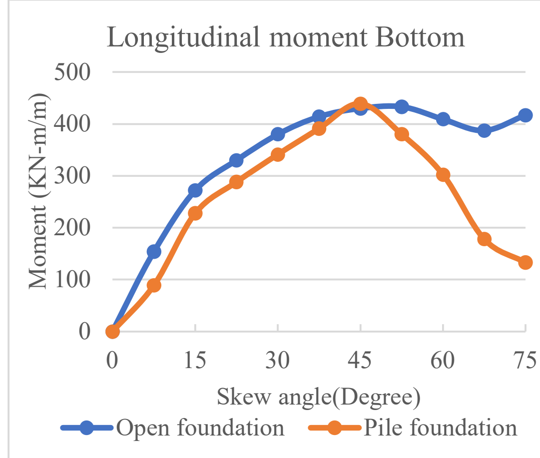

Graph 234. Variation of longitudinal moment at bottom of middle wall w.r.t. skew between open and pile foundation without earth behind abutment.

4.2.7.8 Variation of longitudinal moment at bottom of middle wall with curvature in transverse seismic

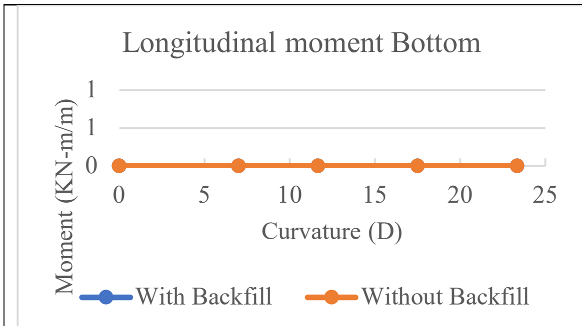

Graph 235. Variation of longitudinal moment at bottom of middle wall w.r.t. curvature with pile foundation with or with earth behind abutment.

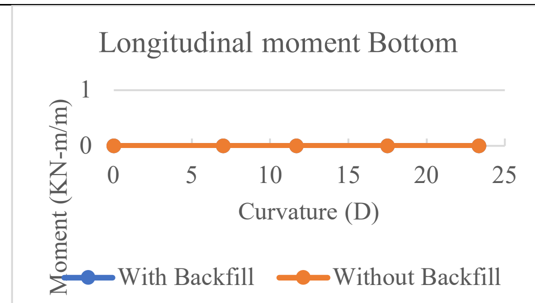

Graph 236. Variation of longitudinal moment at bottom of middle wall w.r.t. curvature with open foundation with or without earth behind abutment.

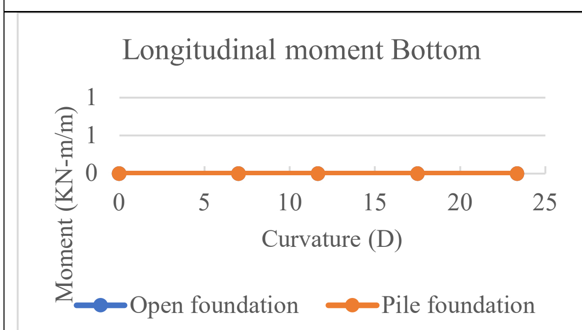

Graph 237. Variation of longitudinal moment at bottom of middle wall w.r.t. curvature between open and pile foundation with earth behind abutment.

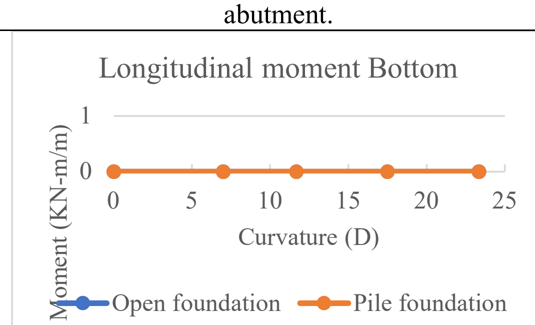

Graph 238. Variation of longitudinal moment at bottom of middle wall w.r.t. curvature between open and pile foundation without earth behind abutment.

4.2.7.9 Variation of transverse moment at bottom of middle wall with skew angle in transverse seismic

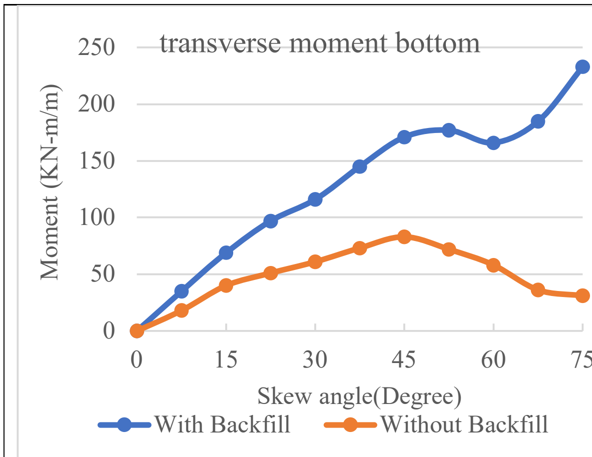

Graph 239. Variation of transverse moment at bottom of middle wall w.r.t. skew with pile foundation with or with earth behind abutment.

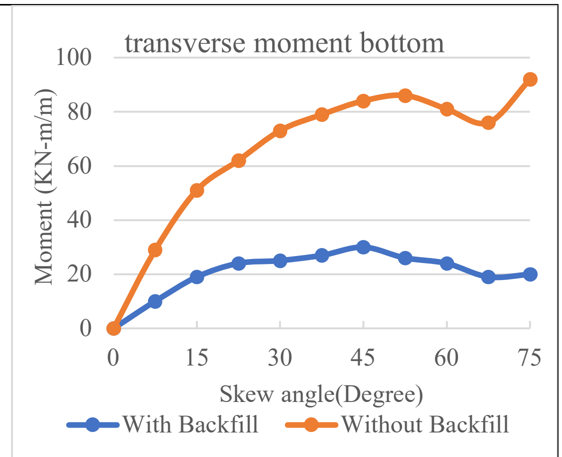

Graph 240. Variation of transverse moment at bottom of middle wall w.r.t. skew with open foundation with or without earth behind abutment.

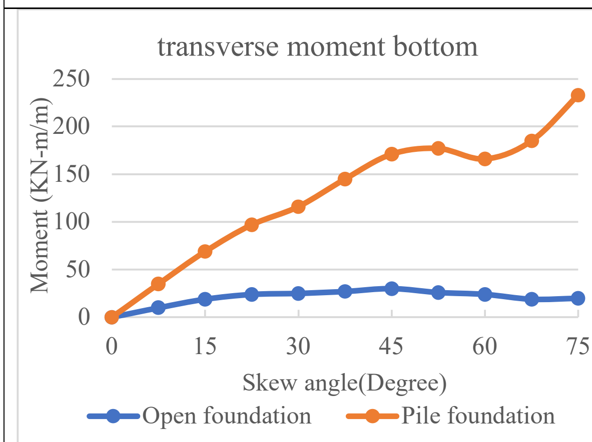

Graph 241. Variation of transverse moment at bottom of middle wall w.r.t. skew between open and pile foundation with earth behind abutment.

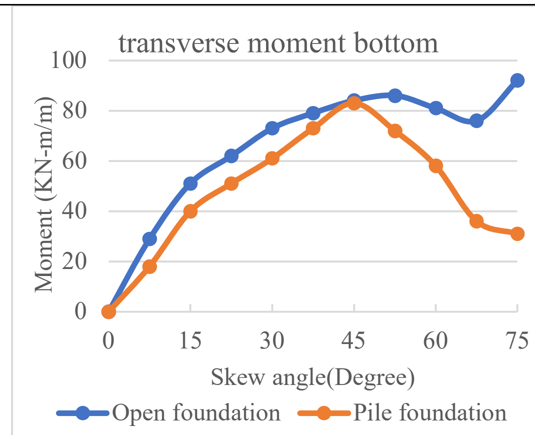

Graph 242. Variation of transverse moment at bottom of middle wall w.r.t. skew between open and pile foundation without earth behind abutment.

4.2.7.10 Variation of transverse moment at bottom of middle wall with curvature in transverse seismic

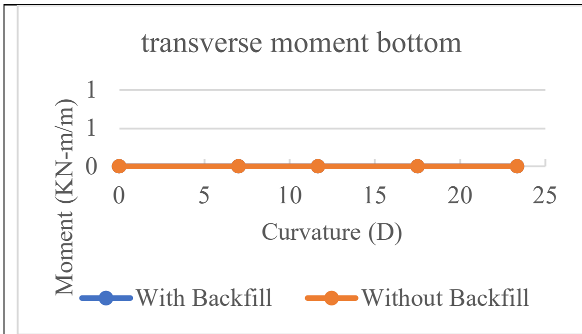

Graph 243. Variation of transverse moment at bottom of middle wall w.r.t. curvature with pile foundation with or with earth behind abutment.

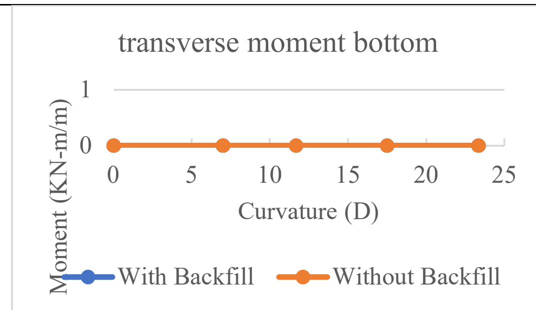

Graph 244. Variation of transverse moment at bottom of middle wall w.r.t. curvature with open foundation with or without earth behind abutment.

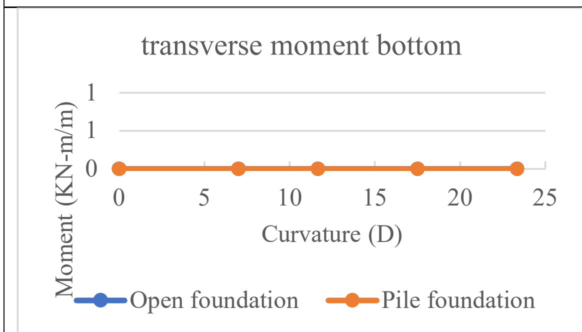

Graph 245. Variation of transverse moment at bottom of middle wall w.r.t. curvature between open and pile foundation with earth behind abutment.

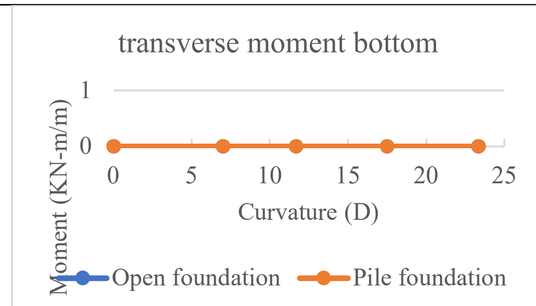

Graph 246. Variation of transverse moment at bottom of middle wall w.r.t. curvature between open and pile foundation without earth behind abutment.

4.2.7.11 Variation of torsional moment at bottom of middle wall with skew angle in transverse seismic

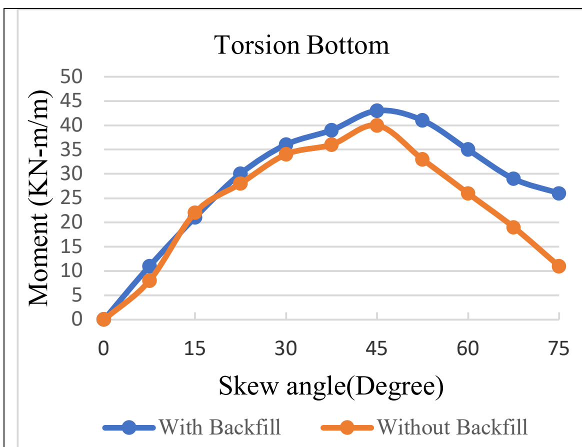

Graph 247. Variation of torsion at bottom of middle wall w.r.t. skew with pile foundation with or with earth behind abutment.

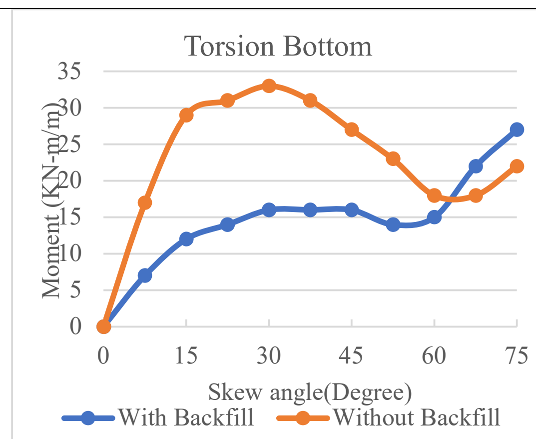

Graph 248. Variation of torsion at bottom of middle wall w.r.t. skew with open foundation with or without earth behind abutment.

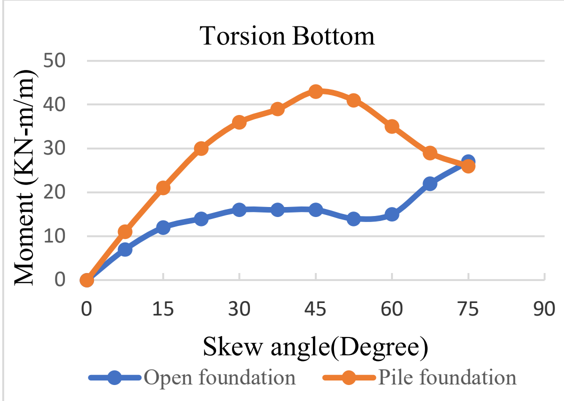

Graph 249. Variation of torsion at bottom of middle wall w.r.t. skew between open and pile foundation with earth behind abutment.

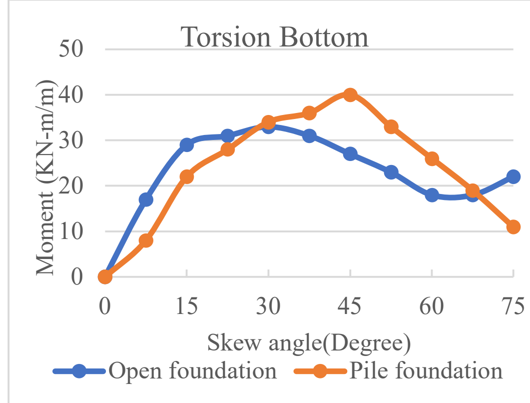

Graph 250. Variation of torsion at bottom of middle wall w.r.t. skew between open and pile foundation without earth behind abutment.

4.2.7.12 Variation of torsional moment at bottom of middle wall with curvature in transverse seismic

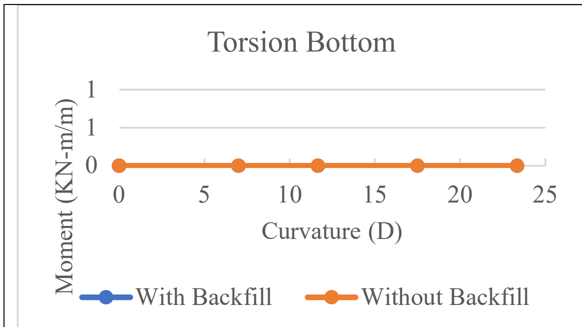

Graph 251. Variation of torsion at bottom of middle wall w.r.t. curvature with pile foundation with or with earth behind abutment.

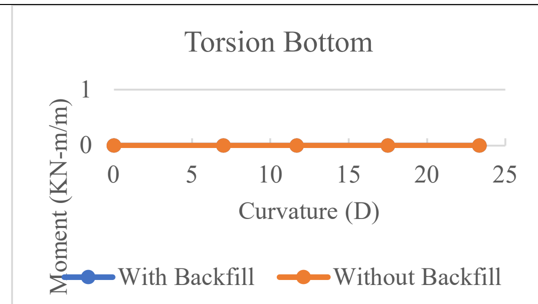

Graph 252. Variation of torsion at bottom of middle wall w.r.t. curvature with open foundation with or without earth behind abutment.

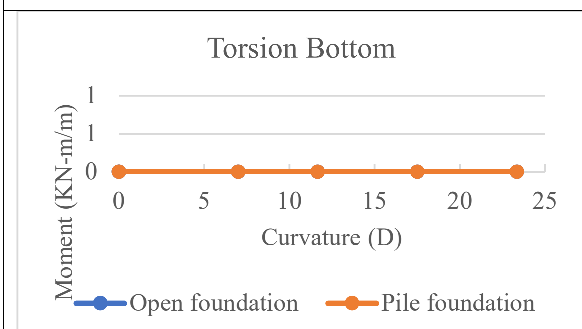

Graph 253. Variation of torsion at bottom of middle wall w.r.t. curvature between open and pile foundation with earth behind abutment.

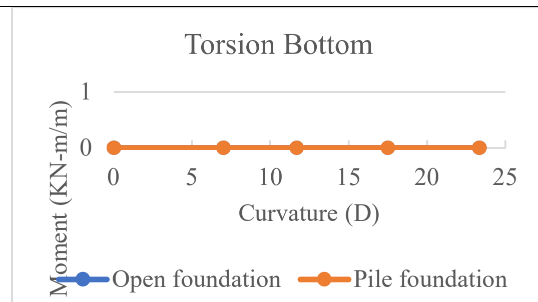

Graph 254. Variation of torsion at bottom of middle wall w.r.t. curvature between open and pile foundation without earth behind abutment.

Hence from the above graphs following observations can be made: -

For transverse seismic case

- Longitudinal moment at top of middle wall initially increases then decreases with increase of skew angle for both open and pile foundation. The moment is more for bridge without backfill than bridge with backfill.
- Longitudinal moment at top of middle is zero for all curvature.
- Transverse moment at top of middle wall initially increases then decreases with increase of skew angle for both open and pile foundation.
- Transverse moment at top of middle wall is zero for all curvature.
- Torsion at top of middle wall increases with increase of skew angle for bridge with backfill. For bridge without backfill it initially increases then decreases.
- Torsion at top of middle wall is zero for all curvature.
- Longitudinal moment at bottom of middle wall increases then decreases with increase of skew angle for both open and pile foundations.
- Longitudinal moment at bottom of middle wall is zero for all curvature.
- Transverse moment at bottom of middle wall increases with increase of skew angle.
- Transverse moment at bottom of middle wall is zero for all curvature.
- Torsion at bottom of middle wall initially increases then decreases with increase of skew angle. It is zero for bridge with all curvature.

Chapter – 5: Conclusions

5.1 General

Four types of bridge responses e.g. time period, base reaction, bending moment, torsion, have been studied in the present thesis. The major point wise conclusion has been presented in Section 5.1; while Section 5.2 indicates the future scope.

An exhaustive parametric study has been carried out to examine the effect of curvature and skewness on various bridge responses of integral bridges. The three-dimensional modeling and finite element analyses of the bridges for various combination of curvature, skewness has been carried out using Midas Civil software package. The study shows that the bridge responses vary significantly with curvature and skewness. In this study it is found that that the dead load increases with the increase of skew angle and it remains almost same for different curvature.

The curves furnished in this thesis will serve as important inputs to designeers and the effect on different design parameters of integral bridges due to changes of curvature and

angle will help practicing engineer in decision making process.

5.1.1 Time period

Time period of 1st mode of vibration is studied in this thesis and it is found that it varies with the variation of skewness and curvature. The following conclusions can be made: -

- Time period for pile foundation without backfill increases with increase of skew angle and for with backfill time period initially decreases then increases.
- Time period for open foundation with backfill decreases rapidly with increase of skew angle and for without backfill time period decreases slowly.
- Time period for integral bridge with pile foundation decrease with increase of curvature i.e. decrease of radius of curve. For bridge with backfill time period decreases more than without backfill.
- Time period for bridge with pile foundation is higher than the same bridge with open foundation.

Simplified formula for calculation of time period as per IRC: SP: 114- 2018 is $T= 2.0\sqrt{\frac{D}{1000F}}$

Where T= fundamental natural period (in seconds)

D = Appropriate dead load of the superstructure and live load in kN

F = Horizontal force in kN required to be applied at the centre of mass of superstructure for one mm horizontal deflection at the top of the pier/ abutment for the earthquake in the transverse direction; and the force to be applied at the top of the bearings for the earthquake in the longitudinal direction

For bridge with pile foundation required horizontal force F is lesser than the bridge with open foundation as for pile foundation soil stiffness of the pile plays main role for the deflection so required force is lesser.

Again, for increase of skew angle of bridge with backfill the length of backfill increases. So the resistance to deflection increases. So the time period decreases. For increase of curvature the resistance of earth increases so the time period decreases. For the same reason the time period of bridge with backfill is lesser than bridge without backfill.

5.1.2 Base reaction

During this study it is found that the base reaction varies with the variation of skew and curvature. The dead load of the structure increases with increase of skew angle so total base reaction increases. So, the effect of skewness will not be prominent if we compare the variation of total base shear. So, variation of base shear/vertical reaction is compared. It gives the clear idea of variation with skew and curvature.

For longitudinal seismic case following observations can be made.

- Longitudinal base shear/Vertical reaction decreases with increase of skew angle. For bridge with backfill the rate of decrease is more than bridge without backfill. The ratio is more for bridge with pile foundation than open foundation. Again, it is more for bridge with backfill than bridge without backfill. The ratio decreases slightly with increase of curvature.
- Transverse base shear/Vertical reaction initially increases then decreases with increase of skew angle. For bridge with backfill the rate of increase is more than bridge without backfill. The ratio is more for bridge with open foundation.
- Transverse base shear is zero for bridge of all curvature without skew.

For transverse seismic case following observations can be made.

- Longitudinal base shear/Vertical reaction is more for bridge with backfill than bridge without backfill. The same initially increases with increase of skew angle then decreases.
- Transverse base shear/Vertical reaction increases in case of bridge with backfill and

decreases for bridge without backfill.

The ratio represents the effective seismic coefficient. As per IRC: SP: 114- 2018 horizontal seismic coefficient is derived by the following formula.

$$Ah = \frac{\frac{Z}{2}\frac{Sa}{g}}{\frac{R}{I}}$$

Z = Zone factor, I= Importance factor, R= Response reduction factor. These three factors are same for all bridges. Sa/g depends upon the time period. As per IRC: SP: 114- 2018 relation of Sa/g with time period can be obtained by the Figure 44.

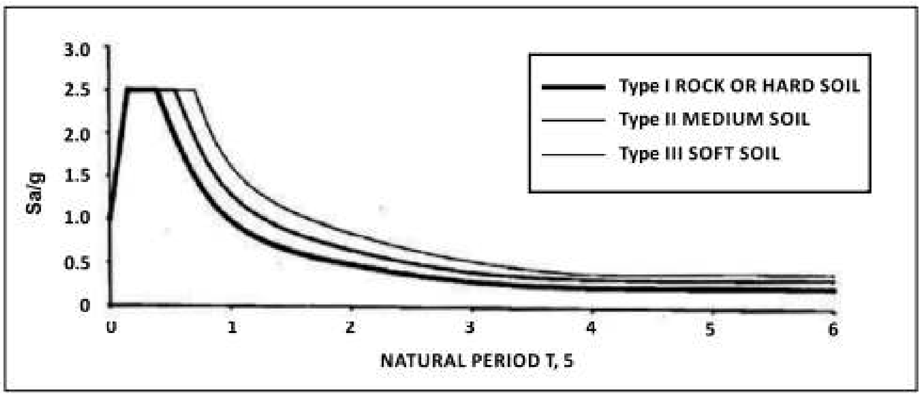

Fig 44. Natural time period vs sa/g

With the increase of skew angle the time period increases so the ratio decreases. Again to increases in skew angle the force of longitudinal direction decreases and in transverse direction increases. For this in longitudinal seismic case the reaction in longitudinal direction decreases and in transverse direction increases. The opposite thing happens for transverse seismic case for the same reason. As the time period of open foundation is lesser than the time period of pile foundation, the ratio is more fore open foundation than pile foundation. As, there is no other directional effect for bridge with curvature so the transverse reaction is zero for longitudinal seismic and longitudinal reaction is zero for transverse seismic.

5.1.2 Moment and torsion of side wall

During this study it is found that the moment and torsion of side wall varies with the variation of skew and curvature. The following conclusions can be made: -

For longitudinal seismic case

- Longitudinal moment at top and bottom of side wall decreases with increase of skew angle for both open and pile foundation. The moment is more for bridge without backfill than bridge with backfill. Moment is more for pile foundation than open foundation. The moment at top and bottom of side wall increases with increase of curvature for both open and pile foundation. The moment is more for bridge without backfill than bridge with backfill. Moment is more for pile foundation than open foundation.
- Transverse moment at top of side wall decreases with increase of skew angle for both open and pile foundation. The rate of decrease is more for bridge without backfill. Moment is more for pile foundation than open foundation. The moment increases with increase of curvature for pile foundation and it is more for bridge without backfill. For open foundation it is almost same. Moment at bottom of side wall decreases with increase of skew angle for bridge without backfill. For bridge with backfill it increases initially then decreases with increase of skew angle. Moment at bottom of side wall increases slightly with increase of curvature.
- Torsion at top of side wall initially increases then decreases with increase of skew angle for both open and pile foundation. Torsion increases with increase of curvature for both open and pile foundation. The rate of increase is more for bridge with backfill than bridge without backfill.
- Torsion at bottom of side wall initially increases then decreases with increase of skew angle except the bridge with open foundation without backfill. For bridge with open foundation and without backfill torsion decreases with increase of skew angle. Torsion increases with the increase of curvature. And for curved bridges torsion is more for bridges with pile foundation than open foundation.

From the above observation the following conclusion may be drawn:-

- ✓ The longitudinal and transverse moment in the bridges with backfill is lesser than the bridges without backfill. As the backfill behind the abutment provides provide a uniform flexible support behind the abutment and cause the resistance to movement and this also increases the time period of the bridge. So the moment is lesser for the bridge with backfill. Longitudinal moment at top of bottom of side wall decreases with increase of skew angle as, the time period increases with the increase of skew angle. As the time period of pile foundation is lesser than the time period of open foundation, moment is more for pile foundation than open foundation. Torsion increases with increase with skew angle as it tends to rotate more but after a certain value to skew angle it decreases.

- ✓ Longitudinal, transverse and torsional moment increases with increase of curvature as the time period decreases with increase of curvature.

For transverse seismic case

- ➢ Longitudinal moment at top and bottom of side wall initially increases then decreases with increase of skew angle for both open and pile foundation. The moment is more for bridge without backfill than bridge with backfill. Longitudinal moment at top and bottom of side wall increases with increase of curvature for both open and pile foundation.
- ➢ Transverse moment at top of side wall initially increases then decreases with increase of skew angle for both open and pile foundation. The moment at top and bottom of side wall increases with increase of curvature for open and pile foundation. The moment also increases with increase of curvature. Transverse moment at bottom of side wall increases with increase of skew angle
- ➢ Torsion at top of side wall initially increases then decreases with increase of skew angle for bridges without backfill. For bridges with backfill it increases with increase of skew angle. Torsion at top of side wall increases with increase of curvature for both open and pile foundations.
- ➢ Torsion at bottom of side wall decreases with increase of skew angle and also with increase of curvature. The rate of decrease is more for bridge without backfill.

From the above observation the following conclusion may be drawn:-

- ✓ The longitudinal and transverse moment in the bridges with backfill is lesser than the bridges without backfill. As the backfill behind the abutment provides provide a uniform flexible support behind the abutment and cause the resistance to movement and this also increases the time period of the bridge. So the moment is lesser for the bridge with backfill. Longitudinal moment at top of bottom of side wall initially increases with increase of skew angle and then decreases as, the time period increases with the increase of skew angle but after a certain skew angle the effect of time period is dominated by the length of the wall so per m moment reduced. Torsion increases with increase with skew angle as it tends to rotate more but after a certain value to skew angle it decreases.
- ✓ Longitudinal, transverse and torsional moment increases with increase of curvature as the time period decreases with increase of curvature.

5.1.2 Moment and torsion of middle wall

During this study it is found that the moment and torsion of middle wall varies with the variation of skew and curvature. The following conclusions can be made: -

For longitudinal seismic case

- Longitudinal moment at top and bottom of middle wall decreases with increase of skew angle for both open and pile foundation. The moment is more for bridge without backfill and bridge with pile foundation than bridge with backfill.
- Transverse moment at top and bottom of middle wall decreases with increase of skew angle for both open and pile foundation. The rate of decrease is more for bridge without backfill. The moment is more for bridge without backfill and bridge with pile foundation than bridge with backfill and bridge with open foundation.
- Torsion at top of middle wall initially increases then decreases with increase of skew angle for bridges without backfill. For bridges with backfill it decreases with increase of skew angle. Torsion at top of middle wall increases with increase of curvature for both open and pile foundations. It is more for bridge without backfill and bridge with pile foundation than bridge with backfill and bridge with open foundation.
- Torsion at bottom of middle wall decreases with increase of skew angle for bridge without backfill. The rate of decrease is more for bridge without backfill.

From the above observation the following conclusion may be drawn:-

- ✓ The longitudinal and transverse moment in the bridges with backfill is lesser than the bridges without backfill. As the backfill behind the abutment provides provide a uniform flexible support behind the abutment and cause the resistance to movement and this also increases the time period of the bridge. So the moment is lesser for the bridge with backfill. Longitudinal moment at top of bottom of middle wall decreases with increase of skew angle as, the time period increases with the increase of skew angle.
- ✓ Longitudinal, transverse and torsional moment increases with increase of curvature as the time period decreases with increase of curvature.

For transverse seismic case

- Longitudinal moment at top and bottom of middle wall initially increases then decreases with increase of skew angle for both open and pile foundation. The moment is more for bridge without backfill than bridge with backfill. The moment at top and bottom of middle is zero for all curvature.

- Transverse moment at top of middle wall initially increases then decreases with increase of skew angle for both open and pile foundation. The moment at top of middle wall is zero for all curvature. Transverse moment at bottom of middle wall increases with increase of skew angle
- Torsion at top of middle wall increases with increase of skew angle. Torsion at top and bottom of middle wall is zero for all curvature.
- Torsion at bottom of middle wall initially increases then decreases with increase of skew angle.

From the above observation the following conclusion may be drawn:-

- ✓ The longitudinal and transverse moment in the bridges with backfill is lesser than the bridges without backfill. As the backfill behind the abutment provides provide a uniform flexible support behind the abutment and cause the resistance to movement and this also increases the time period of the bridge. So the moment is lesser for the bridge with backfill. Longitudinal and transverse moment at top of bottom of middle wall initially increases with increase of skew angle and then decreases as, the time period increases with the increase of skew angle but after a certain skew angle the effect of time period is dominated by the length of the wall so per m moment reduced
- ✓ Longitudinal, transverse and torsional moment is zero for curvature as the structure is symmetrical and the wall is totally perpendicular with the seismic wave direction. So no moment is generated.

5.2 Future scope of study

The critical discussion of the review of the accumulated literature, mentioned in Chapter 23, highlights the different areas which needs attention, from researches of integral bridge. The primary five responses for skewed-curved integral slab bridges e.g. time period, base reaction, bending moment, torsion, has been studied in the present thesis. There is vast area remaining unexplored; may be studied in future. For example, the same parametric study can be carried out for different spans, to increase the accuracy of the response coefficients further. The study can be carried out for Integral bridge with other type of superstructures like T beam, Composite girder etc. In this type of bridges variation of moment, shear and torsion in girder of superstructure also can be studied. The effect of earth behind abutment can be studied with the variation of abutment height of same span. Moreover, for dynamic analysis most important case can be studied that the effect of response reduction due to integral action and presence of backfill. All the studies also can be done with different type of substructure also.

. ***REFERENCES***

1. IRC:SP: 115: 2018: Guidelines for Design of Integral Bridges.
2. IRC:SP: 114: 2018: Guidelines for Seismic Design of Road Bridges.
3. Faraji S, Ting J M, Crovo D S, and Ernst H, *"Nonlinear Analysis of Integral Bridges: Finite-Element Model",* J. Geotech. Geoenviron. Eng. 2001.127:454-461.
4. Dicleli M, Erhan S, *"Analysis of Effect of Modelling Simplifications on Nonlinear Seismic Analysis of Integral Bridges Including Dynamic Soil-Structure Interaction",* 34th International Symposium on Bridge and Structural Engineering, Venice, 2010,
5. Bardakis V J, Fardis M N, *"Nonlinear Dynamic V Elastic Analysis for Seismic Deformation Demands in Concrete Bridges Having Deck Integral with The Piers",* Bull Earthquake Eng (2011) 9:519–535.
6. Zordan T, Briseghella B, Lan C, *"Parametric and Pushover Analyses on Integral Abutment Bridge",* Engineering Structures 33 (2011) 502–5151.
7. Shreedhar R, Hosur V, *"Soil-Pile Interaction for Integral Abutment Bridges",* National Conference, NET-2011.
8. Fartaria C, *"Soil-Structure Interaction in Integral Abutment Bridges",* Instituto Superior Técnico, Av. Rovisco Pais, 1,1049-001 Lisbon, Portugal.
9. Mohtashami E, Shooshtari A, *"Seismic Assessment of Integral Reinforced Concrete Bridges using adaptive Multi-Modal Pushover Analysis",* 15 WCEE, LISBOA 2012.
10. Bloodworth A G, Xu M, Banks J R, Clayton C R I, *"Predicting the Earth Pressure on Integral Bridge Abutments",* 15 Journal of Bridge Engineering, ASCE,2012.
11. Masrilayanti M, *"The Behaviour of Integral Bridges under Vertical and Horizontal Earthquake Ground Motion",* School of Science, Computing and Engineering University of Salford, United Kingdom.
12. Erhan S, Dicleli M, *"Comparative assessment of the seismic performance of integral and conventional bridges with respect to the differences at the abutments",* Bull Earthquake Eng (2015) 13:653–677.
13. Far N E, Maleki S, Barghian M, *"Design of integral abutment bridges for combined thermal and seismic loads",* The 2015 world congress on Advanced on Structural Engineering and Mechanics (ASEM15), Incheon Korea, August 25-29 2015,
14. Wood J H, *"Earthquake Design of Bridges with Integral Abutments",* 6th International Conference on Earthquake Geotechnical Engineering 1-4 November 2015 Christchurch, New Zealand.
15. Peric´ D, Miletic´ M, Shah B R, Esmaeily A, Wang H, *"Thermally induced soil structure*

interaction in the existing integral bridge", Engineering Structures 106 (2016) 484–494.

16. Haymanmyintmaung, Kyawlinnhtat, *"Investigation of Integral Bridge effect under dynamic loading",* International Journal of Advances in Mechanical and Civil Engineering, ISSN: 2250-3153, Volume-7, Issue-5, Aug.-2017
17. Panikkavettil K R, Raveendran K G, *"Seismic Analysis of Integral Bridges Research",* International Journal of Scientific and Engineering Research Volume 8, Issue 11, November-2017, ISSN 2229-5518.
18. Haymanmyintmaung, Kyawlinnhtat, *"Effect of Integral Bridge with Span Variation Under Dynamic Loading",* International Journal of Recent Advances in Engineering and Technology (IJRAET), ISSN (Online): 2347 - 2812, Volume-5, Issue-6, Aug.-2017.
19. Kozak D L, LaFave J M, Fahnestoc L A, *"Seismic modeling of integral abutment bridges in Illinois",* Engineering Structures 165 (2018) 170-183.
20. Mahjoubi, S, Maleki S, *"Finite element modelling and seismic behaviour of integral abutment bridges considering soil– structure interaction",* European Journal of Environmental and Civil Engineering 24, no. 6 (2020): 767-786.
21. Choi B H, Moreno L B, Lim C S, Nguyen D D, Lee T H, *"Seismic Performance Evaluation of a Fully Integral Concrete Bridge with End-restraining Abutments",* Hindawi, Advances in Civil Engineering Volume 2019, Article ID 6873096.
22. Ibrahim M K, Rahman A A, Ahmad B H, Abas F Z M, *"Theoretical Modal Characteristics of Integral Abutment Bridge with Bored Piles Foundation:",* IOP Conf. Series: Materials Science and Engineering 620 (2019) 012068J.
23. Malekjafarian A, Prendergast L J, Obrien E J, *"Use of mode shape ratios for pier scour monitoring in two-span integral bridges under changing environmental conditions.",* Canadian Journal of Civil Engineering 47, no. 8 (2020): 962973.
24. Naji M, Firoozi A A, Firoozi A A, *"A Review: Study of Integral Abutment Bridge with Consideration of Soil-Structure Interaction.",* Latin American Journal of Solids and Structures, 2020, 17(2), e252.
25. Joshi A, Patel R, *"A Review on Analysis and Design of Integral Bridges for Different Type of Span using Finite Element.",* ISSN (Online): 2348-4098.
26. Shilpa S, Thejashwini P T, Shruthi N P, *"Seismic Analysis of Integral Bridges",* International Research Journal of Engineering and Technology (IRJET).
27. Greimann, L F, Wolde-Tinsae, A M, Yang P S, *"Skewed Bridges with Integral Abutments",* 62nd Annual Meeting of the Transportation Research Board, Washington District of Columbia, United States.
28. Kaviani P, Zareian F, Taciroglu E, Sarraf M, *"Simplified Method for Seismic Performance*

Assessment of Skewed Bridges", COMPDYN 2011, 3rd ECCOMAS Thematic Conference on Computational Methods in Structural Dynamics and Earthquake Engineering, Greece, 25–28 May 2011.

29. Akib S, Moatasem Fayyadh M, Othman I, *"Structural Behaviour of a Skewed Integral Bridge affected by Different Parameters",* The Baltic Journal of Road and Bridge Engineering 2011, 6(2): 107–114.
30. Wright B, LaFave J, Fahnestock L, Jarrett M, Riddle J, Svatora J S, *"Field Monitoring of Skewed Integral Abutment Bridges",* 6th International Conference on Advances in Experimental Structural Engineering, August 1-2, 2015, University of Illinois, Urbana-Champaign, United States.
31. Oladele.O P, John W, *"The Long Term Performance Of Skew Integral Bridges",* Journal of Multidisciplinary Engineering Science and Technology (JMEST) ISSN: 3159-0040 Vol. 2 Issue 8, August – 2015.
32. Mallick M, Raychowdhury P, *"Seismic Analysis of Highway Skew Bridges with Nonlinear Soil–Pile Interaction",* Transportation Geotechnicsb3 (2015) 36–47.
33. Muhammad A, Abdullah R, Hassan I O, *"Long-Term Response Prediction of Skewed Integral Bridges under Creep Effects",* International Journal of Scientific Engineering and Technology, Volume No.4 Issue No.1, pp : 20-23.
34. Haymanmyintmaung, Kyawlinnhtat, *"Performance of skew integral bridge under dynamic loading",* International Journal of Advances in Mechanical and Civil Engineering, ISSN: 2394-2827, Volume-4, Issue-4, Aug.-2017.
35. Parachos A, Made A, *"Predrilled Holes for Pile Support of Skewed Integral Abutment Bridges",* Civil Engineering Practice, ISSN: 0886-9685, Boston Society of Civil Engineers Section / ASCE.
36. Zhao Q, Dong S, Wang Q, *"Seismic Response of Skewed Integral Abutment Bridges under Near-Fault Ground Motions, Including Soil–Structure Interaction",* MDPI Applied science journal.
37. Kalayci E, Breña S F, Civjan S A, *"Curved Integral Abutment Bridges – Thermal Response Prediction through Finite Element Analysis",* Structures 2009, ASCE 191 2015, 72-191.
38. Kalayci E, Civjan S A, Breña S F, *"Parametric study on the thermal response of curved integral abutment bridges",* Engineering Structures 43 (2012) 129–138.
39. Kataria N P, Jangid R S, *"Seismic performance and effect of curved geometry on isolation system in horizontally curved",* The 2013 World Congress on Advances in Structural Engineering and Mechanics (ASEM13), Jeju, Korea, September 8-12, 2013.
40. Phares B M, *"Field Monitoring of Curved Girder Bridges with Integral Abutments",* Bridge

Engineering Center, Iowa State University.

41. Deng Y, Phares B M, Greimann L, Shryack G L, Hoffman J J, *"Behavior of Curved and Skewed Bridges with Integral Abutments",* Journal of Constructional Steel Research 109 (2015) 115–136,

42. Jayeshbhai D M, Sanghvi C S, *"Review on Behavior of Curved Integral Bridges",* 2020 JETIR July 2020, Volume 7, Issue 7.

43. Civjan S, Lacroix J, Takeuchi A, Higgins K, *"Curved Steel Girder Integral Abutment Bridges in Vermont, USA",* Civil Engineering Practice, Boston Society of Civil Engineers Section / ASCE ISSN: 0886-9685.

44. Midas Civil user manual http://manual.midasuser.com/EN_Common/Civil/910/index.htm

45. Integral Bridge Function in Midas Civil at https://www.midasbridge.com/en/blog/